

Andrés Arturo Gómez Quinto

*Effective Superpotential and the Renormalization  
Group Equation in a Supersymmetric  
Chern-Simons-Matter Model in the Superfield  
Formalism*



Thesis presented to the Graduate Program in Physics of the Universidade Federal do ABC (UFABC), as a partial requirement to obtain the title of PhD in Physics.

Advisor: Prof. Dr. Alysson Fábio Ferrari

Santo Andre - SP

2016

*Este trabajo esta dedicado a mi  
esposa, Indira, a mis viejos, Juan y  
Cenia y a mis hermanos, Laura y  
Juan Carlos.*

---

## Acknowledgments

First, I would like to thank Prof. Alysson Ferrari for his guidance, help, patience, for many conversations and friendship.

I also thank

- *Coordenação de Aperfeiçoamento de Pessoal de Nivel Superior* (CAPES) for the financial support,
- the professors of the graduate program in Physics at *Universidade Federal do ABC* (UFABC), who were responsible for a large part of my scientific training, with classes, discussions, seminars, etc.,
- all the university staff of UFABC,
- my colleagues and friends in the group: Carlos Palechor and Luiz Borges for their discussions and contributions in my studies,
- the friends I made here: Marcela, Andrés, Diana, Camilo, Julian, Liliana, John, Dona Ana, Don Salu, Marcio and those who probably I forgot to mention (apologize me!),
- my old friends, with whom I am still sharing great moments: Melissa, Carlos, Fernando, Robinson, Mawin, Jeiner, Cynthia, Rodolfo, and those who probably I forgot to mention (apologize me!), thank you for your friendship, there is no happiness without friends specially when you are far from the family.

I would also give a special thanks to Prof. André Lehum, for the immense contribution of our discussions.

Finally, and so very important for me, I would like to thank my family: my wife Indira Vargas; my parents, Cenia Quinto and Juan Gomez; my sister, Laura and my brother Juan Carlos, my immense thanks for the support in these years of study.

---

---

# Abstract

In this thesis we study the Dynamical Symmetry Breaking (DSB) mechanism in a supersymmetric Chern-Simons theory in  $(2 + 1)$  dimensions coupled to  $N$  matter superfields in the superfield formalism. For this purpose, we developed a mechanism to calculate the effective superpotential  $K_{\text{eff}}(\sigma_{\text{cl}}, \alpha)$ , where  $\sigma_{\text{cl}}$  is a background superfield, and  $\alpha$  a gauge-fixing parameter that is introduced in the quantization process. The possible dependence of the effective potential on the gauge parameter have been studied in the context of quantum field theory, and it can have nontrivial consequences to the study of DSB in gauge theories. Therefore, we did not assume from the start the gauge independence of the effective potential in our model, as it is customary in the literature. We developed the formalism of the Nielsen identities in the superfield language, which is the appropriate formalism to study DSB when the effective potential is gauge dependent. We also discuss how to calculate the effective superpotential via the Renormalization Group Equation (RGE) from the knowledge of the renormalization group functions of the theory, i.e.,  $\beta$  functions and anomalous dimensions  $\gamma$ . We perform a detailed calculation of these functions at two loops, finding that these do not depend on  $\alpha$ , and therefore, by using the RGE, we calculate the effective superpotential  $K_{\text{eff}}$ , showing that it is also independent of  $\alpha$ . Then we discuss the improvement of the calculation of  $K_{\text{eff}}$  by summing up leading logarithms, and we compare this improvement with the one obtained in the non supersymmetric version of the model. Finally, we study the DSB finding that it is operational for all reasonable values of the free parameters, while the improvement obtained from the RGE in general only produces a small quantitative correction in the results, instead of the more dramatic qualitative change found in non supersymmetric models.

**Keywords:** Chern-Simons, Supersymmetry, Renormalization Group Equation, Nielsen Identity, Superfields, Superpotential, BRST transformations and Dynamical Symmetry Breaking.



# Contents

<b>1</b>	<b>Introduction</b>	<b>13</b>
<b>2</b>	<b>Supersymmetry in <math>(2 + 1)</math> Dimensions</b>	<b>21</b>
2.1	Conventions . . . . .	21
2.2	Supersymmetry and superfields . . . . .	22
2.2.1	Superfields . . . . .	22
2.2.2	D-algebras . . . . .	24
2.2.3	Components by expansion and projections . . . . .	26
2.3	Scalar multiplet . . . . .	26
2.4	Vector multiplet . . . . .	28
<b>3</b>	<b>Nielsen Identity</b>	<b>31</b>
3.1	Building a Lagrangian invariant under BRST transformations . . . . .	31
3.2	Obtaining the Nielsen identity . . . . .	34
3.3	On the gauge (in)dependence of the Effective Superpotential . . . . .	38
<b>4</b>	<b>Renormalization Group Functions</b>	<b>41</b>
4.1	Gauge invariance of the renormalization group functions . . . . .	41
4.2	Feynman rules . . . . .	42
4.2.1	Scalar propagator . . . . .	42
4.2.2	Gauge propagator . . . . .	43
4.2.3	Vertices . . . . .	44
4.3	Quantum corrections up two loops and renormalization group functions . .	47
<b>5</b>	<b>Renormalization Group Improvement and Dynamical Symmetry Breaking</b>	<b>55</b>
5.1	Calculation of the Effective Superpotential . . . . .	55
5.2	RGE improvement and DSB: A short review of the four dimensional case .	59
5.3	RGE improvement in the three dimensional supersymmetric case . . . . .	62
5.4	Dynamical Breaking of Symmetry . . . . .	65
<b>6</b>	<b>Conclusions and perspectives</b>	<b>73</b>

<b>A</b>	<b>One Loop Correction</b>	<b>75</b>
A.1	Example: Two-point vertex function of gauge superfield . . . . .	75
<b>B</b>	<b>Two loops corrections</b>	<b>79</b>
B.1	Two-point vertex function to gauge superfield . . . . .	79
B.2	Two-point vertex function to the scalar superfield . . . . .	84
B.3	Four-point vertex function to the scalar superfield . . . . .	87
<b>C</b>	<b>Useful integrals</b>	<b>133</b>
C.1	One loop integrals . . . . .	133
C.2	Two loops massless integrals . . . . .	135
C.3	Integrals used in the gauge superfield corrections . . . . .	138

# List of Figures

1.1	Characteristic of the partial differential equation, Eq. (1.4), where the effective potential is constant in the plane $\phi - \alpha [1]$ . . . . .	15
4.1	Elementary vertices of the model, where a continuous line is associated to a scalar superfield, and a wavy line to the gauge superfield. . . . .	45
4.2	Two loops diagrams contributing to the two-point vertex function of the scalar superfield $\Phi$ . . . . .	47
4.3	Two loop diagrams contributing to the two-point vertex function of the gauge superfield $\Gamma_\alpha$ . . . . .	49
4.4	The complete set of two loops diagrams contributing to the four-point scalar vertex function. . . . .	50
5.1	Solutions for $\lambda$ in the improved case: one (gray region), zero (white region) and two (black region) . . . . .	67
5.2	Same as Figure (5.1), but with larger $N$ . We observe that for larger values of $N$ , the region where we have two solutions for $\lambda$ dominates the parameter space of the model. . . . .	69
5.3	Behavior of the unimproved $\lambda$ (blue line) and improved $\lambda^I$ (red line) with the variation of the coupling constant $y$ : a) for $N = 1, 10, 50, 100$ and b) $N = 10 \times 10^2, 10 \times 10^4, 10 \times 10^5, 10 \times 10^6$ . . . . .	70
5.4	Comparison of the unimproved (blue line) and improved (red line) effective superpotential, for $y = 0.5$ and $N = 65$ . . . . .	71
A.1	$\mathcal{S}_{\Gamma\Gamma}^{(a)-1l}$ . . . . .	76
B.1	$\mathcal{S}_{\Gamma\Gamma}$ . . . . .	80
B.2	$\mathcal{S}_{\bar{\Phi}\Phi}$ . . . . .	84
B.3	$\mathcal{S}_{(\bar{\Phi}\Phi)^2}^{(D1)}$ . . . . .	87
B.4	$\mathcal{S}_{(\bar{\Phi}\Phi)^2}^{(D2)}$ . . . . .	88
B.5	$\mathcal{S}_{(\bar{\Phi}\Phi)^2}^{(D3)}$ . . . . .	90
B.6	$\mathcal{S}_{(\bar{\Phi}\Phi)^2}^{(D4)}$ . . . . .	91

B.7	$\mathcal{S}_{(\overline{\Phi}\Phi)^2}^{(D5)}$	93
B.8	$\mathcal{S}_{(\overline{\Phi}\Phi)^2}^{(D6)}$	94
B.9	$\mathcal{S}_{(\overline{\Phi}\Phi)^2}^{(D7)}$	95
B.10	$\mathcal{S}_{(\overline{\Phi}\Phi)^2}^{(D8)}$	96
B.11	$\mathcal{S}_{(\overline{\Phi}\Phi)^2}^{(D9)}$	97
B.12	$\mathcal{S}_{(\overline{\Phi}\Phi)^2}^{(D10)}$	98
B.13	$\mathcal{S}_{(\overline{\Phi}\Phi)^2}^{(D11)}$	99
B.14	$\mathcal{S}_{(\overline{\Phi}\Phi)^2}^{(D12)}$	101
B.15	$\mathcal{S}_{(\overline{\Phi}\Phi)^2}^{(D13)}$	101
B.16	$\mathcal{S}_{(\overline{\Phi}\Phi)^2}^{(D14)}$	102
B.17	$\mathcal{S}_{(\overline{\Phi}\Phi)^2}^{(D15)}$	103
B.18	$\mathcal{S}_{(\overline{\Phi}\Phi)^2}^{(D16)}$	105
B.19	$\mathcal{S}_{(\overline{\Phi}\Phi)^2}^{(D17)}$	106
B.20	$\mathcal{S}_{(\overline{\Phi}\Phi)^2}^{(D18)}$	107
B.21	$\mathcal{S}_{(\overline{\Phi}\Phi)^2}^{(D19)}$	109
B.22	$\mathcal{S}_{(\overline{\Phi}\Phi)^2}^{(D20)}$	110
B.23	$\mathcal{S}_{(\overline{\Phi}\Phi)^2}^{(D21)}$	111
B.24	$\mathcal{S}_{(\overline{\Phi}\Phi)^2}^{(D22)}$	112
B.25	$\mathcal{S}_{(\overline{\Phi}\Phi)^2}^{(D23)}$	113
B.26	$\mathcal{S}_{(\overline{\Phi}\Phi)^2}^{(D24)}$	115
B.27	$\mathcal{S}_{(\overline{\Phi}\Phi)^2}^{(D25)}$	116
B.28	$\mathcal{S}_{(\overline{\Phi}\Phi)^2}^{(D26)}$	117
B.29	$\mathcal{S}_{(\overline{\Phi}\Phi)^2}^{(D27)}$	118
B.30	$\mathcal{S}_{(\overline{\Phi}\Phi)^2}^{(D28)}$	119
B.31	$\mathcal{S}_{(\overline{\Phi}\Phi)^2}^{(D29)}$	120
B.32	$\mathcal{S}_{(\overline{\Phi}\Phi)^2}^{(D30)}$	121
B.33	$\mathcal{S}_{(\overline{\Phi}\Phi)^2}^{(D31)}$	122
B.34	$\mathcal{S}_{(\overline{\Phi}\Phi)^2}^{(D32)}$	122
B.35	$\mathcal{S}_{(\overline{\Phi}\Phi)^2}^{(D33)}$	123

B.36	$\mathcal{S}_{(\bar{\Phi}\Phi)}^{(D34)2}$	124
B.37	$\mathcal{S}_{(\bar{\Phi}\Phi)}^{(D35)2}$	125
B.38	$\mathcal{S}_{(\bar{\Phi}\Phi)}^{(D36)2}$	126
B.39	$\mathcal{S}_{(\bar{\Phi}\Phi)}^{(D37)2}$	127
B.40	$\mathcal{S}_{(\bar{\Phi}\Phi)}^{(D38)2}$	128
B.41	$\mathcal{S}_{(\bar{\Phi}\Phi)}^{(D39)2}$	129
B.42	$\mathcal{S}_{(\bar{\Phi}\Phi)}^{(D40)2}$	130
B.43	$\mathcal{S}_{(\bar{\Phi}\Phi)}^{(D41)2}$	131

# List of Tables

4.1	Divergent contributions from each diagram presented in Figure 4.2, with the common factor $\frac{1}{8} \left( \frac{i}{32\pi^2\epsilon} \right) \int \frac{d^3p}{(2\pi)^3} d^2\theta \bar{\Phi}_i(p, \theta) D^2\Phi_i(-p, \theta)$ omitted. . . . .	48
4.2	Divergent contributions from each diagram in Figure 4.3, omitting the common factor $\frac{1}{8} \left( \frac{N}{192\pi^2\epsilon} \right) i g^4 \int \frac{d^3p}{(2\pi)^3} d^2\theta \Gamma^\alpha(p, \theta) \Gamma^\beta(-p, \theta)$ . . . . .	48
4.3	Divergent contributions arising from the diagrams presented in Figure 4.4; all contributions include the common factor $\frac{i}{32\pi^2\epsilon} (\delta_{im} \delta_{nj} + \delta_{jm} \delta_{ni}) \int d^2\theta \Phi_n \Phi_m \bar{\Phi}_i \bar{\Phi}_j$ , where all external momenta were set to zero. . . . .	51
B.1	Values of the diagrams in Figure B.3 with common factor $-\frac{1}{32\pi^2\epsilon} i \frac{\lambda^3}{8} \int_\theta \bar{\Phi}_i \Phi_m \Phi_n \bar{\Phi}_j$ . . . . .	88
B.2	Values of the diagrams in Figure B.4 with common factor $-\frac{a}{8(32\pi^2\epsilon)} i \lambda^2 g^2 \int_\theta \bar{\Phi}_i \Phi_m \Phi_n \bar{\Phi}_j$ . . . . .	89
B.3	Values of the diagrams in Figure B.5 with common factor $-\frac{a}{8(32\pi^2\epsilon)} i \lambda^2 g^2 \int_\theta \bar{\Phi}_i \Phi_m \Phi_n \bar{\Phi}_j$ . . . . .	89
B.4	Values of the diagrams in Figure B.7 with common factor $\frac{(a-b)}{16(32\pi^2\epsilon)} i \lambda^2 g^2 \int_\theta \bar{\Phi}_i \Phi_m \Phi_n \bar{\Phi}_j$ . . . . .	92
B.5	Values of the diagrams in Figure B.8 with common factor $\frac{(a-b)}{16(32\pi^2\epsilon)} i \lambda^2 g^2 \int_\theta \bar{\Phi}_i \Phi_m \Phi_n \bar{\Phi}_j$ . . . . .	92
B.6	Values of the diagrams in Figure B.10 with common factor $\frac{1}{32} \left( \frac{b^2-4ab+3a^2}{32\pi^2\epsilon} \right) i \lambda g^4 \int_\theta \bar{\Phi}_i \Phi_m \Phi_n \bar{\Phi}_j$ . . . . .	97
B.7	Values of the diagrams in Figure B.11 with common factor $\frac{1}{32} \left( \frac{(a-b)^2}{32\pi^2\epsilon} \right) i \lambda g^4 \int_\theta \bar{\Phi}_i \Phi_m \Phi_n \bar{\Phi}_j$ . . . . .	98
B.8	Values of the diagrams in Figure B.13 with common factor $\frac{8}{128} \left( \frac{ab-a^2}{32\pi^2\epsilon} \right) i \lambda g^4 \int_\theta \bar{\Phi}_i \Phi_m \Phi_n \bar{\Phi}_j$ . . . . .	100
B.9	Values of the diagrams in Figure B.17 with common factor $\frac{1}{32} \left( \frac{(a-b)^2}{32\pi^2\epsilon} \right) i \lambda g^4 \int_\theta \bar{\Phi}_i \Phi_m \Phi_n \bar{\Phi}_j$ . . . . .	104
B.10	Values of the diagrams in Figure B.19 with common factor $\frac{1}{16} \left( \frac{(a-b)^2}{32\pi^2\epsilon} \right) i \lambda g^4 \int_\theta \bar{\Phi}_i \Phi_m \Phi_n \bar{\Phi}_j$ . . . . .	105
B.11	Values of the diagrams in Figure B.20 with common factor $\frac{1}{16} \left( \frac{(a+b)^2}{32\pi^2\epsilon} \right) (1+N) i \lambda g^4 \int_\theta \bar{\Phi}_i \Phi_m \Phi_n \bar{\Phi}_j$ . . . . .	107

B.12	Values of the diagrams in Figure B.22 with common factor	
	$\frac{1}{32} \left( \frac{(a-b)^2}{32\pi^2\epsilon} \right) i \lambda g^4 \int_{\theta} \bar{\Phi}_i \Phi_m \Phi_n \bar{\Phi}_j \dots$	108
B.13	Values of the diagrams in Figure B.23 with common factor	
	$\frac{1}{32} \left( \frac{b^3-3a^3+7a^2b-5ab^2}{32\pi^2\epsilon} \right) i g^6 \int_{\theta} \bar{\Phi}_i \Phi_m \Phi_n \bar{\Phi}_j \dots$	111
B.14	Values of the diagrams in Figure B.24 with common factor	
	$\frac{1}{16} \left( \frac{a(a-b)^2}{32\pi^2\epsilon} \right) i g^6 \int_{\theta} \bar{\Phi}_i \Phi_m \Phi_n \bar{\Phi}_j \dots$	113
B.15	Values of the diagrams in Figure B.25 with common factor	
	$\frac{1}{16} \left( \frac{(a+b)^3}{32\pi^2\epsilon} \right) N i g^6 \int_{\theta} \bar{\Phi}_i \Phi_m \Phi_n \bar{\Phi}_j \dots$	113
B.16	Values of the diagrams in Figure B.26 with common factor	
	$\frac{1}{64} \left( \frac{(a-b)^3}{32\pi^2\epsilon} \right) i g^6 \int_{\theta} \bar{\Phi}_i \Phi_m \Phi_n \bar{\Phi}_j \dots$	114
B.17	Values of the diagrams in Figure B.27 with common factor	
	$-\frac{1}{16} \left( \frac{(a-b)(a^2+b^2)}{32\pi^2\epsilon} \right) i g^6 \int_{\theta} \bar{\Phi}_i \Phi_m \Phi_n \bar{\Phi}_j \dots$	115
B.18	Values of the diagrams in Figure B.28 with common factor	
	$\frac{1}{16} \left( \frac{a(a-b)^2}{32\pi^2\epsilon} \right) i g^6 \int_{\theta} \bar{\Phi}_i \Phi_m \Phi_n \bar{\Phi}_j \dots$	117
B.19	Values of the diagrams in Figure B.29 with common factor	
	$\frac{1}{32} \left( \frac{(a-b)^3}{32\pi^2\epsilon} \right) i g^6 \int_{\theta} \bar{\Phi}_i \Phi_m \Phi_n \bar{\Phi}_j \dots$	118
B.20	Values of the diagrams in Figure B.30 with common factor	
	$\frac{1}{4} \left( \frac{a^3+2ab^2}{32\pi^2\epsilon} \right) i g^6 \int_{\theta} \bar{\Phi}_i \Phi_m \Phi_n \bar{\Phi}_j \dots$	119
B.21	Values of the diagrams in Figure B.31 with common factor	
	$\frac{1}{32} \left( \frac{(a-b)(a+b)^2}{32\pi^2\epsilon} \right) i g^6 \int_{\theta} \bar{\Phi}_i \Phi_m \Phi_n \bar{\Phi}_j \dots$	120
B.22	Values of the diagrams in Figure B.32 with common factor	
	$\frac{1}{32} \left( \frac{b^3+5a^2b-4ab^2-2a^3}{32\pi^2\epsilon} \right) i g^6 \int_{\theta} \bar{\Phi}_i \Phi_m \Phi_n \bar{\Phi}_j \dots$	120
B.23	Values of the diagrams in Figure B.33 with common factor	
	$\frac{1}{16} \left( \frac{a^2b-a^3}{32\pi^2\epsilon} \right) i g^6 \int_{\theta} \bar{\Phi}_i \Phi_m \Phi_n \bar{\Phi}_j \dots$	121
B.24	Values of the diagrams in Figure B.35 with common factor	
	$\frac{1}{16} \left( \frac{a(a-b)^2}{32\pi^2\epsilon} \right) i g^6 \int_{\theta} \bar{\Phi}_i \Phi_m \Phi_n \bar{\Phi}_j \dots$	123
B.25	Values of the diagrams in Figure B.37 with common factor	
	$-\frac{1}{32} \left( \frac{a(a-b)^2}{32\pi^2\epsilon} \right) i g^6 \int_{\theta} \bar{\Phi}_i \Phi_m \Phi_n \bar{\Phi}_j \dots$	124
B.26	Values of the diagrams in Figure B.38 with common factor	
	$\frac{1}{64} \left( \frac{3a^3-7a^2b+5ab^2-b^3}{32\pi^2\epsilon} \right) i g^6 \int_{\theta} \bar{\Phi}_i \Phi_m \Phi_n \bar{\Phi}_j \dots$	126
B.27	Values of the diagrams in Figure B.40 with common factor	
	$\frac{1}{64} \left( \frac{(a-b)^3}{32\pi^2\epsilon} \right) i g^6 \int_{\theta} \bar{\Phi}_i \Phi_m \Phi_n \bar{\Phi}_j \dots$	128
B.28	Values of the diagrams in Figure B.42 with common factor	
	$\frac{1}{16} \left( \frac{a(a-b)^2}{32\pi^2\epsilon} \right) i g^6 \int_{\theta} \bar{\Phi}_i \Phi_m \Phi_n \bar{\Phi}_j \dots$	130
B.29	Values of the diagrams in Figure B.43 with common factor	
	$\frac{1}{64} \left( \frac{(b-a)^3}{32\pi^2\epsilon} \right) i g^6 \int_{\theta} \bar{\Phi}_i \Phi_m \Phi_n \bar{\Phi}_j \dots$	131
C.1	Integrals of diagram $\mathcal{S}_{\Gamma\Gamma}^{(a)}$ in the two-point vertex function of gauge super-field, with $I_d = \frac{1}{192\pi^2\epsilon}$ and $\mathcal{I}^{(a)} \equiv \int \frac{d^D k d^D q}{(2\pi)^{2D}} \frac{1}{(k+p)^2 (k+q)^2 q^2 k^2} \dots$	139

C.2 Integrals of diagram  $\mathcal{S}_{\text{rr}}^{(b)}$  in the two-point vertex function of gauge superfield, with  $I_d = \frac{1}{192\pi^2\epsilon}$  and  $\mathcal{I}^{(a)} \equiv \int \frac{d^D k d^D q}{(2\pi)^{2D}} \frac{1}{(k+p)^2 (k+q)^2 q^2 k^2} \dots$  139

C.3 Integrals of diagram  $\mathcal{S}_{\text{rr}}^{(c)}$  in the two-point vertex function of gauge superfield, with  $I_d = \frac{1}{192\pi^2\epsilon}$  and  $\mathcal{I}^{(b)} \equiv \int \frac{d^D k d^D q}{(2\pi)^{2D}} \frac{1}{(k+p)^2 (k+q)^2 q^2 (k^2)^2} \dots$  139

C.4 Integrals of diagram  $\mathcal{S}_{\text{rr}}^{(d)}$  in the two-point vertex function of gauge superfield, with  $I_d = \frac{1}{192\pi^2\epsilon}$  and  $\mathcal{I}^{(c)} \equiv \int \frac{d^D k d^D q}{(2\pi)^{2D}} \frac{1}{(k+p)^2 (q+p)^2 (k-q)^2 q^2 k^2} \dots$  140



# Chapter 1

## Introduction

In the 1970s supersymmetry was discovered in a series of articles on string theory. Ramond [2] proposed an equation for free fermions based on a dual structure theory for bosons, and in the same period Neveu and Schwarz [3, 4] proposed the inclusion of particles with quantum number of interacting pions in the Ramond model. Another example of a precursor paper to what would come to be called supersymmetry was the symmetry of a two-dimensional field theory discussed by Gervais and Sakita [5]. On the other hand, almost simultaneously, the Soviet researchers Gol'fand and Likhtman [6] extended the algebra of the Poincare group to a superalgebra and from this built a supersymmetric theory in four-dimensional space-time. These papers, although seminal, were generally ignored until much later. Regardless, Volkov and Akulov [7] discovered what today might be called spontaneous breaking of supersymmetry, but they used their formalism to identify the Goldstone fermion associated with supersymmetry breaking with the neutrino, one idea that was unsuccessful. In a widely known paper, Wess and Zumino [8] related the bosonic and fermionic states in a quantum field theory in four dimensions, describing the combination of states with different spin (integer and half-integer) as a supermultiplet. The Wess-Zumino model in  $(3 + 1)$  dimensions is described by the Lagrangian,

$$\begin{aligned} \mathcal{L} = & -\frac{1}{2}\partial_\mu A\partial^\mu A - \frac{1}{2}\partial_\mu B\partial^\mu B - \frac{1}{2}\bar{\psi}\gamma^\mu\partial_\mu\psi + \frac{1}{2}(F^2 + G^2) \\ & + m\left[FA + GB - \frac{1}{2}\bar{\psi}\psi\right] + g\left[F(A^2 + B^2) + 2GAB - \bar{\psi}(A + i\gamma_5 B)\psi\right], \end{aligned} \quad (1.1)$$

where  $A$  and  $B$  are the scalar and pseudo-scalar (bosonic) fields respectively,  $\psi$  is a Majorana (fermionic) field, and  $F$  and  $G$  are auxiliary scalar and pseudo-scalar fields, respectively. The auxiliary fields are non-dynamical, being determined by their algebraic equations of motion,

$$F = -mA - g(A^2 + B^2), \quad G = -mB - 2gAB. \quad (1.2)$$

The Lagrangian in Eq. (1.1) is invariant under the following infinitesimal supersym-

metric transformations:

$$\delta A = \bar{\xi}\psi, \quad (1.3a)$$

$$\delta B = -i\bar{\xi}\gamma_5\psi, \quad (1.3b)$$

$$\delta\psi = \partial_\mu (A + i\gamma_5 B) \gamma^\mu \xi + (F - i\gamma_5 G) \xi, \quad (1.3c)$$

$$\delta F = \bar{\xi}\gamma^\mu \partial_\mu \psi, \quad (1.3d)$$

$$\delta G = -i\bar{\xi}\gamma_5 \gamma^\mu \partial_\mu \psi, \quad (1.3e)$$

where  $\xi$  is a Grassmannian parameter that acts as an infinitesimal transformation parameter. The supersymmetry transformation is generated by a Grassmannian generator  $Q$  that satisfies

$$\{Q, Q\} = 2P,$$

with  $P$  being the generator of space-time translations.

In essence, the supersymmetry is an extension of the symmetry of space-time (Galilean, Poincare and conformal symmetries) by fermionic generators, which works as a theoretical method which naturally unifies fermions and bosons. Therefore, it is natural that supersymmetry is part of the most modern theoretical physics approaches to find an unified theory of all fundamental interactions. A fact that suggests why supersymmetry is important for the unification of interactions is as follows: the supersymmetry (SUSY) offers a possible way to prevent the no-go theorem of Coleman and Mandula [9], establishing that the Lie group of all symmetries of a given quantum field theory is composed of a direct product of the Poincare group with an internal symmetry group, or, in other words, the internal symmetry transformations always commute with the Poincare transformations. The hypotheses of this theorem are very general, consisting of the axioms of quantum field theory and the assumption that all the symmetries can be described in terms of Lie groups. One way around this theorem was found by Haag and Łopuszański [10], making the assumption that the infinitesimal generators of symmetry obey a superalgebra, or supersymmetric Lie algebra. The superalgebra is a generalization of the notion of Lie algebra, where some generators are fermionic, which means that some commutation rules are replaced by anti-commutators.

Besides this formal motivation, supersymmetry is also a possible solution to hierarchy problems in particle physics. In the Standard Model (SM) of particles, which is composed of the electroweak theory together with Quantum Chromodynamics (QCD), the electroweak scale ( $m_{EW} \sim 10^3 GeV$ ) acquires huge quantum corrections at the Planck scale ( $M_{Pl} \sim 10^{18} GeV$ ), creating a hierarchy problem between these scales, that must be accounted for with some extraordinary fine tuning. SUSY solves this problem, since in a supersymmetric version of the SM the hierarchy between these scales is attained in a natural manner, without fine tuning. Supersymmetry can also help us to understand

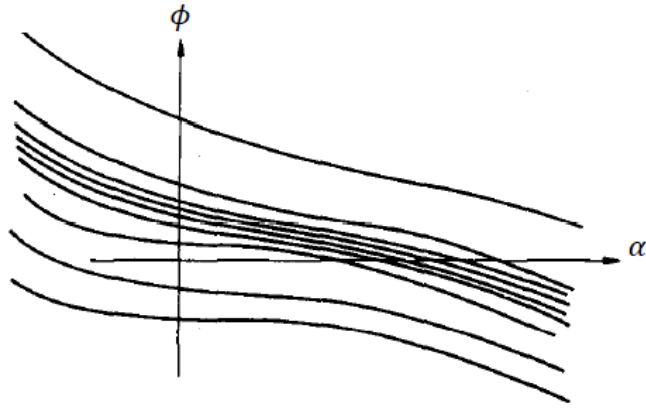


Figure 1.1: Characteristic of the partial differential equation, Eq. (1.4), where the effective potential is constant in the plane  $\phi - \alpha [1]$ .

Grand Unified Theories (GUTs) [11, 12, 13, 14, 15], where the gauge group of the SM is embedded in a larger group, but in general the gauge couplings do not unify properly at a given scale. However, in the supersymmetric version of the SM called Minimal Supersymmetric Standard Model (MSSM), the gauge couplings do unify nicely, provided the scale of supersymmetry breaking is about  $1TeV$ .

If supersymmetry has anything to do with nature, then it must be a local symmetry. When SUSY is imposed as a local symmetry, Einstein's theory of general relativity is included automatically, and the result is said to be a theory of supergravity [15, 16, 17]. In the context of string theory, which attempts to be a consistent quantum gravity theory, the supersymmetry is an essential ingredient, because all realistic models of string theory are built from superstrings [18, 19, 20].

After this mainly historical review of supersymmetry, we will discuss some concepts developed in Quantum Field Theory (QFT), since we will be interested in understanding how the effective superpotential work in the context of supersymmetric models.

In QFT the effective potential is used to calculate physically meaningful quantities, such as the masses for physical particles, and therefore its possible gauge dependence is an important question that has been studied in the literature for quite some time. Given that physical observables cannot depend on the choice of gauge-fixing parameter, it is essential to understand how to extract gauge independent information from perturbative calculations of the effective action in gauge theories [21, 22, 23]. A very robust formalism to address this question was developed by Nielsen, Kugo and Fukuda [1, 24], providing identities that encode the behavior of the effective action under changes of the gauge-fixing parameter. The so-called Nielsen identities imply that the gauge dependence of the effective action is compensated by a nonlocal field redefinition. For the effective potential,

for example, the Nielsen identity reads

$$\left( \alpha \frac{\partial}{\partial \alpha} + C(\phi; \alpha) \frac{\partial}{\partial \phi} \right) V_{\text{eff}}(\phi; \alpha) = 0, \quad (1.4)$$

where  $\alpha$  is the gauge-fixing parameter,  $\phi$  is the vacuum expectation value of the scalar field,  $V_{\text{eff}}$  is the quantum effective potential, and  $C(\phi; \alpha)$  is a functional that can be calculated in terms of Feynman diagrams. Equation (1.4) defines characteristic curves in the  $\phi$ – $\alpha$  plane, such as the ones represented in Figure 1.1, over which the effective potential is constant. This means that changes in the gauge-fixing parameter are compensated by changes in the vacuum expectation value. A consequence of this relation is that physical quantities defined at extrema of the effective potential become gauge independent [1, 25, 26]. We find in the literature many examples of the application of the Nielsen identities: in condensed matter physics, QCD, Quantum Electrodynamics (QED), the SM, and Aharony-Bergman-Jafferis-Maldacena (ABJM) theory, to name a few [27, 28, 29, 30, 31, 32, 33].

The Dynamical Symmetry Breaking (DSB) studied by Coleman and Weinberg [34] constitutes a very appealing scenario in QFT, where quantum corrections are entirely responsible for the appearance of nontrivial minima of the effective potential. When a given Lagrangian  $\hat{\mathcal{L}}$  depends on the fields  $\varphi$  and dimensionless coupling constants, and there is no mass parameter in the classical Lagrangian, we say that the model is scale invariant or conformally invariant. The essence of the Coleman-Weinberg mechanism is to naturally generate mass via quantum corrections, starting from a given conformal model. In the case of massless scalar electrodynamics, for example, the classical potential  $\frac{\lambda}{4!}\varphi_c^4$  receives quantum corrections and becomes

$$V_{\text{eff}} = \frac{\lambda}{4!}\phi^4 + \left( \frac{5}{1152\pi^2} \lambda^2 + \frac{3}{64\pi^2} e^2 \right) \phi^4 \left( \ln \left[ \frac{\phi^2}{M^2} \right] - \frac{25}{6} \right), \quad (1.5)$$

where  $\lambda$  is the scalar coupling constant,  $e$  is the gauge coupling constant and  $M$  is the renormalization scale. This corrected potential has a minimum at  $\phi \neq 0$ , signaling the presence of symmetry breaking in  $\lambda = \frac{33}{8\pi^2} e^4$ . In the case of a classically scale invariant model, all mass scales are generated by these quantum corrections and are fixed as functions of the symmetry breaking scale. This scenario would be particularly interesting in the SM, but earlier calculations pointed to a dead end [35]. The one loop effective potential for the SM reads [36]

$$V_{\text{eff}} = \frac{\lambda}{4!}\phi^4 + \phi^4 \left[ \frac{12\lambda^2 - 3g_t^3}{64\pi^2} + \frac{3(3g_2^4 + 2g_2^2 g'^2 + g'^4)}{1024\pi^2} \right] \left( \ln \left[ \frac{\phi^2}{M^2} \right] - \frac{25}{6} \right), \quad (1.6)$$

where  $g_2$ ,  $g'$  and  $g_t$  are the  $SU(2)$ , the  $U(1)$  and the top quark Yukawa coupling constants, respectively. The large value of  $g_t^2 \sim 1 \gg g_2^2, g'^2$  makes  $\lambda \sim \mathcal{O}(g_t^2) \sim 1$ , so that subsequent leading-logarithm terms such as  $\sim \lambda^3 \phi^4 \ln^2 \left[ \frac{\phi^2}{M^2} \right]$  would be too large to ignore, rendering

---

the one-loop approximation useless to study a possible DSB.

However, it has been shown that this conclusion, based on the effective potential calculated up to one loop level, could be modified substantially by using the Renormalization Group Equation (RGE) [37, 36, 38, 39, 40, 41, 42, 43, 44] to sum up infinite subsets of higher loop contributions to the effective potential. Indeed, in [36] the authors were the first to use the RGE to sum up all leading-logarithm terms, finding an improved version of effective potential. More than a quantitative correction over the one loop result, this improvement lead to a new scenario, where DSB was operational, in the sense that a consistent perturbative minimum of the effective potential were found at  $\phi \neq 0$ . More recent calculations were able to include corrections up to five loops in the effective potential [45, 46], bringing the prediction for the Higgs mass relatively close to the experimental value indicated by the Large Hadron Collider (LHC) (for other works regarding conformal symmetry in the SM, see for example [47, 48]).

Besides being a viable ingredient to the phenomenology of SM, DSB also occurs in other contexts, such as lower dimensional theories. Particularly interesting are models involving the Chern-Simons (CS) term in  $(2 + 1)$  dimensions [49, 50], which exhibit fascinating properties such as massive gauge fields, exotic statistics, and fractional spin, relevant qualities for the study of the quantum Hall effect [51]. Supersymmetric CS theories have also been studied for quite some time [52, 53, 54, 55, 56]. In the context of superstring field theory and supergravity, they have recently attracted much attention due to their relation to M2-branes [57]: the superconformal field theory describing multiple M2-branes is dual to the  $D = 11$  supergravity on  $AdS_4 \times S^7$ , which has  $\mathcal{N} = 8$  supersymmetry. However, the on-shell degrees of freedom of this theory are exhausted by bosons and physical fermions making its gauge sector to have no on-shell degrees of freedom. These requirements are satisfied by a CS-matter theory called Bagger–Lambert–Gustavsson (BLG) theory [58, 59, 60, 61, 62], which describes two M2-branes. Relaxing the requirement of manifest  $\mathcal{N} = 8$  supersymmetry, this approach can be generalized to  $\mathcal{N} = 6$  CS-matter theory with the gauge group  $U_k(N) \times U_{-k}(N)$  ( $k$  and  $-k$  are CS levels) [63, 64], known as ABJM theory. The quantization of such model was thoroughly studied in [65, 66, 67, 68, 69, 70, 71, 72, 73]. Also, detailed calculations of the effective superpotential within  $\mathcal{N} = 2$  superfield theories in  $(2 + 1)$  dimension have been reported in [74, 75].

The basic renormalization properties of CS models have been studied in [76, 52, 77, 78, 79, 80, 81]. We shall be particularly interested in models with scale invariance at the classical level, that is, with a pure CS field coupled to massless scalars and fermions with Yukawa quartic interactions, and scalar  $\varphi^6$  self-interactions. In these models, the one-loop corrections calculated using the dimensional reduction scheme [82] are rather trivial, since no singularities appear, and no DSB happens either; at the two loop level, however, one finds renormalizable divergences. Also, the two loops effective potential  $V_{\text{eff}}$  exhibits a

nontrivial minimum, signaling the appearance of DSB. Due to the nontrivial  $\beta$  and  $\gamma$  functions at two loops level, one may obtain an improvement in the calculation of  $V_{\text{eff}}$  by imposing the RGE,

$$\left[ \mu \frac{\partial}{\partial \mu} + \beta_{x_i} \frac{\partial}{\partial x_i} - \gamma_\varphi \phi \frac{\partial}{\partial \phi} \right] V_{\text{eff}}(\phi; \mu, x_i, L) = 0, \quad (1.7)$$

where  $x$  denotes collectively the coupling constants of the theory,  $\mu$  is the mass scale introduced by the regularization,  $\gamma_\varphi$  is the anomalous dimension of scalar field  $\varphi$ ,

$$L = \ln \left[ \frac{\phi^2}{\mu} \right], \quad (1.8)$$

and  $\phi$  is the vacuum expectation value of  $\varphi$ . This improved effective potential was calculated in [83], and it was shown to imply in considerable changes in the properties of DSB in this model, thus providing another context where the consideration of the RGE is essential to a proper analysis of the phase structure of the model.

The supersymmetric CS model in the superfield formalism was considered by Avdeev *et.al.* [52, 84], which computed the renormalization group functions in the Abelian and non-Abelian cases using a particular gauge-fixing parameter in the  $R_\xi$  gauge, assuming as true the gauge invariance. However, one must keep in mind that, on general grounds, renormalization group functions can depend on the choice of the gauge-fixing parameter [85, 86, 87, 88, 89]. More recently, a perturbative study of a supersymmetric CS model in  $(2+1)$  dimensions coupled to Higgs field were presented in [54], showing the spontaneous breaking of the gauge symmetry  $U(1)$  by the first quantum corrections of the effective action. The dynamical breaking of gauge symmetry in a scale invariant supersymmetric CS model in  $(2+1)$  dimensions was studied in [55], where the masses of the gauge and matter superfields are dynamically generated by quantum corrections, at two loops. A similar study in an abelian supersymmetric CS model in  $(2+1)$  dimensions with  $\mathcal{N} = 1, 2$  supersymmetry in the large  $N$  limit, with arbitrary gauge-fixing parameter, was presented in [56].

In this work, we will consider supersymmetric models containing the CS field with arbitrary gauge-fixing parameter in  $(2+1)$  dimension in the superfield formalism. Our objective is to verify whether the consideration of the RGE also induces considerable modifications in the scenario of DSB in these models. We also want to settle the question of a possible gauge dependence of the effective superpotential. In order to do that, we start with the study of the Nielsen identity in the context of supersymmetric CS theory, working in the superfield formalism. We find the general Becchi-Rouet-Stora-Tyutin (BRST) transformations associated to this theory, then use this result to obtain the Nielsen identity for the effective superpotential  $V_{\text{eff}}^S$ . The complete development of the Nielsen formalism in the superfield language is the first result of this thesis. We then calculate the renor-

---

malization group functions with arbitrary gauge-fixing parameter, and we show explicitly that these are gauge independent, a result we will show can provide information on the gauge independence of the effective potential. These results are reported in [90]

The direct application of the Nielsen identity for superfield models in  $(2 + 1)$  space-time dimensions is complicated by the difficulty in calculating the complete effective superpotential  $V_{\text{eff}}^S$  in the superfield language [91]. Because of that, we will focus on the part of the effective superpotential which does not depend on supercovariant derivatives of the background scalar superfield,  $K_{\text{eff}}$ . We will show that  $K_{\text{eff}}$  can be calculated from the renormalization group functions of the theory, together with the RGE. It follows then, from the gauge invariance of the renormalization group functions, that  $K_{\text{eff}}$  also does not depend on the gauge choice. We briefly discuss how to extend these results to calculate the complete  $V_{\text{eff}}^S$ .

Then, we calculate the effective superpotential of a supersymmetric CS theory coupled to  $N$  matter superfields, up to two loops. To this end, we use the RGE and the  $\beta$  and  $\gamma$  function calculated in [90]. With this result at hand, we discuss how we can reorganize the expansion of the effective superpotential in terms of Leading Logs (LL), Next-to-Leading Logs (NLL) contributions, and so on, in a way that allows us to calculate coefficients arising from higher orders corrections, thus improving the two loops evaluation of the effective superpotential. We are able to find an improved effective superpotential, which will be used to study DSB in our model. We show that, contrary to what happens in the non-supersymmetric case [83], here the RGE improvement in general leads only to a slight modification in the DSB scenario. Most of these results are presented in [92].

In this thesis, all calculations are done in the superfield language [93, 94], in which the supersymmetry is manifest in all stages of the calculations. The thesis is organized as follows: in Chapter 2, we present the conventions and some definitions about supersymmetry in  $(2 + 1)$  dimensions to be used here. In Chapter 3, we study the BRST transformations and the Nielsen identity for the effective superpotential  $V_{\text{eff}}^S(\alpha, \sigma_{\text{cl}})$ . In Chapter 4, we calculate the renormalization group functions,  $\beta$  and  $\gamma$  functions, up to two loops, with arbitrary gauge-fixing parameter. In Chapter 5, we calculate the effective superpotential  $K_{\text{eff}}(\alpha, \sigma_{\text{cl}})$  and its improvement using the RGE. From this result, we study the DSB properties. Chapter 6 presents our conclusions and perspectives for the future. In Appendix A we give an explicit example on how to calculate a one loop superdiagram. Appendix B contains all the details about the calculation of superdiagrams involved in the two loops evaluation of the renormalization group functions. Finally, in Appendix C we present the set of Feynman integrals used in this work.





# Chapter 2

## Supersymmetry in $(2 + 1)$ Dimensions

In this chapter we review the notations and conventions necessary to work with supersymmetry in  $(2 + 1)$  dimensions, providing an elementary introduction to the concept and the different types of superfields that will be used here and the D-algebra that is important in the evaluation of superdiagrams.

### 2.1 Conventions

We show the notations and conventions to be used in this thesis, following [93]. In the  $(2 + 1)$  dimensional space-time with metric  $\eta_{mn} = \text{diag}(-, +, +)$ , where  $m, n = 0, 1, 2$ , the Lorentz group is  $\text{SL}(2, \mathbb{R})$  instead of  $\text{SL}(2, \mathbb{C})$  as in a  $(3 + 1)$  dimensional space-time, and the fundamental representation of the Lorentz group operate on two real components spinors  $\psi^\alpha = (\psi^1, \psi^2)^1$ . All the spinor used here belong to a Grassmann algebra, meaning they anti-commute,

$$\psi^\alpha \psi^\beta = -\psi^\beta \psi^\alpha, \quad (2.1)$$

therefore  $\psi^\alpha \psi^\alpha = 0$  and, as  $\alpha = 1, 2$ , we have  $\psi^{\alpha_1} \psi^{\alpha_2} \dots \psi^{\alpha_n} = 0, \forall n > 2$ . Greek letters  $\alpha, \beta, \mu \dots$  will always be used to label the components of a spinor, and a vector will be represented by a bi-spinor,

$$x^{\alpha\beta} = x^m (\gamma_m)^{\alpha\beta}, \quad (2.2)$$

where the  $\gamma$  matrices are,

$$(\gamma^0)^\alpha_\beta = -i\sigma^2, \quad (\gamma^1)^\alpha_\beta = \sigma^1, \quad (\gamma^2)^\alpha_\beta = \sigma^3, \quad (2.3)$$

---

<sup>1</sup>Which happens to be a Majorana spinor.

$\sigma^i$  being the Pauli matrices, and

$$\{(\gamma_m)^\alpha_\beta, (\gamma_n)^\sigma_\alpha\} = 2\eta_{mn}\delta^\sigma_\beta. \quad (2.4)$$

The  $\gamma$  matrices with both lower indices  $(\gamma^m)_{\alpha\beta} = (-1, -\sigma^3, \sigma^1)$  are symmetrical, therefore all vectors are represented by symmetric bi-spinors.

The indices of the spinors are raised or lowered by contraction with the anti-symmetric symbol,

$$C_{\alpha\beta} = -C_{\beta\alpha} = -C^{\alpha\beta} = \begin{pmatrix} 0 & -i \\ i & 0 \end{pmatrix}, \quad (2.5)$$

with the property

$$C_{\alpha\beta}C^{\gamma\delta} \equiv \delta^\gamma_\alpha\delta^\delta_\beta - \delta^\gamma_\beta\delta^\delta_\alpha. \quad (2.6)$$

The contraction of the spinor indices is defined by,

$$\psi^\alpha = C^{\alpha\beta}\psi_\beta, \quad \psi_\alpha = \psi^\beta C_{\beta\alpha}, \quad (2.7)$$

and the following combination is a scalar,

$$\psi^2 = \frac{1}{2}\psi^\alpha\psi_\alpha. \quad (2.8)$$

Due to the anti-symmetry of  $C_{\alpha\beta}$ , the order in which the indices are contracted is important, and Eq. (2.7) define the order to be used in this work. It is important to say that, due to the fact that  $C_{\alpha\beta}$  is purely imaginary,  $\psi^\alpha$  is real, whereas  $\psi_\alpha$  is imaginary, and therefore  $\psi^2$  is Hermitian.

## 2.2 Supersymmetry and superfields

### 2.2.1 Superfields

The superspace is an extension of the usual space-time that include anti-commutative coordinates. Superfields are functions defined over this space, with supercoordinates  $z = (x^{\mu\nu}, \theta^\alpha) = (x, \theta)$ , which have the property  $z^\dagger = z$ . We define the following derivatives,

$$\partial_\mu\theta^\nu \equiv \delta_\mu^\nu, \quad (2.9)$$

$$\partial_{\mu\nu}x^{\sigma\tau} \equiv \frac{1}{2}(\delta_\mu^\sigma\delta_\nu^\tau + \delta_\nu^\sigma\delta_\mu^\tau), \quad (2.10)$$

where Eq. (2.9) define the derivation with respect to a spinor coordinate and (2.10) the derivation with respect to a space-time coordinate. The momentum operator satisfies

$$(i \partial_{\mu\nu})^\dagger = i \partial_{\mu\nu} . \quad (2.11)$$

The integration over an anti-commutative variable  $\theta_\alpha$  is defined by

$$\int d\theta_\alpha = \partial_\alpha , \quad (2.12a)$$

$$\int d\theta_\alpha \theta^\beta = \delta_\alpha^\beta , \quad (2.12b)$$

$$\int d^2\theta \theta^2 = -1 . \quad (2.12c)$$

We can define a function with the usual properties of the Dirac delta for Grassmannian variables; if we compare the previous equation with  $\int d^2\theta \delta^2(\theta) = 1$ , we can define

$$\delta^2(\theta) = -\theta^2 = -\frac{1}{2}\theta^\alpha\theta_\alpha , \quad (2.13)$$

or, in general

$$\delta^2(\theta - \theta') = \prod_{j=1}^2 (\theta_j - \theta'_j) . \quad (2.14)$$

Superfields are functions defined over the superspace, for example:  $\Phi(z)$ ,  $\Phi_\alpha(z)$ ... A superfield without a Lorentz index  $\Phi(z)$  is called a scalar superfield, a superfield with one index  $\Phi_\alpha(z)$  is a spinor superfield, and so on. Only these two types of superfields will be relevant for our study. The transformations of these functions under the action of the generators of the Poincare group,  $P_{\mu\nu}$  (translations) and  $M_{\alpha\beta}$  (rotations), are the usual from field theory, taking into account that the bosonic coordinates  $x^{\mu\nu}$  transform as a vector, and the fermionic coordinates  $\theta^\alpha$  transforms as spinors.

The superalgebra or graded Poincare algebra is obtained by the inclusion of a new supersymmetric spinor generator  $Q_\alpha$ , which satisfies the following supersymmetric algebra or superalgebra:

$$[P_{\mu\nu}, P_{\rho\sigma}] = 0 , \quad (2.15a)$$

$$\{Q_\mu, Q_\nu\} = 2P_{\mu\nu} , \quad (2.15b)$$

$$[Q_\mu, P_{\nu\rho}] = 0 . \quad (2.15c)$$

This superalgebra is realized as differential operators acting on superfields  $\Phi(z)$ ,  $\Phi_\alpha(z)$ , ...

as follows

$$Q_\mu = i (\partial_\mu - i\theta^\nu \partial_{\nu\mu}) , \quad (2.16a)$$

$$P_{\mu\nu} = i \partial_{\mu\nu} . \quad (2.16b)$$

The supersymmetric transformation acting on a scalar superfield is

$$\Phi(x^{\mu\nu}, \theta^\nu) = \exp \left( i \left[ \xi^{\lambda\rho} P_{\lambda\rho} + \eta^\lambda Q_\lambda \right] \right) \Phi(x'^{\mu\nu}, \theta'^\nu) , \quad (2.17)$$

where the infinitesimal generator  $\xi^{\lambda\rho} P_{\lambda\rho} + \eta^\lambda Q_\lambda$  generates the following transformation on the supercoordinates,

$$x'^{\mu\nu} = x^{\mu\nu} + \xi^{\mu\nu} - \frac{1}{2} i (\theta^\mu \eta^\nu - \theta^\nu \eta^\mu) , \quad (2.18a)$$

$$\theta'^\mu = \theta^\mu + \eta^\mu , \quad (2.18b)$$

with  $\xi^{\lambda\rho}$  and  $\eta^\lambda$  being real constants parameters,  $\xi$  a vector and  $\eta$  an anti-commutative spinor. These parameters generate a translation on space-time and Grassmann coordinates.

### 2.2.2 D-algebras

Equations (2.16a) - (2.18b) provide a representation of the superalgebra given in Eqs. (2.15a) - (2.15c). We notice that due to Eqs. (2.15a), (2.15b), (2.16a) and (2.16b), not only  $\Phi$  and functions of  $\Phi$ , but also their space-time derivatives  $\partial_{\mu\nu}\Phi$ , ..., lead to a supersymmetric representation. Nevertheless, this is not the case for the spinor derivative  $\partial_\mu$  because it does not commute with the supersymmetric spinor generator  $Q_\mu$ . This motivates the introduction of the supercovariant derivatives,

$$D_\alpha = \partial_\alpha - i \theta^\beta \partial_{\beta\alpha} , \quad (2.19)$$

that anticommute with the generators of the supersymmetry. We will provide a brief summary on the properties of these supercovariant derivatives, since they are essential in defining many relevant supersymmetric actions.

The supercovariant derivative anticommute with the supersymmetric generators,

$$\{D_\mu, Q_\nu\} = 0, \quad (2.20)$$

and commute with the translation generators,

$$[D_\mu, P_{\beta\gamma}] = 0. \quad (2.21)$$

Finally, from Eq. (2.19), we can show that,

$$\{D_\mu, D_\nu\} = 2i \partial_{\mu\nu} = 2P_{\mu\nu}. \quad (2.22)$$

Next, multiplying  $D_\alpha D_\beta (C^{\alpha\beta} C_{\mu\nu})$  and using Eq. (2.6), we find

$$[D_\mu, D_\nu] = -2 C_{\mu\nu} D^2. \quad (2.23)$$

We will now deduce some identities that will be of much help for the manipulation of supercovariant derivatives. We start by adding Eqs. (2.22) and (2.23) to obtain

$$D_\mu D_\nu = i \partial_{\mu\nu} - C_{\mu\nu} D^2. \quad (2.24)$$

If we multiply by  $D^\nu$  in the left hand side of Eq. (2.22), using Eq. (2.24) we get,

$$D^\nu D_\mu D_\nu = 0, \quad (2.25)$$

and using Eqs. (2.22) - (2.25) we obtain

$$(D^2)^2 = \square, \quad (2.26)$$

where it was used the identity

$$\partial^{\alpha\beta} \partial_{\nu\beta} = \delta_\nu^\alpha \square, \quad (2.27)$$

and  $\square = 1/2 \partial^{\alpha\beta} \partial_{\alpha\beta}$  is called the d'Alembertian. Finally, if we multiply  $D^\nu$  in the left hand side of Eq. (2.22), using Eq. (2.24) and (2.25), we have

$$D^2 D_\mu = -D_\mu D^2 = i \partial_{\mu\beta} D^\beta. \quad (2.28)$$

Supercovariant derivatives satisfy the Leibniz rules and can be integrated by parts when they appear inside of an integral  $d^3x d^2\theta$ , since they are composed of derivatives in  $x$  and  $\theta$ . Finally, from Eq. (2.13) and the  $(D^\alpha, D^2 \dots)$ , we can prove the following rules that will be used for the calculation of superdiagrams,

$$\begin{aligned} \delta^2 (\theta_n - \theta_m) \delta^2 (\theta_m - \theta_n) &= 0, \\ \delta^2 (\theta_n - \theta_m) D_\alpha \delta^2 (\theta_m - \theta_n) &= 0, \\ \delta^2 (\theta_n - \theta_m) D^2 \delta^2 (\theta_m - \theta_n) &= \delta^2 (\theta_n - \theta_m). \end{aligned} \quad (2.29)$$

### 2.2.3 Components by expansion and projections

Superfields can be expanded in a power series with respect to the Grassmannian coordinates  $\theta$ , and since these have the property that their square is zero, the power series have a finite number of terms. For example, we consider a scalar superfield written in terms of a power series in  $\theta$ ,

$$\Phi(x, \theta) = \varphi(x) + \theta^\alpha \Psi_\alpha(x) - \theta^2 E(x), \quad (2.30)$$

where  $\varphi(x)$ ,  $\Psi_\alpha(x)$  and  $E(x)$  are a scalar field, a Dirac field and an auxiliary scalar field, respectively. They are the component fields of the superfield  $\Phi(x^{\mu\nu}, \theta^\mu)$ , as obtained by power expansion in  $\theta$ . A more efficient way to them comes from observing that the components in Eq. (2.30) can also be defined by projection:

$$\varphi(x) = \Phi(x, \theta) |, \quad (2.31a)$$

$$\Psi_\alpha(x) = D_\alpha \Phi(x, \theta) |, \quad (2.31b)$$

$$E(x) = D^2 \Phi(x, \theta) |. \quad (2.31c)$$

where  $|$  means that after the differentiation, just the  $\theta$  independent part is kept. Finally, it is convenient to notice that

$$\int d^3x d^2\theta \Phi(x, \theta) = \int d^3x \partial^2 \Phi(x, \theta) = \int d^3x D^2 \Phi(x, \theta) |. \quad (2.32)$$

## 2.3 Scalar multiplet

We consider a complex scalar superfield

$$\Phi(x, \theta) = \frac{1}{\sqrt{2}} [\Phi_1(x, \theta) + i\Phi_2(x, \theta)], \quad (2.33a)$$

$$\bar{\Phi}(x, \theta) = \frac{1}{\sqrt{2}} [\Phi_1(x, \theta) - i\Phi_2(x, \theta)], \quad (2.33b)$$

where  $\Phi_1(x, \theta)$  and  $\Phi_2(x, \theta)$  are real scalar superfields. On dimensional grounds, we postulate the free Lagrangian

$$\mathcal{S}_K = -\frac{1}{2} \int d^3x d^2\theta (D^\alpha \bar{\Phi} D_\alpha \Phi), \quad (2.34)$$

which is invariant under constant phase transformations,

$$\Phi \rightarrow \Phi' = e^{i\mathcal{K}} \Phi, \quad (2.35a)$$

$$\bar{\Phi} \rightarrow \bar{\Phi}' = \bar{\Phi} e^{-i\mathcal{K}}. \quad (2.35b)$$

where  $\mathcal{K}$  is a constant scalar superfield. In the case of a gauge theory, we will have to consider  $\mathcal{K}$  as a general, non-constant scalar superfield  $\mathcal{K}(x, \theta)$ , i.e.,

$$\mathcal{K}(x, \theta) = \omega(x) + \theta^\mu \sigma_\mu(x) - \theta^2 \tau(x), \quad (2.36)$$

where  $\omega(x)$ ,  $\tau(x)$  and  $\sigma_\mu(x)$  can be defined by projection as

$$\omega(x) = \mathcal{K}|, \quad (2.37a)$$

$$\sigma_\alpha(x) = D_\alpha \mathcal{K}|, \quad (2.37b)$$

$$\tau(x) = D^2 \mathcal{K}|. \quad (2.37c)$$

From Eq. (2.15b), we can see that  $\theta$  has mass dimension  $-\frac{1}{2}$ . Therefore, we can say that  $[\Phi(x, \theta)] = M^{\frac{1}{2}}$  and then  $[\Psi_\mu(x)] = M^1$ . Thus  $[\varphi(x)] = M^{\frac{1}{2}}$  and  $[E(x)] = M^{\frac{3}{2}}$ , this imply that  $E(x)$  will not be a dynamical field, so it is called an auxiliary field; the same applies to the  $\tau$  field in (2.36). These dimensional considerations are also the motivation for the definition of the free massless kinetic action in Eq. (2.34).

The action in terms of components fields can be obtained by power expansion and integration in  $\theta$ . Notwithstanding, we prefer to use the alternative procedure, based in projection, Eq. (2.31c), which consist in integrating by parts Eq. (2.34),

$$\mathcal{S}_K = - \underbrace{\frac{1}{2} \int d^3x d^2\theta D^\alpha (\bar{\Phi} D_\alpha \Phi)}_{\text{surface integral}} + \frac{1}{2} \int d^3x d^2\theta \bar{\Phi} D^\alpha D_\alpha \Phi = \int d^3x d^2\theta \bar{\Phi} D^2 \Phi, \quad (2.38)$$

next, using the identity (2.32),

$$\mathcal{S}_K = \int d^3x D^2 (\bar{\Phi} D^2 \Phi) | = \int d^3x \left[ D^2 \bar{\Phi} D^2 \Phi + \bar{\Phi} (D^2)^2 \Phi + D^\alpha \bar{\Phi} D_\alpha D^2 \Phi \right] |,$$

and finally, using the projections defined in (2.31c), we obtain

$$\mathcal{S}_K = \frac{1}{2} \int d^3x \left[ \bar{E}(x) E(x) + \bar{\varphi}(x) \square \varphi(x) + \bar{\Psi}^\alpha(x) i \partial_\alpha^\beta \Psi_\beta(x) \right], \quad (2.39)$$

where the auxiliary fields  $E(x)$  and  $\bar{E}(x)$  can be eliminated by means of their equation of motion ( $E = 0$  and  $\bar{E} = 0$  in the massless case). Mass and interaction terms can be included in Eq. (2.34):

$$\mathcal{S}_I = \int d^2\theta d^3x \left( m \bar{\Phi} \Phi + V(\Phi, \bar{\Phi}) \right), \quad (2.40)$$

where  $V(\Phi, \bar{\Phi})$  is a function involving monomials of three or more powers of the scalar superfield.

## 2.4 Vector multiplet

A spinor gauge superfield  $\Gamma_\alpha(x, \theta)$  can be used to describe a massless gauge vector field, together with its fermionic superpartner.

If the supercovariant spinor derivative  $D_\alpha$  is substituted by the gauge supercovariant derivative  $\nabla_\alpha$ ,

$$D_\alpha \rightarrow \nabla_\alpha = D_\alpha - ig \Gamma_\alpha, \quad (2.41)$$

and using Eq. (2.34), we obtain

$$\mathcal{S} = -\frac{1}{2} \int d^3x d^2\theta \left( \overline{\nabla_\alpha \Phi} \nabla^\alpha \Phi \right), \quad (2.42)$$

where this Lagrangian describes the coupling of a spinor superfield with a complex scalar superfield, and it is invariant over local phase transformations of the form Eq. (2.35).

We can expand the gauge superfield  $\Gamma_\alpha(x, \theta)$  in power series of  $\theta$ ,

$$\Gamma_\alpha(x, \theta) = \chi_\alpha(x) - \theta_\alpha R(x) + i\theta^\beta A_{\beta\alpha}(x) - \theta^2 \Lambda_\alpha(x), \quad (2.43)$$

where

$$\chi_\alpha(x) = \Gamma_\alpha(x, \theta)|, \quad (2.44a)$$

$$R(x) = \frac{1}{2} D^\alpha \Gamma_\alpha(x, \theta)|, \quad (2.44b)$$

$$A_{\alpha\beta}(x) = -\frac{i}{2} [D_\alpha \Gamma_\beta(x, \theta) + D_\beta \Gamma_\alpha(x, \theta)]|, \quad (2.44c)$$

$$\Lambda_\alpha(x) = 2\rho_\alpha(x) + i\partial_{\beta\alpha}\chi^\beta(x) = D^2\Gamma_\alpha(x, \theta)|, \quad (2.44d)$$

where  $\chi_\alpha(x)$  and  $R(x)$  are auxiliary fields and  $A_{\alpha\beta}$  is the vector potential written as a bi-spinor. The mass dimensions of these fields can be shown to be  $[\Gamma_\alpha(x, \theta)] = M^{\frac{1}{2}}$ ,  $[\chi_\alpha(x)] = M^{\frac{1}{2}}$ ,  $[R(x)] = M^1$  and  $[A_{\alpha\beta}(x)] = M^1$ .

Introducing the so-called field strength superfield,

$$W_\alpha(x, \theta) \equiv \frac{1}{2} D^\beta D_\alpha \Gamma_\beta(x, \theta) = \frac{1}{2} D_\alpha D^\beta \Gamma_\beta(x, \theta) + D^2 \Gamma_\alpha(x, \theta), \quad (2.45)$$



we can check that  $W_\alpha$  is gauge invariant and satisfies a Bianchi identity<sup>2</sup>,

$$D^\alpha W_\alpha = 0. \quad (2.46)$$

We expand the superfield  $W_\alpha(x, \theta)$  in power series in  $\theta$ ,

$$W_\alpha(x, \theta) = \rho_\alpha(x) + \theta^\beta f_{\beta\alpha}(x) - \theta^2 \Theta(x), \quad (2.47)$$

where

$$\rho_\alpha(x) = W_\alpha(x, \theta)|, \quad (2.48a)$$

$$f_{\beta\alpha}(x) = \frac{1}{2} [\partial_{\beta\rho} A_\alpha^\rho + \partial_{\alpha\rho} A_\beta^\rho] = D_\beta W_\alpha(x, \theta)|, \quad (2.48b)$$

$$\Theta(x) = i\partial_\alpha^\beta \rho_\beta(x) = D^2 W_\alpha(x, \theta)|, \quad (2.48c)$$

with  $\rho_\alpha(x)$  being the photino field, and  $f_{\alpha\beta}(x)$  the bi-spinor Maxwell field strength. We can verify that  $[W_\alpha(x, \theta)] = M^{\frac{3}{2}}$ ,  $[\rho_\alpha(x)] = M^{\frac{3}{2}}$  and  $[f_{\alpha\beta}(x)] = M^2$  are their mass dimensions.

We can also define a Lagrangian involving the vector superfield. In this thesis, we will be interested in studying the Abelian supersymmetric CS action defined as

$$\mathcal{S}_{\text{CS}} = -\frac{1}{2} \int d^3x d^2\theta \Gamma^\alpha W_\alpha, \quad (2.49)$$

or, in terms of components fields,

$$\mathcal{S}_{\text{CS}} = - \int d^3x (A^{\alpha\beta}(x) f_{\alpha\beta}(x) - \rho^\alpha(x) \rho_\alpha(x)). \quad (2.50)$$

To rewrite Eq. (2.42), describing the interaction between the gauge and the scalar superfields, in terms of component fields, the more efficient way is to define the components of  $\Phi$  via projection,

$$\begin{aligned} \varphi(x) &= \Phi(x, \theta)| \\ \Psi_\alpha(x) &= \nabla_\alpha \Phi(x, \theta)| \\ F(x) &= \nabla^2 \Phi(x, \theta)|, \end{aligned} \quad (2.51)$$

---

<sup>2</sup>In usual Abelian gauge field theory, the field strength tensor  $F_{\mu\nu}$  satisfy the Bianchi identity because they are written in terms of the vector potential as  $F_{\mu\nu} = \partial_\mu A_\nu - \partial_\nu A_\mu$ ; these are identities that do not bring dynamic information. For gauge theories described by supercovariant derivatives, the Bianchi identities are just the Jacobi identities,

$$[\nabla_\alpha, [\nabla_\beta, \nabla_\gamma]] = 0,$$

where  $[\ ]$  is the graduated anti-symmetrization symbol, similar to the usual anti-symmetrization symbol but with an extra factor of  $(-1)$  for each interchange between fermion indices.

and use that

$$\int d^3x d^2\theta = \int d^3x D^2| = \int d^3x \nabla^2|. \quad (2.52)$$

Therefore, Eq. (2.42) can be written as follows,

$$\begin{aligned} \mathcal{S} &= \int d^3x \nabla^2 [\bar{\Phi} \nabla^2 \Phi] | \\ &= \int d^3x \left[ \nabla^2 \bar{\Phi} \nabla^2 \Phi + \frac{1}{2} \nabla^\alpha \bar{\Phi} \nabla_\alpha \nabla^2 \Phi + \frac{1}{2} C_{\alpha\beta} \nabla^\beta \bar{\Phi} C^{\alpha\rho} \nabla_\rho \nabla^2 \Phi + \bar{\Phi} (\nabla^2)^2 \Phi \right] | \\ &= \int d^3x \left[ \bar{F}(x) F(x) + i \bar{\Psi}^\alpha(x) (\partial_\alpha^\beta - ig A_\alpha^\beta(x)) \Psi_\beta(x) + i \bar{\Psi}^\alpha(x) \Lambda_\alpha(x) \varphi(x) \right. \\ &\quad \left. - i \bar{\varphi}(x) \Lambda^\alpha(x) \Psi_\alpha(x) + \bar{\varphi}(x) (\partial_{\alpha\beta} - ig A_{\alpha\beta}(x))^2 \varphi(x) \right], \end{aligned} \quad (2.53)$$

where we used the algebra of supercovariant derivatives and the property,

$$(\nabla^2)^2 = \square - i W^\alpha \nabla_\alpha. \quad (2.54)$$

# Chapter 3

## Nielsen Identity

In this chapter we study the Nielsen identity for the supersymmetric CS matter model in the superfield formalism. The Nielsen identity is essential to understand the gauge invariance of the symmetry breaking mechanism, and it is calculated by using the BRST invariance of the model. We will also discuss the technical difficulties in applying this identity to the complete effective superpotential  $V_{\text{eff}}^S$ .

### 3.1 Building a Lagrangian invariant under BRST transformations

We will investigate the BRST transformations in  $\mathcal{N} = 1$  supersymmetric CS-Higgs model in  $(2 + 1)$  dimensions

$$\mathcal{S}_{\text{CS}} = \int d^5z \mathcal{L}_{\text{CSM}}(z) = \int d^5z \left\{ -\frac{1}{2} \Gamma^\alpha W_\alpha - \frac{1}{2} \overline{\nabla}^\alpha \Phi \nabla_\alpha \Phi - m \overline{\Phi} \Phi + \frac{\lambda}{4} (\overline{\Phi} \Phi)^2 \right\}, \quad (3.1)$$

where  $m$  is a mass parameter. In this chapter, we work with a nonvanishing mass parameter  $m$  (Higgs model), instead of a theory with conformal invariance at the classical level (Coleman-Weinberg [34] model) for the sake of generality, and also because the  $m = 0$  case would be more complicated to analyze in the context of the Nielsen identities [95, 1, 25].

The action in Eq. (3.1) is invariant under the gauge transformations

$$\delta \Phi = ig \mathcal{K} \Phi, \quad \delta \overline{\Phi} = -ig \mathcal{K} \overline{\Phi}, \quad \delta \Gamma_\alpha = D_\alpha \mathcal{K}, \quad (3.2)$$

where  $\mathcal{K}$  is a scalar superfield. From the gauge transformations we can obtain a set of BRST transformations [96, 97, 98]. First we define  $\mathcal{K} = \varepsilon C$ , where  $C$  is a ghost superfields and  $\varepsilon$  is a constant infinitesimal parameter, both being Grassmannian (so that  $\varepsilon^2 = 0$ ).

Therefore, Eq. (3.2) can be rewritten as

$$\delta_B \Phi = i\varepsilon g C \Phi, \quad \delta_B \bar{\Phi} = -i\varepsilon g C \bar{\Phi}, \quad \delta_B \Gamma_\alpha = -\varepsilon D_\alpha C. \quad (3.3)$$

The BRST transformations for ghosts fields  $C$  and  $\bar{C}$  are defined as usual, i.e., in the Abelian model,

$$\delta_B C = 0, \quad (3.4)$$

since  $\delta_B C$  would depend on the structure constants of the gauge group, and

$$\delta_B \bar{C} = \epsilon B(z), \quad (3.5)$$

where  $B(z)$  is a scalar superfield, known as the Nakanishi-Lautrup auxiliary field in quantum field theory. Also, it is known that all BRST transformations are nilpotent, i.e.,

$$\delta_B^2 C = \delta_B^2 \bar{C} = \delta_B^2 \Gamma_\alpha = \delta_B^2 \Phi = \delta_B^2 \bar{\Phi} = 0, \quad (3.6)$$

which implies that  $\delta_B B(z) = 0$ .

We define the total Lagrangian as

$$\mathcal{L}_t = \mathcal{L}_{\text{CSM}} + \delta_B \mathcal{O}, \quad (3.7)$$

which is invariant by the BRST transformations, Eqs. (3.3) - (3.5). We choose the operator

$$\mathcal{O}(z) = \bar{C}(z) \left( -\alpha \frac{1}{4} B(z) + \frac{1}{2} F(z) \right),$$

where  $F(z)$  and  $\alpha$  are the gauge fixing function and a gauge-fixing parameter, respectively. Applying the BRST transformation on the operator  $\mathcal{O}(z)$ , we have

$$\delta_B \mathcal{O} = -\varepsilon \frac{\alpha}{4} B^2 + \varepsilon \frac{1}{2} B F + \frac{1}{2} \bar{C} (\delta_B F). \quad (3.8)$$

There is no derivatives acting on the scalar superfield  $B(z)$ , which appears only quadratically and linearly in  $\delta_B \mathcal{O}$ . Therefore, we can perform the path integral over it, the result being equivalent to solving the classical equation of motion with respect to  $B$ ,

$$\frac{\partial \delta_B \mathcal{O}}{\partial B} = -\varepsilon \frac{\alpha}{2} B + \varepsilon \frac{1}{2} F = 0, \quad (3.9)$$

and from this, we find

$$B = \alpha F, \quad (3.10)$$

which leads to

$$\mathcal{O}(z) = \frac{1}{4} \overline{C}(z) F(z), \quad (3.11)$$

and therefore

$$\delta_B \mathcal{O} = \varepsilon \frac{1}{4\alpha} F^2 + \frac{1}{2} \overline{C} (\delta_B F). \quad (3.12)$$

The total Lagrangian, Eq. (3.7) becomes

$$\mathcal{L}_t = \mathcal{L}_{\text{CSM}} + \frac{1}{4\alpha} F^2 + \frac{1}{2} \overline{C} \frac{\delta F}{\delta \mathcal{K}} C. \quad (3.13)$$

By rewriting the scalar superfields as in Eq. (2.33), we obtain

$$\begin{aligned} \mathcal{L}_t = & \frac{1}{2} \Gamma_\alpha W^\alpha + \frac{1}{2} (\Phi_1 D^2 \Phi_1 + \Phi_2 D^2 \Phi_2) - \frac{1}{2} m (\Phi_1^2 + \Phi_2^2) - \frac{1}{4} g^2 C^{\alpha\beta} \Gamma_\beta \Gamma_\alpha (\Phi_1^2 + \Phi_2^2) \\ & + \frac{1}{2} g [\Phi_1 D^\alpha \Phi_2 - \Phi_2 D^\alpha \Phi_1] \Gamma_\alpha - \frac{\lambda}{16} (\Phi_1^2 + \Phi_2^2)^2 + \frac{1}{4\alpha} F^2 + \frac{1}{2} \overline{C} \frac{\delta F}{\delta \mathcal{K}} C. \end{aligned} \quad (3.14)$$

We will use a supersymmetric generalization of the  $R_\xi$  defined in usual QFT [98, 55, 54], defined by the gauge fixing function

$$F = D^\alpha \Gamma_\alpha + d g \Phi_2, \quad (3.15)$$

where  $d$  is an arbitrary parameter that can be chosen to eliminate the mixing between the  $\Phi_2$  and  $\Gamma_\alpha$ , for example [55, 54]. We will leave the value of  $d$  unspecified, in which case in general one would need to consider mixed propagators to evaluate quantum corrections [1, 25, 26, 27]. With this choice of gauge fixing, we end up with the Lagrangian

$$\begin{aligned} \mathcal{L}_t = & \frac{1}{4} \Gamma_\alpha W^\alpha + \frac{1}{2} (\Phi_1 [D^2 - m] \Phi_1 + \Phi_2 [D^2 - m] \Phi_2) + \frac{1}{2} g [\Phi_1 D^\alpha \Phi_2 - \Phi_2 D^\alpha \Phi_1] \Gamma_\alpha \\ & - \frac{1}{4} g^2 C^{\alpha\beta} \Gamma_\beta \Gamma_\alpha (\Phi_1^2 + \Phi_2^2) + \frac{\lambda}{16} (\Phi_1^2 + \Phi_2^2)^2 + \frac{1}{4\alpha} F^2 + \overline{C} D^2 C + \frac{1}{2} d g^2 \Phi_1 \overline{C} C, \end{aligned} \quad (3.16)$$

which is invariant under the BRST transformations

$$\delta_B \Gamma_\alpha = -\varepsilon D_\alpha C, \quad (3.17a)$$

$$\delta_B \Phi_1 = -\varepsilon g \Phi_2 C, \quad (3.17b)$$

$$\delta_B \Phi_2 = \varepsilon g \Phi_1 C, \quad (3.17c)$$

$$\delta_B \overline{C} = -\varepsilon \frac{1}{\alpha} F, \quad (3.17d)$$

$$\delta_B C = 0. \quad (3.17e)$$

Finally, we add to the Lagrangian the source terms

$$\mathcal{L}_{\text{source}} = J^\mu \Gamma_\mu + \bar{\eta} C + \bar{C} \eta + f_1 \Phi_1 + f_2 \Phi_2 - g K_1 \Phi_2 C + g K_2 \Phi_1 C + h \mathcal{O}, \quad (3.18)$$

where  $J^\mu$ ,  $\bar{\eta}$ ,  $\eta$ ,  $f_1$ , and  $f_2$  are the sources for the basic superfields, while  $K_1$ ,  $K_2$  and  $h$  are sources for the composite operators.

## 3.2 Obtaining the Nielsen identity

Our starting point is the generating functional,

$$Z[J_a] = e^{iW[J_a]} = N \int \mathcal{D}\phi_a e^{iS}, \quad (3.19)$$

or

$$W[J_a] = -i \ln Z[J_a], \quad (3.20)$$

where  $J_a$  represent all the sources and  $\mathcal{D}\phi_a$  the path integral over all superfields present in the action

$$S = \int d^5 z (\mathcal{L}_t + \mathcal{L}_{\text{source}}). \quad (3.21)$$

Applying the BRST transformation  $\phi_a \rightarrow \phi_a + \delta_B \phi_a$  on  $W[J_a]$ , we observe that the generating functional does not change since the functional integration covers all the possible field configurations; in other words, the functional only depends on the sources and not on the superfields. Therefore, this BRST transformation leaves  $\mathcal{L}_t$  and the functional measure invariant. This implies that

$$0 = \frac{1}{Z[J_a]} N \int \mathcal{D}\phi_a e^{iS} \int d^5 z (\delta_B \mathcal{L}_{\text{source}}), \quad (3.22)$$

where

$$\delta_B \mathcal{L}_{\text{source}} = \varepsilon J^\mu D_\mu C - \varepsilon \frac{1}{\alpha} F \eta - \varepsilon g f_1 \Phi_2 C + \varepsilon g f_2 \Phi_1 C + h \varepsilon \tilde{\mathcal{O}}, \quad (3.23)$$

and

$$\delta_B \mathcal{O} = \varepsilon \tilde{\mathcal{O}}. \quad (3.24)$$

We also quote the useful relations, familiar from standard QFT,

$$\frac{\delta W[J_a]}{\delta J_\mu} = \frac{1}{Z[J_a]} N \int \mathcal{D}\phi_a e^{iS} \Gamma_\mu = \langle \Gamma_\mu \rangle, \quad (3.25)$$

as well as

$$\frac{\delta W[J_a]}{\delta \eta} = -\bar{C}, \quad \frac{\delta W[J_a]}{\delta \bar{\eta}} = C, \quad (3.26a)$$

$$\frac{\delta W[J_a]}{\delta f_1} = \Phi_1, \quad \frac{\delta W[J_a]}{\delta f_2} = \Phi_2, \quad (3.26b)$$

$$\frac{\delta W[J_a]}{\delta K_1} = -g \Phi_2 C, \quad \frac{\delta W[J_a]}{\delta K_2} = g \Phi_1 C. \quad (3.26c)$$

Substituting Eqs. (3.25) and (3.26) into Eq. (3.22), we obtain

$$\begin{aligned} & -\frac{1}{Z[J_a]} N \int \mathcal{D}\phi_a e^{iS} \int d^5 z (h \tilde{\mathcal{O}}) = \\ & \int d^5 z \left( J^\mu D_\mu \frac{\delta W[J_a]}{\delta \bar{\eta}} - \frac{1}{\alpha} \left( D^\mu \frac{\delta W[J_a]}{\delta J_\mu} + d g \frac{\delta W[J_a]}{\delta f_2} \right) \eta \right. \\ & \left. + f_1 \frac{\delta W[J_a]}{\delta K_1} + f_2 \frac{\delta W[J_a]}{\delta K_2} \right). \end{aligned} \quad (3.27)$$

The quantum effective action is defined by means of a partial Legendre transformation,

$$\Gamma[\phi_a] = W[J_a] - \int d^5 z \left( J^\mu \Gamma_\mu + \bar{\eta} C + \bar{C} \eta + f_1 \Phi_1 + f_2 \Phi_2 \right), \quad (3.28)$$

where the sources  $h$  and  $K_i$  are not Legendre transformed. Besides the usual relations,

$$\frac{\delta \Gamma[\phi_a]}{\delta \Gamma^\mu} = J^\mu, \quad \frac{\delta \Gamma[\phi_a]}{\delta \bar{C}} = \eta, \quad (3.29a)$$

$$\frac{\delta \Gamma[\phi_a]}{\delta C} = -\bar{\eta}, \quad \frac{\delta \Gamma[\phi_a]}{\delta \Phi_1} = -f_1, \quad (3.29b)$$

$$\frac{\delta \Gamma[\phi_a]}{\delta \Phi_2} = -f_2. \quad (3.29c)$$

one can also prove that [25],

$$\frac{\delta \Gamma[\phi_a]}{\delta h} = \frac{\delta W[J_a]}{\delta h}, \quad (3.30a)$$

$$\frac{\delta \Gamma[\phi_a]}{\delta K_1} = \frac{\delta W[J_a]}{\delta K_i}, \quad (3.30b)$$

$$\frac{\partial \Gamma[\phi_a]}{\partial \alpha} = \frac{\partial W[J_a]}{\partial \alpha}. \quad (3.30c)$$

Now, substituting Eqs. (3.25), (3.26), (3.29) and (3.30) into Eq. (3.27), we find

$$\begin{aligned} & -\frac{1}{Z[J_a]} N \int \mathcal{D}\phi_a e^{iS} \int d^5 z (h \tilde{\mathcal{O}}) = \int d^5 z \left( \frac{\delta \Gamma[\phi_a]}{\delta \Gamma^\mu} D_\mu C - \frac{1}{\alpha} F \frac{\delta \Gamma[\phi_a]}{\delta \bar{C}} \right. \\ & \left. - \frac{\delta \Gamma[\phi_a]}{\delta \Phi_1} \frac{\delta \Gamma[\phi_a]}{\delta K_1} - \frac{\delta \Gamma[\phi_a]}{\delta \Phi_2} \frac{\delta \Gamma[\phi_a]}{\delta K_2} \right), \end{aligned} \quad (3.31)$$

which after functional differentiation with respect to  $h$  and taking  $h = 0$ , reduces to

$$\begin{aligned}
 -\frac{1}{Z[J_a]} N \int \mathcal{D}\phi_a e^{iS} \tilde{\mathcal{O}} = \int d^5 z \left( \frac{\delta\Gamma[\mathcal{O}(z)]}{\delta\Gamma^\mu} D_\mu C - \frac{1}{\alpha} F \frac{\delta\Gamma[\mathcal{O}(z)]}{\delta\bar{C}} \right. \\
 \left. - \frac{\delta\Gamma[\mathcal{O}(z)]}{\delta\Phi_1} \frac{\delta\Gamma[J_a]}{\delta K_1} - \frac{\delta\Gamma[\phi_a]}{\delta\Phi_1} \frac{\delta\Gamma[\mathcal{O}(z)]}{\delta K_1} \right. \\
 \left. - \frac{\delta\Gamma[\mathcal{O}(z)]}{\delta\Phi_2} \frac{\delta\Gamma[\phi_a]}{\delta K_2} - \frac{\delta\Gamma[\phi_a]}{\delta\Phi_2} \frac{\delta\Gamma[\mathcal{O}(z)]}{\delta K_2} \right), \quad (3.32)
 \end{aligned}$$

where

$$\delta\Gamma[\mathcal{O}(z)] = \left. \frac{\delta\Gamma[\phi_a]}{\delta h} \right|_{h=0}. \quad (3.33)$$

The operator  $\tilde{\mathcal{O}}$  in Eq. (3.32), in the class of supersymmetric  $R_\xi$  gauge we are considering, is given explicitly by

$$\tilde{\mathcal{O}} = \frac{1}{4\alpha} F^2 + \bar{C} D^2 C + \frac{1}{2} d g^2 \Phi_1 \bar{C} C. \quad (3.34)$$

By using the equation of motion  $\delta S / \delta \bar{C} = 0$ , we have

$$-\bar{C} \eta = \bar{C} D^2 C + \frac{1}{2} d g^2 \Phi_1 \bar{C} C, \quad (3.35)$$

which, substituted into Eq. (3.34), leads to

$$\tilde{\mathcal{O}} = \frac{1}{4\alpha} F^2 - \bar{C} \eta. \quad (3.36)$$

By differentiation of Eq. (3.20) with respect to the gauge-fixing parameter  $\alpha$ , considering Eq. (3.16), one obtains that

$$\alpha \frac{\partial W[J_a]}{\partial \alpha} = -\frac{1}{Z[J_a]} N \int \mathcal{D}\phi_a \int d^5 z \frac{1}{4\alpha} F^2 e^{iS}, \quad (3.37)$$

and proceeding similarly, one can show that

$$\frac{\delta W[J_a]}{\delta \eta(r)} = -\frac{1}{Z[J_a]} N \int \mathcal{D}\phi_a e^{iS} \int d^5 z \delta^5(r-z) \bar{C}(z), \quad (3.38)$$

then, after functional integration,

$$-\int d^5 r \eta(r) \frac{\delta W[J_a]}{\delta \eta(r)} = \frac{1}{Z[J_a]} N \int \mathcal{D}\phi_a e^{iS} \int d^5 r \eta(r) \bar{C}(r). \quad (3.39)$$



Theses relations, Eqs. (3.37) and (3.39) together with Eqs. (3.36) in (3.32), lead us to

$$\begin{aligned} & \alpha \frac{\partial W[J_a]}{\partial \alpha} - \int d^5 z \eta(z) \frac{\delta W[J_a]}{\delta \eta(z)} \\ &= \int d^5 r \int d^5 z \left( \frac{\delta \Gamma[\mathcal{O}(z)]}{\delta \Gamma^\mu} D_\mu C - \frac{1}{\alpha} F \frac{\delta \Gamma[\mathcal{O}(z)]}{\delta \bar{C}} - \frac{\delta \Gamma[\mathcal{O}(z)]}{\delta \Phi_1} \frac{\delta \Gamma[\phi_a]}{\delta K_1} \right. \\ & \quad \left. - \frac{\delta \Gamma[\phi_a]}{\delta \Phi_1} \frac{\delta \Gamma[\mathcal{O}(z)]}{\delta K_1} - \frac{\delta \Gamma[\mathcal{O}(z)]}{\delta \Phi_2} \frac{\delta \Gamma[\phi_a]}{\delta K_2} - \frac{\delta \Gamma[\phi_a]}{\delta \Phi_2} \frac{\delta \Gamma[\mathcal{O}(z)]}{\delta K_2} \right), \end{aligned} \quad (3.40)$$

then, using Eqs. (3.30), (3.29) and (3.26) on the left hand side, we obtain

$$\begin{aligned} \alpha \frac{\partial \Gamma[\phi_a]}{\partial \alpha} + \int d^5 z \frac{\delta \Gamma[\phi_a]}{\delta \bar{C}} \bar{C} &= \int d^5 r \int d^5 z \left( \frac{\delta \Gamma[\mathcal{O}(z)]}{\delta \Gamma^\mu} D_\mu C - \frac{1}{\alpha} F \frac{\delta \Gamma[\mathcal{O}(z)]}{\delta \bar{C}} \right. \\ & \quad - \frac{\delta \Gamma[\mathcal{O}(z)]}{\delta \Phi_1} \frac{\delta \Gamma[\phi_a]}{\delta K_1} - \frac{\delta \Gamma[\phi_a]}{\delta \Phi_1} \frac{\delta \Gamma[\mathcal{O}(z)]}{\delta K_1} - \frac{\delta \Gamma[\mathcal{O}(z)]}{\delta \Phi_2} \frac{\delta \Gamma[\phi_a]}{\delta K_2} \\ & \quad \left. - \frac{\delta \Gamma[\phi_a]}{\delta \Phi_2} \frac{\delta \Gamma[\mathcal{O}(z)]}{\delta K_2} \right). \end{aligned} \quad (3.41)$$

This expression is the base for obtaining the Nielsen identity. By taking  $\bar{C} = C = \Phi_2 = \Gamma_\alpha = 0$ , and using the ghost number conservation in Eq. (3.41), we arrive to a simple result:

$$\alpha \frac{\partial \Gamma[\phi_a]}{\partial \alpha} = - \int d^5 r \int d^5 z \left( \frac{\delta \Gamma[\phi_a]}{\delta \Phi_1} \frac{\delta \Gamma[\mathcal{O}(z)]}{\delta K_1} + \frac{\delta \Gamma[\phi_a]}{\delta \Phi_2} \frac{\delta \Gamma[\mathcal{O}(z)]}{\delta K_2} \right). \quad (3.42)$$

The effective superpotential is obtained by setting  $\Phi_1 = \sigma_{\text{cl}}$  in the effective action,

$$\Gamma[\Phi_1, \alpha]|_{\Phi_1=\sigma_{\text{cl}}} = V_{\text{eff}}^S(\sigma_{\text{cl}}, \alpha), \quad (3.43)$$

where

$$\sigma_{\text{cl}} = \sigma_1 - \theta^2 \sigma_2, \quad (3.44)$$

is the space-time constant expectation value of the scalar superfield, called of *background superfield*, where  $\sigma_1$  is a scalar field and  $\sigma_2$  is an auxiliary scalar field. The superfield  $\sigma_{\text{cl}}$  has the same properties of a scalar superfield, except there is not a spinor component because its presence would imply a Lorentz violation. Consdering Eq. (3.42) for the case of the effective superpotential, we have

$$\left[ \alpha \frac{\partial}{\partial \alpha} + C^S(\sigma_{\text{cl}}, \alpha) \frac{\partial}{\partial \sigma_{\text{cl}}} \right] V_{\text{eff}}^S(\sigma_{\text{cl}}, \alpha) = 0, \quad (3.45)$$

where

$$C^S(\sigma_{\text{cl}}, \alpha) = \int d^5 z \frac{\delta^2 \Gamma[\mathcal{O}(z)]}{\delta K_1(0) \delta h(y)} \Big|_{K_1=h=0}, \quad (3.46)$$

which is the Nielsen identity for the effective superpotential.

### 3.3 On the gauge (in)dependence of the Effective Superpotential

The effective superpotential in three space-time dimensions has the general form

$$V_{\text{eff}}^S(\sigma_{\text{cl}}, \alpha) = - \int d^5 z \left[ K_{\text{eff}}(\sigma_{\text{cl}}, \alpha) + \mathcal{F}(D_\alpha \sigma_{\text{cl}}, D^\alpha \sigma_{\text{cl}}, D^2 \sigma_{\text{cl}}, \sigma_{\text{cl}}, \alpha) \right], \quad (3.47)$$

where we made explicit the potential gauge dependence. Here,  $K_{\text{eff}}$  is the part of the effective superpotential that does not depend on derivatives of the background classical superfield  $\sigma_{\text{cl}}$ , similar to the Kählerian effective superpotential defined in four-dimensional models [93, 94]. In the context of dynamical gauge symmetry breaking, it is enough to consider only the  $K_{\text{eff}}$  [55, 92, 54, 56, 69], while a study of a possible supersymmetry breaking would involve also the knowledge of  $\mathcal{F}$  [99, 100].

An explicit perturbative evaluation of  $V_{\text{eff}}^S$  starting from Eq. (3.16), within the superfield formalism, is in general quite difficult. The root of this problem is the fact that the classical superfield  $\sigma_{\text{cl}}$  is space-time constant, but its supercovariant derivatives do not vanish,  $D_\alpha \sigma_{\text{cl}} \neq 0$ . This, for example, complicates the calculation of the free superpropagators of the model, since powers of  $\sigma_{\text{cl}}$  appear in the quadratic operators that have to be inverted. This leads to the appearance of non-covariant superpropagators, as discussed in [101, 99]. In these works, the effective superpotential of SCSM and SQED models was calculated up to two loops. Part of these calculations was performed in an arbitrary gauge, but the final results for the effective superpotential were only obtained in the Landau gauge. Another perspective on the difficulties of evaluating the full effective superpotential in the superfield formalism, using heat kernel techniques, can be found in [91].

One possibility to obtain a full computation of  $V_{\text{eff}}^S$  within the superfield formalism would involve the use of the RGE. This approach will be used to calculate  $K_{\text{eff}}$  in the massless limit in Chapter 5. Essentially, one may consider  $K_{\text{eff}}$  as a function of the single mass scale  $\sigma_1$ , and this constrains the form of the radiative corrections to  $K_{\text{eff}}$ , so that a simple ansatz can be made, which inserted in the RGE provides a set of recursive equations from which the coefficients of the leading logs contributions to  $K_{\text{eff}}$  can be found. In principle this technique could be extended for the full effective superpotential  $V_{\text{eff}}^S$ , but in this case more complicated, multiscale techniques would be needed [102, 103], since  $V_{\text{eff}}^S$  should be considered as a function of both  $\sigma_1$  and  $\sigma_2$ .

The derivation of the effective superpotential from the renormalization group functions, by means of the RGE, may allow one to infer from the gauge (in)dependence of the beta functions and anomalous dimensions the gauge (in)dependence of the effective

superpotential itself. This is something we can do for the  $K_{\text{eff}}$ , since we establish in Chapter 5 that it can be calculated from the renormalization group functions without any ambiguity. Therefore, in the next Chapter, we will present a detailed computation of the beta and gamma functions in an arbitrary gauge, showing that the result is indeed gauge independent. By this reasoning, we can conclude that  $K_{\text{eff}}$  does not depend on the gauge parameter. That means, when only  $K_{\text{eff}}$  is considered, the Nielsen identity (3.45) is trivially satisfied with  $C^S = 0$ .

These results may suggest the gauge independence of the whole effective superpotential  $V_{\text{eff}}^S$ , but without explicitly establishing that the RGE fixes the form of  $\mathcal{F}$  in some approximation, without ambiguities, from the renormalization group functions (which we know are gauge independent), we believe this is still an open question. The discussion of [101, 99] is not conclusive in this regard, since most of the results are presented in a specific gauge, but some gauge dependence was found in the effective superpotential of the supersymmetric QED model. It is also not simple to use the Nielsen identity itself to investigate this point since, as discussed in [1, 25], the calculation of  $C^S$  in the massless case is complicated by the fact that different loop orders contribute to  $C^S$  in a given order in the coupling constants.



## Chapter 4

# Renormalization Group Functions

In this chapter we calculate the renormalization group functions of the model for arbitrary gauge-fixing parameter, finding them to be independent of the gauge choice. This result will be used to argue that  $K_{\text{eff}}$  also does not depend on the gauge-fixing parameter.

### 4.1 Gauge invariance of the renormalization group functions

In this section, we consider the  $m = 0$  version of Eq. (3.1), generalized to exhibit a global  $SU(N)$  symmetry,

$$\mathcal{S}_{\text{CS}} = \int d^5 z \left\{ -\frac{1}{2} \Gamma^\alpha W_\alpha - \frac{1}{2} \overline{\nabla^\alpha \Phi_a} \nabla_\alpha \Phi_a + \frac{\lambda}{4} (\overline{\Phi_a} \Phi_a)^2 \right\}, \quad (4.1)$$

where  $a = 1, \dots, N$ . We follow the basic conventions for three-dimensional supersymmetry described in Chapter 2.

In the quantization process, we introduce the gauge-fixing action,

$$\mathcal{S}_{\text{GF}} = \frac{1}{4\alpha} \int d^5 z (D^\alpha \Gamma_\alpha)^2, \quad (4.2)$$

but differently from what is done in the literature [52, 54, 56], we will perform all calculations with an arbitrary gauge-fixing parameter. Then, from Eqs. (4.1) and (4.2) we have

$$\begin{aligned} \mathcal{S} = \int d^5 z \left\{ \frac{1}{4} \Gamma_\alpha \left[ D^\beta D^\alpha + \frac{1}{\alpha} D^\alpha D^\beta \right] \Gamma_\beta - \frac{1}{2} g^2 C_{\beta\alpha} \Gamma^\alpha \Gamma^\beta \overline{\Phi_a} \Phi_a \right. \\ \left. + \overline{\Phi_a} D^2 \Phi_a - \frac{1}{2} i g \left[ \Gamma^\alpha \overline{\Phi_a} D_\alpha \Phi_a - (D^\alpha \overline{\Phi_a}) \Gamma_\alpha \Phi_a \right] + \frac{\lambda}{4} (\overline{\Phi_a} \Phi_a)^2 + \mathcal{L}_{ct} \right\}, \end{aligned} \quad (4.3)$$

where the counterterm Lagrangian is

$$\mathcal{L}_{ct} = \frac{1}{4} (Z_\Gamma - 1) \Gamma_\alpha D^\beta D^\alpha \Gamma_\beta + \frac{1}{2} (Z_\Phi - 1) \bar{\nabla}^\alpha \bar{\Phi}_a \nabla_\alpha \Phi_a + \frac{\lambda}{4} Z_\lambda (\bar{\Phi}_a \Phi_a)^2, \quad (4.4)$$

$Z_\Gamma$ ,  $Z_\Phi$ , and  $Z_\lambda$  being the counterterms needed to make the renormalized quantities finite in each order of perturbation theory.

## 4.2 Feynman rules

In this section we present the explicit derivation of the Feynman rules in our model.

### 4.2.1 Scalar propagator

From Eq. (4.3) we can find the scalar propagator. For this purpose, we start with the generating functional

$$Z[J_a, \bar{J}_a] = \int \mathcal{D}\Phi_a \mathcal{D}\bar{\Phi}_a \exp \left[ i \int d^5 z \left( \bar{\Phi}_a D^2 \Phi_a + \bar{J}_a \Phi_a + J_a \bar{\Phi}_a \right) \right], \quad (4.5)$$

where  $J_a$  and  $\bar{J}_a$  are the sources associated to the scalar superfields  $\Phi_a$  and  $\bar{\Phi}_a$ , respectively. Then, the two-point Green's function in position space is

$$\langle 0 | T \bar{\Phi}_i(z_1) \Phi_j(z_2) | 0 \rangle = \frac{1}{Z_0} \left( \frac{1}{i} \frac{\delta}{\delta J_i(z_1)} \right) \left( -\frac{1}{i} \frac{\delta}{\delta \bar{J}_j(z_2)} \right) Z[J_a, \bar{J}_a] \Big|_{J=\bar{J}=0}. \quad (4.6)$$

By shifting the superfields  $\Phi_a$  and  $\bar{\Phi}_a$

$$\Phi_a \rightarrow \Phi_a - \frac{J_a}{D^2}, \quad (4.7)$$

$$\bar{\Phi}_a \rightarrow \bar{\Phi}_a - \frac{\bar{J}_a}{D^2}, \quad (4.8)$$

and substituting in (4.5), we find

$$\begin{aligned} Z[J_a, \bar{J}_a] &= \int \mathcal{D}\Phi_a \mathcal{D}\bar{\Phi}_a \exp \left[ i \int d^5 z \left( \bar{\Phi}_a D^2 \Phi_a - \frac{\bar{J}_a J_a}{D^2} \right) \right] \\ &= Z_0 \int \mathcal{D}\Phi_a \mathcal{D}\bar{\Phi}_a \exp \left[ -i \int d^5 z d^5 z' \bar{J}_a(z) \triangle(z, z') J_a(z') \right], \end{aligned} \quad (4.9)$$

where

$$\triangle(z, z') = \frac{1}{D^2} \delta^5(z - z') = \frac{1}{D^2} \delta^3(x - x') \delta^2(\theta - \theta'). \quad (4.10)$$

If we substitute Eq. (4.9) into Eq. (4.6) and perform the functional derivations, we

obtain

$$\langle 0 | T \bar{\Phi}_i(z_1) \Phi_j(z_2) | 0 \rangle = -\frac{i \delta_{ij}}{D^2} \delta^5(z_1 - z_2) = -\frac{i \delta_{ij} D^2}{\square} \delta^5(z_1 - z_2). \quad (4.11)$$

We know that  $G_{ij}^{(2)}(z_1, z_2) = \langle 0 | T \bar{\Phi}_i(z_1) \Phi_j(z_2) | 0 \rangle$ , so by using the Fourier transformation in Eq. (4.11), we have

$$\begin{aligned} G_{ij}^{(2)}(k_1, k_2) &= \int d^3x_1 d^3x_2 \exp[-i(k_1x_1 + k_2x_2)] \tilde{G}^{(2)}(z_1, z_2) \\ &= (2\pi)^3 \delta^2(k_1 + k_2) \left( \frac{i \delta_{ij} D^2}{k_1} \delta^2(\theta_1 - \theta_2) \right), \end{aligned} \quad (4.12)$$

where it was used that  $(D^2)^2 = -k^2$  (see Eq. (2.26)). Therefore, we find the scalar propagator in momentum space to be

$$\overline{\Phi_i(k, \theta_1) \Phi_j(-k, \theta_2)} = \langle 0 | T \bar{\Phi}_i(k, \theta_1) \Phi_j(-k, \theta_2) | 0 \rangle = i \delta_{ij} \frac{D^2}{k^2} \delta^2(\theta_1 - \theta_2). \quad (4.13)$$

## 4.2.2 Gauge propagator

We calculate the gauge propagator associated to the gauge superfield  $\Gamma_\alpha$ , see Eq. (4.3). The relevant part of the generating functional is

$$Z[J^\alpha] = \int \mathcal{D}\Gamma \exp \left[ \frac{1}{2} i \int d^5z \left( \Gamma_\alpha P^{\alpha\beta} \Gamma_\beta + 2 J^\rho \Gamma_\rho \right) \right], \quad (4.14)$$

where  $J^\alpha$  is the source of the gauge superfield, which behaves as a spinor, and

$$P^{\alpha\beta} = \frac{1}{2} D^\beta D^\alpha + \frac{1}{2\alpha} D^\alpha D^\beta. \quad (4.15)$$

We shift the gauge superfield in Eq. (4.14) as,

$$\Gamma_\rho \rightarrow \Gamma_\rho + Q_{\rho\theta} J^\theta, \quad (4.16)$$

where

$$P^{\alpha\beta} Q_{\beta\theta} = \delta_\theta^\alpha, \quad (4.17)$$

$$Q_{\beta\theta} = b_1 D_\theta D_\beta + b_2 D_\beta D_\theta, \quad (4.18)$$

and  $b_1$  and  $b_2$  are constants to be determined. We obtain

$$\begin{aligned} Z[J_\alpha] &= \int \mathcal{D}\Gamma \exp \left[ \frac{1}{2} i \int d^5 z \left( \Gamma_\alpha P^{\alpha\beta} \Gamma_\beta + J_\alpha Q^{\alpha\beta} J_\beta \right) \right] \\ &= Z_0 \int \mathcal{D}\Gamma \exp \left[ \frac{1}{2} \int d^5 z d^5 z' J_\alpha(z) \Delta_{zz'}^{\alpha\beta} J_\beta(z') \right], \end{aligned} \quad (4.19)$$

where

$$\Delta_{zz'}^{\alpha\beta} = i Q^{\alpha\beta} \delta^5(z - z'). \quad (4.20)$$

The two-point Green's function in position space is

$$\begin{aligned} \overline{\Gamma_\beta(z_1) \Gamma_\theta(z_2)} &= \frac{1}{Z_0} \left( \frac{1}{i} \frac{\delta}{\delta J_\beta(z_1)} \right) \left( \frac{1}{i} \frac{\delta}{\delta J_\theta(z_2)} \right) Z[J_\alpha] \Big|_{J_\beta=J_\theta=0} \\ &= i Q_{\beta\theta} \delta^5(z_1 - z_2). \end{aligned} \quad (4.21)$$

To calculate the explicit form of  $Q$ , we use Eq.(4.17) and the identities shown in Section 2.2.2, which lead to

$$\begin{cases} \delta_\theta^\alpha &= -2 b_1 \delta_\theta^\alpha \square, \\ 0 &= b_1 D^2 D^\alpha D_\theta - b_2 D^2 D^\alpha D_\theta, \end{cases} \quad (4.22)$$

from this system of equations, we find

$$b_2 = \alpha b_1 = -\frac{\alpha}{2 \square}. \quad (4.23)$$

This fixes the form of the gauge superpropagator to be

$$\overline{\Gamma_\beta(z_1) \Gamma_\theta(z_2)} = -\frac{1}{2 \square} i (D_\theta D_\beta + \alpha D_\beta D_\theta) \delta^5(z_1 - z_2), \quad (4.24)$$

or, in momentum space,

$$\overline{\Gamma_\beta(k, \theta_1) \Gamma_\theta(-k, \theta_2)} = \frac{i}{2k^2} (D_\theta D_\beta + \alpha D_\beta D_\theta) \delta^2(\theta_1 - \theta_2), \quad (4.25)$$

where

$$D_\rho D_\beta + \alpha D_\beta D_\rho = b(\alpha) k_{\rho\beta} + a(\alpha) C_{\beta\alpha} D^2, \quad (4.26)$$

and

$$a(\alpha) = 1 - \alpha; \quad b(\alpha) \equiv 1 + \alpha. \quad (4.27)$$

### 4.2.3 Vertices

To compute the vertices of the theory, we use the Wick's theorem. For this purpose, we start with the correlation functions, which are vacuum expectation values of time-ordered



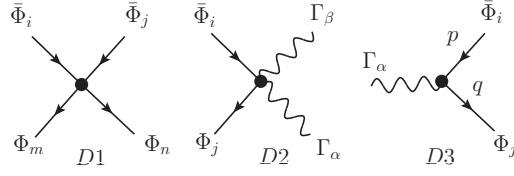


Figure 4.1: Elementary vertices of the model, where a continuous line is associated to a scalar superfield, and a wavy line to the gauge superfield.

products of a finite number of free superfield operators,

$$\langle 0 | T \Phi(z_1) \dots \Phi(z_n) | 0 \rangle . \quad (4.28)$$

As an example, for  $n = 2$  Eq. (4.28) represents the scalar propagator,

$$\overline{\Phi(z_1) \Phi(z_2)} = \langle 0 | T \Phi(z_1) \Phi(z_2) | 0 \rangle . \quad (4.29)$$

Wick's theorem allows us to turn any expression of the form Eq. (4.28) into a sum of products of Feynman propagators. This theorem can be extended to gauge superfields, taking care of the signals appearing due to the anti-commuting properties of spinors.

If we consider n-point Green's functions,

$$G^{(n)}(z_1, \dots, z_n) = \frac{\langle 0 | T \Phi(z_1) \Gamma_\alpha(z_2) \dots \Phi(z_n) \Gamma_\beta(z_m) \exp[i \int d^5 z \mathcal{L}_{\text{int}}(\Phi(z), \Gamma_\alpha(z))] | 0 \rangle}{\langle 0 | T \exp[i \int d^5 z \mathcal{L}_{\text{int}}(\Phi(z), \Gamma_\alpha(z))] | 0 \rangle} , \quad (4.30)$$

where the interaction Lagrangian  $\mathcal{L}_{\text{int}}$  is a function of the complex scalar  $\Phi_a(z)$  and the gauge superfields  $\Gamma_\alpha(z)$ , it is possible to find the elementary vertices of the theory. . We start with the four-point Green's function associated to the complex scalar superfield, for this we only need to use the numerator in (4.30) and (4.1),

$$\langle 0 | T \bar{\Phi}_i(x) \Phi_j(y) \bar{\Phi}_k(w) \Phi_l(s) \left[ 1 + i \left( \frac{\lambda}{4} \right) \int d^5 z \left( \bar{\Phi}_a(z) \Phi_a(z) \right)^2 + \dots \right] | 0 \rangle , \quad (4.31)$$

after expanding the exponential function. In our case, we need only the order  $\mathcal{O}(\lambda)$  term, then choosing only the second term of the previous equation, we have

$$i \left( \frac{\lambda}{4} \right) \langle 0 | T \bar{\Phi}_i(x) \Phi_j(y) \bar{\Phi}_k(w) \Phi_l(s) \int d^5 z \bar{\Phi}_a(z) \Phi_a(z) \bar{\Phi}_b(z) \Phi_b(z) | 0 \rangle$$

$$\begin{aligned}
 &= i \left( \frac{\lambda}{4} \right) \int d^5 z \left( \overbrace{\bar{\Phi}_i(x) \Phi_j(y) \bar{\Phi}_k(w) \Phi_l(s) \bar{\Phi}_a(z) \Phi_a(z) \bar{\Phi}_b(z) \Phi_b(z)}^{\text{Diagram 1}} \right. \\
 &\quad + \overbrace{\bar{\Phi}_i(x) \Phi_j(y) \bar{\Phi}_k(w) \Phi_l(s) \bar{\Phi}_a(z) \Phi_a(z) \bar{\Phi}_b(z) \Phi_b(z)}^{\text{Diagram 2}} \\
 &\quad + \overbrace{\bar{\Phi}_i(x) \Phi_j(y) \bar{\Phi}_k(w) \Phi_l(s) \bar{\Phi}_a(z) \Phi_a(z) \bar{\Phi}_b(z) \Phi_b(z)}^{\text{Diagram 3}} \\
 &\quad \left. + \overbrace{\bar{\Phi}_i(x) \Phi_j(y) \bar{\Phi}_k(w) \Phi_l(s) \bar{\Phi}_a(z) \Phi_a(z) \bar{\Phi}_b(z) \Phi_b(z)}^{\text{Diagram 4}} \right) \\
 &= i \frac{\lambda}{2} (\delta_{ij} \delta_{kl} + \delta_{il} \delta_{jk}) \int d^5 z \Delta(x, y, w, s - z)
 \end{aligned}$$

where  $\Delta$  was introduced to denote the product of the scalar propagators. From this expression, we can find in momentum space the four-point vertex function, at tree level,

$$i V_{(\bar{\Phi}_a \Phi_a)^2} = \frac{1}{2} i \lambda (\delta_{in} \delta_{jm} + \delta_{im} \delta_{jn}) \int d^2 \theta, \quad (4.32)$$

where the corresponding Feynman diagram is represented by  $D1$  in the Figure 4.1.

Next, we do the same procedure described before for the vertices involving the gauge superfield, taking care of the signs generated by the interchange of gauge superfields  $\Gamma_\alpha(z)$ . We start with

$$\langle 0 | T \Gamma^\beta(w) \Gamma_\beta(s) \bar{\Phi}_i(x) \Phi_j(y) \left[ 1 + i \left( -\frac{1}{2} g^2 \right) \int d^5 z \Gamma^\alpha(z) \Gamma_\alpha(z) \bar{\Phi}_a(z) \Phi_a(z) + \dots \right] | 0 \rangle,$$

considering the second term on the expansion, we have

$$\begin{aligned}
 &\langle 0 | T \Gamma_\sigma(w) \Gamma_\lambda(s) \bar{\Phi}_i(x) \Phi_j(y) \left[ -\frac{1}{2} i g^2 C^{\alpha\beta} \int d^5 z \Gamma_\beta(z) \Gamma_\alpha(z) \bar{\Phi}_a(z) \Phi_a(z) \right] | 0 \rangle \\
 &= -\frac{1}{2} i g^2 C^{\alpha\beta} \int d^5 z \left( \overbrace{\Gamma_\sigma(w) \Gamma_\lambda(s) \bar{\Phi}_i(x) \Phi_j(y) \Gamma_\beta(z) \Gamma_\alpha(z) \bar{\Phi}_a(z) \Phi_a(z)}^{\text{Diagram 1}} \right. \\
 &\quad \left. + \overbrace{\Gamma_\sigma(w) \Gamma_\lambda(s) \bar{\Phi}_i(x) \Phi_j(y) \Gamma_\beta(z) \Gamma_\alpha(z) \bar{\Phi}_a(z) \Phi_a(z)}^{\text{Diagram 2}} \right) \\
 &= i g^2 C^{\alpha\beta} \int d^5 z \overbrace{\Gamma_\sigma(w) \Gamma_\beta(z)}^{\text{Diagram 3}} \overbrace{\Gamma_\lambda(s) \Gamma_\alpha(z)}^{\text{Diagram 4}} \overbrace{\bar{\Phi}_i(x) \Phi_a(z)}^{\text{Diagram 5}} \overbrace{\bar{\Phi}_a(z) \Phi_j(y)}^{\text{Diagram 6}}
 \end{aligned}$$

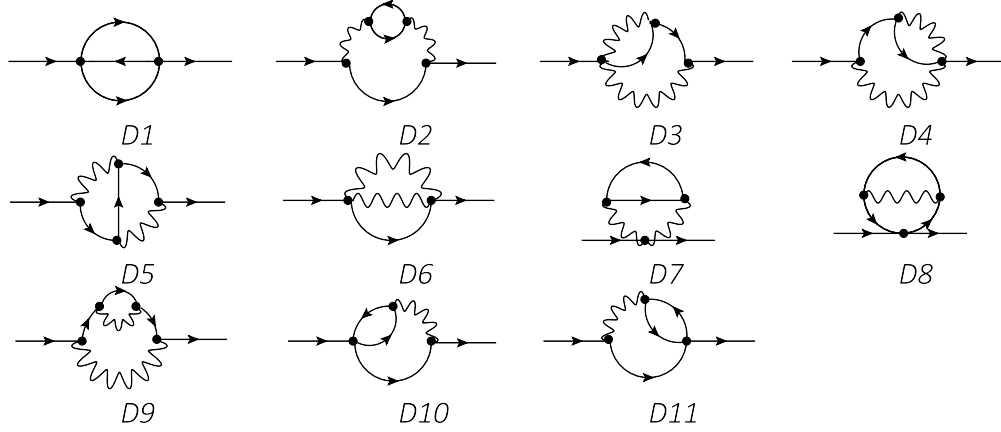


Figure 4.2: Two loops diagrams contributing to the two-point vertex function of the scalar superfield  $\Phi$ .

and in momentum space, we find

$$i V_{\bar{\Phi}_a \Phi_a \Gamma_\beta \Gamma_\alpha} = i g^2 \delta_{ij} C^{\alpha\beta} \int d^2\theta, \quad (4.33)$$

where the corresponding Feynman diagram is represented by  $D2$  in the Figure 4.1.

Finally, performing a similar procedure, we find

$$i V_{\bar{\Phi}_a D^\alpha \bar{\Phi}_a \Gamma_\alpha - \Phi_a D^\alpha \Phi_a \Gamma_\alpha} = \frac{1}{2} \delta_{ij} g [D^\alpha(p) - D^\alpha(-q)] \int d^2\theta, \quad (4.34)$$

where the corresponding Feynman diagram is represented by  $D3$  in the Figure 4.1.

### 4.3 Quantum corrections up two loops and renormalization group functions

In this section we calculate the quantum corrections to the vertices functions, up two loops, using the Feynman rules derived in Section 4.2; from these, we will be able to calculate the  $\beta$  and  $\gamma$  functions of our model. The use of regularization by dimensional reduction means that all super-algebra manipulations are performed in three dimensions, while momentum integrals are calculated at dimension  $d = 3 - \epsilon$  (see in Appendix C more details about the momentum integrals). The use of this regularization scheme guarantees that the one loop corrections are finite, see an example given in Appendix A. The full set of topologies was generated using the MATHEMATICA package FEYNARTS [104], and the final diagrams drawn with the program JAXODRAW [105]. All algebraic manipulations of supercovariant derivatives needed for the evaluation of the superdiagrams were performed with the MATHEMATICA package SUSYMATH [106]; explicit details about our calculations are presented in the Appendix B.

$D1$	$-2(N+1)\lambda^2$	$D2$	$(a+b)^2 g^4 N$	$D3$	$a(b-3a)g^4$
$D4$	$a(b-3a)g^4$	$D5$	$\frac{1}{2}(3a^2 + 2ab + 3b^2)g^4$	$D6$	$2a^2 g^4$
$D7$	$0$	$D8$	$0$	$D9$	$4a^2 g^4$
$D10$	$0$	$D11$	$0$		

Table 4.1: Divergent contributions from each diagram presented in Figure 4.2, with the common factor  $\frac{1}{8} \left( \frac{i}{32\pi^2\epsilon} \right) \int \frac{d^3 p}{(2\pi)^3} d^2\theta \bar{\Phi}_i(p, \theta) D^2\Phi_i(-p, \theta)$  omitted.

$D1$	$(3a-b)(-p_{\alpha\beta} + 3C_{\beta\alpha}D^2)$	$D2$	$(3a-b)(-p_{\alpha\beta} + 3C_{\beta\alpha}D^2)$
$D3$	$(3a-b)(-p_{\alpha\beta} + 3C_{\beta\alpha}D^2)$	$D4$	$(3a-b)(-p_{\alpha\beta} + 3C_{\beta\alpha}D^2)$
$D5$	$-2a(p_{\alpha\beta} + 3C_{\beta\alpha}D^2)$	$D6$	$-2a(p_{\alpha\beta} + 3C_{\beta\alpha}D^2)$
$D7$	$4((4a+b)p_{\alpha\beta} + 3bC_{\beta\alpha}D^2)$	$D8$	$-bp_{\alpha\beta} - 3aC_{\beta\alpha}D^2$
$D9$	$0$		

Table 4.2: Divergent contributions from each diagram in Figure 4.3, omitting the common factor  $\frac{1}{8} \left( \frac{N}{192\pi^2\epsilon} \right) i g^4 \int \frac{d^3 p}{(2\pi)^3} d^2\theta \Gamma^\alpha(p, \theta) \Gamma^\beta(-p, \theta)$ .

We start by calculating the two-point vertex functions associated to scalar and gauge superfields. For the case of the scalar superfield, the diagrams that contribute are represented in Figure 4.2, and the corresponding results are given in Table 4.1. For the divergent part of the two points vertex function, at two loops, we can write

$$S_{\Phi}^{2\text{loop}} = \frac{i}{4(32\pi^2\epsilon)} \left[ -(N+1)\lambda^2 + \frac{1}{4}(a+b)^2(2N+3)g^4 \right] \times \int \frac{d^3 p}{(2\pi)^3} d^2\theta \bar{\Phi}_i(p, \theta) D^2\Phi_i(-p, \theta), \quad (4.35)$$

which fixes the value of the  $Z_\Phi$  counterterm as

$$Z_\Phi = 1 + \frac{1}{4(32\pi^2\epsilon)} \left[ -(N+1)\lambda^2 + \frac{1}{4}(a+b)^2(2N+3)g^4 \right]. \quad (4.36)$$

Remembering Eq. (4.27), we see that  $Z_\Phi$  depends only on the gauge independent combination  $(a+b)$ . From this, it follows that the anomalous dimension  $\gamma_\Phi$  will also be gauge independent.

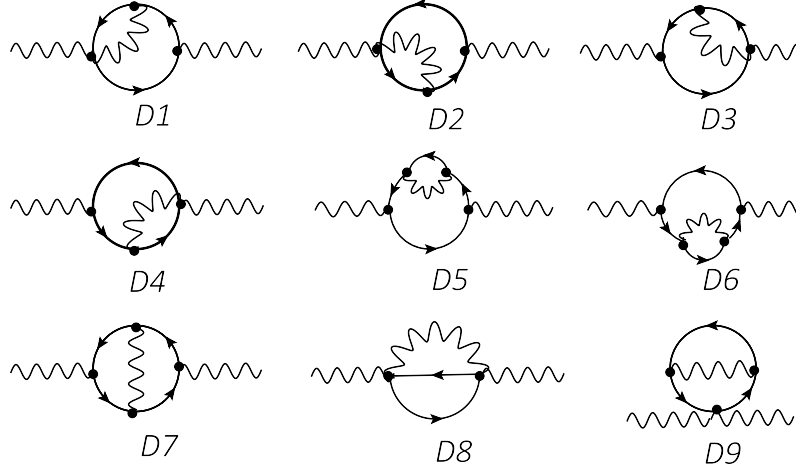


Figure 4.3: Two loop diagrams contributing to the two-point vertex function of the gauge superfield  $\Gamma_\alpha$ .

The next step is to compute, up to two loops, the two-point vertex function of the gauge superfield  $\Gamma_\alpha$ . The diagrams involved are represented in Figure 4.3, with the respective divergent contributions given in Table 4.2. We verify that, for any gauge choice, all divergences cancel among the diagrams in Figure 4.3. As a consequence, no infinite wave function renormalization of the CS superfield is needed, and therefore the anomalous dimension  $\gamma_\Gamma$  vanishes ( $Z_\Gamma = 1$ ). This result extends for the massless matter case according to the Coleman-Hill theorem [107], which states that in Abelian theories there are no quantum correction above one loop order for the CS coefficient, and it was also verified in previous calculations performed in a specific gauge [52], as well as in the non-supersymmetric version of the model [81].

Finally, the evaluation of the divergent part of the four-point vertex function associated to the scalar superfield  $\Phi$ , up to two loops, involve all diagrams in Figure 4.4, these 41 topologies being equivalent to 371 diagrams, see Appendix B.3 for more details. The results are given in Table 4.3, and lead to

$$S_{(\bar{\Phi}\Phi)^2}^{2\text{loop}} = \frac{i}{4(32\pi^2\epsilon)} \left[ -(5N + 11)\lambda^3 - (a + b)\lambda^2 g^2 + \frac{1}{4}(a + b)^2(2N + 5)\lambda g^4 + \frac{1}{4}(a + b)^3(N + 3)g^6 \right] (\delta_{im}\delta_{nj} + \delta_{jm}\delta_{ni}) \int_\theta \bar{\Phi}_i \Phi_m \Phi_n \bar{\Phi}_j, \quad (4.37)$$

where  $\int_\theta \bar{\Phi}_i \Phi_m \Phi_n \bar{\Phi}_j \equiv \int d^2\theta \bar{\Phi}_i(0, \theta) \Phi_m(0, \theta) \Phi_n(0, \theta) \bar{\Phi}_j(0, \theta)$ . Here we chose all the external momenta to be zero, since the tree-level vertex factor

$$\frac{1}{2} i \lambda Z_\lambda (\delta_{in}\delta_{jm} + \delta_{im}\delta_{jn}) \int d^2\theta, \quad (4.38)$$

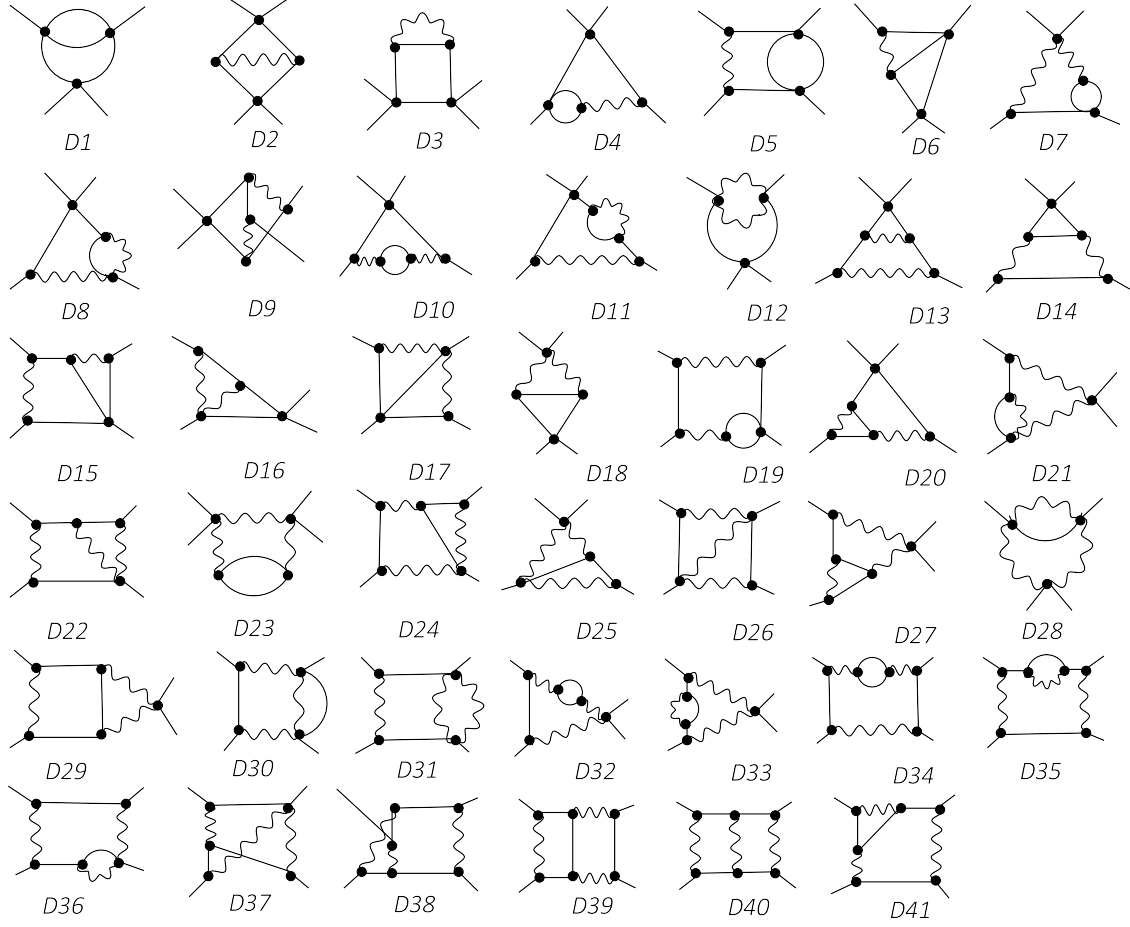


Figure 4.4: The complete set of two loops diagrams contributing to the four-point scalar vertex function.

does not depend of external momenta. Equation (4.37) implies that

$$\begin{aligned}
 Z_\lambda = 1 + \frac{1}{2(32\pi^2\epsilon)} & \left[ (5N + 11)\lambda^2 + (a + b)\lambda g^2 - \frac{1}{4}(a + b)^2(2N + 5)g^4 \right. \\
 & \left. - \frac{1}{4}(a + b)^3(N + 3)\lambda^{-1}g^6 \right]. \quad (4.39)
 \end{aligned}$$

Again, this results turns out to be independent of the gauge parameter  $\alpha$ .

In conclusion, all the renormalization constants  $Z_\Phi$ ,  $Z_\Gamma$ , and  $Z_\lambda$  are independent of the choice of the gauge-fixing parameter. This same property will follow for the renormalization group functions that are calculated from these constants.

$D1$	$-\frac{1}{4}(5N+11)\lambda^3$	$D2$	$\frac{1}{4}a(N+2)\lambda^2g^2$
$D3$	$-\frac{1}{4}a(N+4)\lambda^2g^2$	$D4$	0
$D5$	$-\frac{1}{4}(a-b)\lambda^2g^2$	$D6$	$\frac{1}{2}(a-b)\lambda^2g^2$
$D7$	0	$D8$	$\frac{1}{8}(b^2-4ab+3a^2)\lambda g^4$
$D9$	$\frac{3}{16}(a-b)^2\lambda g^4$	$D10$	0
$D11$	$\frac{1}{4}a(b-a)\lambda g^4$	$D12$	$\frac{3}{4}a^2\lambda g^4$
$D13$	$\frac{3}{4}a(a-b)\lambda g^4$	$D14$	0
$D15$	$-\frac{1}{4}(a-b)^2\lambda g^4$	$D16$	$\frac{3}{2}a(b-a)\lambda g^4$
$D16$	$\frac{3}{2}a(b-a)\lambda g^4$	$D17$	$\frac{1}{4}(a-b)^2\lambda g^4$
$D18$	$\frac{1}{8}(a+b)^2(1+N)\lambda g^4$	$D19$	0
$D20$	$-\frac{1}{8}(a-b)^2\lambda g^4$	$D21$	$-\frac{1}{8}(a-b)^2(3a-b)g^6$
$D22$	0	$D23$	$\frac{1}{16}(a+b)^3Ng^6$
$D24$	$\frac{1}{8}(a-b)^3g^6$	$D25$	$-\frac{1}{4}(a-b)(a^2+b^2)g^6$
$D26$	0	$D27$	$\frac{1}{8}(a-b)^3g^6$
$D28$	$\frac{1}{2}a(a^2+2b^2)g^6$	$D29$	$\frac{1}{16}(a-b)(a+b)^2g^6$
$D30$	$-\frac{1}{8}(a-b)^2(2a-b)g^6$	$D31$	0
$D32$	0	$D33$	$\frac{1}{8}a(a-b)^2g^6$
$D34$	0	$D35$	$-\frac{1}{8}a(a-b)^2g^6$
$D36$	$\frac{1}{8}(a-b)^2(3a-b)g^6$	$D37$	0
$D38$	0	$D39$	0
$D40$	0	$D41$	$\frac{1}{8}(b-a)^3g^6$

Table 4.3: Divergent contributions arising from the diagrams presented in Figure 4.4; all contributions include the common factor  $\frac{i}{32\pi^2\epsilon}(\delta_{im}\delta_{nj} + \delta_{jm}\delta_{ni})\int d^2\theta\Phi_n\Phi_m\bar{\Phi}_i\bar{\Phi}_j$ , where all external momenta were set to zero.

The explicit relations between bare and renormalized quantities are given by

$$\Gamma_0^\alpha = Z_\Gamma^{\frac{1}{2}} \Gamma^\alpha, \quad (4.40a)$$

$$\Phi_0 = Z_\Phi^{\frac{1}{2}} \Phi, \quad (4.40b)$$

$$\alpha_0 = \alpha Z_\Gamma, \quad (4.40c)$$

$$g_0 = \mu^{\frac{\epsilon}{2}} g Z_\Gamma^{-\frac{1}{2}}, \quad (4.40d)$$

$$\lambda_0 = \mu^\epsilon \lambda Z_\lambda Z_\Phi^{-2}, \quad (4.40e)$$

where  $\mu$  is a mass parameter introduced to keep  $g$  and  $\lambda$  dimensionless. From these, we can obtain the renormalization group functions,

$$\gamma_\Gamma \equiv -\frac{\mu}{\Gamma} \frac{d}{d\mu} \Gamma = \frac{\mu}{2 Z_\Gamma} \frac{d}{d\mu} Z_\Gamma, \quad (4.41a)$$

$$\gamma_\Phi = \frac{\mu}{2 Z_\Phi} \frac{d}{d\mu} Z_\Phi, \quad (4.41b)$$

$$\beta_\alpha \equiv \mu \frac{d}{d\mu} \alpha = -2 \alpha \gamma_\Gamma, \quad (4.41c)$$

$$\beta_g = g \gamma_\Gamma, \quad (4.41d)$$

$$\beta_\lambda = \epsilon \frac{\lambda^2}{Z_\lambda} \frac{\partial}{\partial \lambda} Z_\lambda + \frac{\epsilon \lambda g}{2 Z_\lambda} \frac{\partial}{\partial g} Z_\lambda + 4 \lambda \gamma_\Phi. \quad (4.41e)$$

From these definitions, and the results presented in this section, we obtain

$$\beta_\lambda = c_3 \lambda^3 + c_2 \lambda^2 y + c_1 \lambda y^2 + c_0 y^3, \quad (4.42a)$$

$$\gamma_\Gamma = \beta_\alpha = \beta_y = 0, \quad (4.42b)$$

$$\gamma_\Phi = d_2 \lambda^2 + d_0 y^2, \quad (4.42c)$$

in terms of the redefined gauge coupling constant

$$y = g^2. \quad (4.43)$$

The numerical coefficients present in (4.42) are given by

$$\begin{aligned} c_3 &= \frac{3}{16\pi^2} (N+2), & c_2 &= \frac{1}{16\pi^2}, \\ c_1 &= -\frac{2}{16\pi^2} (N+2), & c_0 &= -\frac{1}{16\pi^2} (N+3), \\ d_2 &= \frac{1}{4(32\pi^2)} (N+1), & d_1 &= 0, \\ d_0 &= -\frac{1}{4(32\pi^2)} (2N+3). \end{aligned} \quad (4.44)$$



As stated before, these functions are independent of the gauge-fixing parameter. Our results agree with [52], except for overall numerical factors that arise due to their different definition of the scale  $\mu$ . We stress however that in [52] the authors considered as true the gauge independence of these functions, a fact that has been checked explicitly here.



# Chapter 5

## Renormalization Group Improvement and Dynamical Symmetry Breaking

In this chapter, we investigate the consequences of the RGE in the determination of the effective superpotential and the study of DSB in an  $\mathcal{N} = 1$  supersymmetric theory including an Abelian CS superfield coupled to  $N$  scalar superfields in  $(2+1)$  dimensional space-time, as already detailed in Chapter 4. The classical Lagrangian presents scale invariance, which is broken by radiative corrections to the effective superpotential. We calculate the effective superpotential up to two-loops by using the RGE and the beta functions and anomalous dimensions found in Chapter 4. We then show how the RGE can be used to improve this calculation, by summing up properly defined series of leading logs (LL), next-to-leading logs (NLL) contributions, and so on... We conclude that even if the RGE improvement procedure can indeed be applied in a supersymmetric model, the effects of the consideration of the RGE are not so dramatic as it happens in the non-supersymmetric case.

### 5.1 Calculation of the Effective Superpotential

The main object we shall be interested in studying is the three-dimensional effective superpotential. To define this object, we consider a shift in the  $N$ -th component of  $\Phi_a$  in (4.1),

$$\Phi_N = \Phi_N^q + \sigma_{\text{cl}}, \quad (5.1)$$

where  $\sigma_{\text{cl}}$  was defined in Eq. (3.44). On general grounds, the effective superpotential is given by Eq. (3.47).

As discussed in [55], the knowledge of  $K_{\text{eff}}(\sigma_{\text{cl}}, \alpha)$  in (3.47) is sufficient for investigating

the dynamical breaking of gauge symmetry, and consequential generation of a mass scale in the model. For simplicity, in this work we will restrict ourselves to the calculation of  $K_{\text{eff}}(\sigma_{\text{cl}}, \alpha)$ , which we shall call the *effective superpotential* from now on. The effective superpotential  $K_{\text{eff}}(\sigma_{\text{cl}}, \alpha)$  is particularly well suited for the approach that we develop in this thesis, since we will be able to calculate it by using a simple ansatz, from the renormalization group functions for the model (4.1) found in Chapter 4, see Eq. (4.42).

We shall use for  $K_{\text{eff}}(\sigma_{\text{cl}}, \alpha)$  the ansatz

$$K_{\text{eff}}(\sigma_{\text{cl}}, \alpha) = -\frac{1}{4}\sigma_{\text{cl}}^4 S_{\text{eff}}(\sigma_{\text{cl}}, \lambda, y, \alpha, L) , \quad (5.2)$$

where

$$S_{\text{eff}}(\sigma_{\text{cl}}, \lambda, y, \alpha, L) = A(y, \lambda, \alpha) + B(y, \lambda, \alpha)L + C(y, \lambda, \alpha)L^2 + \dots , \quad (5.3)$$

and  $A, B, C, \dots$  are defined as series in powers of the coupling constants  $y$  and  $\lambda$ , and  $L = \ln \left[ \frac{\sigma_{\text{cl}}^2}{\mu} \right]$ . We will eventually adopt a shorthand notation where  $x$  denotes any of the two couplings in our model, so that a monomial like  $y^n \lambda^m$  will be written as  $x^{m+n}$ . These ansatz comes from the conformal invariance at tree-level, leading to the fact that we can have only one type of logarithm appearing in the quantum corrections. Comparison with the tree level action (4.1) shows us that

$$A(y, \lambda, \alpha) = \lambda + \mathcal{O}(x^2) . \quad (5.4)$$

The value of  $A(y, \lambda, \alpha)$  will be fixed by the CW normalization of the effective superpotential,

$$\frac{1}{4!} \frac{d^4 K_{\text{eff}}(\sigma_{\text{cl}}, \alpha)}{d^4 \sigma_{\text{cl}}} = \frac{\lambda}{4} , \quad (5.5)$$

so only the  $L$  dependent pieces of  $K_{\text{eff}}(\sigma_{\text{cl}}, \alpha)$ , involving  $B, C, \dots$ , have to be calculated.

The other ingredient that we will need is the RGE. To obtain this equation, we start with

$$K_{\text{eff}}^0(\sigma_{\text{cl}}; \lambda_0, y_0, \alpha_0) = K_{\text{eff}}(\sigma_{\text{cl}}; \lambda(\mu), y(\mu), \alpha(\mu), \mu, L) , \quad (5.6)$$

where  $K^0$  is independent of the arbitrary mass scale  $\mu$ . By deriving Eq. (5.6) with respect to  $\mu$

$$0 = \left( \mu \frac{\partial}{\partial \mu} + \mu \frac{d\lambda}{d\mu} \frac{\partial}{\partial \lambda} + \mu \frac{dy}{d\mu} \frac{\partial}{\partial y} + \mu \frac{d\alpha}{d\mu} \frac{\partial}{\partial \alpha} + \mu \frac{d\sigma_{\text{cl}}}{d\mu} \frac{\partial}{\partial \sigma_{\text{cl}}} \right) K_{\text{eff}}(\sigma_{\text{cl}}; \lambda, y, \alpha, \mu, L) , \quad (5.7)$$

and using Eqs. (4.41), we have

$$0 = \left( \mu \frac{\partial}{\partial \mu} + \beta_\lambda \frac{\partial}{\partial \lambda} + \beta_y \frac{\partial}{\partial y} + \beta_\alpha \frac{\partial}{\partial \alpha} - \gamma_\Phi \sigma_{\text{cl}} \frac{\partial}{\partial \sigma_{\text{cl}}} \right) K_{\text{eff}}(\sigma_{\text{cl}}; \lambda, y, \alpha, \mu, L), \quad (5.8)$$

where we used that  $\gamma_\Phi = \gamma_\sigma$ <sup>1</sup>. From Eq. (1.8), it follows that

$$\partial_L = \frac{1}{2} \sigma_{\text{cl}} \partial_{\sigma_{\text{cl}}} = -\mu \partial_\mu, \quad (5.11)$$

where it was used the notation  $\partial_t \equiv \frac{\partial}{\partial t}$ , and inserting (5.2) into (5.8), we obtain an alternative form for the RGE,

$$[-(1 + 2\gamma_\Phi) \partial_L + \beta_\lambda \partial_\lambda - 4\gamma_\Phi] S_{\text{eff}}(\sigma_{\text{cl}}, \lambda, y, \alpha, L) = 0, \quad (5.12)$$

where it was used that  $\beta_y = \beta_\alpha = 0$ , which will be used hereafter.

Inserting the ansatz (5.3) in (5.12), and separating the resulting expression by orders of  $L$ , we obtain a series of equations, of which we quote the first two:

$$-(1 + 2\gamma_\Phi) B(y, \lambda, \alpha) + \beta_\lambda \partial_\lambda A(y, \lambda, \alpha) - 4\gamma_\Phi A(y, \lambda, \alpha) = 0, \quad (5.13)$$

and

$$-2(1 + 2\gamma_\Phi) C(y, \lambda, \alpha) + \beta_\lambda \partial_\lambda B(y, \lambda, \alpha) - 4\gamma_\Phi B(y, \lambda, \alpha) = 0. \quad (5.14)$$

We now consider that all functions appearing in these equations are defined as series in powers of the couplings  $x$ , writing Eq. (5.13) as

$$\begin{aligned} & - \left( B^{(1)} + B^{(2)} + B^{(3)} + \dots \right) - 2 \left( \gamma_\Phi^{(2)} + \gamma_\Phi^{(3)} + \dots \right) \left( B^{(1)} + B^{(2)} + B^{(3)} + \dots \right) \\ & + \left( \beta_\lambda^{(3)} + \beta_\lambda^{(4)} + \dots \right) \left( \partial_\lambda A^{(1)} + \partial_\lambda A^{(2)} + \dots \right) - 4 \left( \gamma_\Phi^{(2)} + \gamma_\Phi^{(3)} + \dots \right) \left( A^{(1)} + A^{(2)} + \dots \right) = 0, \end{aligned} \quad (5.15)$$

where the numbers in the superscripts denote the power of  $x$  of each term. Since all terms of the previous equation start at order  $x^3$ , except the first, we conclude that  $B^{(1)} = B^{(2)} = 0$ , and obtain the relation

$$B^{(3)} = \beta_\lambda^{(3)} - 4\lambda \gamma_\Phi^{(2)}, \quad (5.16)$$

---

<sup>1</sup>Using the shift of superfield  $\Phi$ , Eq. (5.1) and (4.40) we have

$$\Phi_0 = Z_\Phi^{\frac{1}{2}} (\Phi + \sigma_{\text{cl}}), \quad (5.9)$$

by deriving with respect to  $\mu$ , we find

$$\Phi \left( \gamma_\Phi - \frac{1}{2} \frac{\mu}{Z_\Phi} \frac{d}{d\mu} Z_\Phi \right) + \sigma_{\text{cl}} \left( \gamma_\sigma - \frac{1}{2} \frac{\mu}{Z_\Phi} \frac{d}{d\mu} Z_\Phi \right) = 0, \quad (5.10)$$

and from this, we have  $\gamma_\Phi = \gamma_\sigma$ .

after using Eq. (5.4). This last equation fixes the coefficients of  $B^{(3)}$  in terms of the (known) coefficients of  $\beta_\lambda^{(3)}$  and  $\gamma_\Phi^{(2)}$ , in the following form,

$$B^{(3)} = b_3 \lambda^3 + b_2 \lambda^2 y + b_1 \lambda y^2 + b_0 y^3, \quad (5.17)$$

where

$$b_0 = c_0, \quad (5.18a)$$

$$b_1 = c_1 - 4 d_0, \quad (5.18b)$$

$$b_2 = c_2, \quad (5.18c)$$

$$b_3 = c_3 - 4 d_2. \quad (5.18d)$$

We observe that  $B^{(3)}$  do not depend on the gauge-fixing parameter, inheriting this property from the renormalization group function. The corrections of order  $x^3 L$ , which we have found for  $S_{\text{eff}}$ , could be obtained by a two-loop calculation of the effective superpotential, using supergraph methods. Since we do not know the coefficients of  $\beta_\lambda^{(4)}$  and  $\gamma_\Phi^{(3)}$ , which would appear from higher loop corrections, we cannot use Eq. (5.13) to calculate further coefficients of  $B$  or  $A$ .

Now looking at Eq. (5.14) expanded in powers of the couplings,

$$\begin{aligned} & -2 \left( C^{(1)} + C^{(2)} + C^{(3)} + C^{(4)} + C^{(5)} + \dots \right) + \left( \beta_\lambda^{(3)} + \beta_\lambda^{(4)} + \dots \right) \partial_\lambda B^{(3)} \\ & -4 \left( \gamma_\Phi^{(2)} + \gamma_\Phi^{(3)} + \dots \right) \left( C^{(1)} + C^{(2)} + C^{(3)} + \dots \right) - 4 \left( \gamma_\Phi^{(2)} + \gamma_\Phi^{(3)} + \dots \right) B^{(3)} = 0, \end{aligned} \quad (5.19)$$

one may conclude that  $C(\lambda, y, \alpha)$  starts at order  $x^5$ , and obtain the relation,

$$C^{(5)} = \frac{1}{2} \beta_\lambda^{(3)} \partial_\lambda B^{(3)} - 2 \gamma_\Phi^{(2)} B^{(3)}, \quad (5.20)$$

from which the coefficients of the form  $x^5 L^2$  of  $S_{\text{eff}}$  are calculated from known coefficients of the beta functions, anomalous dimension, and  $B^{(3)}$ . The end result is as follows,

$$\begin{aligned} C^{(5)} = & \lambda^5 \left( \frac{3}{2} c_3 b_3 - 2 d_2 b_3 \right) + \lambda^4 y \left( c_3 b_2 + \frac{3}{2} c_2 b_3 - 2 d_2 b_2 \right) \\ & + \lambda^3 y^2 \left( \frac{1}{2} c_3 b_1 + c_2 b_2 + \frac{3}{2} c_1 b_3 - 2 d_0 b_3 - 2 d_2 b_1 \right) \\ & + \lambda^2 y^3 \left( \frac{1}{2} c_2 b_1 + c_1 b_2 + \frac{3}{2} c_0 b_3 - 2 d_0 b_2 - 2 d_2 b_0 \right) \\ & + \lambda y^4 \left( \frac{1}{2} c_1 b_1 + c_0 b_2 - 2 d_0 b_1 \right) + y^5 \left( \frac{1}{2} c_0 b_1 - 2 d_0 b_0 \right). \end{aligned} \quad (5.21)$$

As before, we see that  $C^{(5)}$  do not depend on the gauge-fixing parameter. As a result, the RGE allows us to calculate terms of order  $x^5 L^2$  which, in our model, would appear only at four loops in an explicit evaluation of  $K_{\text{eff}}$ . The Eq. (5.14) does not provide us with

order  $x^6 L^2$ ,  $x^7 L^2$ , ... terms, since we do not have knowledge of higher orders coefficients of  $\beta_\lambda$  and  $\gamma_\Phi$ .

At this point, it is clear that one could go on calculating order  $x^7 L^3$ ,  $x^9 L^4$ , ... terms from Eqs. (5.3) and (5.12), obtaining contributions to the effective superpotential arising from higher loop orders, based only on the information we have from the two loop calculation of  $\beta_\lambda$  and  $\gamma_\Phi$ . Therefore, we can conclude that the effective superpotential does not depend on the gauge-fixing parameter. In the next section, we will give an explanation of this pattern of coefficients we are able to calculate, interpreting it as a leading logs summation of the effective superpotential.

## 5.2 RGE improvement and DSB: A short review of the four dimensional case

We now review the procedure for the RGE improvement of the effective potential that was applied to the Standard Model in [37, 38, 45, 46] and to the non supersymmetric version of the model studied in this work in [83]. In doing so, we will be able to pinpoint the differences we find in the supersymmetric three dimensional case, still recognizing that the procedure outlined in the previous section is essentially the same used in these works.

Consider a scale invariant  $\varphi^4$  model in  $(3+1)$  dimensions, coupled to other fermionic or gauge fields via a set of couplings denoted collectively by  $x$ . The effective potential  $\mathcal{V}_{\text{eff}}(\phi; \mu, x, \mathcal{L})$  satisfy the RGE

$$\left[ \mu \frac{\partial}{\partial \mu} + \beta_x \frac{\partial}{\partial x} - \gamma_\varphi \phi \frac{\partial}{\partial \phi} \right] \mathcal{V}_{\text{eff}}(\phi; \mu, x, \mathcal{L}) = 0, \quad (5.22)$$

where now

$$\mathcal{L} = \ln \left[ \frac{\phi^2}{\mu^2} \right]. \quad (5.23)$$

As before, we can rewrite this in a more convenient fashion by defining

$$\mathcal{V}_{\text{eff}}(\phi; \mu, x, \mathcal{L}) = \phi^4 \mathcal{S}_{\text{eff}}(\mu, x, \mathcal{L}), \quad (5.24)$$

so that Eq. (5.24) implies

$$\left[ -(2 + 2\gamma_\varphi) \frac{\partial}{\partial \mathcal{L}} + \beta_x \frac{\partial}{\partial x} - 4\gamma_\varphi \right] \mathcal{S}_{\text{eff}}(\mu, x, \mathcal{L}) = 0. \quad (5.25)$$

The central point of the general approach to RGE improvement discussed in the aforementioned references is to reorganize the contributions to  $\mathcal{S}_{\text{eff}}(\mu, x, \mathcal{L})$  arising from different loop orders according to the difference between the aggregate power of the couplings

$x$  and the logs  $\mathcal{L}$ , that is to say,

$$\mathcal{S}_{\text{eff}}(x, \mathcal{L}) = \mathcal{S}_{\text{eff}}^{\text{LL}}(x, \mathcal{L}) + \mathcal{S}_{\text{eff}}^{\text{NLL}}(x, \mathcal{L}) + \dots, \quad (5.26)$$

where  $\mathcal{S}_{\text{eff}}^{\text{LL}}$  contains the leading logs contributions,

$$\mathcal{S}_{\text{eff}}^{\text{LL}}(x, \mathcal{L}) = \sum_{n \geq 1} \mathcal{C}_n^{\text{LL}} x^n \mathcal{L}^{n-1}, \quad (5.27)$$

$\mathcal{S}_{\text{eff}}^{\text{NLL}}$  contains the next to leading logs terms,

$$\mathcal{S}_{\text{eff}}^{\text{NLL}}(x, \mathcal{L}) = \sum_{n \geq 2} \mathcal{C}_n^{\text{NLL}} x^n \mathcal{L}^{n-2}, \quad (5.28)$$

and so on. Insertion of the ansatz (5.26) into the RGE (5.25) gives a set of coupled differential equations, of which we quote the first two,

$$\left[ -2 \frac{\partial}{\partial \mathcal{L}} + \beta_x^{(2)} \frac{\partial}{\partial x} \right] \mathcal{S}_{\text{eff}}^{\text{LL}}(x, \mathcal{L}) = 0, \quad (5.29)$$

and

$$\left[ -2 \frac{\partial}{\partial \mathcal{L}} + \beta_x^{(2)} \frac{\partial}{\partial x} \right] \mathcal{S}_{\text{eff}}^{\text{NLL}}(x, \mathcal{L}) + \left[ \beta_x^{(3)} \frac{\partial}{\partial x} - 4 \gamma_\varphi^{(2)} \right] \mathcal{S}_{\text{eff}}^{\text{LL}}(x, \mathcal{L}) = 0. \quad (5.30)$$

Equation (5.29) results in a first order difference equation for  $\mathcal{C}_n^{\text{LL}}$ , so the knowledge of the initial coefficient  $\mathcal{C}_1^{\text{LL}}$  and the order  $x^2$  contribution to the beta function from loop calculations allows one to calculate all  $\mathcal{C}_n^{\text{LL}}$ , therefore summing up all the leading logs contributions to the effective potential. This summation was the key to making the DSB scenario viable in the scale invariant Standard Model as shown in [37]. One does not need to stop at this point, however, since Eq. (5.30) can also be used to sum up the next to leading logs, after  $\mathcal{S}_{\text{eff}}^{\text{LL}}$  was calculated, provided one knows the first coefficient  $\mathcal{C}_2^{\text{NLL}}$  of the series, as well as  $\beta_x^{(3)}$  and  $\gamma_\varphi^{(2)}$ . That means one can sum up sequentially several subseries of coefficients contributing to the effective potential, until exhausting the perturbative information encoded in  $\beta_x$ ,  $\gamma_\varphi$ , and the  $V_{\text{eff}}$  calculated up to a certain loop order. This is a systematic procedure to extract the maximum amount of information concerning the effective potential from a perturbative calculation.

One important technical detail is that the renormalization group functions are usually calculated in the Minimal Subtraction (MS) renormalization scheme, and they need to be adapted to the procedure outlined in this section, as it was first pointed out in [108]. For simplicity, let us consider the case of a theory with a single coupling  $x$ . In the MS scheme, divergent integrals (in four space-time dimension) appear with a factor

$$\tilde{\mathcal{L}} = \ln \left[ \frac{x \phi^2}{2 \mu^2} \right], \quad (5.31)$$



while in the so-called CW scheme, the effective potential depends on a log of the form (5.23). Both schemes can be related by a redefinition of the mass scale  $\mu$ ,

$$\mu_{\text{MS}}^2 = f(x) \mu_{\text{CW}}^2, \quad (5.32)$$

which can be shown to imply the following relation between the beta functions in both schemes,

$$\beta_{\text{CW}} = \beta_{\text{MS}} \left( 1 - \frac{1}{2} \beta_{\text{MS}} \partial_x \ln f \right)^{-1}. \quad (5.33)$$

In four space-time dimensions, divergences usually start at one loop, generating order  $x^2$  contributions to  $\beta_{\text{MS}}$ , therefore,

$$\begin{aligned} \beta_{\text{CW}} &= \left( \beta_{\text{MS}}^{(2)} + \beta_{\text{MS}}^{(3)} + \dots \right) (1 + \mathcal{O}(x)) \\ &= \beta_{\text{MS}}^{(2)} + \mathcal{O}(x^3). \end{aligned} \quad (5.34)$$

The conclusion is that at one loop level, both beta functions can be used interchangeably, but if calculations are done at two loops or more, one has to adapt the MS functions to be used in the calculation of the CW effective potential. The same reasoning concerning the beta functions can be applied to the anomalous dimension, with similar conclusions.

To gain further insight into this problem, we present the following argument: in the MS and CW schemes, the effective potential would be calculated at one loop level in the forms

$$V_{\text{MS}} = \phi^4 \left( \tilde{A}(x) + \tilde{B}(x) \tilde{\mathcal{L}} \right), \quad (5.35)$$

and

$$V_{\text{CW}} = \phi^4 \left( A(x) + B(x) \mathcal{L} \right). \quad (5.36)$$

From Eqs. (5.23) and (5.31), we have

$$\tilde{\mathcal{L}} = \mathcal{L} + \ln \left[ \frac{x}{2} \right], \quad (5.37)$$

and therefore one can rewrite  $V_{\text{MS}}$  in a form compatible with the CW scheme as follows,

$$V_{\text{MS}} = \phi^4 \left[ \left( \tilde{A}(x) + \ln \frac{x}{2} \tilde{B}(x) \right) + \tilde{B}(x) \mathcal{L} \right]. \quad (5.38)$$

Since the value of  $A(x)$  is immaterial in the CW potential, being fixed by the CW condition (5.5), we conclude that  $\tilde{B}(x) = B(x)$  and that both  $V_{\text{MS}}$  and  $V_{\text{CW}}$  end up giving identical results at one loop. At two loops, however,  $V_{\text{MS}}$  contains a term of the form  $\tilde{C}(x) \tilde{\mathcal{L}}^2$ , so after employing (5.37), one would find a difference in the relevant term proportional to  $\mathcal{L}$ , meaning both potentials are not equivalent at two loops. The net result is

that, at the two loop level, the RGE can be used to relate renormalization group functions and the effective potential in the CW and the MS scheme, but not interchangeably.

### 5.3 RGE improvement in the three dimensional supersymmetric case

Now we discuss how to adapt the procedure outlined in Section 5.2 to our model. First of all, we consider the problem of interchangeability of MS and CW renormalization group functions when using the RGE to calculate the effective potential. In the supersymmetric three-dimensional model considered by us, divergences only start at two loops, and the beta functions start at order  $x^3$ . This means that instead of Eq. (5.34) we have

$$\begin{aligned}\beta_{\text{CW}} &= \left( \beta_{\text{MS}}^{(3)} + \beta_{\text{MS}}^{(4)} + \cdots \right) (1 + \mathcal{O}(x)) \\ &= \beta_{\text{MS}}^{(3)} + \mathcal{O}(x^4) .\end{aligned}\tag{5.39}$$

Also,  $K_{\text{eff}}$  acquires a term proportional to  $\tilde{\mathcal{L}}^2$  only at loop orders greater than two. This means we are safe to use interchangeably functions calculated in the MS and the CW scheme, as we have done in Section 5.1.

It is still not clear that the series of terms we calculated in section 5.1, of orders  $x^{2n+1}L^n$ , have any relation to the leading logs summation described in Section 5.2. Indeed, by repeating the steps outlined in the start of that section for our model, the fact that  $\beta_{\lambda}^{(2)} = 0$  together with Eq. (5.29) would imply  $\mathcal{C}_n^{LL} = 0$  for  $n > 1$ , which in its turn would also trivialize Eq. (5.30). The conclusion would be that the RGE does not allow us to calculate any new contribution for the effective superpotential.

Actually, this apparent problem is a consequence of the particular pattern of divergences that appear in our model, whenever we use dimensional regularization to evaluate Feynman integrals. In four dimensional non supersymmetric theories, divergences in general occur at any loop order  $n$ , the leading logs being of the order  $x^{n+1}L^n$ . In three dimensional supersymmetric models, divergences start only at two loops, and are of the order  $x^3L$ . At three loops, the only divergences arise from two loops subdiagrams, of the order  $x^4L$ . At four loops, we find again superficially divergent diagrams, of order  $x^5L^2$ , while five loops diagrams contain at most four and two loops divergent subdiagrams, of order  $x^6L^2$  and  $x^6L$ . This pattern suggests that new superficial divergences appear only at even loops, and are of the order  $x^{2n+1}L^n$ , and these terms should be identified as “leading logs” in our case, despite the fact that the difference between the power of coupling constants and logs is not the same for these terms. Careful consideration of this divergence pattern suggests for supersymmetric three dimensional models the definition,

$$S_{\text{eff}}(x, L) = S_{\text{eff}}^{\text{LL}}(x, L) + S_{\text{eff}}^{\text{NLL}}(x, L) + \cdots ,\tag{5.40}$$

where leading logs contributions are of the form

$$S_{\text{eff}}^{\text{LL}}(x, L) = \sum_{n \geq 0} C_n^{\text{LL}} x^{2n+1} L^n, \quad (5.41)$$

next to leading logs are given by

$$S_{\text{eff}}^{\text{NLL}}(x, L) = \sum_{n \geq 0} \left( C_n^{\text{NLL}} x^{2n+2} L^n + D_n^{\text{NLL}} x^{2n+3} L^n \right), \quad (5.42)$$

and so on. Using Eqs. (5.41), (5.42) and the RGE (5.12), we obtain

$$\partial_L S_{\text{eff}}^{\text{LL}} = \sum_{n \geq 0} (n+1) C_{n+1}^{\text{LL}} x^{2n+3} L^n, \quad (5.43a)$$

$$C_{\gamma_\Phi^{(2)}} x^2 \partial_L S_{\text{eff}}^{\text{LL}} = C_{\gamma_\Phi^{(2)}} \sum_{n \geq 0} (n+1) C_n^{\text{LL}} x^{2n+5} L^n, \quad (5.43b)$$

$$C_{\beta_\lambda^{(3)}} x^3 \partial_x S_{\text{eff}}^{\text{LL}} = C_{\beta_\lambda^{(3)}} \sum_{n \geq 0} (2n+1) C_n^{\text{LL}} x^{2n+3} L^n, \quad (5.43c)$$

$$C_{\gamma_\Phi^{(2)}} x^2 S_{\text{eff}}^{\text{LL}} = C_{\gamma_\Phi^{(2)}} \sum_{n \geq 0} C_n^{\text{LL}} x^{2n+3} L^n, \quad (5.43d)$$

$$\partial_L S_{\text{eff}}^{\text{NLL}} = \sum_{n \geq 0} (n+1) \left( C_{n+1}^{\text{NLL}} x^{2n+4} L^n + D_{n+1}^{\text{NLL}} x^{2n+5} L^n \right), \quad (5.43e)$$

$$C_{\gamma_\Phi^{(2)}} x^2 \partial_L S_{\text{eff}}^{\text{NLL}} = C_{\gamma_\Phi^{(2)}} \sum_{n \geq 0} (n+1) \left( C_{n+1}^{\text{NLL}} x^{2n+6} L^n + D_{n+1}^{\text{NLL}} x^{2n+7} L^n \right), \quad (5.43f)$$

$$C_{\beta_\lambda^{(3)}} x^3 \partial_x S_{\text{eff}}^{\text{NLL}} = C_{\beta_\lambda^{(3)}} \sum_{n \geq 0} \left( (2n+2) C_n^{\text{NLL}} x^{2n+4} L^n + (2n+3) D_n^{\text{NLL}} x^{2n+5} L^n \right), \quad (5.43g)$$

$$C_{\gamma_\Phi^{(2)}} x^2 S_{\text{eff}}^{\text{NLL}} = C_{\gamma_\Phi^{(2)}} \sum_{n \geq 0} \left( C_n^{\text{NLL}} x^{2n+4} L^n + D_n^{\text{NLL}} x^{2n+5} L^n \right), \quad (5.43h)$$

where  $C_{\beta_\lambda^{(3)}}$  and  $C_{\gamma_\Phi^{(2)}}$  are the coefficients of the renormalization group functions. Inserting Eq. (5.43) into the RGE (5.12) gives us

$$\sum_{n \geq 0} \left[ \left( -(n+1) C_{n+1}^{\text{LL}} + (2n+1) C_{\beta_\lambda^{(3)}} C_n^{\text{LL}} - 4 C_{\gamma_\Phi^{(2)}} C_n^{\text{LL}} \right) x^{2n+3} L^n + \mathcal{O}(x^{2n+5} L^n) \right] = 0, \quad (5.44)$$

which, very much like Eq. (5.29), provides a first order difference equation for  $C_n^{\text{LL}}$ , now involving the order  $x^3$  terms in the beta function, as well as the order  $x^2$  terms of the anomalous dimension. From this equation, the whole series of leading logs coefficients,

$$C_{n+1}^{\text{LL}} = \left( \frac{2n+1}{n+1} C_{\beta_\lambda^{(3)}} - \frac{4}{n+1} C_{\gamma_\Phi^{(2)}} \right) C_n^{\text{LL}} \quad (5.45)$$

may be (in principle) determined, and so  $S_{\text{eff}}^{\text{LL}}(x, L)$  is obtained from the two loop information we have at hand. Looking at other coefficients of the sum in Eq. (5.44) would provide equations for the calculation of next to leading log contributions, and so on. The result

is that the leading logs summation procedure can be applied to three dimensional supersymmetric models, yet with nontrivial modifications, taking into account the peculiar divergence structure of such models.

To actually apply this technique to our model, one has to generalize the equations in the last paragraph to the case of two couplings, which involves dealing with double sums of the form

$$S_{\text{eff}}^{\text{LL}}(\lambda, y, L) = \sum_{n \geq 0} \sum_{0 \leq \ell \leq 2n+1} C_{\ell, 2n+1-\ell}^{\text{LL}} \lambda^\ell y^{2n+1-\ell} L^n. \quad (5.46)$$

We will only need the first, third and fourth terms from the RGE (5.12), since the second, involving  $\gamma_\Phi \partial_L$ , can be shown to appear only at the next-to-leading log level. According to the coefficients in (4.44), we obtain the initial values for  $S_{\text{eff}}^{\text{LL}}$ ,

$$C_{01}^{\text{LL}} = 0, C_{10}^{\text{LL}} = 1, \quad (5.47)$$

$$C_{30}^{\text{LL}} = b_3, C_{21}^{\text{LL}} = b_2, C_{12}^{\text{LL}} = b_1, C_{03}^{\text{LL}} = b_0. \quad (5.48)$$

Substituting (4.42) into  $S_{\text{eff}}^{\text{LL}}$  we obtain

$$\partial_L S_{\text{eff}}^{\text{LL}} = \sum_{n \geq 0} \sum_{0 \leq \ell \leq 2n+3} (n+1) C_{\ell, 2n+3-\ell}^{\text{LL}} \lambda^\ell y^{2n+3-\ell} L^n, \quad (5.49)$$

$$\begin{aligned} \gamma_\Phi^{(2)} \partial_L S_{\text{eff}}^{\text{LL}} &= \sum_{n \geq 0} \sum_{0 \leq \ell \leq 2n+3} (n+1) \left( d_2 C_{\ell, 2n+3-\ell}^{\text{LL}} \lambda^{\ell+2} y^{2n+3-\ell} \right. \\ &\quad \left. + d_0 C_{\ell, 2n+5-\ell}^{\text{LL}} \lambda^\ell y^{2n+5-\ell} \right) L^n, \end{aligned} \quad (5.50)$$

$$\beta_\lambda^{(3)} \partial_\lambda S_{\text{eff}}^{\text{LL}} = \sum_{n \geq 0} \sum_{m \leq \ell \leq 2n+m} \sum_{0 \leq m \leq 3} (l-m+1) c_m C_{l-m+1, 2n-\ell+m}^{\text{LL}} \lambda^l y^{2n+3-l} L^n, \quad (5.51)$$

$$\begin{aligned} \gamma_\Phi^{(2)} S_{\text{eff}}^{\text{LL}} &= \sum_{n \geq 0} \sum_{0 \leq \ell \leq 2n+1} \left( d_2 C_{\ell, 2n+1-\ell}^{\text{LL}} \lambda^{\ell+2} y^{2n+1-\ell} \right. \\ &\quad \left. + d_0 C_{\ell, 2n+1-\ell}^{\text{LL}} \lambda^\ell y^{2n+3-\ell} \right) L^n. \end{aligned} \quad (5.52)$$

To calculate the first terms of the leading logs series, we expand explicitly these sums for  $n = 0$  and  $n = 1$ ,

$$\begin{aligned} \partial_L S_{\text{eff}}^{\text{LL}} &= C_{30}^{\text{LL}} \lambda^3 + C_{2,1}^{\text{LL}} \lambda^2 y + C_{12}^{\text{LL}} \lambda y^2 + C_{03}^{\text{LL}} y^3 + 2 C_{50}^{\text{LL}} \lambda^5 L + 2 C_{41}^{\text{LL}} \lambda^4 y L, \\ &\quad + 2 C_{32}^{\text{LL}} \lambda^3 y^2 L + 2 C_{23}^{\text{LL}} \lambda^2 y^3 L + 2 C_{14}^{\text{LL}} \lambda y^4 L + 2 C_{05}^{\text{LL}} y^5 L + \dots, \end{aligned} \quad (5.53)$$

$$\begin{aligned}
 \gamma_{\Phi}^{(2)} \partial_L S_{\text{eff}}^{\text{LL}} &= d_2 C_{12}^{\text{LL}} \lambda^3 y^2 + d_0 C_{14}^{\text{LL}} \lambda y^4 + d_2 C_{21}^{\text{LL}} \lambda^4 y + d_0 C_{23}^{\text{LL}} \lambda^2 y^3 \\
 &+ d_2 C_{30}^{\text{LL}} \lambda^5 + d_0 C_{32}^{\text{LL}} \lambda^3 y^2 + 2 \left( d_2 C_{05}^{\text{LL}} \lambda^2 y^5 + d_0 C_{07}^{\text{LL}} y^7 \right) L \\
 &+ 2 \left( d_2 C_{14}^{\text{LL}} \lambda^3 y^4 + d_0 C_{16}^{\text{LL}} \lambda y^6 \right) L + 2 \left( d_2 C_{23}^{\text{LL}} \lambda^4 y^3 + d_0 C_{25}^{\text{LL}} \lambda^2 y^5 \right) L, \\
 &+ 2 \left( d_2 C_{32}^{\text{LL}} \lambda^5 y^2 + d_0 C_{34}^{\text{LL}} \lambda^3 y^4 \right) L + 2 \left( d_2 C_{41}^{\text{LL}} \lambda^6 y + d_0 C_{43}^{\text{LL}} \lambda^4 y^3 \right) L, \\
 &+ 2 \left( d_2 C_{41}^{\text{LL}} \lambda^6 y + d_0 C_{43}^{\text{LL}} \lambda^4 y^3 \right) L + \dots, \tag{5.54}
 \end{aligned}$$

$$\begin{aligned}
 \beta_{\lambda}^{(3)} \partial_{\lambda} S_{\text{eff}}^{\text{LL}} &= C_{10}^{\text{LL}} \left( c_3 \lambda^3 + c_2 \lambda^2 y + c_1 \lambda y^2 + c_0 y^3 \right) + 3 c_3 C_{30}^{\text{LL}} \lambda^5 L \\
 &+ \left( 3 c_2 C_{30}^{\text{LL}} + 2 c_3 C_{21}^{\text{LL}} \right) \lambda^4 y L + \left( 3 c_1 C_{30}^{\text{LL}} + 2 c_2 C_{21}^{\text{LL}} + c_3 C_{12}^{\text{LL}} \right) \lambda^3 y^2 L \\
 &+ \left( 3 c_0 C_{30}^{\text{LL}} + 2 c_1 C_{21}^{\text{LL}} + c_2 C_{12}^{\text{LL}} \right) \lambda^2 y^3 L + \left( 2 c_0 C_{21}^{\text{LL}} + c_1 C_{12}^{\text{LL}} \right) \lambda y^4 L \\
 &+ c_0 C_{12}^{\text{LL}} y^5 L + \dots, \tag{5.55}
 \end{aligned}$$

$$\begin{aligned}
 \gamma_{\Phi}^{(2)} S_{\text{eff}}^{\text{LL}} &= d_2 \left( C_{10}^{\text{LL}} \lambda^3 + C_{01}^{\text{LL}} \lambda^2 y \right) + d_0 \left( C_{10}^{\text{LL}} \lambda y^2 + C_{01}^{\text{LL}} y^3 \right) + d_2 C_{30}^{\text{LL}} \lambda^5 L \\
 &+ d_2 C_{21}^{\text{LL}} \lambda^4 y L + \left( d_2 C_{12}^{\text{LL}} + d_0 C_{30}^{\text{LL}} \right) \lambda^3 y^2 L + \left( d_2 C_{03}^{\text{LL}} + d_0 C_{21}^{\text{LL}} \right) \lambda^2 y^3 L \\
 &+ d_0 C_{12}^{\text{LL}} \lambda y^4 L + d_0 C_{03}^{\text{LL}} y^5 L + \dots. \tag{5.56}
 \end{aligned}$$

Substituting these results in Eq. (5.12), at order  $L^0$  we have the relations

$$\begin{cases} \left( -C_{30}^{\text{LL}} + C_{10}^{\text{LL}} c_3 - 4 d_2 C_{10}^{\text{LL}} \right) \lambda^3 &= 0 \\ \left( -C_{21}^{\text{LL}} + C_{10}^{\text{LL}} c_2 - 4 d_2 C_{01}^{\text{LL}} \right) \lambda^2 y &= 0 \\ \left( -C_{12}^{\text{LL}} + C_{10}^{\text{LL}} c_1 - 4 d_0 C_{10}^{\text{LL}} \right) \lambda y^2 &= 0 \\ \left( -C_{03}^{\text{LL}} + C_{10}^{\text{LL}} c_0 - 4 d_0 C_{01}^{\text{LL}} \right) y^3 &= 0 \end{cases} \tag{5.57}$$

From this system of equations and (5.47), we find the same result obtained in (5.18). If we continue with the order  $L^1$ , we reproduce the results obtained in (5.20).

To systematically calculate higher order coefficients, we developed a MATHEMATICA code to calculate the coefficients  $C^{\text{LL}}$  up to an arbitrary (finite) order. With this code we could calculate corrections to  $S_{\text{eff}}^{\text{LL}}$  up to the order  $x^{41} L^{20}$  in a few seconds, for example. This result will be used, in the next section, to study the modifications introduced by the leading logs summation in the DSB in our model. The code as well as the explicit results are available as a Supplementary Material in [92].

## 5.4 Dynamical Breaking of Symmetry

In this section we study the dynamical breaking of the conformal symmetry that occurs in the theory we are considering, based on the improved effective superpotential that

was obtained in the previous section by summing up leading logs contributions. More explicitly, we consider,

$$K_{\text{eff}}^I(\sigma_{\text{cl}}) = -\frac{1}{4}\sigma_{\text{cl}}^4 \left[ S_{\text{eff}}^{\text{LL}}(\lambda, y, L) + \rho \right], \quad (5.58)$$

$\rho$  being a finite renormalization constant. The constant  $\rho$  is fixed using the CW normalization condition (5.5). Requiring that the  $K_{\text{eff}}^I(\sigma_{\text{cl}})$  has a minimum at  $\sigma_{\text{cl}}^2 = \mu$  means imposing that

$$\left. \frac{d}{d\sigma} K_{\text{eff}}^I(\sigma_{\text{cl}}) \right|_{\sigma_{\text{cl}}^2 = \mu} = 0, \quad (5.59)$$

which can be used to determine the value of  $\lambda$  as a function of the free parameters  $y$  and  $N$ .

Upon explicit calculation, Eq. (5.59) turns out to be a polynomial equation in  $\lambda$ , and among its solutions we look for those which are real and positive, and correspond to a minimum of the potential, i.e.,

$$M_{\Sigma} = \left. \frac{d^2}{d\sigma^2} K_{\text{eff}}^I(\sigma_{\text{cl}}) \right|_{\sigma_{\text{cl}}^2 = \mu} > 0. \quad (5.60)$$

This procedure was implemented in a MATHEMATICA program, and we can verify whether DSB is operational for any given value of  $y \leq 1$  and  $N$ , both considering the unimproved (which is the effective superpotential calculated at two loops, i.e., including only the  $B^{(3)}$  term in (5.3)) and the improved effective superpotential (the one including all higher order leading logs corrections, calculated by the procure described in the last section). This way, we can verify whether the effect of the RGE improvement is so dramatic as it has found to be in other cases.

In general, we found DSB being operational for most reasonable value of its free parameters. For the case of the unimproved effective superpotential, this is true for any  $y \leq 1$  and  $N$ . In the case of the improved effective superpotential, Figure 5.1 displays a plot of the allowed regions in the  $y - N$  parameter space. We notice that the region of the parameter space where DSB is operational is slightly smaller for the improved superpotential compared to the unimproved case. The same pattern were found in the non supersymmetric version of this model [83], but in that case this difference was much more relevant. It is also noteworthy that for some values of  $y$  and  $N$ , one may find actually two viable solutions for  $\lambda$  as a function of the free parameters. For larger values of  $N$ , this multiplicity of solutions dominates the parameter space of the model, as can be seen in Fig. 5.2.

Choosing for example the values  $y = 0.5$  and  $N = 1$ , we find using the improved superpotential calculated including corrections up to order  $x^{41}L^{20}$  that  $\lambda^I = 0.0118182863005$ .

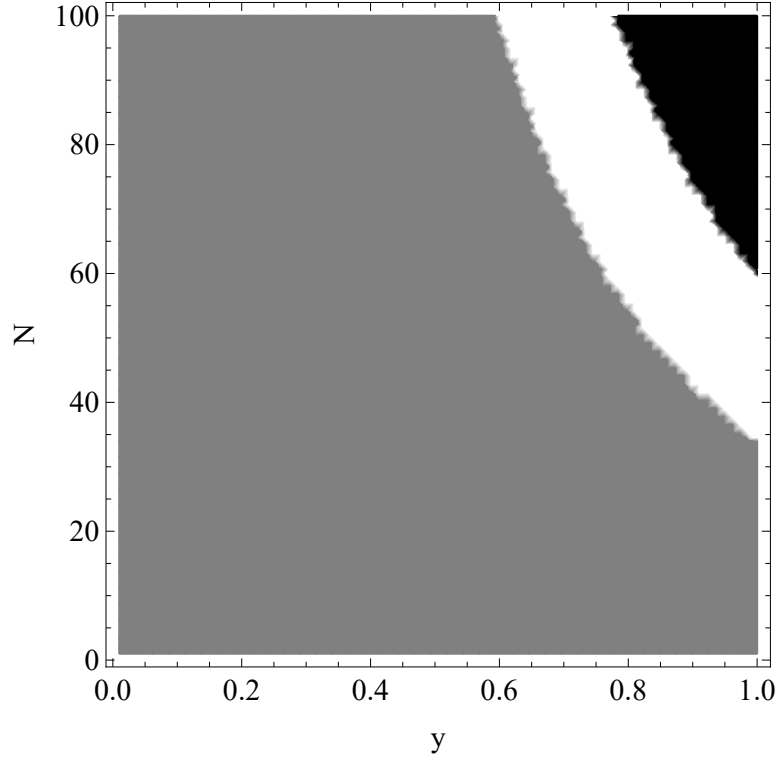


Figure 5.1: Solutions for  $\lambda$  in the improved case: one (gray region), zero (white region) and two (black region)

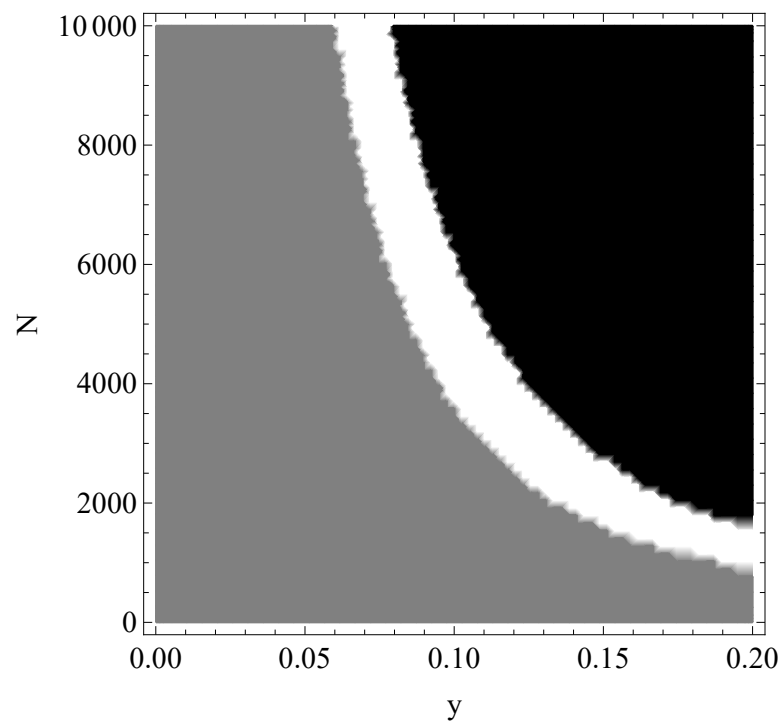
To compare, by choosing the same values of  $y$  and  $N$ , but using the unimproved two-loop effective superpotential, we find  $\lambda = 0.0118485063225$ . The difference between the two values being only of order 0.255%, we say that for these values of  $y$  and  $N$ , the improvement of the effective superpotential by means of the summation of the leading logs contributions provides only a small quantitative change on the parameters of the DSB. We verify this happens for most of the parameter space of the model.

In Figure 5.3a, we show the behavior of  $\lambda^I$  and  $\lambda$  for a range of values of  $y \in [0, 1]$ , with specific values of  $N$ , to wit  $N = 1, 10, 50, 100$ . It becomes evident that the difference between the DSB described by the improved and the unimproved superpotential is significant only for larger values of  $N$ , and even so, for not so small values of  $y$ . In particular, for large  $N$ , such as  $N = 10 \times 10^3, 10 \times 10^4, 10 \times 10^5, 10 \times 10^6$ , the Figure 5.3b show us that in essentially the whole range of values of  $y$  (in the perturbative regime) two solutions can be found for  $\lambda^I$ .

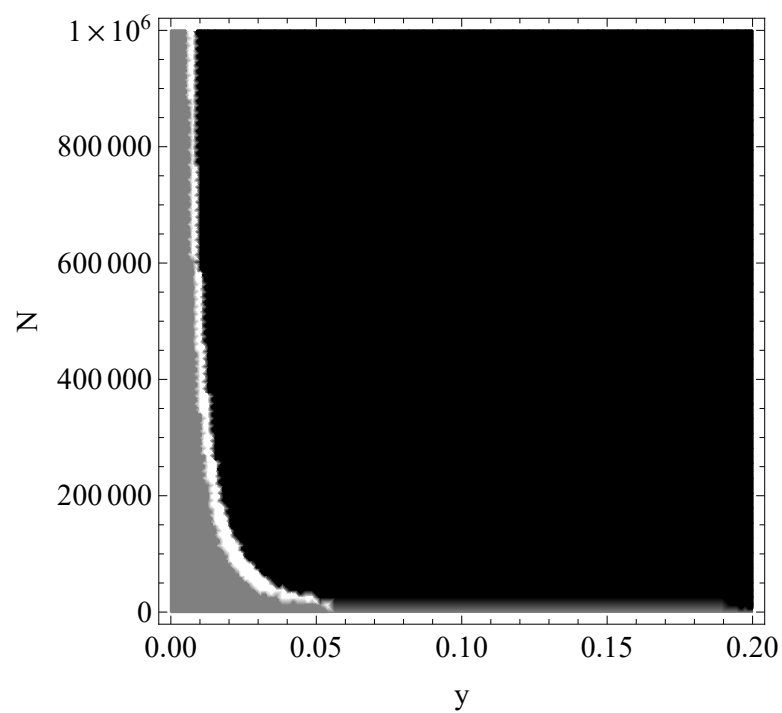
Finally, the incremental aspect of the RGE improvement in the present case can also be seen by plotting both the improved and unimproved effective superpotentials as in Figure 5.4, where only by choosing relatively high values of  $y$  and  $N$  we were able to get two graphs that do not superimpose. We note that the improved superpotential is shallower than the unimproved one, which is a general feature observed also in four dimensional cases [37, 109, 39].







(a)



(b)

Figure 5.2: Same as Figure (5.1), but with larger  $N$ . We observe that for larger values of  $N$ , the region where we have two solutions for  $\lambda$  dominates the parameter space of the model.

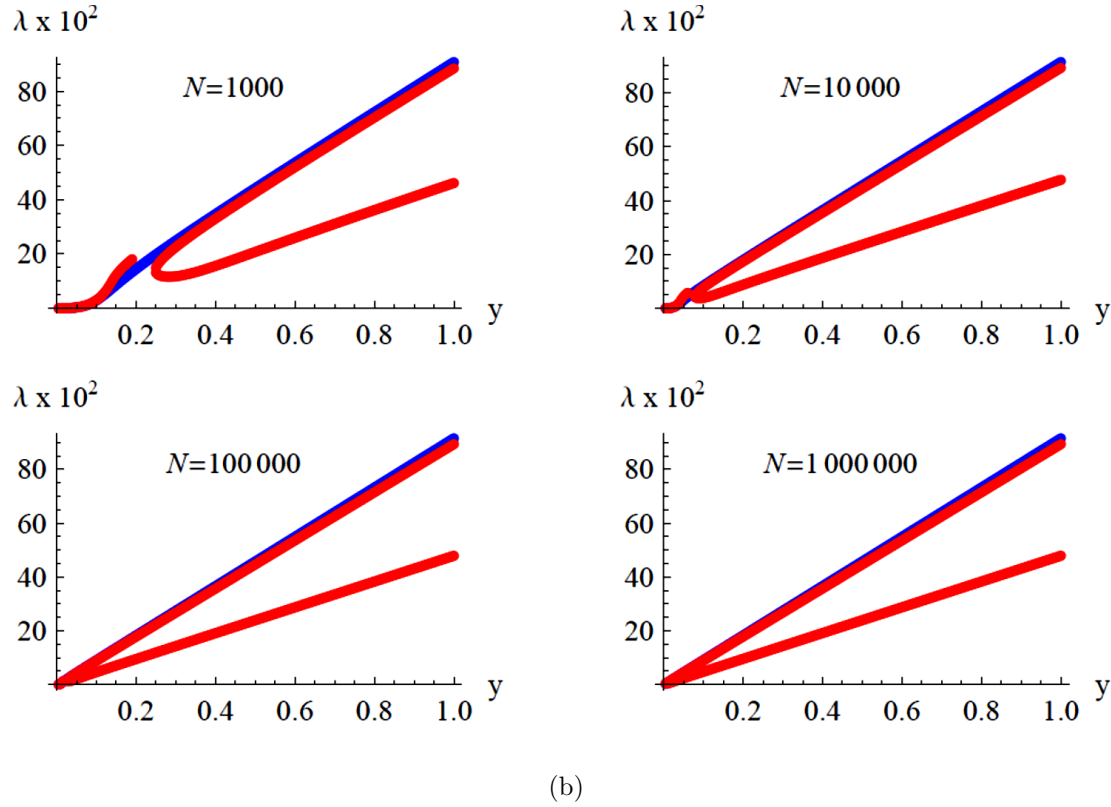
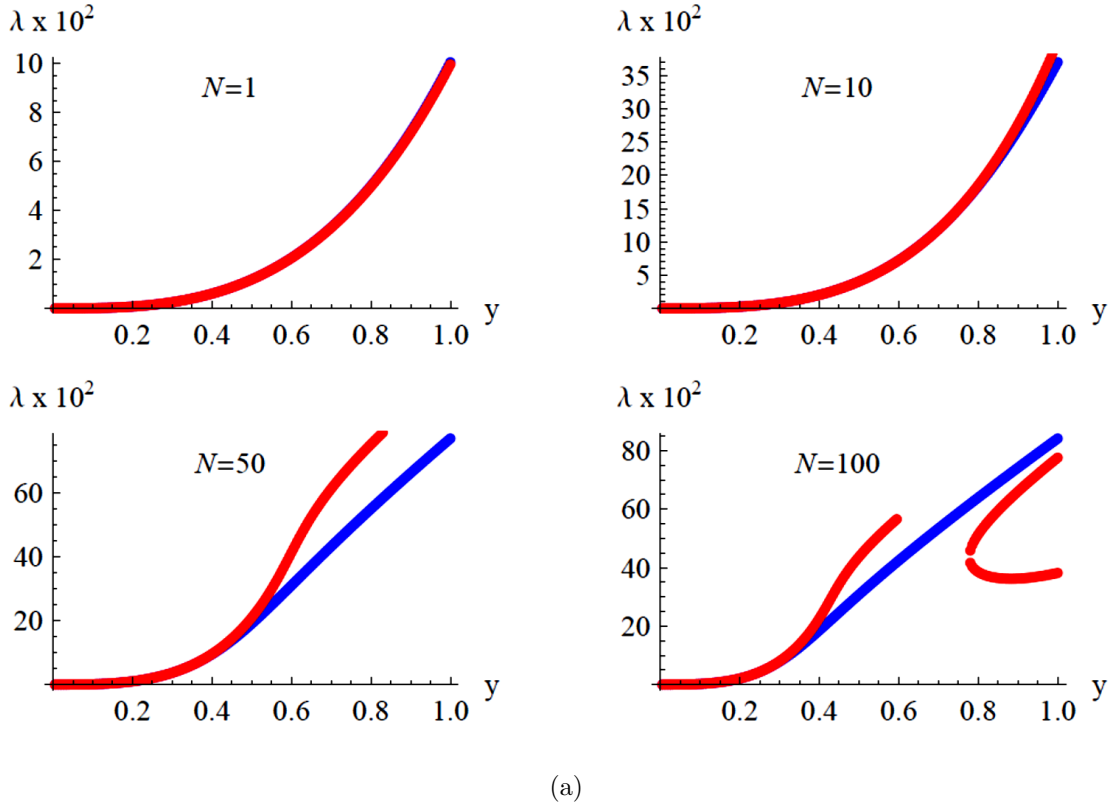


Figure 5.3: Behavior of the unimproved  $\lambda$  (blue line) and improved  $\lambda^I$  (red line) with the variation of the coupling constant  $y$ : a) for  $N = 1, 10, 50, 100$  and b)  $N = 10 \times 10^2, 10 \times 10^4, 10 \times 10^5, 10 \times 10^6$ .

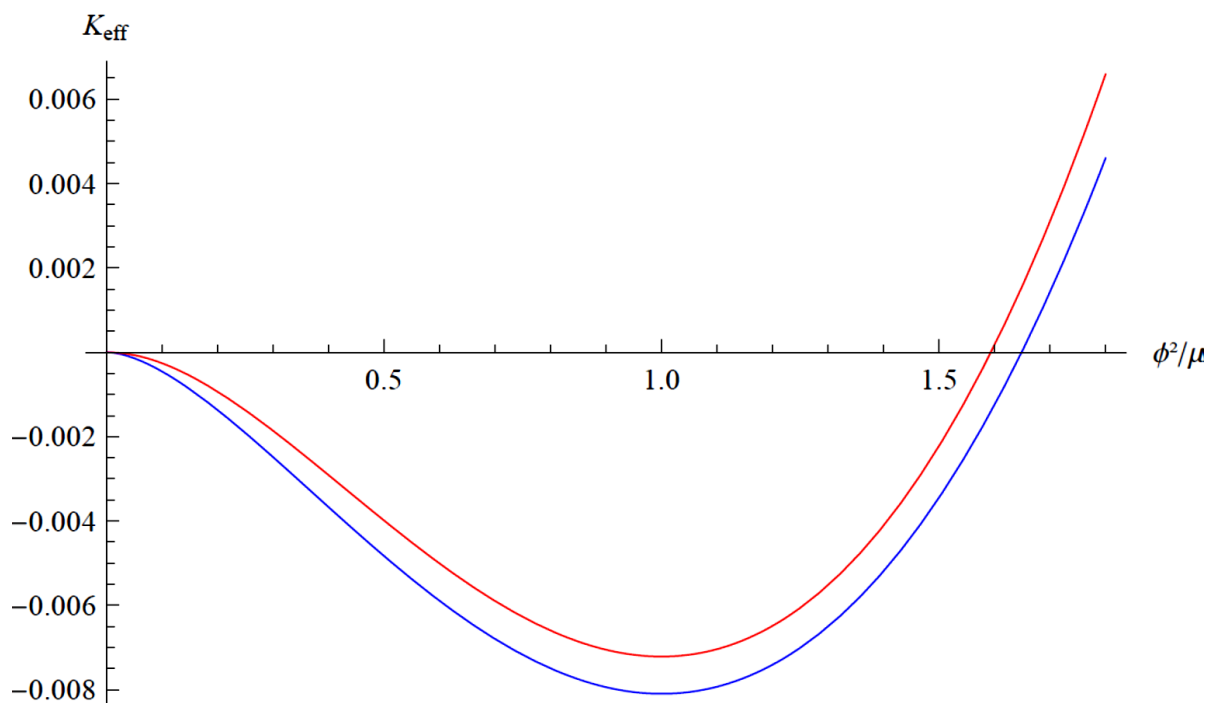


Figure 5.4: Comparison of the unimproved (blue line) and improved (red line) effective superpotential, for  $y = 0.5$  and  $N = 65$ .



# Chapter 6

## Conclusions and perspectives

The gauge independence of physical observables is an essential point to consider when studying gauge theories. In relation to the effective potential, which plays an essential role in the DSB mechanism in many relevant models, the Nielsen identity is the key to understand how the effective potential can depend on the gauge choice, and yet physical quantities evaluated at its minima can be gauge independent. The DSB mechanism is central for the formulation of a consistent quantum field theory of the known elementary interactions, and the possibility that quantum corrections of a symmetric potential could alone induce such symmetry breaking is a rather interesting one, not only for its mathematical elegance, but also for physical reasons. Recently, for example, a DSB mechanism in a scale-invariant version of the Standard Model is being discussed as a viable mechanism for generating a mass for the Higgs particle compatible with experimental observations. The idea of using the RGE to improve the calculation of the effective potential, summing up terms arising from higher loop orders organized as leading logarithms, next to leading logarithms, and so on, is central to this approach. We have shown how this program can be applied to a supersymmetric model in the superfield formalism, which is the main technical result of this thesis.

In this thesis we studied the Nielsen identity for a supersymmetric CS model in the superfield formalism. After deriving the Nielsen identity in the superfield language, we argue that an explicit calculation of the complete effective superpotential  $V_{\text{eff}}^S$ , including any possible gauge dependence, is still a technically difficult task. As a first step in this direction, we calculated the part of the effective superpotential that do not depend on supercovariant derivatives of the background scalar superfield,  $K_{\text{eff}}$  [91, 94]. This calculation was made without fixing the gauge-fixing parameter  $\alpha$ , and we were able to verify explicitly that all divergent corrections to the vertex functions at two loop order are independent of  $\alpha$ . From these vertex functions, we calculate the renormalization group functions. Our results agree with the ones previously found in the literature [52, 84], that were calculated in a specific gauge. We developed a method where the use of the renormalization group functions together with the RGE allows us to calculate the improved

effective superpotential in the superfield formalism and showing its independence on the gauge-fixing parameter. The effective superpotential is used to study the DSB mechanism in our model. The end result is that DSB is operational for reasonable values of the free parameters, and the RGE improvement produces in general only a small quantitative change in the properties of the model. Only for higher values of the gauge coupling and the number of matter fields we obtain a significant difference on the properties of DSB from the RGE improvement.

In this particular model, therefore, the effects of the RGE improvement were not so dramatic as in its non supersymmetric counterpart, however the question remains whether the same might happen in different models. As a future perspective, we will try to extend these results to the full effective superpotential  $V_{\text{eff}}^S$ . This should be possible with the results given in this thesis, and the same techniques used here, generalized to the multiscale case as discussed in [102, 103]. Also, a generalization of this study for non Abelian models and ABJM theories would be an interesting endeavor.

To finish, we would like to briefly comment on another study that was made by us during the development of this thesis, where we studied the improvement of the effective potential in the context of the scalar QED and QCD with a colorless scalar, in order to verify the effect of a possible non-perturbative infrared fixed points associated to a conformal phase [44]. This work represent another instance of the use of the RGE to gain further physical insights on the dynamics of four dimensional gauge theory.

# Appendix A

## One Loop Correction

### A.1 Example: Two-point vertex function of gauge superfield

In this section, for didactic purposes, we present the explicit calculation of the two-point vertex function at one loop associated to the gauge superfield, Figure A.1.

First, we need to find the correct sign in front of the, for this purpose, one may use the Wick's theorem, but we note that for practical reasons we will use the Wick's contractions only to determine the correct sign of the amplitude. We start with,

$$\frac{1}{2}g \left[ D_{\Phi}^{\alpha} - D_{\Phi}^{\alpha} \right]_1 \bar{\Phi}_{1a} \Phi_{1a} \Gamma_{1\alpha} = \left( \frac{1}{2} g \right) \mathcal{D}_1^{\alpha} \bar{\Phi}_{1a} \Phi_{1a} \Gamma_{1\alpha},$$

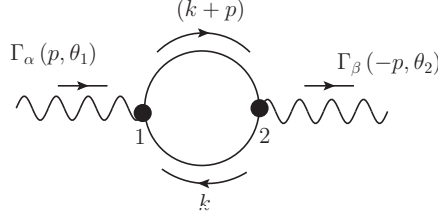
this term is the complete trilinear vertex, and we introduced the notation

$$\mathcal{D}^{\alpha} = D_{\Phi}^{\alpha} - D_{\Phi}^{\alpha},$$

to facilitate the manipulations of the contractions, for example,

$$\begin{aligned} & \left( \frac{1}{2} g \right)^4 \mathcal{D}_1^{\alpha} \bar{\Phi}_{1a} \Phi_{1a} \Gamma_{1\alpha} \mathcal{D}_2^{\beta} \bar{\Phi}_{2b} \Phi_{2b} \Gamma_{2\beta} \\ &= -\frac{1}{16} g^4 \mathcal{D}_1^{\alpha} \mathcal{D}_2^{\beta} : \bar{\Phi}_{1a} \Phi_{1a} \Gamma_{1\alpha} : \bar{\Phi}_{2b} \Phi_{2b} \Gamma_{2\beta} \\ &= -\frac{1}{16} g^4 \mathcal{D}_1^{\alpha} \mathcal{D}_2^{\beta} \overbrace{\bar{\Phi}_{1a} \Phi_{1a} \Gamma_{1\alpha} \bar{\Phi}_{2b} \Phi_{2b} \Gamma_{2\beta}} \\ &= -\frac{1}{16} g^4 \mathcal{D}_1^{\alpha} \mathcal{D}_2^{\beta} \overbrace{\bar{\Phi}_{1a} \Phi_{2b}} \overbrace{\Phi_{1a} \bar{\Phi}_{2b}} \overbrace{\Gamma_{1\alpha} \Gamma_{2\beta}}, \end{aligned}$$

Now, with this procedure, we find the correct sign of the amplitude. Using the Feynman rules shown in Section 4.2, we can calculate the diagram  $\mathcal{S}_{\Gamma\Gamma}^{(a)-1l}$ , in the Figure A.1,


 Figure A.1:  $\mathcal{S}_{\Gamma\Gamma}^{(a)-1l}$ .

finding

$$\begin{aligned} \mathcal{S}_{\Gamma\Gamma}^{(a)-1l} = & -\frac{1}{s} \left( \frac{g}{2} \delta_{ij} \mathcal{D}_1^\alpha \right) \left( \frac{g}{2} \delta_{kl} \mathcal{D}_2^\beta \right) \int d^2\theta_1 d^2\theta_2 \int \frac{d^3p}{(2\pi)^3} \int \frac{d^Dk}{(2\pi)^3} \frac{i\delta_{jk} D^2}{(k+p)^2} \delta_{12}^{(-(k+p))} \\ & \times \frac{i\delta_{il} D^2}{(k)^2} \delta_{21}^{(-k)} \Gamma_\alpha(p, \theta_1) \Gamma_\beta(-p, \theta_2), \end{aligned} \quad (\text{A.1})$$

where  $s$  is a symmetric factor, we compute it as,  $\frac{1}{s} = \frac{1}{2!} \times 2 \times 1 \times 1$ , meaning: the  $2!$  in the denominator come from the Taylor expansion because we have two identical vertices, the first numerical factor “2” come from the external gauge lines (wave line) of the vertices 1 and 2, the second numerical factor “1” come from the symmetric factor from the trilinear vertex, and the last numerical factor come from the combinations of the internal lines that connect vertex 1 with vertex 2, which in the case amount to a single choice because the scalar superfield is complex.

Also,

$$\mathcal{D}_1^\alpha \equiv [D_1^\alpha(k) - D_1^\alpha(-(k+p))], \quad (\text{A.2})$$

$$\mathcal{D}_2^\beta \equiv [D_2^\beta(k+p) - D_2^\beta(-(k))], \quad (\text{A.3})$$

which substituted into Eq. (A.1), leads to

$$\begin{aligned} \mathcal{S}_{\Gamma\Gamma}^{(a)-1l} = & -i^2 \frac{g^2}{4} N \int d^2\theta_1 \int d^2\theta_2 \int \frac{d^3p}{(2\pi)^3} \int \frac{d^Dk}{(2\pi)^3} \frac{1}{(k+p)^2 k^2} \times \\ & \left\{ -D_2^\beta(k+p) D^2 \delta_{12}^{(-(k+p))} D_1^\alpha(k) D^2 \delta_{21}^{(-k)} \Gamma_\alpha(p, \theta_1) \Gamma_\beta(-p, \theta_2) \right. \\ & - D_1^\alpha(-(k+p)) D_2^\beta(k+p) D^2 \delta_{12}^{(-(k+p))} D^2 \delta_{21}^{(-k)} \Gamma_\alpha(p, \theta_1) \Gamma_\beta(-p, \theta_2) \\ & + D^2 \delta_{12}^{(-(k+p))} D_2^\beta(-(k)) D_1^\alpha(k) D^2 \delta_{21}^{(-k)} \Gamma_\alpha(p, \theta_1) \Gamma_\beta(-p, \theta_2) \\ & \left. + D_1^\alpha(-(k+p)) D^2 \delta_{12}^{(-(k+p))} D_2^\beta(-(k)) D^2 \delta_{21}^{(-k)} \Gamma_\alpha(p, \theta_1) \Gamma_\beta(-p, \theta_2) \right\}, \end{aligned} \quad (\text{A.4})$$



then, integrating by parts the first term in the second line in Eq. (A.4),

$$\begin{aligned}
 & -D_2^\beta (k+p) D^2 \delta_{12}^{-(k+p)} D_1^\alpha (k) D^2 \delta_{21}^{(-k)} \Gamma_\alpha (p, \theta_1) \Gamma_\beta (-p, \theta_2) = \\
 & = -\frac{1}{2} \delta_{12} \left\{ D_{\rho 1} D_1^\rho D_2^\beta D_1^\alpha D_2^2 \delta_{21} \Gamma_\alpha^{(1)} \Gamma_\beta^{(2)} + D_{\rho 1} D_2^\beta D_1^\alpha D_2^2 \delta_{21} D_1^\rho \Gamma_\alpha^{(1)} \Gamma_\beta^{(2)} \right. \\
 & + D_{\rho 1} D_1^\rho D_1^\alpha D_2^2 \delta_{21} \Gamma_\alpha^{(1)} D_2^\beta \Gamma_\beta^{(2)} - D_{\rho 1} D_1^\alpha D_2^2 \delta_{21} D_1^\rho \Gamma_\alpha^{(1)} D_2^\beta \Gamma_\beta^{(2)} \\
 & - D_1^\rho D_2^\beta D_1^\alpha D_2^2 \delta_{21} D_{\rho 1} \Gamma_\alpha^{(1)} \Gamma_\beta^{(2)} + D_2^\beta D_1^\alpha D_2^2 \delta_{21} D_{\rho 1} D_1^\rho \Gamma_\alpha^{(1)} \Gamma_\beta^{(2)} \\
 & \left. + D_1^\rho D_1^\alpha D_2^2 \delta_{21} D_{\rho 1} \Gamma_\alpha^{(1)} D_2^\beta \Gamma_\beta^{(2)} + D_1^\alpha D_2^2 \delta_{21} D_{\rho 1} D_1^\rho \Gamma_\alpha^{(1)} D_2^\beta \Gamma_\beta^{(2)} \right\}, \tag{A.5}
 \end{aligned}$$

where  $\Gamma_\alpha (p, \theta_1) = \Gamma_\alpha^{(1)}$ .

By using Eq. (2.29), we can see that some terms are zero, therefore the previous equation is reduced to

$$\begin{aligned}
 & -D_2^\beta (k+p) D^2 \delta_{12}^{-(k+p)} D_1^\alpha (k) D^2 \delta_{21}^{(-k)} \Gamma_\alpha (p, \theta_1) \Gamma_\beta (-p, \theta_2) = \\
 & \delta_{12} \left\{ -D_2^\beta D_2^2 D_2^\alpha D_2^2 \delta_{21} \Gamma_\alpha^{(1)} \Gamma_\beta^{(1)} - D_2^\beta D_2^2 D_2^\alpha D_2^2 \delta_{21} D_1^2 \Gamma_\alpha^{(1)} \Gamma_\beta^{(1)} \right. \\
 & \left. + D_2^2 D_2^\alpha D_2^\rho \delta_{21} D_{\rho 1} \Gamma_\alpha^{(1)} D_2^\beta \Gamma_\beta^{(2)} \right\}, \tag{A.6}
 \end{aligned}$$

now, using the D-algebra, Section 2.2.2 in Eq. (A.6) and integrating in  $\theta_2$ , we obtain

$$\begin{aligned}
 & -\int d^2 \theta_2 D_2^\beta (k+p) D^2 \delta_{12}^{-(k+p)} D_1^\alpha (k) D^2 \delta_{21}^{(-k)} \Gamma_\alpha (p, \theta_1) \Gamma_\beta (-p, \theta_2) \\
 & = \left( k^2 + k^{\alpha\rho} p_\rho^\beta \right) \Gamma_\alpha (p, \theta) \Gamma_\beta (-p, \theta). \tag{A.7}
 \end{aligned}$$

Using a similar procedure, we can find the form of the second term in the third line of Eq. (A.4),

$$\begin{aligned}
 & -\int d^2 \theta_2 D_1^\alpha (- (k+p)) D_2^\beta (k+p) D^2 \delta_{12}^{-(k+p)} D^2 \delta_{21}^{(-k)} \Gamma_\alpha (p, \theta_1) \Gamma_\beta (-p, \theta_2) \\
 & = \left( k^2 + p^2 + 2 k \cdot p \right) \Gamma_\alpha (p, \theta) \Gamma^\alpha (-p, \theta) + \left( k^{\alpha\beta} + p^{\alpha\beta} \right) \Gamma_\alpha (p, \theta) D^2 \Gamma_\beta (-p, \theta). \tag{A.8}
 \end{aligned}$$

For the third term in the four line of Eq. (A.4),

$$\begin{aligned}
 & \int d^2 \theta D^2 \delta_{12}^{-(k+p)} D_2^\beta (- (k)) D_1^\alpha (k) D^2 \delta_{21}^{(-k)} \Gamma_\alpha (p, \theta_1) \Gamma_\beta (-p, \theta_2) \\
 & = - \left( k^2 + k^{\beta\alpha} D^2 \right) \Gamma_\alpha (p, \theta) \Gamma_\beta (-p, \theta). \tag{A.9}
 \end{aligned}$$

The fourth term in Eq. (A.4) yields

$$\begin{aligned}
 & \int d^2 \theta D_1^\alpha (- (k+p)) D^2 \delta_{12}^{-(k+p)} D_2^\beta (- (k)) D^2 \delta_{21}^{(-k)} \Gamma_\alpha (p, \theta_1) \Gamma_\beta (-p, \theta_2) \\
 & = - \left( k^2 + k^{\beta\rho} p_\rho^\alpha \right) \Gamma_\alpha (p, \theta) \Gamma_\beta (-p, \theta). \tag{A.10}
 \end{aligned}$$

Finally, substituting Eqs. (A.7) - (A.10) into Eq. (A.4) we find

$$\begin{aligned} \mathcal{S}_{\Gamma\Gamma}^{(a)-1l} = & \frac{g^2}{4} N \int d^2\theta \int \frac{d^3p}{(2\pi)^3} \int \frac{d^Dk}{(2\pi)^3} \frac{1}{(k+p)^2 k^2} \left\{ - \left( 4k^2 + p^2 + 2k \cdot p \right) C^{\alpha\beta} \right. \\ & \left. + \left( k^{\alpha\rho} p_\rho^\beta - k^{\beta\rho} p_\rho^\alpha + p^{\beta\alpha} D^2 \right) \right\} \Gamma_\alpha(p, \theta) \Gamma_\beta(-p, \theta) . \end{aligned} \quad (\text{A.11})$$

If it use the dimensional regularization this contribution turns out to be finite.

# Appendix B

## Two loops corrections

Here we give details about the perturbative calculations presented in Chapter 4. The general procedure was exemplified for an one-loop graph in Appendix A. For the two-loop diagrams considered here, we use the MATHEMATICA packages FEYNARTS [104] to perform all the topologies and the MATHEMATICA package SUSYMATH [106] to perform the integration by parts, and then we use a set of integrals that are given in Appendix C.

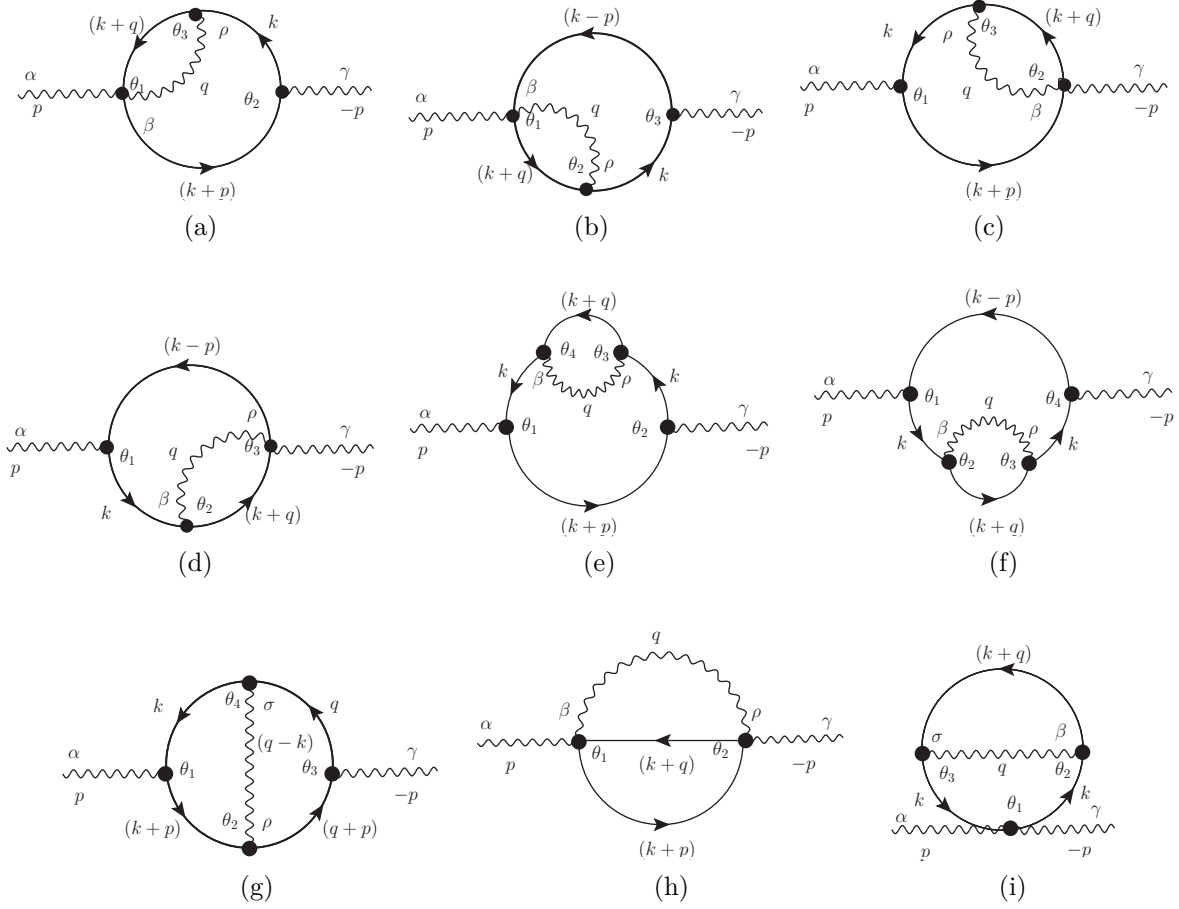
### B.1 Two-point vertex function to gauge superfield

We present a summary of the details of the calculation of the two-point vertex function, up to two loops, for each diagram presented in Figure B.1.

We start with the first diagram, i.e.  $\mathcal{S}_{\Gamma\Gamma}^{(a)}$ ,

$$\begin{aligned} \mathcal{S}_{\Gamma\Gamma}^{(a)} = & \frac{1}{8} i g^4 N \int \frac{d^3 p}{(2\pi)^3} d^2 \theta_1 d^2 \theta_2 d^2 \theta_3 \frac{d^D k d^D q}{(2\pi)^{2D}} \Gamma^\alpha(p, \theta_1) \Gamma_\gamma(-p, \theta_2) \\ & \left\{ + D_2^\gamma(k+p) \frac{D^2}{(k+p)^2} \delta_{12} D_3^\rho(k) \frac{D^2}{k^2} \delta_{23} \frac{D^2}{(k+q)^2} \delta_{31} \frac{(-b q_{\rho\alpha} + a C_{\alpha\rho} D^2)}{q^2} \delta_{13} \right. \\ & - D_2^\gamma(k+p) \frac{D^2}{(k+p)^2} \delta_{12} \frac{D^2}{k^2} \delta_{23} D_3^\rho(-(k+q)) \frac{D^2}{(k+q)^2} \delta_{31} \frac{(-b q_{\rho\alpha} + a C_{\alpha\rho} D^2)}{q^2} \delta_{13} \\ & - \frac{D^2}{(k+p)^2} \delta_{12} D_2^\gamma(-k) \frac{D^2}{k^2} \delta_{23} D_3^\rho(k) \frac{D^2}{(k+q)^2} \delta_{31} \frac{(-b q_{\rho\alpha} + a C_{\alpha\rho} D^2)}{q^2} \delta_{13} \\ & \left. + \frac{D^2}{(k+p)^2} \delta_{12} D_2^\gamma(-k) \frac{D^2}{k^2} \delta_{23} D_3^\rho(-(k+q)) \frac{D^2}{(k+q)^2} \delta_{31} \frac{(-b q_{\rho\alpha} + a C_{\alpha\rho} D^2)}{q^2} \delta_{13} \right\}, \end{aligned} \quad (\text{B.1})$$

where we used a similar procedure as in the one loop case to find the correct sign and the symmetric factor. Now, we can use the SUSYMATH package to perform the integration


 Figure B.1:  $\mathcal{S}_{\Gamma\Gamma}$ 

by parts, then Eq. (B.1) is reduced to,

$$\mathcal{S}_{\Gamma\Gamma}^{(a)} = \frac{1}{8} i g^4 N \int \frac{d^3 p}{(2\pi)^3} d^2 \theta \int \frac{d^D k d^D q}{(2\pi)^{2D}} \Gamma^\alpha(p, \theta) \left\{ \frac{\Delta_{\alpha\beta}^{\Gamma\Gamma} + \Delta_{\alpha\beta}^{\Gamma D^2 \Gamma} D^2}{(k+p)^2 (k+q)^2 q^2 k^2} \right\} \Gamma^\beta(-p, \theta), \quad (\text{B.2})$$

where

$$\begin{aligned} \Delta_{\alpha\beta}^{\Gamma\Gamma} = & -2a (k \cdot p) k_{\alpha\beta} - 2a (k \cdot q) k_{\alpha\beta} - 2a (k \cdot p) q_{\alpha\beta} - b p_{\beta\gamma} q_{\alpha\delta} k^{\gamma\delta} - a C_{\beta\gamma} C^{\delta\epsilon} k_{\alpha\epsilon} q_{\delta\zeta} k^{\gamma\zeta} \\ & + a k_{\alpha\gamma} k_{\beta\delta} p^{\gamma\delta} + a k_{\beta\gamma} q_{\alpha\delta} p^{\gamma\delta} - 4a k_{\alpha\beta} k^2 - a p_{\alpha\beta} k^2 - (a+2b) q_{\alpha\beta} k^2, \end{aligned} \quad (\text{B.3})$$

$$\Delta_{\alpha\beta}^{\Gamma D^2 \Gamma} = -(a+b) C_{\beta\gamma} q_{\alpha\delta} k^{\gamma\delta} - 2a C_{\beta\alpha} k^2. \quad (\text{B.4})$$

Finally, by doing the two loops integration with help of the integrals in Table C.1, we obtain

$$\mathcal{S}_{\Gamma\Gamma}^{(a)} = \mathcal{S}_{\Gamma\Gamma}^{(b)} = \frac{(3a-b)}{8(192\pi^2\epsilon)} N i g^4 \int \frac{d^3 p}{(2\pi)^3} d^2 \theta \Gamma^\alpha(p, \theta) \left\{ -p_{\alpha\beta} + 3 C_{\beta\alpha} D^2 \right\} \Gamma^\beta(-p, \theta). \quad (\text{B.5})$$

The diagram  $\mathcal{S}_{\Gamma\Gamma}^{(c)}$  in Figure B.1 is

$$\mathcal{S}_{\Gamma\Gamma}^{(c)} = \frac{1}{8} i g^4 N \int \frac{d^3 p}{(2\pi)^3} d^2 \theta \int \frac{d^D k d^D q}{(2\pi)^{2D}} \Gamma^\alpha(p, \theta) \left\{ \frac{\Delta_{\alpha\beta}^{\Gamma\Gamma} + \Delta_{\alpha\beta}^{\Gamma D^2 \Gamma} D^2}{(k+p)^2 (k+q)^2 q^2 k^2} \right\} \Gamma^\beta(-p, \theta), \quad (\text{B.6})$$

where

$$\Delta_{\alpha\beta}^{\Gamma D^2 \Gamma} = (a+b) C_{\alpha\gamma} q_{\beta\delta} k^{\gamma\delta} - 2a C_{\beta\alpha} k^2, \quad (\text{B.7})$$

and

$$\begin{aligned} \Delta_{\alpha\beta}^{\Gamma\Gamma} = & -2a (k \cdot p) k_{\alpha\beta} - \left( \frac{1}{2} a + b \right) p_{\alpha\gamma} q_{\beta\delta} k^{\gamma\delta} + \frac{1}{2} a C_{\alpha\gamma} C^{\delta\epsilon} k_{\beta\delta} p_{\epsilon\zeta} k^{\gamma\zeta} + \frac{1}{2} a k_{\alpha\gamma} k_{\beta\delta} p^{\gamma\delta} \\ & + \frac{1}{2} a C_{\alpha\gamma} C^{\delta\epsilon} k_{\delta\zeta} q_{\beta\epsilon} p^{\gamma\zeta} - 4a k_{\alpha\beta} k^2 - a p_{\alpha\beta} k^2 - 2(a+b) q_{\alpha\beta} k^2, \end{aligned} \quad (\text{B.8})$$

then, using Table C.2, we find

$$\mathcal{S}_{\Gamma\Gamma}^{(c)} = \mathcal{S}_{\Gamma\Gamma}^{(d)} = \frac{1}{8} \left( \frac{(3a-b)}{192\pi^2\epsilon} \right) N i g^4 \int \frac{d^3 p}{(2\pi)^3} d^2 \theta \Gamma^\alpha(p, \theta) \left\{ -p_{\alpha\beta} + 3 C_{\beta\alpha} D^2 \right\} \Gamma^\beta(-p, \theta). \quad (\text{B.9})$$

The diagram  $\mathcal{S}_{\Gamma\Gamma}^{(e)}$  in the Figure B.1 is

$$\mathcal{S}_{\Gamma\Gamma}^{(e)} = -\frac{1}{32} i g^4 N \int \frac{d^3 p}{(2\pi)^3} d^2 \theta \int \frac{d^D k d^D q}{(2\pi)^{2D}} \Gamma^\alpha(p, \theta) \frac{\left\{ \Delta_{\alpha\beta}^{\Gamma\Gamma} + \Delta_{\alpha\beta}^{\Gamma D^2 \Gamma} D^2 \right\}}{(k+p)^2 (k+q)^2 q^2 (k^2)^2} \Gamma^\beta(-p, \theta), \quad (\text{B.10})$$

where

$$\begin{aligned} \Delta_{\alpha\beta}^{\Gamma\Gamma} = & (-20a + 4b) (k \cdot p) (k \cdot q) k_{\alpha\beta} + (2a + 2b) C_{\alpha\gamma} C_{\beta\delta} (k \cdot q) p_{\epsilon\zeta} k^{\gamma\zeta} k^{\delta\epsilon} \\ & + (-2a - 2b) C_{\alpha\gamma} C_{\beta\delta} (k \cdot p) q_{\epsilon\zeta} k^{\gamma\epsilon} k^{\delta\zeta} + \frac{1}{2} a C_{\alpha\gamma} C_{\beta\delta} p_{\epsilon\zeta} q_{\eta\theta} k^{\gamma\theta} k^{\delta\zeta} k^{\epsilon\eta} \\ & + (8a - 4b) (k \cdot q) k_{\alpha\gamma} k_{\beta\delta} p^{\gamma\delta} - \left( \frac{1}{2} a + b \right) C_{\alpha\gamma} C^{\delta\epsilon} k_{\beta\zeta} k_{\epsilon\eta} q_{\delta\theta} k^{\gamma\theta} p^{\zeta\eta} \\ & - 2a (k \cdot p) k_{\alpha\gamma} k_{\beta\delta} q^{\delta\gamma} + a k_{\alpha\gamma} k_{\beta\delta} k_{\epsilon\zeta} p^{\delta\epsilon} q^{\zeta\gamma} - 20a (k \cdot p) k_{\alpha\beta} k^2 \\ & + (-24a + 6b) (k \cdot q) k_{\alpha\beta} k^2 - (8a - 2b) (k \cdot q) p_{\alpha\beta} k^2 - 2a (k \cdot p) q_{\alpha\beta} k^2 \\ & + \frac{7}{2} a C_{\alpha\gamma} C_{\beta\delta} p_{\epsilon\zeta} k^{\gamma\zeta} k^{\delta\epsilon} k^2 - \left( \frac{5}{2} a + 3b \right) C_{\alpha\gamma} C_{\beta\delta} q_{\epsilon\zeta} k^{\gamma\epsilon} k^{\delta\zeta} k^2 \\ & + \frac{13}{2} a k_{\alpha\gamma} k_{\beta\delta} p^{\gamma\delta} k^2 + \frac{1}{2} a k_{\beta\gamma} q_{\alpha\delta} p^{\gamma\delta} k^2 - \left( \frac{1}{2} a + b \right) C_{\alpha\gamma} C_{\beta\delta} q_{\epsilon\zeta} k^{\delta\epsilon} p^{\gamma\zeta} k^2 \end{aligned}$$

$$\begin{aligned}
 & -\frac{1}{2} a k_{\beta\gamma} p_{\alpha\delta} q^{\gamma\delta} k^2 - (a+b) C_{\alpha\gamma} C_{\beta\delta} k_{\epsilon\zeta} p^{\delta\zeta} q^{\gamma\epsilon} k^2 + \frac{1}{2} a C_{\alpha\gamma} C_{\beta\delta} p_{\epsilon\zeta} k^{\delta\epsilon} q^{\gamma\zeta} k^2 \\
 & -\frac{3}{2} a k_{\alpha\gamma} k_{\beta\delta} q^{\delta\gamma} k^2 - (a+b) C_{\alpha\gamma} C_{\beta\delta} k_{\epsilon\zeta} p^{\gamma\zeta} q^{\delta\epsilon} k^2 - 32 a k_{\alpha\beta} k^4 - 14 a p_{\alpha\beta} k^4 \\
 & - (4a+3b) q_{\alpha\beta} k^4,
 \end{aligned} \tag{B.11}$$

$$\begin{aligned}
 \Delta_{\alpha\beta}^{\Gamma D^2 \Gamma} = & - (6a-2b) C_{\beta\alpha} (k \cdot q) k^2 + \left(\frac{3}{2}a-b\right) C_{\beta\gamma} q_{\alpha\delta} k^{\gamma\delta} k^2 + \frac{3}{2} a C_{\alpha\gamma} q_{\beta\delta} k^{\gamma\delta} k^2 \\
 & + \left(\frac{1}{2}a-b\right) C_{\beta\gamma} k_{\alpha\delta} q^{\gamma\delta} k^2 + \frac{5}{2} a C_{\alpha\gamma} k_{\beta\delta} q^{\gamma\delta} k^2 - 8a C_{\beta\alpha} k^4,
 \end{aligned} \tag{B.12}$$

using Table C.3, we find

$$\mathcal{S}_{\Gamma\Gamma}^{(e)} = \mathcal{S}_{\Gamma\Gamma}^{(f)} = -\frac{1}{4} \left( \frac{a N}{192\pi^2\epsilon} \right) i g^4 \int \frac{d^3 p}{(2\pi)^3} d^2\theta \Gamma^\alpha(p, \theta) \left\{ p_{\alpha\beta} + 3 C_{\beta\alpha} D^2 \right\} \Gamma^\beta(-p, \theta). \tag{B.13}$$

The diagram  $\mathcal{S}_{\Gamma\Gamma}^{(g)}$  in the Figure B.1 is

$$\mathcal{S}_{\Gamma\Gamma}^{(g)} = \frac{1}{32} i g^4 N \int \frac{d^3 p}{(2\pi)^3} d^2\theta \int \frac{d^D k d^D q}{(2\pi)^{2D}} \Gamma^\alpha(p, \theta) \frac{\left\{ \Delta_{\alpha\beta(1)}^{\Gamma\Gamma} + \Delta_{\alpha\beta(2)}^{\Gamma\Gamma} + \Delta_{\alpha\beta}^{\Gamma D^2 \Gamma} D^2 \right\}}{(k+p)^2 (q+p)^2 (k-q)^2 q^2 k^2} \Gamma^\beta(-p, \theta), \tag{B.14}$$

where

$$\begin{aligned}
 \Delta_{\alpha\beta(1)}^{\Gamma\Gamma} = & -\frac{1}{2} a C_{\alpha\gamma} C^{\delta\epsilon} p_{\epsilon\zeta} q_{\beta\eta} q_{\delta\theta} k^{\gamma\theta} k^{\zeta\eta} + 3b C_{\alpha\gamma} C^{\delta\epsilon} k_{\epsilon\zeta} q_{\beta\eta} q_{\delta\theta} k^{\gamma\theta} p^{\zeta\eta} \\
 & + \frac{1}{2} a C_{\beta\gamma} C^{\delta\epsilon} k_{\alpha\zeta} p_{\epsilon\eta} q_{\delta\theta} k^{\eta\theta} q^{\gamma\zeta} - a C_{\beta\gamma} C^{\delta\epsilon} k_{\alpha\zeta} k_{\epsilon\eta} q_{\delta\theta} p^{\eta\theta} q^{\gamma\zeta} \\
 & + \frac{1}{2} a C_{\beta\gamma} C^{\delta\epsilon} k_{\alpha\zeta} k_{\delta\eta} q_{\epsilon\theta} p^{\eta\theta} q^{\gamma\zeta} + (a+3b) C_{\beta\gamma} C^{\delta\epsilon} k_{\alpha\zeta} k_{\delta\eta} q_{\epsilon\theta} p^{\zeta\theta} q^{\gamma\eta} \\
 & - a k_{\alpha\gamma} k_{\delta\epsilon} q_{\beta\zeta} p^{\epsilon\zeta} q^{\delta\gamma} - 2a C_{\alpha\gamma} C_{\beta\delta} (k \cdot q) p_{\epsilon\zeta} k^{\gamma\zeta} q^{\delta\epsilon} + (4a-4b) (p \cdot q) k_{\alpha\beta} k^2 \\
 & - \left(\frac{1}{2}a+b\right) C_{\alpha\gamma} C_{\beta\delta} p_{\epsilon\zeta} q_{\eta\theta} k^{\gamma\eta} k^{\zeta\theta} q^{\delta\epsilon} + \frac{1}{2} a C_{\alpha\gamma} C_{\beta\delta} k_{\epsilon\zeta} q_{\eta\theta} k^{\gamma\theta} p^{\zeta\eta} q^{\delta\epsilon} \\
 & + \frac{1}{2} a C_{\alpha\gamma} C_{\beta\delta} k_{\epsilon\zeta} q_{\eta\theta} k^{\gamma\eta} p^{\epsilon\theta} q^{\delta\zeta} - b C_{\alpha\gamma} C_{\beta\delta} k_{\epsilon\zeta} p_{\eta\theta} k^{\gamma\theta} q^{\delta\zeta} q^{\epsilon\eta} - 2a (k \cdot q) q_{\alpha\beta} k^2, \\
 & - \frac{1}{2} a C_{\beta\gamma} C^{\delta\epsilon} k_{\alpha\zeta} k_{\delta\eta} p_{\epsilon\theta} q^{\gamma\theta} q^{\zeta\eta} - \frac{1}{2} a C_{\beta\gamma} C^{\delta\epsilon} k_{\alpha\zeta} k_{\delta\eta} p_{\epsilon\theta} q^{\gamma\eta} q^{\zeta\theta} \\
 & + \frac{1}{2} a p_{\alpha\gamma} q_{\beta\delta} k^{\gamma\delta} k^2 - \left(\frac{3}{2}a-b\right) k_{\alpha\gamma} q_{\beta\delta} p^{\gamma\delta} k^2 - \frac{1}{2} a q_{\alpha\gamma} q_{\beta\delta} p^{\delta\gamma} k^2 - 4a (k \cdot p) q_{\alpha\beta} k^2
 \end{aligned} \tag{B.15}$$

$$\begin{aligned}
 \Delta_{\alpha\beta(2)}^{\Gamma\Gamma} = & - (2a - 2b) C_{\alpha\gamma} C_{\beta\delta} q_{\epsilon\zeta} k^{\gamma\epsilon} p^{\delta\zeta} k^2 + \frac{3}{2} a C_{\alpha\gamma} C_{\beta\delta} p_{\epsilon\zeta} k^{\gamma\zeta} q^{\delta\epsilon} k^2 + 4b (p \cdot q) q_{\alpha\beta} k^2 \\
 & + a C_{\alpha\gamma} C_{\beta\delta} k_{\epsilon\zeta} p^{\gamma\zeta} q^{\delta\epsilon} k^2 + a C_{\alpha\gamma} C_{\beta\delta} k_{\epsilon\zeta} q^{\gamma\zeta} q^{\delta\epsilon} k^2 + 2a C_{\alpha\gamma} C_{\beta\delta} p_{\epsilon\zeta} q^{\gamma\zeta} q^{\delta\epsilon} k^2 \\
 & + b C_{\alpha\gamma} C_{\beta\delta} p_{\epsilon\zeta} k^{\gamma\epsilon} q^{\delta\zeta} k^2 + \frac{1}{2} a C_{\alpha\gamma} C_{\beta\delta} k_{\epsilon\zeta} p^{\gamma\epsilon} q^{\delta\zeta} k^2 + (6a + 4b) (k \cdot p) k_{\alpha\beta} q^2 \\
 & + \left(\frac{1}{2}a + 2b\right) C_{\alpha\gamma} C_{\beta\delta} p_{\epsilon\zeta} q^{\gamma\epsilon} q^{\delta\zeta} k^2 + (4a - 4b) (k \cdot p) q_{\alpha\beta} q^2 + \frac{1}{2} a p_{\alpha\gamma} q_{\beta\delta} k^{\gamma\delta} q^2 \\
 & + (a + 2b) C_{\alpha\gamma} C_{\beta\delta} p_{\epsilon\zeta} k^{\gamma\zeta} k^{\delta\epsilon} q^2 - \frac{1}{2} a C_{\alpha\gamma} C_{\beta\delta} p_{\epsilon\zeta} k^{\gamma\epsilon} k^{\delta\zeta} q^2 + \frac{1}{2} a k_{\alpha\gamma} k_{\beta\delta} p^{\gamma\delta} q^2 \\
 & - \left(\frac{7}{4}a - 2b\right) k_{\alpha\gamma} q_{\beta\delta} p^{\gamma\delta} q^2 - a k_{\alpha\gamma} k_{\beta\delta} p^{\delta\gamma} q^2 + \left(\frac{3}{4}a + b\right) C_{\alpha\gamma} C_{\beta\delta} p_{\epsilon\zeta} k^{\gamma\zeta} q^{\delta\epsilon} q^2 \\
 & - \left(\frac{3}{2}a - b\right) C_{\alpha\gamma} C_{\beta\delta} k_{\epsilon\zeta} p^{\gamma\zeta} q^{\delta\epsilon} q^2 - (a + b) C_{\alpha\gamma} C_{\beta\delta} p_{\epsilon\zeta} k^{\gamma\epsilon} q^{\delta\zeta} q^2 \\
 & - (a - b) C_{\alpha\gamma} C_{\beta\delta} k_{\epsilon\zeta} p^{\gamma\epsilon} q^{\delta\zeta} q^2 + a k_{\alpha\beta} k^2 q^2 - (13a + 4b) p_{\alpha\beta} k^2 q^2, \quad (B.16)
 \end{aligned}$$

and

$$\begin{aligned}
 \Delta_{\alpha\beta}^{\Gamma D^2 \Gamma} = & - (a + 2b) C_{\alpha\gamma} q_{\beta\delta} q_{\epsilon\zeta} k^{\gamma\zeta} k^{\delta\epsilon} + 4a C_{\beta\gamma} (k \cdot q) k_{\alpha\delta} q^{\gamma\delta} + \frac{1}{2} a C_{\beta\gamma} k_{\alpha\delta} k_{\epsilon\zeta} q^{\gamma\zeta} q^{\delta\epsilon} \\
 & - \left(\frac{5}{2}a + 4b\right) C_{\alpha\gamma} C_{\beta\delta} C^{\epsilon\zeta} k_{\zeta\eta} q_{\epsilon\theta} k^{\gamma\theta} q^{\delta\eta} + 2(a + b) C_{\beta\gamma} k_{\alpha\delta} k_{\epsilon\zeta} q^{\gamma\zeta} q^{\delta\epsilon} \\
 & + 2b C_{\alpha\gamma} q_{\beta\delta} k^{\gamma\delta} k^2 + 2b C_{\beta\gamma} k_{\alpha\delta} q^{\gamma\delta} k^2 + \left(\frac{1}{2}a - b\right) C_{\alpha\gamma} q_{\beta\delta} k^{\gamma\delta} q^2 \\
 & + \left(\frac{1}{2}a - b\right) C_{\beta\gamma} k_{\alpha\delta} q^{\gamma\delta} q^2 - (2a + 8b) C_{\beta\alpha} k^2 q^2, \quad (B.17)
 \end{aligned}$$

using Table C.4, we find,

$$\mathcal{S}_{\Gamma\Gamma}^{(g)} = \frac{1}{2} \left( \frac{N}{192\pi^2\epsilon} \right) i g^4 \int \frac{d^3p}{(2\pi)^3} d^2\theta \Gamma^\alpha(p, \theta) \left\{ (4a + b) p_{\alpha\beta} + 3b C_{\beta\alpha} D^2 \right\} \Gamma^\beta(-p, \theta). \quad (B.18)$$

The diagram  $\mathcal{S}_{\Gamma\Gamma}^{(h)}$  in the Figure B.1 is

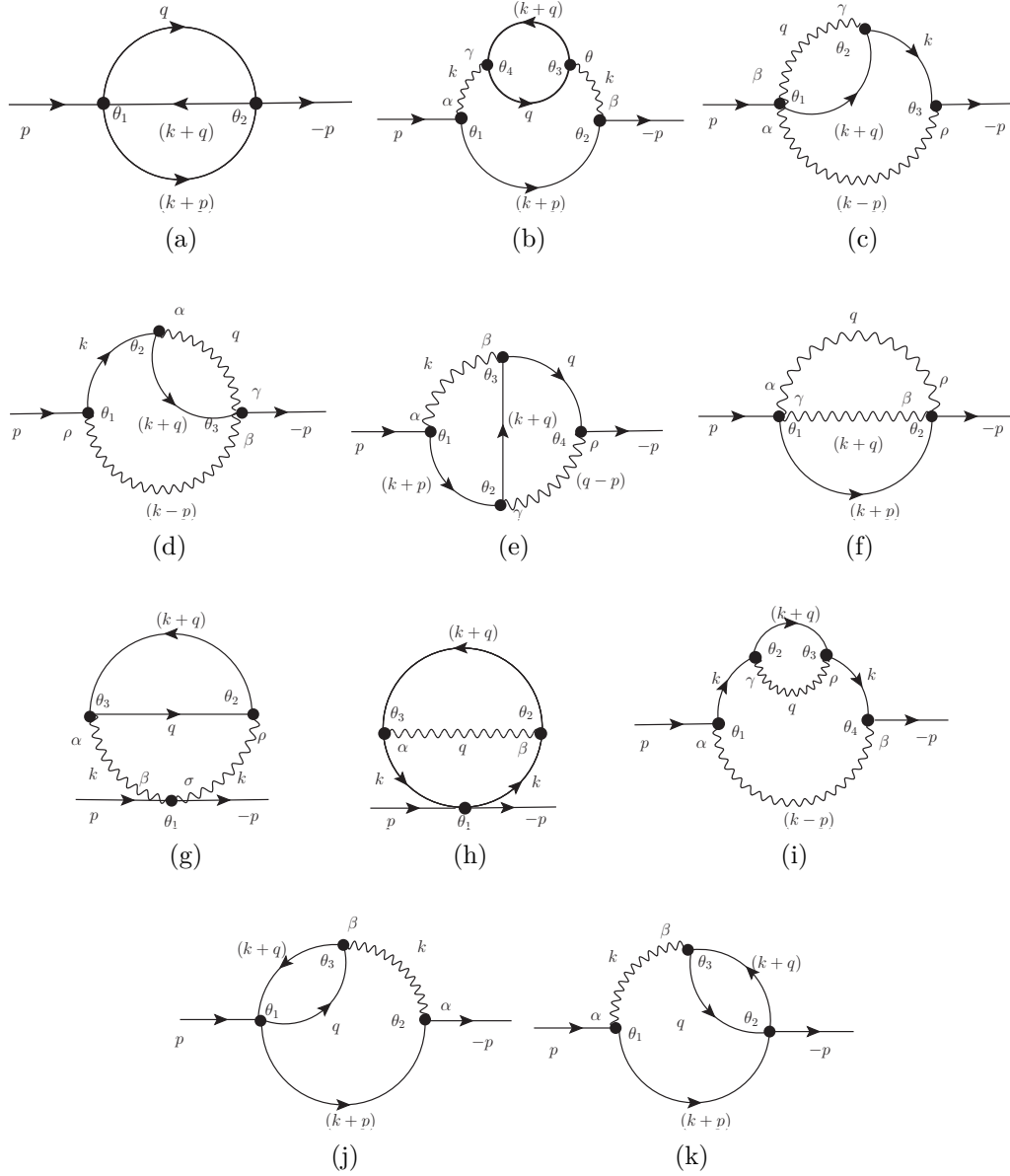
$$\mathcal{S}_{\Gamma\Gamma}^{(h)} = -\frac{1}{2} i g^4 N \int \frac{d^3p}{(2\pi)^3} d^2\theta \frac{d^D k d^D q}{(2\pi)^{2D}} \Gamma^\alpha(p, \theta) \frac{\{-b q_{\alpha\beta} - a C_{\beta\alpha} D^2\}}{(k+p)^2 (k+q)^2 q^2} \Gamma^\beta(-p, \theta), \quad (B.19)$$

using Eq. (C.13) and Eq. (C.14), we find

$$\mathcal{S}_{\Gamma\Gamma}^{(h)} = -\left( \frac{N}{192\pi^2\epsilon} \right) i g^4 \int \frac{d^3p}{(2\pi)^3} d^2\theta \Gamma^\alpha(p, \theta) \left\{ b p_{\alpha\beta} + 3a C_{\beta\alpha} D^2 \right\} \Gamma^\beta(-p, \theta). \quad (B.20)$$

Finally,  $\mathcal{S}_{\Gamma\Gamma}^{(i)}$  in the Figure B.1 is

$$\mathcal{S}_{\Gamma\Gamma}^{(i)} = 0, \quad (B.21)$$


 Figure B.2:  $\mathcal{S}_{\Phi\Phi}$ 

## B.2 Two-point vertex function to the scalar superfield

In this section we give details on the two-point vertex functions associated to the scalar superfield, a set of diagrams represented in Figure B.2.

We start with the computation of diagram  $\mathcal{S}_{\Phi\Phi}^{(a)}$  in Figure B.2,

$$\mathcal{S}_{\Phi\Phi}^{(a)} = i (N+1) \frac{\lambda^2}{4} \int \frac{d^3p}{(2\pi)^3} d^2\theta \frac{d^D k d^D q}{(2\pi)^{2D}} \frac{\bar{\Phi}_i(p, \theta) D^2 \Phi_i(-p, \theta)}{(k+p)^2 (k+q)^2 q^2}, \quad (\text{B.22})$$



using Eq. (C.14), we obtain

$$\mathcal{S}_{\Phi\Phi}^{(a)} = -\frac{i\lambda^2(N+1)}{4(32\pi^2\epsilon)} \int \frac{d^3p}{(2\pi)^3} d^2\theta \bar{\Phi}_i(p, \theta) D^2\Phi_i(-p, \theta) . \quad (\text{B.23})$$

The diagram  $\mathcal{S}_{\Phi\Phi}^{(b)}$  in the Figure B.2 is

$$\begin{aligned} \mathcal{S}_{\Phi\Phi}^{(b)} = & -\frac{1}{64} i g^4 N \int \frac{d^3p}{(2\pi)^3} d^2\theta \bar{\Phi}_i(p, \theta) D^2\Phi_i(-p, \theta) \times \\ & \int \frac{d^D k d^D q}{(2\pi)^{2D}} \left\{ \frac{-8(a^2 + 6ab + b^2)[k \cdot q + q^2]k^2 + 4(a-b)^2(k^2)^2}{(k+p)^2(k+q)^2(k^2)^2 q^2} \right\} , \end{aligned} \quad (\text{B.24})$$

using Eq. (C.14) and Eq. (C.16), by power counting one of these three integrals is finite, then

$$\mathcal{S}_{\Phi\Phi}^{(b)} = \frac{1}{8} \left( \frac{(a+b)^2}{32\pi^2\epsilon} \right) i g^4 N \int \frac{d^3p}{(2\pi)^3} d^2\theta \bar{\Phi}_i(p, \theta) D^2\Phi_i(-p, \theta) . \quad (\text{B.25})$$

Following the same procedure explained before, we consider the next diagrams  $\mathcal{S}_{\Phi\Phi}^{(c)}$  and  $\mathcal{S}_{\Phi\Phi}^{(d)}$  in the Figure B.2,

$$\mathcal{S}_{\Phi\Phi}^{(c)} = \mathcal{S}_{\Phi\Phi}^{(d)} = \frac{1}{16} i g^4 \int \frac{d^3p}{(2\pi)^3} d^2\theta \int \frac{d^D k d^D q}{(2\pi)^{2D}} \frac{4(a^2 + ab)k \cdot q + 8a^2 k^2}{(k-p)^2(k+q)^2 k^2 q^2} \bar{\Phi}_i(p, \theta) D^2\Phi_i(-p, \theta) , \quad (\text{B.26})$$

using Eq. (C.14) and Eq. (C.16), we find

$$\mathcal{S}_{\Phi\Phi}^{(c)} = \mathcal{S}_{\Phi\Phi}^{(d)} = \frac{1}{8} \left( \frac{ab - 3a^2}{32\pi^2\epsilon} \right) i g^4 \int \frac{d^3p}{(2\pi)^3} d^2\theta \bar{\Phi}_i(p, \theta) D^2\Phi_i(-p, \theta) . \quad (\text{B.27})$$

The diagram  $\mathcal{S}_{\Phi\Phi}^{(e)}$  in the Figure B.2 is

$$\begin{aligned} \mathcal{S}_{\Phi\Phi}^{(e)} = & -\frac{1}{64} i g^4 \int \frac{d^3p}{(2\pi)^3} d^2\theta \int \frac{d^D k d^D q}{(2\pi)^{2D}} \frac{\Delta(k, q)}{(k+p)^2(q-p)^2(k+q)^2 k^2 q^2} \\ & \times \bar{\Phi}_i(p, \theta) D^2\Phi_i(-p, \theta) , \end{aligned} \quad (\text{B.28})$$

where

$$\begin{aligned} \Delta(k, q) = & -4(b^2 + 2ab + 4a^2)(k \cdot q)^2 - 3(2ab + b^2) q_{\alpha\beta} q_{\gamma\delta} k^{\alpha\delta} k^{\beta\gamma} \\ & + (20a^2 + 12ab + 14b^2) k^2 q^2 , \end{aligned} \quad (\text{B.29})$$

using Eq. (C.14) and Eq. (C.20), we find

$$\mathcal{S}_{\Phi\Phi}^{(e)} = \frac{1}{16} \left( \frac{3a^2 + 2ab + 3b^2}{32\pi^2\epsilon} \right) i g^4 \int \frac{d^3p}{(2\pi)^3} d^2\theta \bar{\Phi}_i(p, \theta) D^2\Phi_i(-p, \theta) . \quad (\text{B.30})$$

The diagram  $\mathcal{S}_{\Phi\Phi}^{(f)}$  in the Figure B.2 is

$$\mathcal{S}_{\Phi\Phi}^{(f)} = \frac{1}{8} i g^4 \int \frac{d^3p}{(2\pi)^3} d^2\theta \int \frac{d^D k d^D q}{(2\pi)^{2D}} \frac{-2a^2}{q^2(k+p)^2(k+q)^2} \bar{\Phi}_i(p, \theta) D^2\Phi_i(-p, \theta) , \quad (\text{B.31})$$

using Eq. (C.14), we find

$$\mathcal{S}_{\Phi\Phi}^{(f)} = \frac{1}{4} \left( \frac{a^2}{32\pi^2\epsilon} \right) i g^4 \int \frac{d^3p}{(2\pi)^3} d^2\theta \bar{\Phi}_i(p, \theta) D^2\Phi_i(-p, \theta) . \quad (\text{B.32})$$

The diagrams  $\mathcal{S}_{\Phi\Phi}^{(g)}$  and  $\mathcal{S}_{\Phi\Phi}^{(h)}$  in the Figure B.2 are

$$\mathcal{S}_{\Phi\Phi}^{(g)} = \mathcal{S}_{\Phi\Phi}^{(h)} = 0 , \quad (\text{B.33})$$

after  $D$ 's manipulations.

The diagram  $\mathcal{S}_{\Phi\Phi}^{(i)}$  in the Figure B.2 is

$$\begin{aligned} \mathcal{S}_{\Phi\Phi}^{(i)} &= \frac{1}{64} i g^4 \int \frac{d^3p}{(2\pi)^3} d^2\theta \int \frac{d^D k d^D q}{(2\pi)^{2D}} \frac{-64a^2(k \cdot q)k^2 - 64a^2k^4 - 16(a^2 - ab)k^2q^2}{(k-p)^2(k+q)^2q^2(k^2)^2} \\ &\quad \times \bar{\Phi}_i(p, \theta) D^2\Phi_i(-p, \theta) , \end{aligned} \quad (\text{B.34})$$

using Eqs. (C.14), (C.16) and by power counting, we find

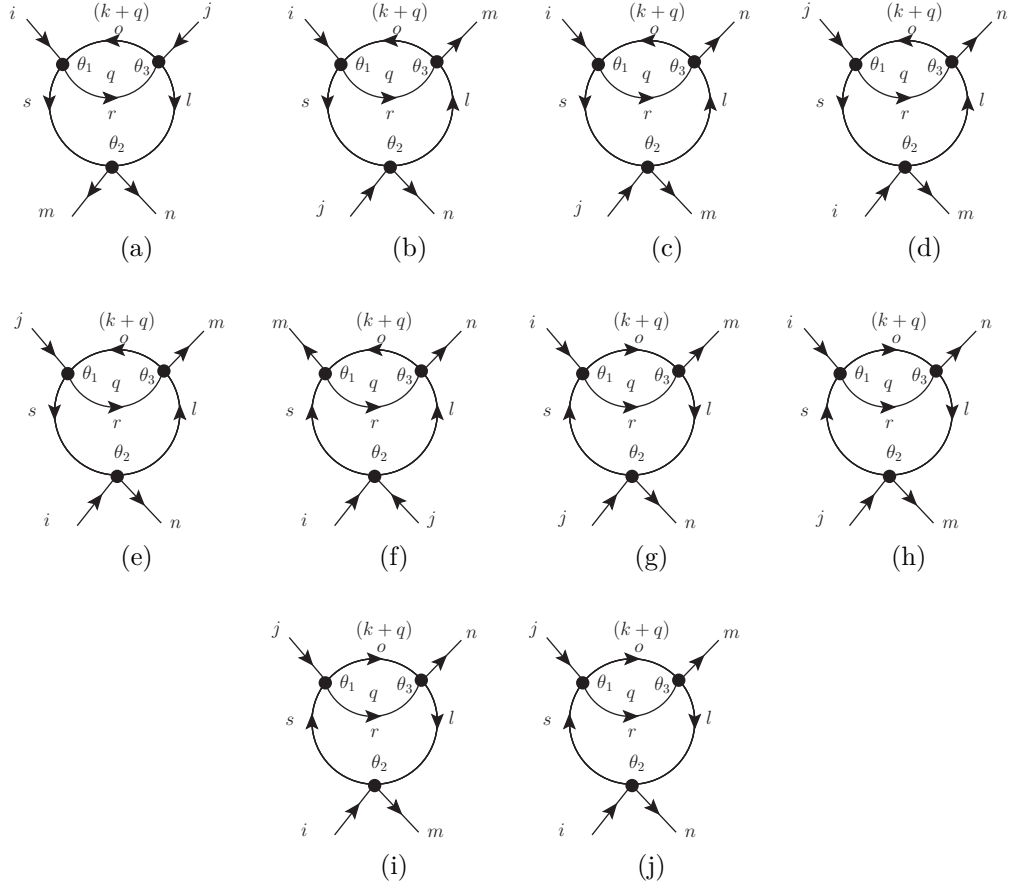
$$\mathcal{S}_{\Phi\Phi}^{(i)} = \frac{1}{2} \left( \frac{a^2}{32\pi^2\epsilon} \right) i g^4 \int \frac{d^3p}{(2\pi)^3} d^2\theta \bar{\Phi}_i(p, \theta) D^2\Phi_i(-p, \theta) . \quad (\text{B.35})$$

Finally, the diagrams  $\mathcal{S}_{\Phi\Phi}^{(j)}$  and  $\mathcal{S}_{\Phi\Phi}^{(k)}$  in the Figure B.2 are

$$\begin{aligned} \mathcal{S}_{\Phi\Phi}^{(j)} &= -\mathcal{S}_{\Phi\Phi}^{(k)} = -\frac{1}{16} i \lambda g^2 (1+N) \int \frac{d^3p}{(2\pi)^3} d^2\theta \int \frac{d^D k d^D q}{(2\pi)^{2D}} \frac{-4(a-b)k \cdot q - 2(a-b)k^2}{(k+p)^2(k+q)^2k^2q^2} \\ &\quad \times \bar{\Phi}_i(p, \theta) D^2\Phi_i(-p, \theta) , \end{aligned} \quad (\text{B.36})$$

using Eqs. (C.14) and (C.16), we find

$$\mathcal{S}_{\Phi\Phi}^{(j)} = \mathcal{S}_{\Phi\Phi}^{(k)} = 0 . \quad (\text{B.37})$$


 Figure B.3:  $\mathcal{S}_{(\bar{\Phi}\Phi)^2}^{(D1)}$ 

### B.3 Four-point vertex function to the scalar superfield

In this section we show all the diagrams that contribute to the four-point vertex function.

We start with the diagrams that contribute with the order  $\mathcal{O}(\lambda^3)$ , in this order there is only one topology that is equivalent to 10 diagrams, the first of then is the diagram  $\mathcal{S}_{(\bar{\Phi}\Phi)^2}^{(D1-a)}$  in the Figure B.3,

$$\mathcal{S}_{(\bar{\Phi}\Phi)^2}^{(D1-a)} = -(3+N) i \frac{\lambda^3}{8} (\delta_{in}\delta_{jm} + \delta_{im}\delta_{jn}) \int \frac{d^D k d^D q}{(2\pi)^{2D}} \frac{-k^2}{(k^2)^2 q^2 (k+q)^2} \int_{\theta} \bar{\Phi}_i \Phi_m \Phi_n \bar{\Phi}_j \quad (\text{B.38})$$

$D1 - a$	$(3 + N) (\delta_{in}\delta_{jm} + \delta_{im}\delta_{jn})$
$D1 - b$	$(2N + 3) \delta_{im}\delta_{jn} + (N + 2) \delta_{in}\delta_{jm}$
$D1 - c$	$(N + 2) \delta_{im}\delta_{jn} + (2N + 3) \delta_{in}\delta_{jm}$
$D1 - d$	$(2N + 3) \delta_{jn}\delta_{im} + (N + 2) \delta_{jm}\delta_{in}$
$D1 - e$	$(N + 2) \delta_{jn}\delta_{im} + (2N + 3) \delta_{jm}\delta_{in}$
$D1 - f$	$(3 + N) (\delta_{in}\delta_{jm} + \delta_{im}\delta_{jn})$
$D1 - g$	$\delta_{in}\delta_{jm} + (2 + N) \delta_{im}\delta_{jn}$
$D1 - h$	$(2 + N) \delta_{in}\delta_{jm} + \delta_{im}\delta_{jn}$
$D1 - i$	$\delta_{in}\delta_{jm} + (N + 2) \delta_{jn}\delta_{im}$
$D1 - j$	$(N + 2) \delta_{jm}\delta_{in} + \delta_{jn}\delta_{im}$

Table B.1: Values of the diagrams in Figure B.3 with common factor  $-\frac{1}{32\pi^2\epsilon} i \frac{\lambda^3}{8} \int_{\theta} \bar{\Phi}_i \Phi_m \Phi_n \bar{\Phi}_j$ .

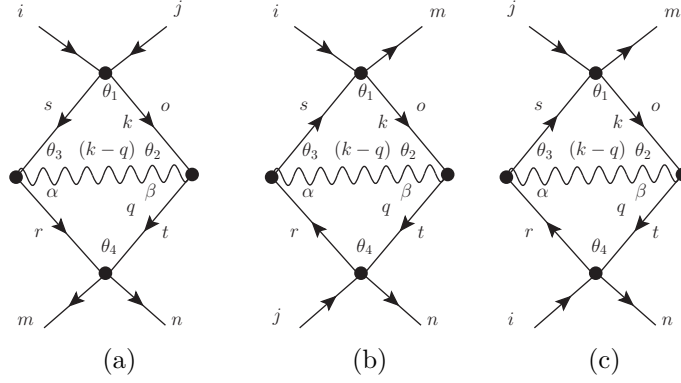


Figure B.4:  $\mathcal{S}_{(\bar{\Phi}\Phi)^2}^{(D2)}$

where  $\int_{\theta} \bar{\Phi}_i \Phi_m \Phi_n \bar{\Phi}_j \equiv \int d^2\theta \bar{\Phi}_i(0, \theta) \Phi_m(0, \theta) \Phi_n(0, \theta) \bar{\Phi}_j(0, \theta)$  and using Eq. (C.14), we find

$$\mathcal{S}_{(\bar{\Phi}\Phi)^2}^{(D1-a)} = -\frac{1}{32\pi^2\epsilon} i \frac{\lambda^3}{8} (3 + N) (\delta_{in}\delta_{jm} + \delta_{im}\delta_{jn}) \int_{\theta} \bar{\Phi}_i \Phi_m \Phi_n \bar{\Phi}_j. \quad (\text{B.39})$$

Then, we can repeat the same procedure for the other diagrams, with the difference between diagrams given only by the manipulations of  $\delta$ 's that can change for each diagram. We provide these values in the Table B.1, for each diagram in Figure B.3. Therefore, the total contribution of diagram  $\mathcal{S}_{(\bar{\Phi}\Phi)^2}^{(D1)}$  turns out to be

$$\mathcal{S}_{(\bar{\Phi}\Phi)^2}^{(D1)} = -i \frac{1}{4(32\pi^2\epsilon)} (5N + 11) \lambda^3 (\delta_{in}\delta_{jm} + \delta_{im}\delta_{jn}) \int_{\theta} \bar{\Phi}_i \Phi_m \Phi_n \bar{\Phi}_j. \quad (\text{B.40})$$

Following with the process, now we consider all diagrams that contribute to the order  $\mathcal{O}(\lambda^2 g^2)$ . In this order there are 5 topologies that are equivalent to 44 diagrams.

$D2 - a$	$-(\delta_{in}\delta_{jm} + \delta_{im}\delta_{jn})$	$D2 - b$	$(N + 2) \delta_{im}\delta_{jn} + \delta_{in}\delta_{mj}$
$D2 - c$	$(N + 2) \delta_{jm}\delta_{in} + \delta_{jn}\delta_{mi}$		

Table B.2: Values of the diagrams in Figure B.4 with common factor

$$-\frac{a}{8(32\pi^2\epsilon)} i \lambda^2 g^2 \int_{\theta} \bar{\Phi}_i \Phi_m \Phi_n \bar{\Phi}_j .$$

$D3 - a$	$2(\delta_{in}\delta_{jm} + \delta_{im}\delta_{jn})$	$D3 - b$	$(N + 2) \delta_{mi}\delta_{jn} + \delta_{mj}\delta_{in}$
$D3 - c$	$(N + 2) \delta_{ni}\delta_{jm} + \delta_{nj}\delta_{im}$	$D3 - d$	$(N + 2) \delta_{mi}\delta_{jn} + \delta_{mj}\delta_{in}$
$D3 - e$	$(N + 2) \delta_{ni}\delta_{jm} + \delta_{nj}\delta_{im}$		

Table B.3: Values of the diagrams in Figure B.5 with common factor

$$-\frac{a}{8(32\pi^2\epsilon)} i \lambda^2 g^2 \int_{\theta} \bar{\Phi}_i \Phi_m \Phi_n \bar{\Phi}_j .$$

We start with  $\mathcal{S}_{(\bar{\Phi}\Phi)^2}^{(D2-a)}$  in the Figure B.4

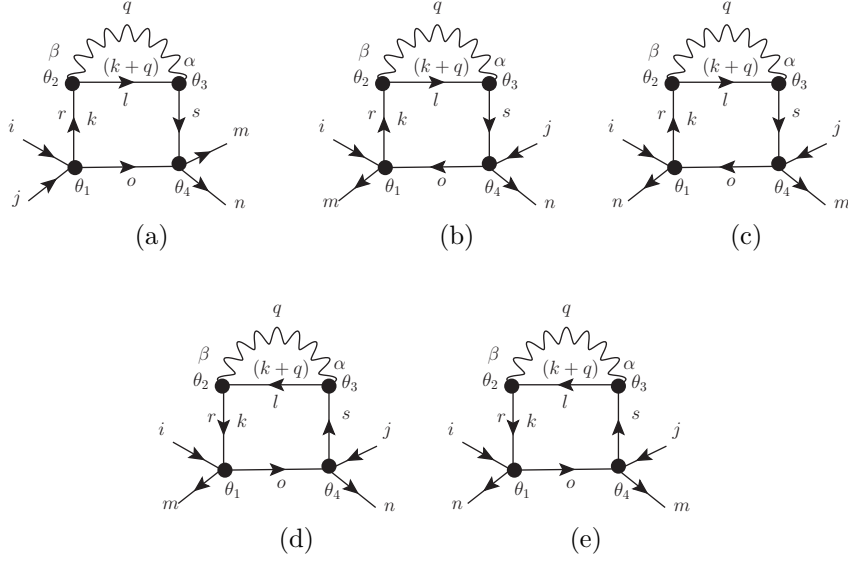
$$\begin{aligned} \mathcal{S}_{(\bar{\Phi}\Phi)^2}^{(D2-a)} &= -\frac{1}{32} i \lambda^2 g^2 (\delta_{im}\delta_{jn} + \delta_{in}\delta_{jm}) \int_{\theta} \bar{\Phi}_i \Phi_m \Phi_n \bar{\Phi}_j \\ &\times \int \frac{d^D k d^D q}{(2\pi)^{2D}} \left\{ \frac{-8 a k^2 q^2}{(k^2)^2 (q^2)^2 (k - q)^2} \right\} , \end{aligned} \quad (\text{B.41})$$

using Eq. (C.14) we find,

$$\mathcal{S}_{(\bar{\Phi}\Phi)^2}^{(D2)} = -\frac{a}{4(32\pi^2\epsilon)} i \lambda^2 g^2 (\delta_{im}\delta_{jn} + \delta_{in}\delta_{jm}) \int_{\theta} \bar{\Phi}_i \Phi_m \Phi_n \bar{\Phi}_j . \quad (\text{B.42})$$

In Table B.2, we give the factors associated to each diagram in Figure B.4. Therefore, the total contribution of diagram  $\mathcal{S}_{(\bar{\Phi}\Phi)^2}^{(D2)}$  is,

$$\mathcal{S}_{(\bar{\Phi}\Phi)^2}^{(D2)} = \frac{a}{4(32\pi^2\epsilon)} (N + 2) i \lambda^2 g^2 (\delta_{im}\delta_{jn} + \delta_{in}\delta_{mj}) \int_{\theta} \bar{\Phi}_i \Phi_m \Phi_n \bar{\Phi}_j . \quad (\text{B.43})$$


 Figure B.5:  $\mathcal{S}_{(\overline{\Phi}\Phi)^2}^{(D3)}$ 

$\mathcal{S}_{(\overline{\Phi}\Phi)^2}^{(D3-a)}$  in the Figure B.5 is

$$\begin{aligned} \mathcal{S}_{(\overline{\Phi}\Phi)^2}^{(D3-a)} &= -\frac{1}{16} i \lambda^2 g^2 (\delta_{in} \delta_{jm} + \delta_{im} \delta_{jn}) \int_{\theta} \overline{\Phi}_i \Phi_m \Phi_n \overline{\Phi}_j \\ &\times \int \frac{d^D k d^D q}{(2\pi)^{2D}} \left\{ \frac{-8a (k \cdot q) k^2 - 8a (k^2)^2 + 2(b-a) k^2 q^2}{(k^2)^3 q^2 (k+q)^2} \right\}, \end{aligned} \quad (\text{B.44})$$

using Eqs. (C.14), (C.16) , we find

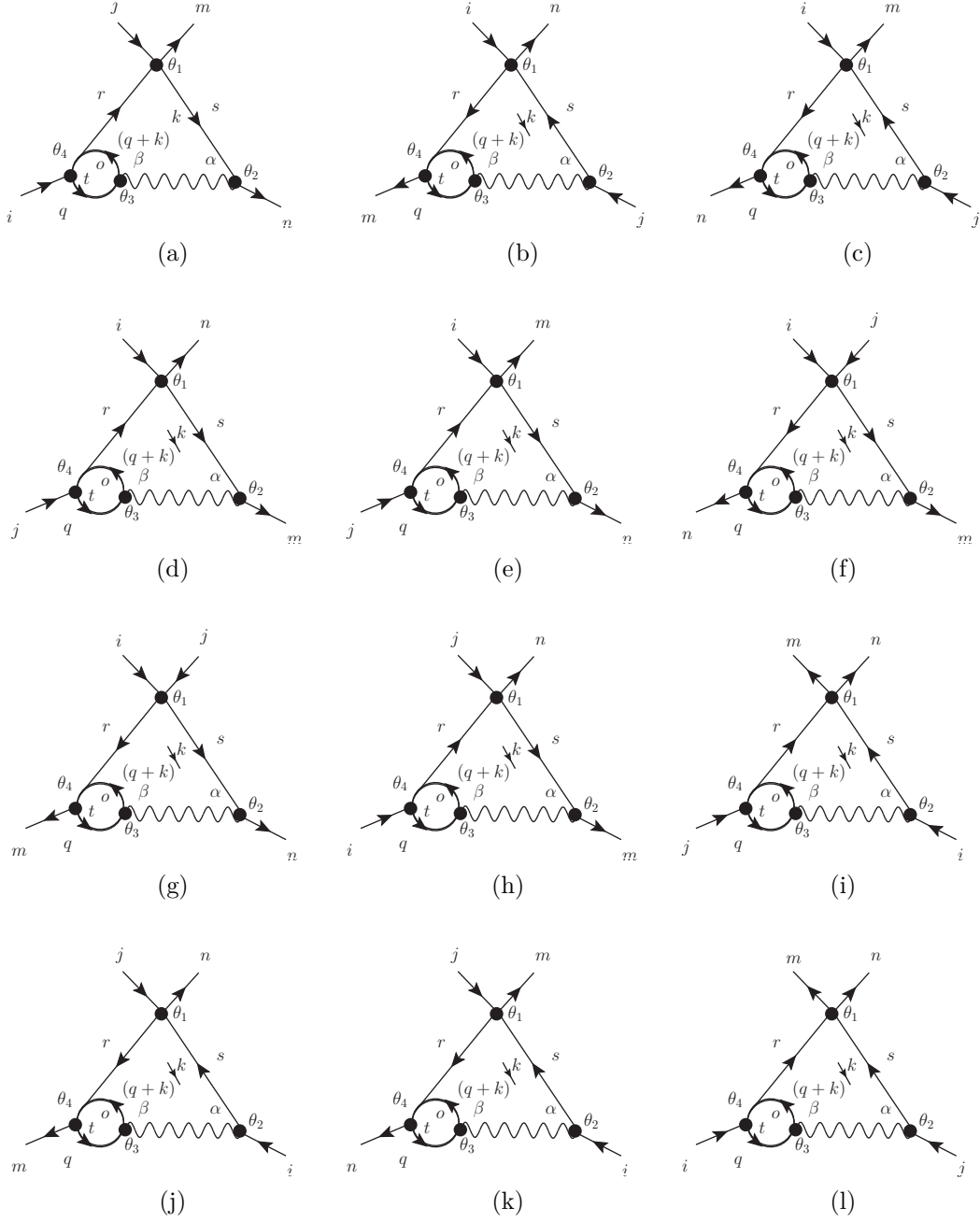
$$\mathcal{S}_{(\overline{\Phi}\Phi)^2}^{(D3-a)} = -\frac{a}{4(32\pi^2\epsilon)} i \lambda^2 g^2 (\delta_{in} \delta_{jm} + \delta_{im} \delta_{jn}) \int_{\theta} \overline{\Phi}_i \Phi_m \Phi_n \overline{\Phi}_j, \quad (\text{B.45})$$

adding the diagrams  $\mathcal{S}_{(\overline{\Phi}\Phi)^2}^{(D3-a)}$  to  $\mathcal{S}_{(\overline{\Phi}\Phi)^2}^{(D3-e)}$  using the values in Table B.3 we find

$$\mathcal{S}_{(\overline{\Phi}\Phi)^2}^{(D3)} = -\frac{a}{4(32\pi^2\epsilon)} (N+4) i \lambda^2 g^2 (\delta_{mi} \delta_{jn} + \delta_{mj} \delta_{in}) \int_{\theta} \overline{\Phi}_i \Phi_m \Phi_n \overline{\Phi}_j. \quad (\text{B.46})$$

$\mathcal{S}_{(\overline{\Phi}\Phi)^2}^{(D4-a)}$  in the Figure B.5 is

$$\begin{aligned} \mathcal{S}_{(\overline{\Phi}\Phi)^2}^{(D4-a)} &= \frac{1}{32} i \lambda^2 g^2 (N+1) (\delta_{jm} \delta_{in} + \delta_{im} \delta_{jn}) \int_{\theta} \overline{\Phi}_i \Phi_m \Phi_n \overline{\Phi}_j \\ &\times \int \frac{d^D k d^D q}{(2\pi)^{2D}} \left\{ \frac{4(a-b) k \cdot q k^2 + 2(a-b) (k^2)^2}{(k^2)^3 q^2 (k+q)^2} \right\}, \end{aligned} \quad (\text{B.47})$$


 Figure B.6:  $\mathcal{S}_{(\bar{\Phi}\Phi)^2}^{(D4)}$

$D5 - a$	$\delta_{in}\delta_{mj} + (N+2)\delta_{im}\delta_{nj}$	$D5 - b$	$-(\delta_{in}\delta_{jm} + \delta_{im}\delta_{jn})$
$D5 - c$	$-(\delta_{mi}\delta_{jn} + (N+2)\delta_{mj}\delta_{ni})$	$D5 - d$	$-((N+2)\delta_{im}\delta_{nj} + \delta_{in}\delta_{mj})$
$D5 - e$	$(N+2)\delta_{jm}\delta_{in} + \delta_{jn}\delta_{mi}$	$D5 - f$	$-(\delta_{ni}\delta_{jm} + \delta_{nj}\delta_{mi})$
$D5 - g$	$-(\delta_{mj}\delta_{in} + (N+2)\delta_{mi}\delta_{jn})$	$D5 - h$	$-(\delta_{mj}\delta_{in} + \delta_{mi}\delta_{jn})$
$D5 - i$	$-((N+2)\delta_{ni}\delta_{jm} + \delta_{im}\delta_{jn})$	$D5 - j$	$-(\delta_{in}\delta_{jm} + \delta_{nj}\delta_{im})$
$D5 - k$	$(N+2)\delta_{ni}\delta_{mj} + \delta_{im}\delta_{jn}$	$D5 - l$	$(N+2)\delta_{mi}\delta_{nj} + \delta_{in}\delta_{jm}$

Table B.4: Values of the diagrams in Figure B.7 with common factor

$$\frac{(a-b)}{16(32\pi^2\epsilon)} i \lambda^2 g^2 \int_{\theta} \bar{\Phi}_i \Phi_m \Phi_n \bar{\Phi}_j .$$

$D6 - a$	$-((N+2)\delta_{im}\delta_{jn} + \delta_{mj}\delta_{ni})$	$D6 - b$	$(N+2)\delta_{im}\delta_{jn} + \delta_{mj}\delta_{ni}$
$D6 - c$	$-(\delta_{jn}\delta_{im} + (N+2)\delta_{jm}\delta_{in})$	$D6 - d$	$\delta_{jn}\delta_{im} + (N+2)\delta_{jm}\delta_{in}$
$D6 - e$	$-(\delta_{jn}\delta_{im} + (N+2)\delta_{jm}\delta_{in})$	$D6 - f$	$\delta_{jn}\delta_{im} + (N+2)\delta_{jm}\delta_{in}$
$D6 - g$	$2(\delta_{jm}\delta_{in} + \delta_{im}\delta_{jn})$	$D6 - h$	$2(\delta_{jm}\delta_{in} + \delta_{im}\delta_{jn})$
$D6 - i$	$2(\delta_{jm}\delta_{in} + \delta_{im}\delta_{jn})$	$D6 - j$	$2(\delta_{jm}\delta_{in} + \delta_{im}\delta_{jn})$
$D6 - k$	$-((N+2)\delta_{jn}\delta_{im} + \delta_{in}\delta_{jm})$	$D6 - l$	$(N+2)\delta_{jn}\delta_{im} + \delta_{in}\delta_{jm}$

Table B.5: Values of the diagrams in Figure B.8 with common factor

$$\frac{(a-b)}{16(32\pi^2\epsilon)} i \lambda^2 g^2 \int_{\theta} \bar{\Phi}_i \Phi_m \Phi_n \bar{\Phi}_j .$$

using Eqs. (C.14) and (C.16), we find

$$\mathcal{S}_{(\bar{\Phi}\Phi)^2}^{(D4-a)} = \mathcal{S}_{(\bar{\Phi}\Phi)^2}^{(D4)} = 0 . \quad (\text{B.48})$$

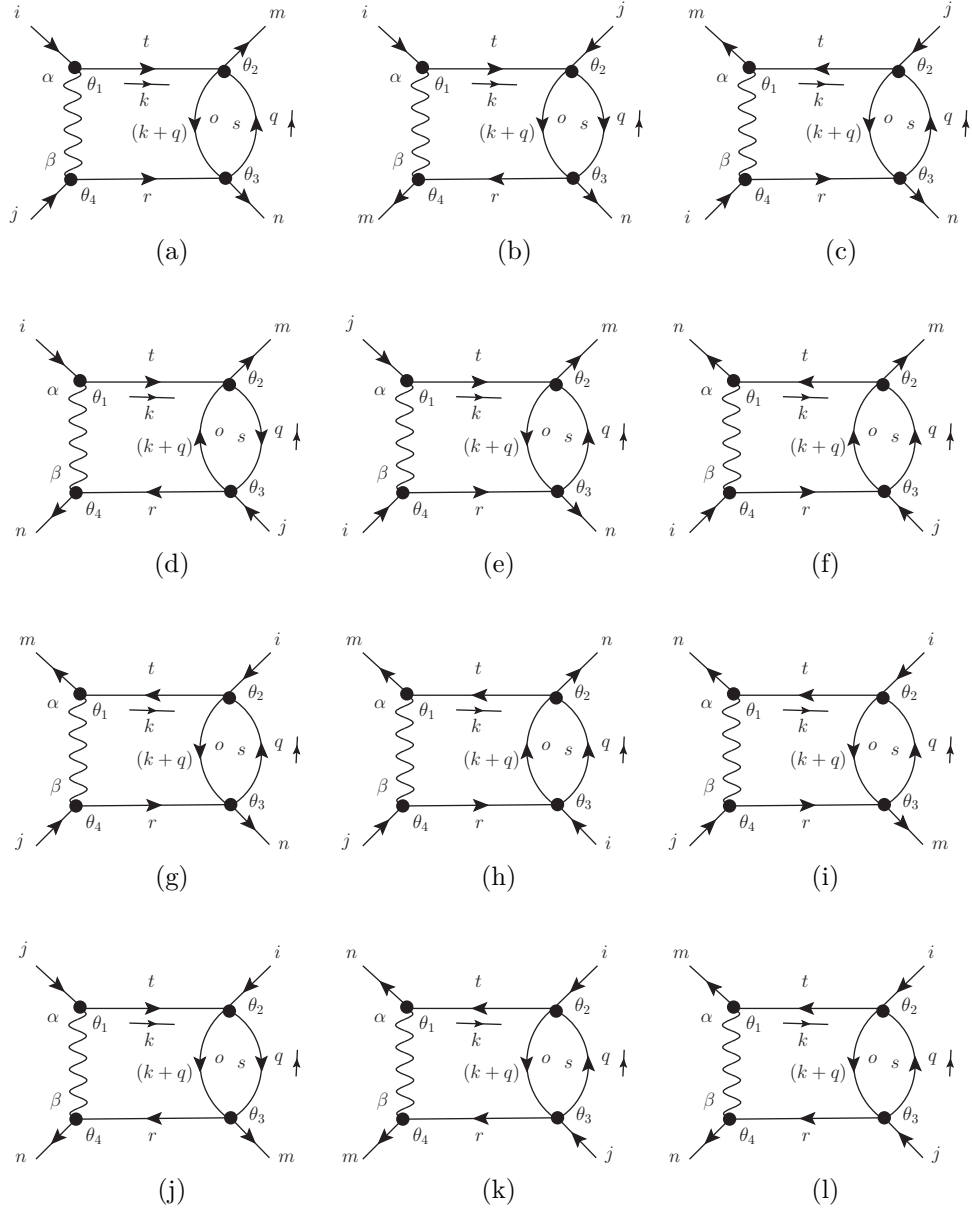
$\mathcal{S}_{(\bar{\Phi}\Phi)^2}^{(D5-a)}$  in the Figure B.5 is

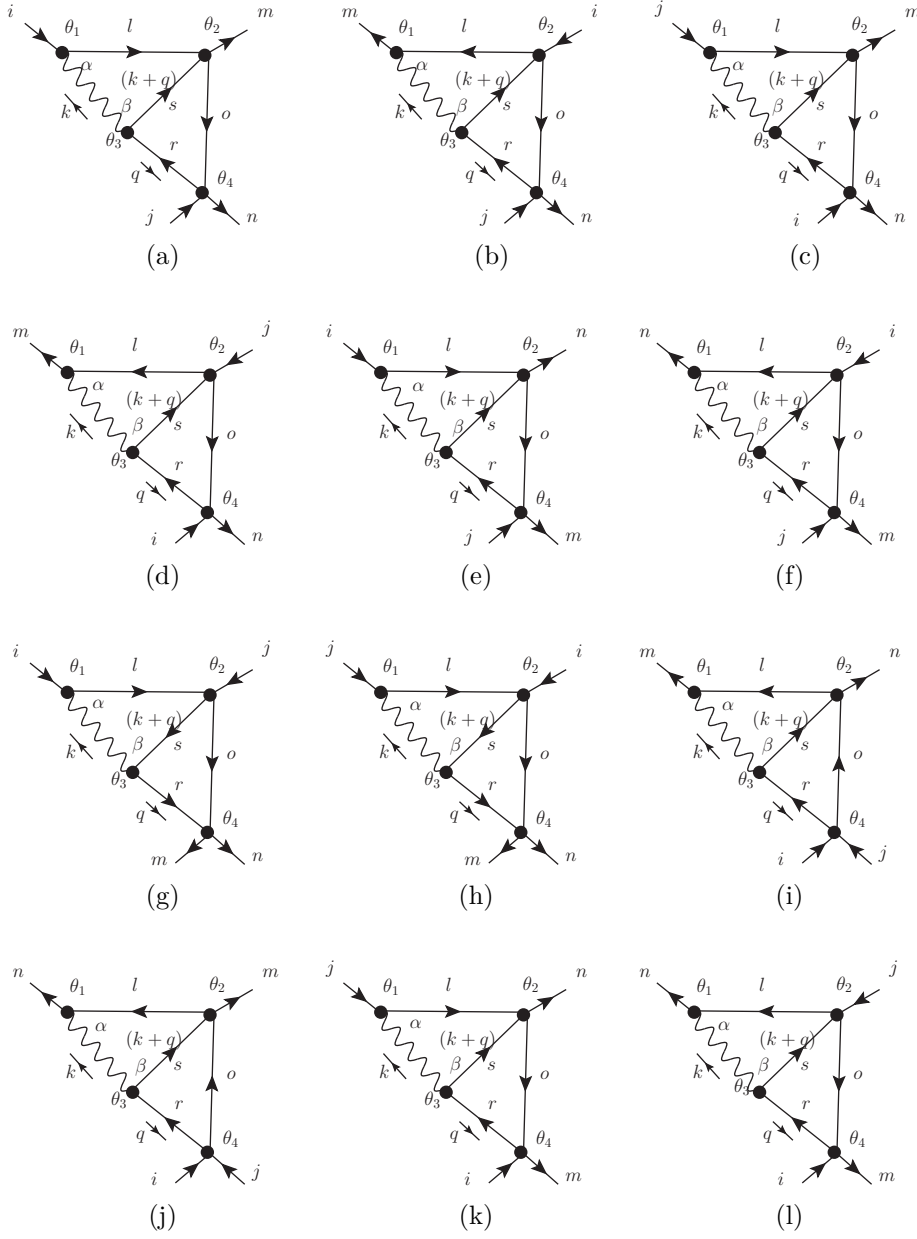
$$\begin{aligned} \mathcal{S}_{(\bar{\Phi}\Phi)^2}^{(D5-a)} &= -\frac{1}{32} i \lambda^2 g^2 [\delta_{in}\delta_{mj} + (N+2)\delta_{im}\delta_{nj}] \int_{\theta} \bar{\Phi}_i \Phi_m \Phi_n \bar{\Phi}_j \\ &\times \int \frac{d^D k d^D q}{(2\pi)^{2D}} \left\{ \frac{2(a-b)(k^2)^2}{(k^2)^3 q^2 (q+k)^2} \right\} , \end{aligned} \quad (\text{B.49})$$

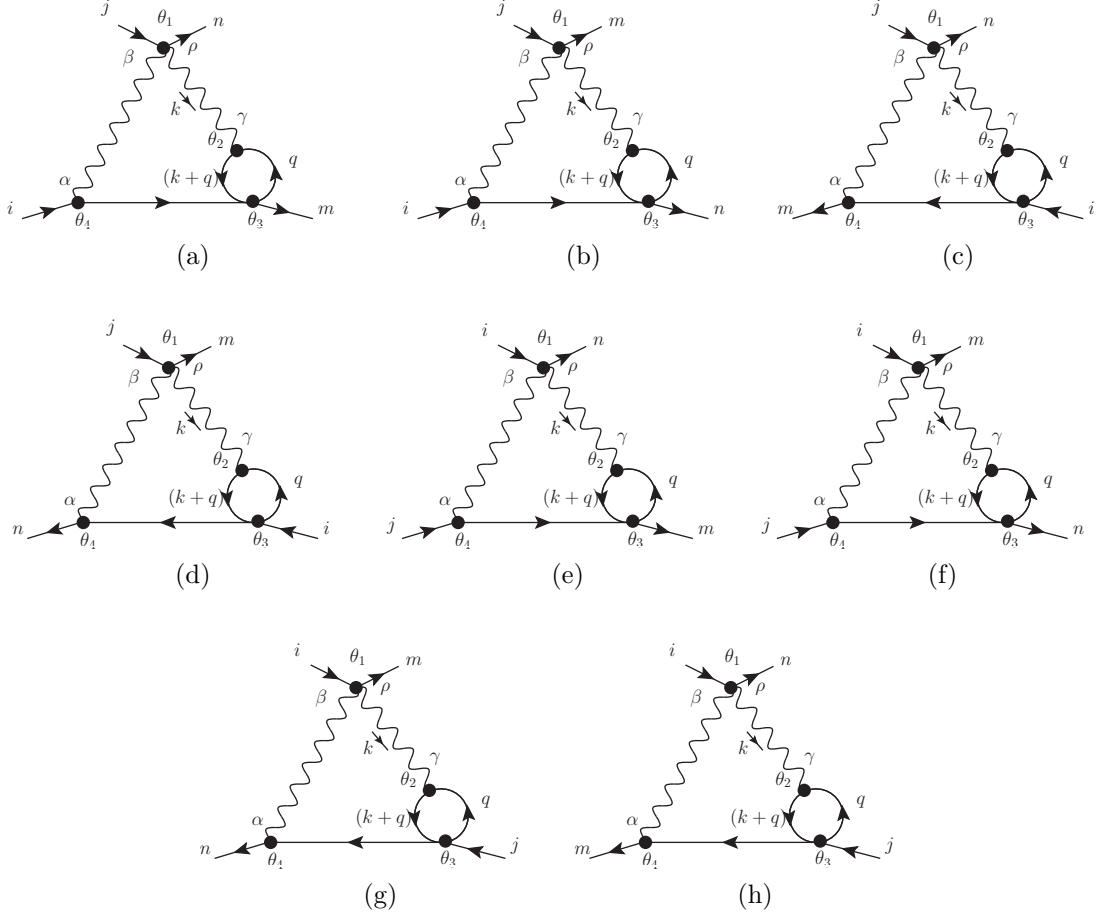
using Eq. (C.14) and adding  $\mathcal{S}_{(\bar{\Phi}\Phi)^2}^{(D5-a)}$  to  $\mathcal{S}_{(\bar{\Phi}\Phi)^2}^{(D5-l)}$  with the values in the Table B.4, we find

$$\mathcal{S}_{(\bar{\Phi}\Phi)^2}^{(D5)} = -\frac{(a-b)}{4(32\pi^2\epsilon)} i \lambda^2 g^2 (\delta_{in}\delta_{jm} + \delta_{mi}\delta_{nj}) \int_{\theta} \bar{\Phi}_i \Phi_m \Phi_n \bar{\Phi}_j . \quad (\text{B.50})$$




 Figure B.7:  $\mathcal{S}_{(\Phi\Phi)}^{(D5)_2}$


 Figure B.8:  $\mathcal{S}_{(\Phi\bar{\Phi})^2}^{(D6)}$


 Figure B.9:  $\mathcal{S}_{(\bar{\Phi}\Phi)^2}^{(D7)}$ 

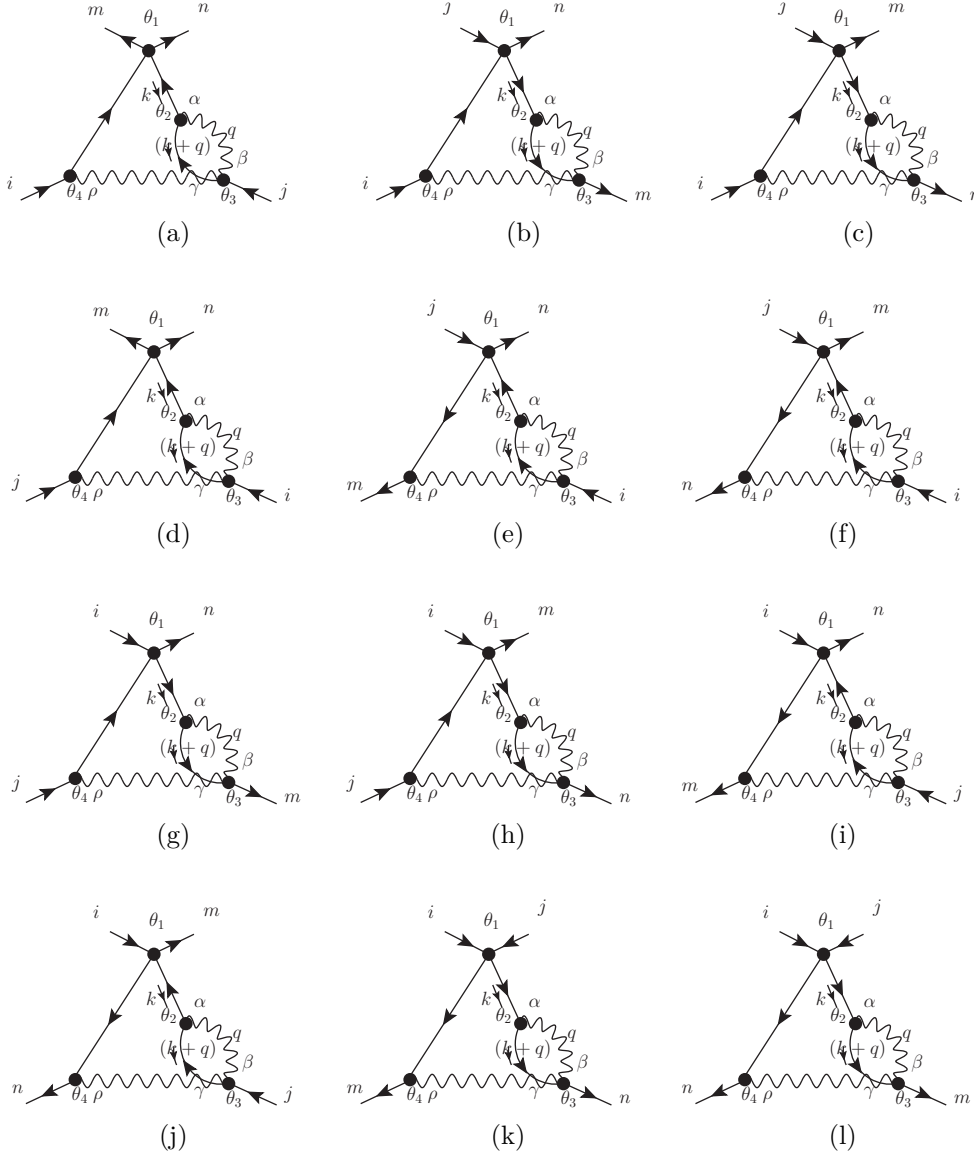
Finally,  $\mathcal{S}_{(\bar{\Phi}\Phi)^2}^{(D6-a)}$  in the Figure B.8 is

$$\mathcal{S}_{(\bar{\Phi}\Phi)^2}^{(D6-a)} = \frac{1}{32} i \lambda^2 g^2 [(N+2) \delta_{im} \delta_{jn} + \delta_{mj} \delta_{ni}] \int_{\theta} \bar{\Phi}_i \Phi_m \Phi_n \bar{\Phi}_j \int \frac{d^D k d^D q}{(2\pi)^{2D}} \left\{ \frac{2(a-b) k^2 q^2}{(k^2)^2 (k+q)^2 (q^2)^2} \right\}, \quad (\text{B.51})$$

using Eq. (C.14) and adding the diagrams  $\mathcal{S}_{(\bar{\Phi}\Phi)^2}^{(D6-a)}$  to  $\mathcal{S}_{(\bar{\Phi}\Phi)^2}^{(D6-l)}$  with the values in Table B.5, we find

$$\mathcal{S}_{(\bar{\Phi}\Phi)^2}^{(D6)} = \frac{(a-b)}{2(32\pi^2\epsilon)} i \lambda^2 g^2 (\delta_{jn} \delta_{im} + \delta_{in} \delta_{jm}) \int_{\theta} \bar{\Phi}_i \Phi_m \Phi_n \bar{\Phi}_j. \quad (\text{B.52})$$

Now, we will consider all the diagrams that contribute with the order  $\mathcal{O}(\lambda g^4)$ , in this order there are 14 topologies that are equivalent to 139 diagrams.


 Figure B.10:  $\mathcal{S}_{(\overline{\Phi}\Phi)^2}^{(D8)}$ 

We start with  $\mathcal{S}_{(\overline{\Phi}\Phi)^2}^{(D7-a)}$  in the Figure B.9,

$$\begin{aligned} \mathcal{S}_{(\overline{\Phi}\Phi)^2}^{(D7-a)} = & -\frac{1}{32} i \lambda g^4 (N+1) \delta_{im} \delta_{jn} \int_{\theta} \overline{\Phi}_i \Phi_m \Phi_n \overline{\Phi}_j \\ & \times \int \frac{d^D k d^D q}{(2\pi)^{2D}} \left\{ \frac{-4(a-b)^2 (k \cdot q) k^2 - 2(a-b)^2 (k^2)^2}{(k^2)^3 q^2 (k+q)^2} \right\}, \end{aligned} \quad (\text{B.53})$$

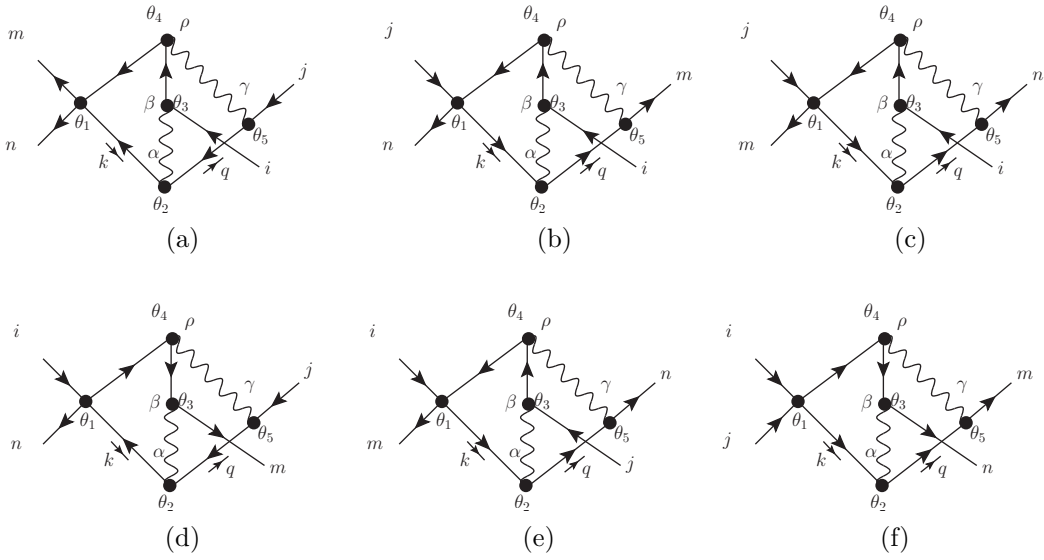
using Eqs. (C.14) and (C.16), we find

$$\mathcal{S}_{(\overline{\Phi}\Phi)^2}^{(D7-a)} = \mathcal{S}_{(\overline{\Phi}\Phi)^2}^{(D7)} = 0. \quad (\text{B.54})$$

$D8 - a$	$-(\delta_{jn}\delta_{im} + \delta_{mj}\delta_{ni})$	$D8 - b$	$\delta_{jn}\delta_{im} + \delta_{mj}\delta_{ni}$
$D8 - c$	$\delta_{jn}\delta_{im} + \delta_{mj}\delta_{ni}$	$D8 - d$	$-(\delta_{jn}\delta_{im} + \delta_{mj}\delta_{ni})$
$D8 - e$	$\delta_{jn}\delta_{im} + \delta_{mj}\delta_{ni}$	$D8 - f$	$\delta_{jn}\delta_{im} + \delta_{mj}\delta_{ni}$
$D8 - g$	$\delta_{jn}\delta_{im} + \delta_{mj}\delta_{ni}$	$D8 - h$	$\delta_{jn}\delta_{im} + \delta_{mj}\delta_{ni}$
$D8 - i$	$\delta_{jn}\delta_{im} + \delta_{mj}\delta_{ni}$	$D8 - j$	$\delta_{jn}\delta_{im} + \delta_{mj}\delta_{ni}$
$D8 - k$	$-(\delta_{jn}\delta_{im} + \delta_{mj}\delta_{ni})$	$D8 - l$	$-(\delta_{jn}\delta_{im} + \delta_{mj}\delta_{ni})$

Table B.6: Values of the diagrams in Figure B.10 with common factor

$$\frac{1}{32} \left( \frac{b^2 - 4ab + 3a^2}{32\pi^2\epsilon} \right) i \lambda g^4 \int_{\theta} \bar{\Phi}_i \Phi_m \Phi_n \bar{\Phi}_j .$$


 Figure B.11:  $\mathcal{S}_{(\bar{\Phi}\Phi)^2}^{(D9)}$ 

$\mathcal{S}_{(\bar{\Phi}\Phi)^2}^{(D8-a)}$  in the Figure B.10 is

$$\begin{aligned} \mathcal{S}_{(\bar{\Phi}\Phi)^2}^{(D8-a)} &= -\frac{1}{32} i \lambda g^4 (\delta_{jn}\delta_{im} + \delta_{mj}\delta_{ni}) \int_{\theta} \bar{\Phi}_i \Phi_m \Phi_n \bar{\Phi}_j \\ &\times \int \frac{d^D k d^D q}{(2\pi)^{2D}} \left\{ \frac{-2(a^2 - b^2)(k \cdot q)k^2 - 4(a^2 - ab)(k^2)^2}{(k^2)^3(k+q)^2 q^2} \right\}, \end{aligned} \quad (\text{B.55})$$

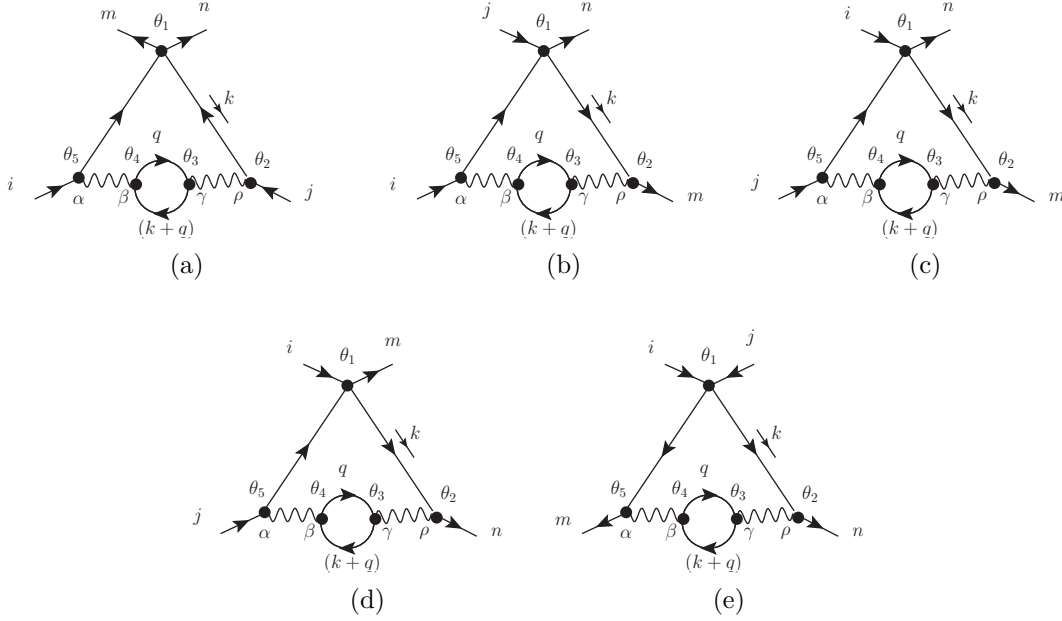
using Eqs. (C.14), (C.16) and adding  $\mathcal{S}_{(\bar{\Phi}\Phi)^2}^{(D8-a)}$  to  $\mathcal{S}_{(\bar{\Phi}\Phi)^2}^{(D8-l)}$  with the values in the Table B.6, we find

$$\mathcal{S}_{(\bar{\Phi}\Phi)^2}^{(D8)} = \frac{1}{8} \left( \frac{b^2 - 4ab + 3a^2}{32\pi^2\epsilon} \right) i \lambda g^4 (\delta_{jn}\delta_{im} + \delta_{mj}\delta_{ni}) \int_{\theta} \bar{\Phi}_i \Phi_m \Phi_n \bar{\Phi}_j. \quad (\text{B.56})$$

$D9 - a$	$\delta_{jn}\delta_{im} + \delta_{mj}\delta_{ni}$	$D9 - b$	$\delta_{jn}\delta_{im} + \delta_{mj}\delta_{ni}$
$D9 - c$	$\delta_{jn}\delta_{im} + \delta_{mj}\delta_{ni}$	$D9 - d$	$\delta_{jn}\delta_{im} + \delta_{mj}\delta_{ni}$
$D9 - e$	$\delta_{jn}\delta_{im} + \delta_{mj}\delta_{ni}$	$D9 - f$	$\delta_{jn}\delta_{im} + \delta_{mj}\delta_{ni}$

Table B.7: Values of the diagrams in Figure B.11 with common factor

$$\frac{1}{32} \left( \frac{(a-b)^2}{32\pi^2\epsilon} \right) i \lambda g^4 \int_{\theta} \bar{\Phi}_i \Phi_m \Phi_n \bar{\Phi}_j .$$

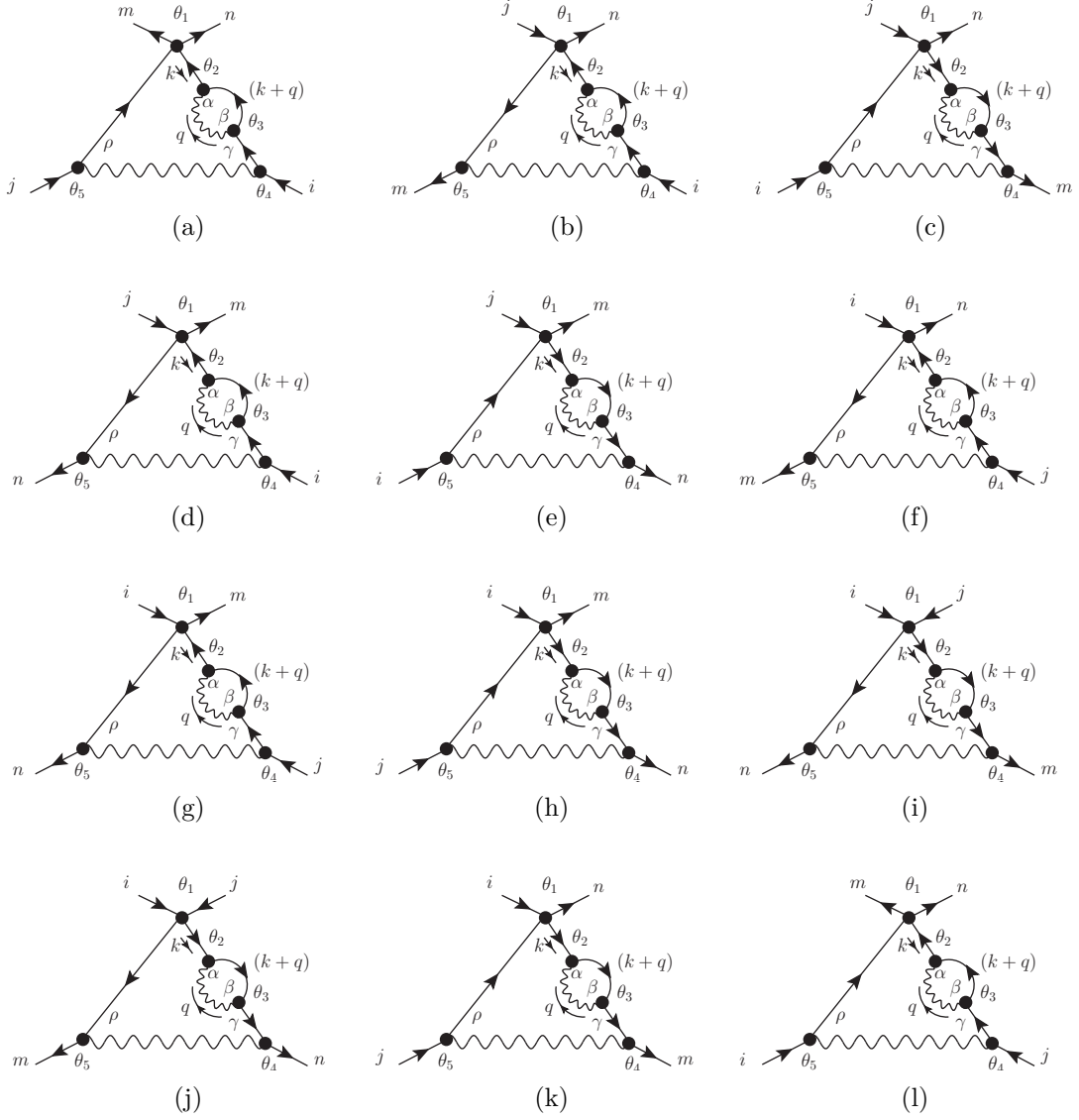

 Figure B.12:  $\mathcal{S}_{(\bar{\Phi}\Phi)^2}^{(D10)}$ 

$\mathcal{S}_{(\bar{\Phi}\Phi)^2}^{(D9-a)}$  in the Figure B.11 is

$$\begin{aligned} \mathcal{S}_{(\bar{\Phi}\Phi)^2}^{(D9-a)} &= \frac{1}{128} i \lambda g^4 (\delta_{jn}\delta_{im} + \delta_{mj}\delta_{ni}) \int_{\theta} \bar{\Phi}_i \Phi_m \Phi_n \bar{\Phi}_j \\ &\times \int \frac{d^D k d^D q}{(2\pi)^{2D}} \left\{ \frac{-4(a-b)^2 k^2 q^2 (k-q)^2}{(k-q)^4 (k^2)^2 (q^2)^2} \right\}, \end{aligned} \quad (B.57)$$

using Eq. (C.14) and adding  $\mathcal{S}_{(\bar{\Phi}\Phi)^2}^{(D9-a)}$  to  $\mathcal{S}_{(\bar{\Phi}\Phi)^2}^{(D9-f)}$  with the values in Table B.7, we find

$$\mathcal{S}_{(\bar{\Phi}\Phi)^2}^{(D9)} = \frac{3}{16} \left( \frac{(a-b)^2}{32\pi^2\epsilon} \right) i \lambda g^4 (\delta_{jn}\delta_{im} + \delta_{mj}\delta_{ni}) \int_{\theta} \bar{\Phi}_i \Phi_m \Phi_n \bar{\Phi}_j . \quad (B.58)$$


 Figure B.13:  $\mathcal{S}_{(\overline{\Phi}\Phi)^2}^{(D11)}$ 

$\mathcal{S}_{(\overline{\Phi}\Phi)^2}^{(D10-a)}$  in the Figure B.12 is

$$\begin{aligned} \mathcal{S}_{(\overline{\Phi}\Phi)^2}^{(D10-a)} &= \frac{1}{128} i \lambda g^4 N (\delta_{jn} \delta_{im} + \delta_{mj} \delta_{ni}) \int_{\theta} \overline{\Phi}_i \Phi_m \Phi_n \overline{\Phi}_j \\ &\times \int \frac{d^D k d^D q}{(2\pi)^{2D}} \left\{ \frac{-4(a-b)^2 (k^2)^2 ((k+q)^2 + q^2)}{(k^2)^4 (k+q)^2 q^2} \right\}, \end{aligned} \quad (\text{B.59})$$

using Eqs. (C.14), (C.16), we find

$$\mathcal{S}_{(\overline{\Phi}\Phi)^2}^{(D10-a)} = \mathcal{S}_{(\overline{\Phi}\Phi)^2}^{(D10)} = 0. \quad (\text{B.60})$$

$D11 - a$	$-(\delta_{jn}\delta_{im} + \delta_{mj}\delta_{ni})$	$D11 - b$	$\delta_{jn}\delta_{im} + \delta_{mj}\delta_{ni}$
$D11 - c$	$\delta_{jn}\delta_{im} + \delta_{mj}\delta_{ni}$	$D11 - d$	$\delta_{jn}\delta_{im} + \delta_{mj}\delta_{ni}$
$D11 - e$	$\delta_{jn}\delta_{im} + \delta_{mj}\delta_{ni}$	$D11 - f$	$\delta_{jn}\delta_{im} + \delta_{mj}\delta_{ni}$
$D11 - g$	$\delta_{jn}\delta_{im} + \delta_{mj}\delta_{ni}$	$D11 - h$	$\delta_{jn}\delta_{im} + \delta_{mj}\delta_{ni}$
$D11 - i$	$-(\delta_{jn}\delta_{im} + \delta_{mj}\delta_{ni})$	$D11 - j$	$-(\delta_{jn}\delta_{im} + \delta_{mj}\delta_{ni})$
$D11 - k$	$\delta_{jn}\delta_{im} + \delta_{mj}\delta_{ni}$	$D11 - l$	$-(\delta_{jn}\delta_{im} + \delta_{mj}\delta_{ni})$

Table B.8: Values of the diagrams in Figure B.13 with common factor

$$\frac{8}{128} \left( \frac{ab-a^2}{32\pi^2\epsilon} \right) i \lambda g^4 \int_{\theta} \bar{\Phi}_i \Phi_m \Phi_n \bar{\Phi}_j .$$

$\mathcal{S}_{(\bar{\Phi}\Phi)^2}^{(D11-a)}$  in the Figure B.13 is

$$\begin{aligned} \mathcal{S}_{(\bar{\Phi}\Phi)^2}^{(D11-a)} &= -\frac{1}{128} i \lambda g^4 (\delta_{in}\delta_{jm} + \delta_{mi}\delta_{nj}) \int_{\theta} \bar{\Phi}_i \Phi_m \Phi_n \bar{\Phi}_j \\ &\times \int \frac{d^D k d^D q}{(2\pi)^{2D}} \left\{ \frac{16 (a^2 - ab) (k^2)^2 ((k \cdot q) + k^2) + 4 (a-b)^2 (k^2)^2 q^2}{(k^2)^4 q^2 (k+q)^2} \right\} , \end{aligned} \quad (\text{B.61})$$

using Eqs. (C.14), (C.16) and the momentum power counting, then adding  $\mathcal{S}_{(\bar{\Phi}\Phi)^2}^{(D11-a)}$  to  $\mathcal{S}_{(\bar{\Phi}\Phi)^2}^{(D11-l)}$  with the values in the Table B.8, we find

$$\mathcal{S}_{(\bar{\Phi}\Phi)^2}^{(D11)} = \frac{1}{4} \left( \frac{ab-a^2}{32\pi^2\epsilon} \right) i \lambda g^4 (\delta_{in}\delta_{jm} + \delta_{mi}\delta_{nj}) \int_{\theta} \bar{\Phi}_i \Phi_m \Phi_n \bar{\Phi}_j . \quad (\text{B.62})$$

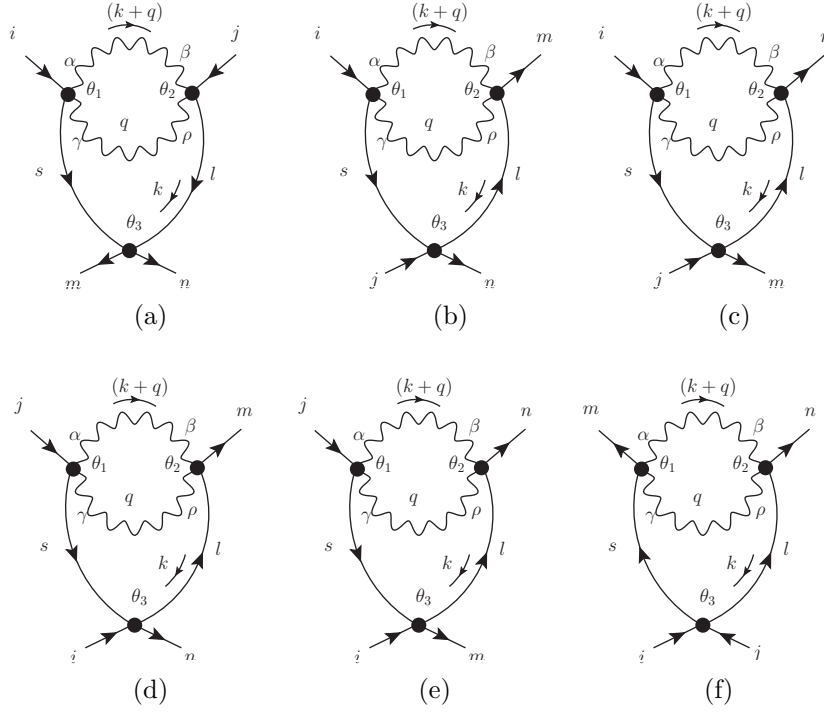
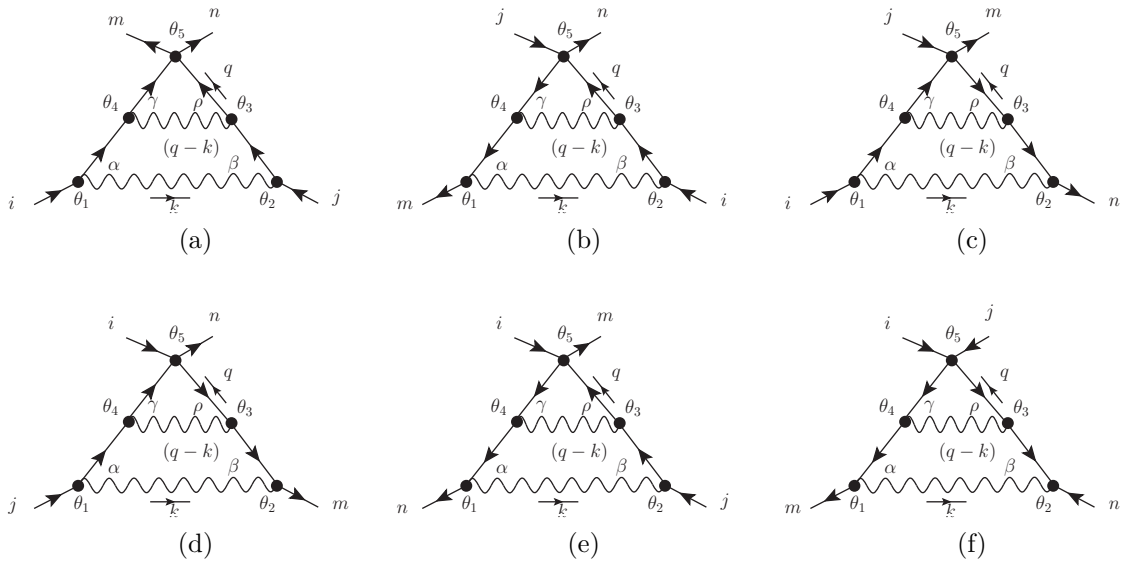
$\mathcal{S}_{(\bar{\Phi}\Phi)^2}^{(D12-a)}$  in the Figure B.14 is

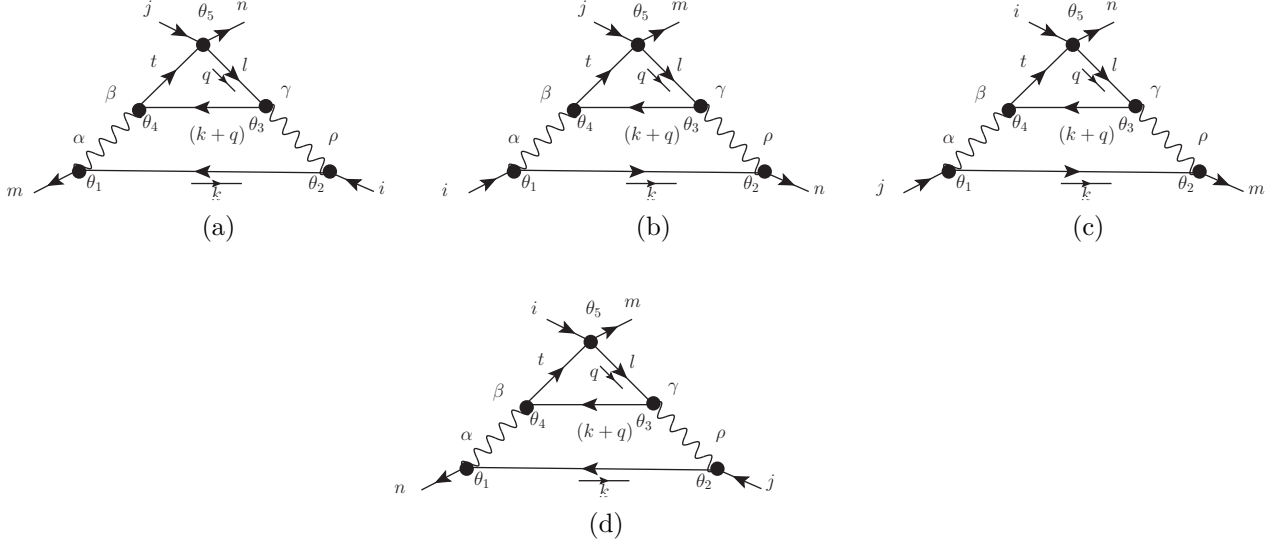
$$\mathcal{S}_{(\bar{\Phi}\Phi)^2}^{(D12-a)} = -\frac{1}{16} i \lambda g^4 (\delta_{jn}\delta_{im} + \delta_{mj}\delta_{ni}) \int_{\theta} \bar{\Phi}_i \Phi_m \Phi_n \bar{\Phi}_j \int \frac{d^D k d^D q}{(2\pi)^{2D}} \left\{ \frac{2 a^2 k^2}{(k^2)^2 q^2 (k+q)^2} \right\} , \quad (\text{B.63})$$

using Eq. (C.14), then adding  $\mathcal{S}_{(\bar{\Phi}\Phi)^2}^{(D12-a)}$  to  $\mathcal{S}_{(\bar{\Phi}\Phi)^2}^{(D12-f)}$ , we have

$$\mathcal{S}_{(\bar{\Phi}\Phi)^2}^{(D12)} = \frac{3}{4} \left( \frac{a^2}{32\pi^2\epsilon} \right) i \lambda g^4 (\delta_{jn}\delta_{im} + \delta_{mj}\delta_{ni}) \int_{\theta} \bar{\Phi}_i \Phi_m \Phi_n \bar{\Phi}_j . \quad (\text{B.64})$$




 Figure B.14:  $\mathcal{S}_{(\Phi\Phi)^2}^{(D12)}$ 

 Figure B.15:  $\mathcal{S}_{(\Phi\Phi)^2}^{(D13)}$


 Figure B.16:  $\mathcal{S}_{(\overline{\Phi}\Phi)^2}^{(D14)}$ 

$\mathcal{S}_{(\overline{\Phi}\Phi)^2}^{(D13-a)}$  in the Figure B.15 is

$$\begin{aligned} \mathcal{S}_{(\overline{\Phi}\Phi)^2}^{(D13-a)} &= \frac{1}{128} i \lambda g^4 (\delta_{jn} \delta_{im} + \delta_{mj} \delta_{ni}) \int_{\theta} \overline{\Phi}_i \Phi_m \Phi_n \overline{\Phi}_j \\ &\times \int \frac{d^D k d^D q}{(2\pi)^{2D}} \left\{ \frac{16 (a b - a^2) (k^2)^2 q^2}{(k^2)^3 (q^2)^2 (q - k)^2} \right\}, \end{aligned} \quad (\text{B.65})$$

using Eq. (C.14), then adding  $\mathcal{S}_{(\overline{\Phi}\Phi)^2}^{(D13-a)}$  to  $\mathcal{S}_{(\overline{\Phi}\Phi)^2}^{(D13-f)}$ , we have

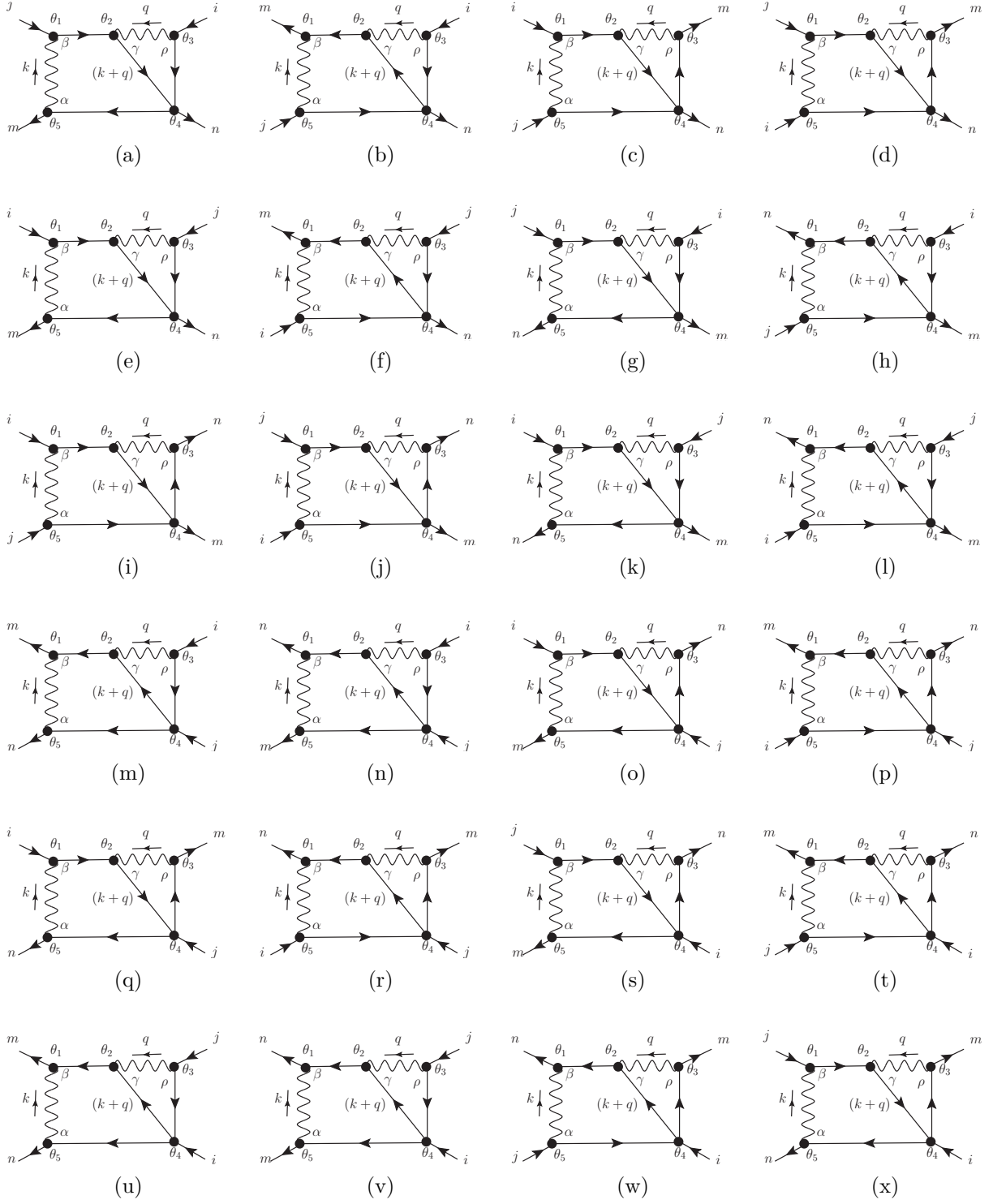
$$\mathcal{S}_{(\overline{\Phi}\Phi)^2}^{(D13)} = \frac{3}{4} a \left( \frac{a - b}{32\pi^2 \epsilon} \right) i \lambda g^4 (\delta_{jn} \delta_{im} + \delta_{mj} \delta_{ni}) \int_{\theta} \overline{\Phi}_i \Phi_m \Phi_n \overline{\Phi}_j. \quad (\text{B.66})$$

$\mathcal{S}_{(\overline{\Phi}\Phi)^2}^{(D14-a)}$  in the Figure B.16 is

$$\mathcal{S}_{(\overline{\Phi}\Phi)^2}^{(D14-a)} = \frac{1}{128} i \lambda g^4 (N + 1) \delta_{jn} \delta_{mi} \int_{\theta} \overline{\Phi}_i \Phi_m \Phi_n \overline{\Phi}_j \int \frac{d^D k d^D q}{(2\pi)^{2D}} \left\{ \frac{-4 (a - b)^2 k^2 q^2 (2 (k \cdot q) + k^2)}{(k^2)^3 (k + q)^2 (q^2)^2} \right\}, \quad (\text{B.67})$$

using Eqs. (C.14), (C.16) and momentum power counting, we find,

$$\mathcal{S}_{(\overline{\Phi}\Phi)^2}^{(D14-a)} = \mathcal{S}_{(\overline{\Phi}\Phi)^2}^{(D14)} = 0. \quad (\text{B.68})$$


 Figure B.17:  $\mathcal{S}_{(\Phi\Phi)^2}^{(D15)}$

$D15 - a$	$-(\delta_{jn}\delta_{im} + \delta_{mj}\delta_{ni})$	$D15 - b$	$\delta_{jn}\delta_{im} + \delta_{mj}\delta_{ni}$
$D15 - c$	$-(\delta_{jn}\delta_{im} + \delta_{mj}\delta_{ni})$	$D15 - d$	$-(\delta_{jn}\delta_{im} + \delta_{mj}\delta_{ni})$
$D15 - e$	$-(\delta_{jn}\delta_{im} + \delta_{mj}\delta_{ni})$	$D15 - f$	$\delta_{jn}\delta_{im} + \delta_{mj}\delta_{ni}$
$D15 - g$	$-(\delta_{jn}\delta_{im} + \delta_{mj}\delta_{ni})$	$D15 - h$	$\delta_{jn}\delta_{im} + \delta_{mj}\delta_{ni}$
$D15 - i$	$-(\delta_{jn}\delta_{im} + \delta_{mj}\delta_{ni})$	$D15 - j$	$-(\delta_{jn}\delta_{im} + \delta_{mj}\delta_{ni})$
$D15 - k$	$-(\delta_{jn}\delta_{im} + \delta_{mj}\delta_{ni})$	$D15 - l$	$\delta_{jn}\delta_{im} + \delta_{mj}\delta_{ni}$
$D15 - m$	$-(\delta_{jn}\delta_{im} + \delta_{mj}\delta_{ni})$	$D15 - n$	$-(\delta_{jn}\delta_{im} + \delta_{mj}\delta_{ni})$
$D15 - o$	$\delta_{jn}\delta_{im} + \delta_{mj}\delta_{ni}$	$D15 - p$	$-(\delta_{jn}\delta_{im} + \delta_{mj}\delta_{ni})$
$D15 - q$	$\delta_{jn}\delta_{im} + \delta_{mj}\delta_{ni}$	$D15 - r$	$-(\delta_{jn}\delta_{im} + \delta_{mj}\delta_{ni})$
$D15 - s$	$\delta_{jn}\delta_{im} + \delta_{mj}\delta_{ni}$	$D15 - t$	$-(\delta_{jn}\delta_{im} + \delta_{mj}\delta_{ni})$
$D15 - u$	$-(\delta_{jn}\delta_{im} + \delta_{mj}\delta_{ni})$	$D15 - v$	$-(\delta_{jn}\delta_{im} + \delta_{mj}\delta_{ni})$
$D15 - w$	$-(\delta_{jn}\delta_{im} + \delta_{mj}\delta_{ni})$	$D15 - x$	$-(\delta_{jn}\delta_{im} + \delta_{mj}\delta_{ni})$

Table B.9: Values of the diagrams in Figure B.17 with common factor

$$\frac{1}{32} \left( \frac{(a-b)^2}{32\pi^2\epsilon} \right) i \lambda g^4 \int_{\theta} \bar{\Phi}_i \Phi_m \Phi_n \bar{\Phi}_j .$$

$\mathcal{S}_{(\bar{\Phi}\Phi)^2}^{(D15-a)}$  in the Figure B.17 is

$$\mathcal{S}_{(\bar{\Phi}\Phi)^2}^{(D15-a)} = \frac{1}{128} i \lambda g^4 (\delta_{jn}\delta_{im} + \delta_{jm}\delta_{in}) \int_{\theta} \bar{\Phi}_i \Phi_m \Phi_n \bar{\Phi}_j \int \frac{d^D k d^D q}{(2\pi)^{2D}} \left\{ \frac{4(a-b)^2 (k^2)^2 q^2}{(k^2)^3 (k+q)^2 (q^2)^2} \right\} , \quad (\text{B.69})$$

using Eq. (C.14) and adding  $\mathcal{S}_{(\bar{\Phi}\Phi)^2}^{(D15-a)}$  to  $\mathcal{S}_{(\bar{\Phi}\Phi)^2}^{(D15-x)}$  with the values in the Table B.9, we find

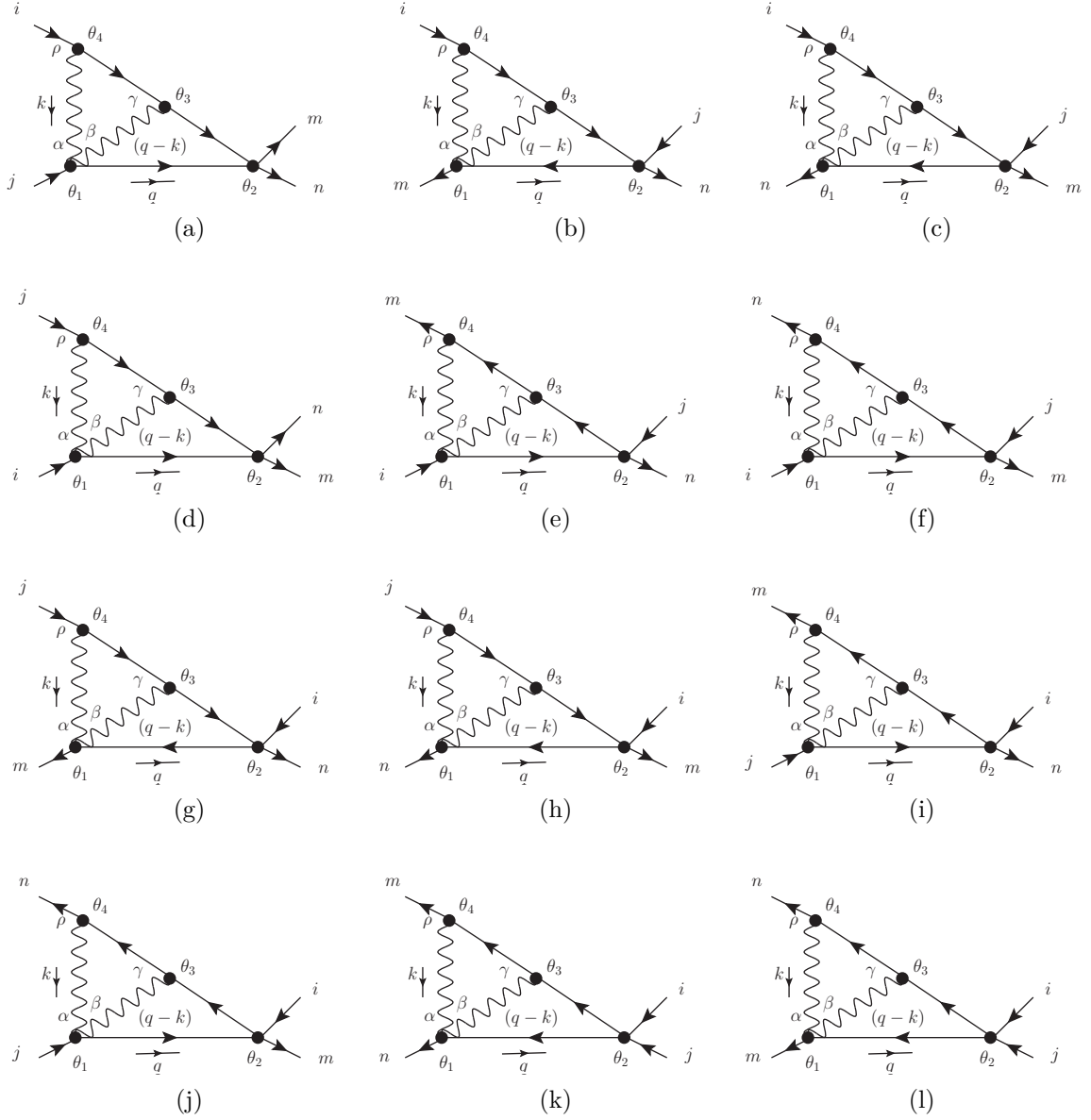
$$\mathcal{S}_{(\bar{\Phi}\Phi)^2}^{(D15)} = -\frac{1}{4} \left( \frac{(a-b)^2}{32\pi^2\epsilon} \right) i \lambda g^4 (\delta_{jn}\delta_{im} + \delta_{jm}\delta_{in}) \int_{\theta} \bar{\Phi}_i \Phi_m \Phi_n \bar{\Phi}_j . \quad (\text{B.70})$$

$\mathcal{S}_{(\bar{\Phi}\Phi)^2}^{(D16-a)}$  in the Figure B.18 is

$$\mathcal{S}_{(\bar{\Phi}\Phi)^2}^{(D16-a)} = -\frac{1}{32} i \lambda g^4 (\delta_{jn}\delta_{im} + \delta_{mj}\delta_{ni}) \int_{\theta} \bar{\Phi}_i \Phi_m \Phi_n \bar{\Phi}_j \int \frac{d^D k d^D q}{(2\pi)^{2D}} \left\{ \frac{(4ab - 4a^2) k^2 q^2}{(k^2)^2 (q-k)^2 (q^2)^2} \right\} , \quad (\text{B.71})$$

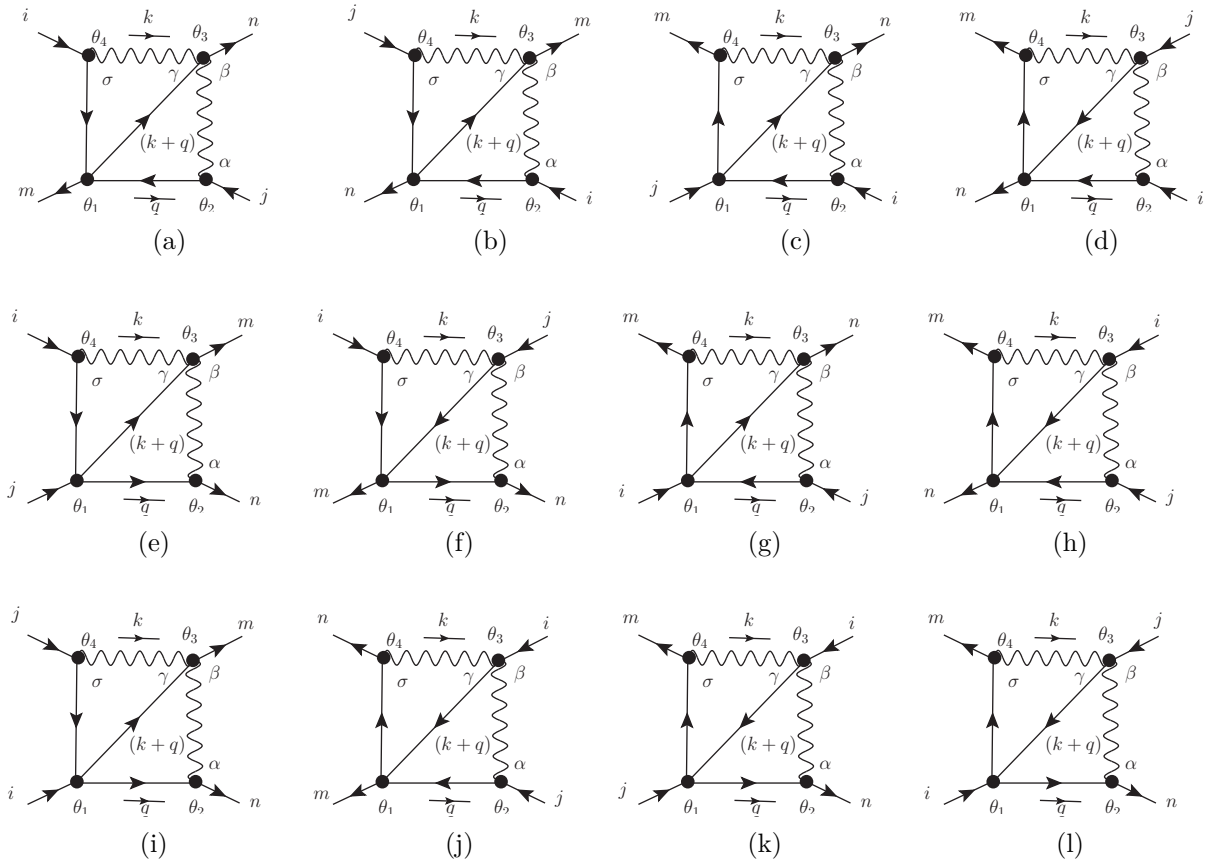
using Eq. (C.14) and adding  $\mathcal{S}_{(\bar{\Phi}\Phi)^2}^{(D15-a)}$  to  $\mathcal{S}_{(\bar{\Phi}\Phi)^2}^{(D15-l)}$  we find,

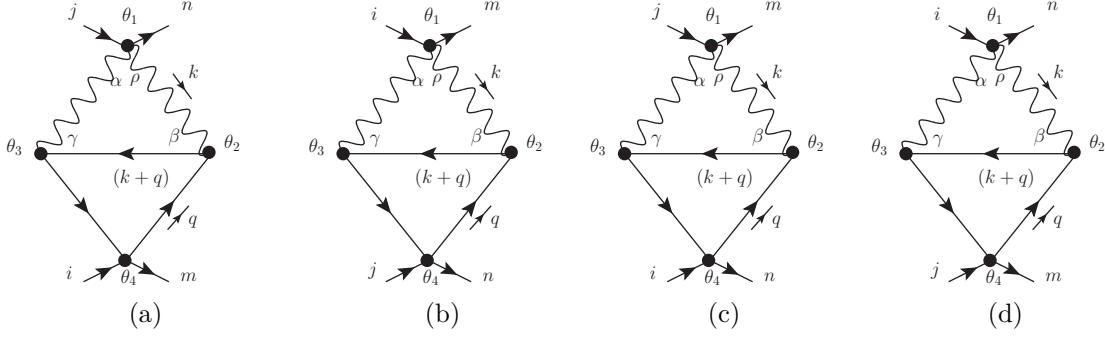
$$\mathcal{S}_{(\bar{\Phi}\Phi)^2}^{(D16)} = \frac{3}{2} a \left( \frac{b-a}{32\pi^2\epsilon} \right) i \lambda g^4 (\delta_{jn}\delta_{im} + \delta_{mj}\delta_{ni}) \int_{\theta} \bar{\Phi}_i \Phi_m \Phi_n \bar{\Phi}_j . \quad (\text{B.72})$$


 Figure B.18:  $\mathcal{S}_{(\overline{\Phi}\Phi)^2}^{(D16)}$ 

$D17 - a$	$-(\delta_{jn}\delta_{im} + \delta_{mj}\delta_{ni})$	$D17 - b$	$-(\delta_{jn}\delta_{im} + \delta_{mj}\delta_{ni})$
$D17 - c$	$\delta_{jn}\delta_{im} + \delta_{mj}\delta_{ni}$	$D17 - d$	$\delta_{jn}\delta_{im} + \delta_{mj}\delta_{ni}$
$D17 - e$	$\delta_{jn}\delta_{im} + \delta_{mj}\delta_{ni}$	$D17 - f$	$\delta_{jn}\delta_{im} + \delta_{mj}\delta_{ni}$
$D17 - g$	$\delta_{jn}\delta_{im} + \delta_{mj}\delta_{ni}$	$D17 - h$	$\delta_{jn}\delta_{im} + \delta_{mj}\delta_{ni}$
$D17 - i$	$\delta_{jn}\delta_{im} + \delta_{mj}\delta_{ni}$	$D17 - j$	$\delta_{jn}\delta_{im} + \delta_{mj}\delta_{ni}$
$D17 - k$	$-(\delta_{jn}\delta_{im} + \delta_{mj}\delta_{ni})$	$D17 - l$	$-(\delta_{jn}\delta_{im} + \delta_{mj}\delta_{ni})$

 Table B.10: Values of the diagrams in Figure B.19 with common factor  $\frac{1}{16} \left( \frac{(a-b)^2}{32\pi^2\epsilon} \right) i \lambda g^4 \int_{\theta} \overline{\Phi}_i \Phi_m \Phi_n \overline{\Phi}_j$ .


 Figure B.19:  $\mathcal{S}_{(\overline{\Phi}\Phi)^2}^{(D17)}$


 Figure B.20:  $\mathcal{S}_{(\Phi\Phi)^2}^{(D18)}$ 

$D18 - a$	$\delta_{jn}\delta_{im}$	$D18 - b$	$\delta_{jn}\delta_{im}$	$D18 - c$	$\delta_{mj}\delta_{ni}$
$D18 - d$	$\delta_{mj}\delta_{ni}$				

Table B.11: Values of the diagrams in Figure B.20 with common factor

$$\frac{1}{16} \left( \frac{(a+b)^2}{32\pi^2\epsilon} \right) (1+N) i \lambda g^4 \int_{\theta} \bar{\Phi}_i \Phi_m \Phi_n \bar{\Phi}_j .$$

$\mathcal{S}_{(\Phi\Phi)^2}^{(D17-a)}$  in the Figure B.19 is

$$\mathcal{S}_{(\Phi\Phi)^2}^{(D17-a)} = -\frac{1}{32} i \lambda g^4 (\delta_{jn}\delta_{im} + \delta_{mj}\delta_{ni}) \int_{\theta} \bar{\Phi}_i \Phi_m \Phi_n \bar{\Phi}_j \int \frac{d^D k d^D q}{(2\pi)^{2D}} \left\{ \frac{-2(a-b)^2 k^2 q^2}{(k^2)^2 (k+q)^2 (q^2)^2} \right\} , \quad (B.73)$$

using Eq. (C.14) and adding  $\mathcal{S}_{(\Phi\Phi)^2}^{(D17-a)}$  to  $\mathcal{S}_{(\Phi\Phi)^2}^{(D17-l)}$  with the values in the Table B.10, we find

$$\mathcal{S}_{(\Phi\Phi)^2}^{(D17)} = \frac{1}{4} \left( \frac{(a-b)^2}{32\pi^2\epsilon} \right) i \lambda g^4 (\delta_{jn}\delta_{im} + \delta_{mj}\delta_{ni}) \int_{\theta} \bar{\Phi}_i \Phi_m \Phi_n \bar{\Phi}_j . \quad (B.74)$$

$\mathcal{S}_{(\Phi\Phi)^2}^{(D18-a)}$  in the Figure B.20 is

$$\begin{aligned} \mathcal{S}_{(\Phi\Phi)^2}^{(D18-a)} &= \frac{1}{32} i \lambda g^4 (1+N) \delta_{nj}\delta_{mi} \int_{\theta} \bar{\Phi}_i \Phi_m \Phi_n \bar{\Phi}_j \\ &\times \int \frac{d^D k d^D q}{(2\pi)^{2D}} \left\{ \frac{-16 a b (k \cdot q) q^2 - 2(a^2 + 6 a b + b^2) k^2 q^2}{(k^2)^2 (k+q)^2 (q^2)^2} \right\} , \end{aligned} \quad (B.75)$$

$D20 - a$	$\delta_{jn}\delta_{im} + \delta_{mj}\delta_{ni}$	$D20 - b$	$\delta_{jn}\delta_{im} + \delta_{mj}\delta_{ni}$
$D20 - c$	$-(\delta_{jn}\delta_{im} + \delta_{mj}\delta_{ni})$	$D20 - d$	$-(\delta_{jn}\delta_{im} + \delta_{mj}\delta_{ni})$
$D20 - e$	$-(\delta_{jn}\delta_{im} + \delta_{mj}\delta_{ni})$	$D20 - f$	$-(\delta_{jn}\delta_{im} + \delta_{mj}\delta_{ni})$
$D20 - g$	$-(\delta_{jn}\delta_{im} + \delta_{mj}\delta_{ni})$	$D20 - h$	$-(\delta_{jn}\delta_{im} + \delta_{mj}\delta_{ni})$
$D20 - i$	$-(\delta_{jn}\delta_{im} + \delta_{mj}\delta_{ni})$	$D20 - j$	$-(\delta_{jn}\delta_{im} + \delta_{mj}\delta_{ni})$
$D20 - k$	$\delta_{jn}\delta_{im} + \delta_{mj}\delta_{ni}$	$D20 - l$	$\delta_{jn}\delta_{im} + \delta_{mj}\delta_{ni}$

Table B.12: Values of the diagrams in Figure B.22 with common factor

$$\frac{1}{32} \left( \frac{(a-b)^2}{32\pi^2\epsilon} \right) i \lambda g^4 \int_{\theta} \bar{\Phi}_i \Phi_m \Phi_n \bar{\Phi}_j .$$

using Eqs. (C.14) and (C.16), then adding  $\mathcal{S}_{(\bar{\Phi}\Phi)^2}^{(D18-a)}$  to  $\mathcal{S}_{(\bar{\Phi}\Phi)^2}^{(D18-d)}$  with the values in Table B.11, we find

$$\mathcal{S}_{(\bar{\Phi}\Phi)^2}^{(D18)} = \frac{1}{8} \left( \frac{(a+b)^2}{32\pi^2\epsilon} \right) (1+N) i \lambda g^4 (\delta_{im}\delta_{jn} + \delta_{jm}\delta_{in}) \int_{\theta} \bar{\Phi}_i \Phi_m \Phi_n \bar{\Phi}_j . \quad (\text{B.76})$$

$\mathcal{S}_{(\bar{\Phi}\Phi)^2}^{(D19-a)}$  in the Figure B.21 is

$$\mathcal{S}_{(\bar{\Phi}\Phi)^2}^{(D19-a)} = -\frac{1}{128} i \lambda g^4 (1+N) \delta_{jn}\delta_{mi} \int_{\theta} \bar{\Phi}_i \Phi_m \Phi_n \bar{\Phi}_j \int \frac{d^D k d^D q}{(2\pi)^{2D}} \left\{ \frac{-4(a-b)^2 (k^2)^2 (2(k \cdot q) + k^2)}{(k^2)^4 (k+q)^2 q^2} \right\} , \quad (\text{B.77})$$

using Eqs. (C.14), (C.16), we find

$$\mathcal{S}_{(\bar{\Phi}\Phi)^2}^{(D19-a)} = \mathcal{S}_{(\bar{\Phi}\Phi)^2}^{(D19)} = 0 . \quad (\text{B.78})$$

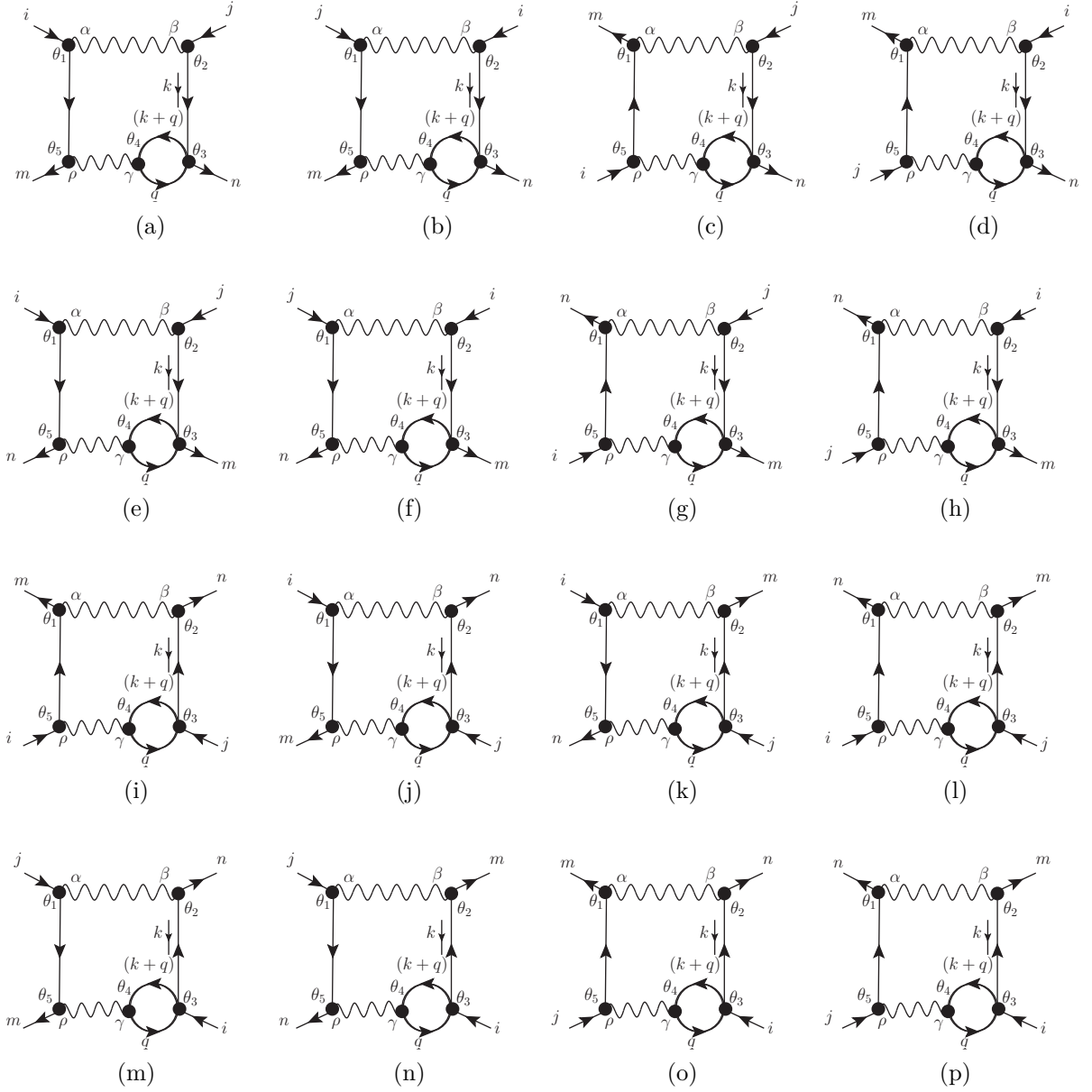
$\mathcal{S}_{(\bar{\Phi}\Phi)^2}^{(D20-a)}$  in the Figure B.22 is

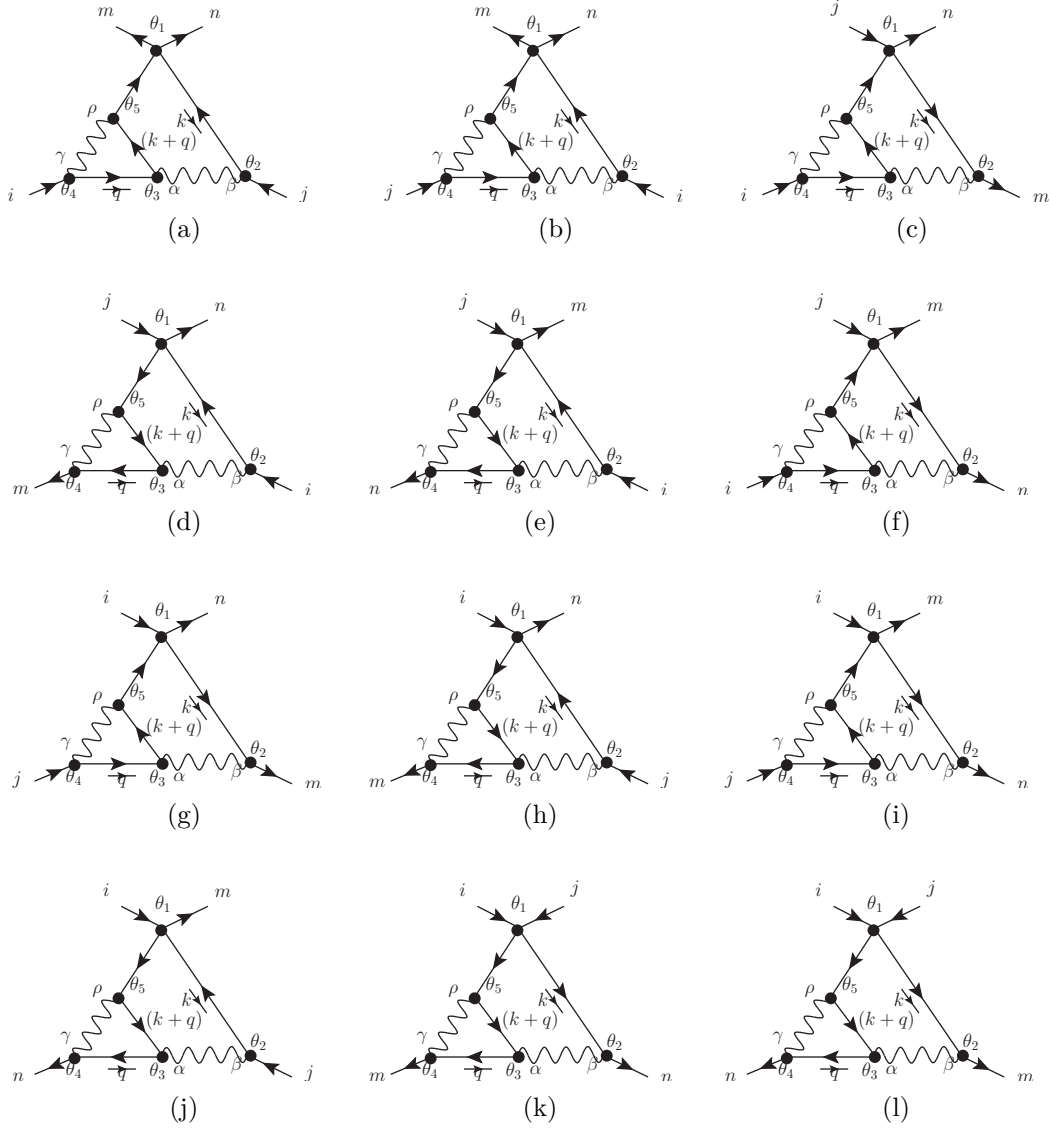
$$\mathcal{S}_{(\bar{\Phi}\Phi)^2}^{(D20-a)} = -\frac{1}{128} i \lambda g^4 (\delta_{jn}\delta_{im} + \delta_{jm}\delta_{in}) \int_{\theta} \bar{\Phi}_i \Phi_m \Phi_n \bar{\Phi}_j \int \frac{d^D k d^D q}{(2\pi)^{2D}} \left\{ \frac{4(a-b)^2 (k^2)^2 q^2}{(k^2)^3 (k+q)^2 (q^2)^2} \right\} , \quad (\text{B.79})$$

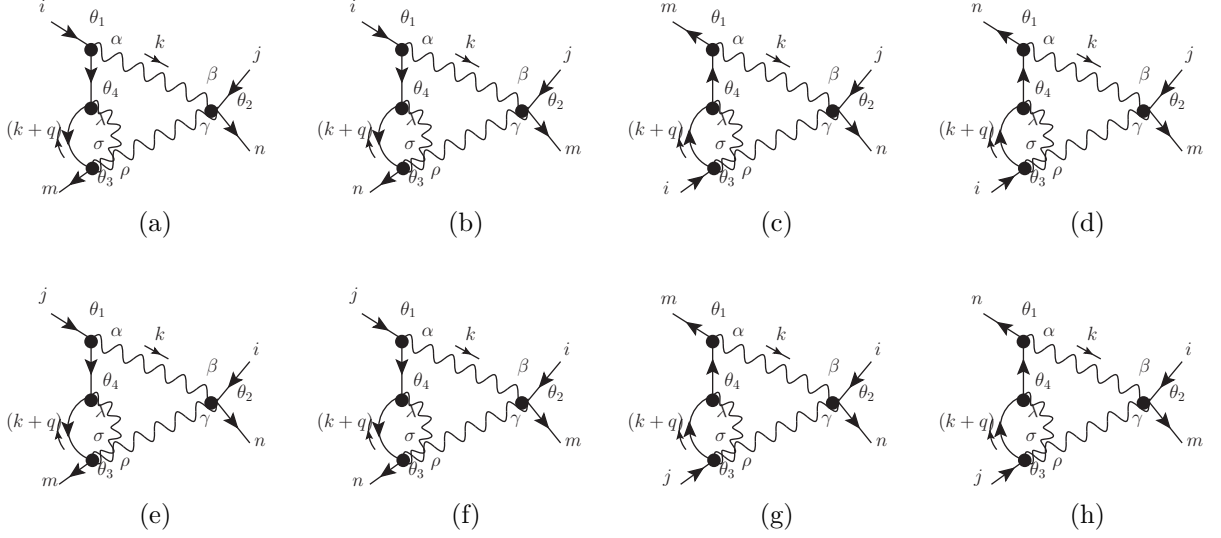
using Eq. (C.14), then adding  $\mathcal{S}_{(\bar{\Phi}\Phi)^2}^{(D20-a)}$  to  $\mathcal{S}_{(\bar{\Phi}\Phi)^2}^{(D20-l)}$  with the values in Table B.12, we find

$$\mathcal{S}_{(\bar{\Phi}\Phi)^2}^{(D20)} = -\frac{1}{8} \left( \frac{(a-b)^2}{32\pi^2\epsilon} \right) i \lambda g^4 (\delta_{jn}\delta_{im} + \delta_{jm}\delta_{in}) \int_{\theta} \bar{\Phi}_i \Phi_m \Phi_n \bar{\Phi}_j . \quad (\text{B.80})$$




 Figure B.21:  $\mathcal{S}^{(D19)}_{(\Phi\Phi)^2}$


 Figure B.22:  $\mathcal{S}_{(\overline{\Phi}\Phi)^2}^{(D20)}$


 Figure B.23:  $\mathcal{S}_{(\Phi\Phi)^2}^{(D21)}$ 

$D21 - a$	$\delta_{jn}\delta_{im}$	$D21 - b$	$\delta_{mj}\delta_{ni}$	$D21 - c$	$\delta_{jn}\delta_{im}$
$D21 - d$	$\delta_{mj}\delta_{ni}$	$D21 - e$	$\delta_{mj}\delta_{ni}$	$D21 - f$	$\delta_{jn}\delta_{im}$
$D21 - g$	$\delta_{mj}\delta_{ni}$	$D21 - h$	$\delta_{jn}\delta_{im}$		

 Table B.13: Values of the diagrams in Figure B.23 with common factor  $\frac{1}{32} \left( \frac{b^3 - 3a^3 + 7a^2b - 5ab^2}{32\pi^2\epsilon} \right) i g^6 \int_{\theta} \bar{\Phi}_i \Phi_m \Phi_n \bar{\Phi}_j$ .

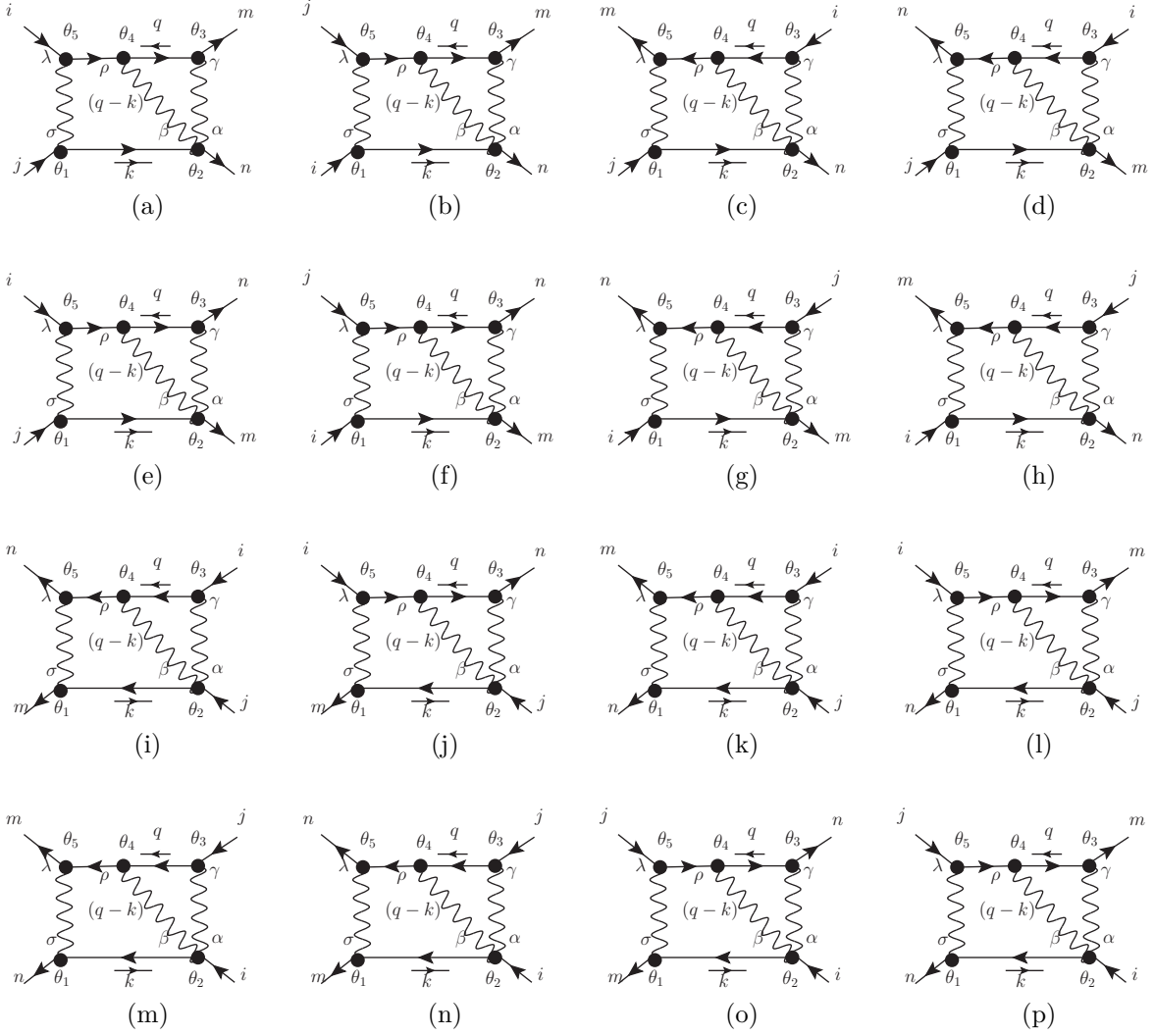
Now, we consider all the diagrams that contribute with the order  $\mathcal{O}(g^6)$ , in this order there are 21 topologies that are equivalent to 178 diagrams.

We start with  $\mathcal{S}_{(\Phi\Phi)^2}^{(D21-a)}$  in the Figure B.23,

$$\mathcal{S}_{(\Phi\Phi)^2}^{(D21-a)} = -\frac{1}{32} i g^6 \delta_{mi} \delta_{jn} \int_{\theta} \bar{\Phi}_i \Phi_m \Phi_n \bar{\Phi}_j \int \frac{d^D k d^D q}{(2\pi)^{2D}} \times \left\{ \frac{-2(a^3 - a^2 b - a b^2 + b^3)(k \cdot q) k^2 - 4a(a-b)^2(k^2)^2}{(k^2)^3 (k+q)^2 q^2} \right\}, \quad (\text{B.81})$$

using Eqs. (C.14) and (C.16), then adding  $\mathcal{S}_{(\Phi\Phi)^2}^{(D21-a)}$  to  $\mathcal{S}_{(\Phi\Phi)^2}^{(D21-h)}$  with the values in Table B.13, we find

$$\mathcal{S}_{(\Phi\Phi)^2}^{(D21)} = -\frac{1}{8} \left( \frac{(a-b)^2(3a-b)}{32\pi^2\epsilon} \right) i g^6 (\delta_{mj}\delta_{in} + \delta_{mi}\delta_{jn}) \int_{\theta} \bar{\Phi}_i \Phi_m \Phi_n \bar{\Phi}_j. \quad (\text{B.82})$$


 Figure B.24:  $\mathcal{S}_{(\Phi\Phi)^2}^{(D22)}$ 

$\mathcal{S}_{(\Phi\Phi)^2}^{(D22-a)}$  in the Figure B.24 is

$$\mathcal{S}_{(\Phi\Phi)^2}^{(D22-a)} = \frac{1}{128} i \delta_{jn} \delta_{mi} g^6 \int_{\theta} \bar{\Phi}_i \Phi_m \Phi_n \bar{\Phi}_j \int \frac{d^D k d^D q}{(2\pi)^{2D}} \left\{ \frac{-8 a (a-b)^2 (k^2)^2 q^2}{(k^2)^3 (q-k)^2 (q^2)^2} \right\}, \quad (\text{B.83})$$

using Eq. (C.14), then adding  $\mathcal{S}_{(\Phi\Phi)^2}^{(D21-a)}$  to  $\mathcal{S}_{(\Phi\Phi)^2}^{(D21-p)}$  with the values in Table B.14, we find

$$\mathcal{S}_{(\Phi\Phi)^2}^{(D22-a)} = \mathcal{S}_{(\Phi\Phi)^2}^{(D22)} = 0. \quad (\text{B.84})$$

$D22 - a$	$\delta_{jn}\delta_{im}$	$D22 - b$	$\delta_{mj}\delta_{ni}$	$D22 - c$	$-\delta_{jn}\delta_{im}$
$D22 - d$	$-\delta_{mj}\delta_{ni}$	$D22 - e$	$\delta_{mj}\delta_{ni}$	$D22 - f$	$\delta_{jn}\delta_{im}$
$D22 - g$	$-\delta_{jn}\delta_{im}$	$D22 - h$	$-\delta_{mj}\delta_{ni}$	$D22 - i$	$\delta_{mj}\delta_{ni}$
$D22 - j$	$-\delta_{mj}\delta_{ni}$	$D22 - k$	$\delta_{jn}\delta_{im}$	$D22 - l$	$-\delta_{jn}\delta_{im}$
$D22 - m$	$\delta_{mj}\delta_{ni}$	$D22 - n$	$\delta_{jn}\delta_{im}$	$D22 - o$	$-\delta_{jn}\delta_{im}$
$D22 - p$	$-\delta_{mj}\delta_{ni}$				

Table B.14: Values of the diagrams in Figure B.24 with common factor  $\frac{1}{16} \left( \frac{a(a-b)^2}{32\pi^2\epsilon} \right) i g^6 \int_{\theta} \bar{\Phi}_i \Phi_m \Phi_n \bar{\Phi}_j$ .

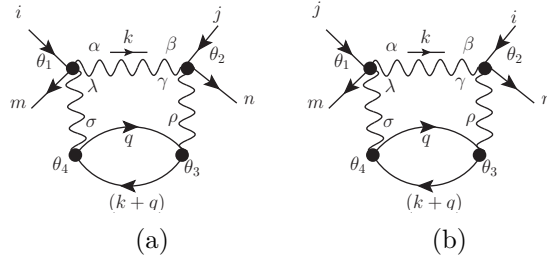


Figure B.25:  $\mathcal{S}_{(\bar{\Phi}\Phi)^2}^{(D23)}$

$D23 - a$	$\delta_{jn}\delta_{im}$	$D23 - b$	$\delta_{mj}\delta_{ni}$
-----------	--------------------------	-----------	--------------------------

Table B.15: Values of the diagrams in Figure B.25 with common factor  $\frac{1}{16} \left( \frac{(a+b)^3}{32\pi^2\epsilon} \right) N i g^6 \int_{\theta} \bar{\Phi}_i \Phi_m \Phi_n \bar{\Phi}_j$ .

$D24 - a$	$\delta_{mj}\delta_{ni}$	$D24 - b$	$\delta_{mj}\delta_{ni}$	$D24 - c$	$\delta_{jn}\delta_{im}$
$D24 - d$	$\delta_{jn}\delta_{im}$	$D24 - e$	$\delta_{jn}\delta_{im}$	$D24 - f$	$\delta_{jn}\delta_{im}$
$D24 - g$	$\delta_{mj}\delta_{ni}$	$D24 - h$	$\delta_{mj}\delta_{ni}$	$D24 - i$	$\delta_{jn}\delta_{im}$
$D24 - j$	$\delta_{jn}\delta_{im}$	$D24 - k$	$\delta_{mj}\delta_{ni}$	$D24 - l$	$\delta_{mj}\delta_{ni}$
$D24 - m$	$\delta_{mj}\delta_{ni}$	$D24 - n$	$\delta_{mj}\delta_{ni}$	$D24 - o$	$\delta_{jn}\delta_{im}$
$D24 - p$	$\delta_{jn}\delta_{im}$				

Table B.16: Values of the diagrams in Figure B.26 with common factor

$$\frac{1}{64} \left( \frac{(a-b)^3}{32\pi^2\epsilon} \right) i g^6 \int_{\theta} \bar{\Phi}_i \Phi_m \Phi_n \bar{\Phi}_j .$$

$\mathcal{S}_{(\bar{\Phi}\Phi)^2}^{(D23-a)}$  in the Figure B.25 is

$$\begin{aligned} \mathcal{S}_{(\bar{\Phi}\Phi)^2}^{(D23-a)} &= -\frac{1}{32} i N g^6 \delta_{im} \delta_{jn} \int_{\theta} \bar{\Phi}_i \Phi_m \Phi_n \bar{\Phi}_j \\ &\times \int \frac{d^D k d^D q}{(2\pi)^{2D}} \left\{ \frac{-8(a^3 + 3ab^2)k^2((k \cdot q) + q^2) - 2(a-b)^3(k^2)^2}{(k^2)^3(k+q)^2 q^2} \right\}, \end{aligned} \quad (\text{B.85})$$

using Eqs. (C.14), (C.16), then adding  $\mathcal{S}_{(\bar{\Phi}\Phi)^2}^{(D23-a)}$  to  $\mathcal{S}_{(\bar{\Phi}\Phi)^2}^{(D23-b)}$  with the values in Table B.15, we find

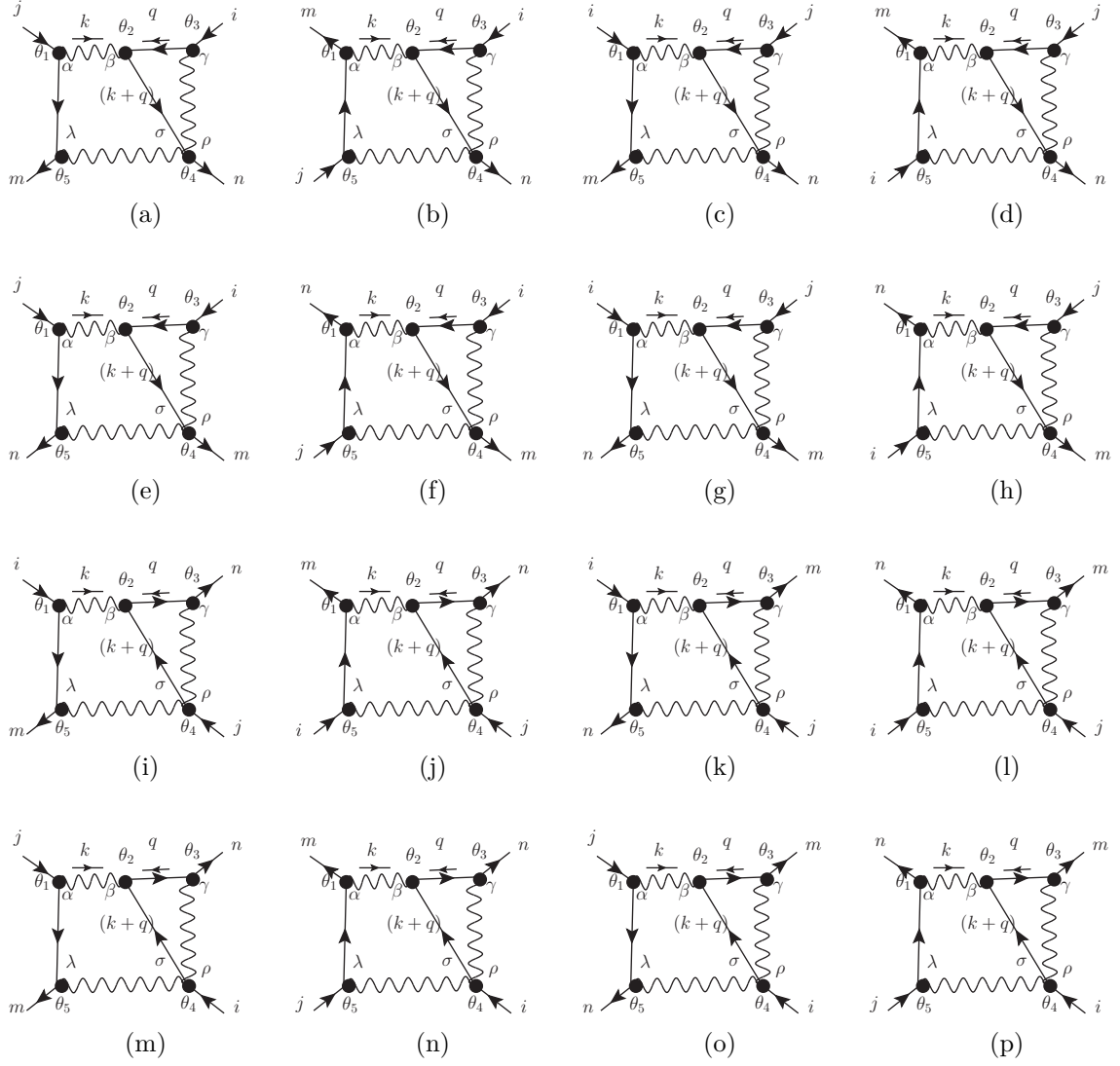
$$\mathcal{S}_{(\bar{\Phi}\Phi)^2}^{(D23)} = \frac{1}{16} \left( \frac{(a+b)^3}{32\pi^2\epsilon} \right) i N g^6 (\delta_{im}\delta_{jn} + \delta_{jm}\delta_{in}) \int_{\theta} \bar{\Phi}_i \Phi_m \Phi_n \bar{\Phi}_j . \quad (\text{B.86})$$

$\mathcal{S}_{(\bar{\Phi}\Phi)^2}^{(D24-a)}$  in the Figure B.26 is

$$\mathcal{S}_{(\bar{\Phi}\Phi)^2}^{(D24-a)} = \frac{1}{128} i \delta_{in} \delta_{mj} g^6 \int_{\theta} \bar{\Phi}_i \Phi_m \Phi_n \bar{\Phi}_j \int \frac{d^D k d^D q}{(2\pi)^{2D}} \left\{ \frac{4(a-b)^3(k \cdot q)k^2 q^2}{(k^2)^3(k+q)^2(q^2)^2} \right\}, \quad (\text{B.87})$$

using Eq. (C.16), then adding  $\mathcal{S}_{(\bar{\Phi}\Phi)^2}^{(D24-a)}$  to  $\mathcal{S}_{(\bar{\Phi}\Phi)^2}^{(D24-p)}$  with the values in Table B.16, we find

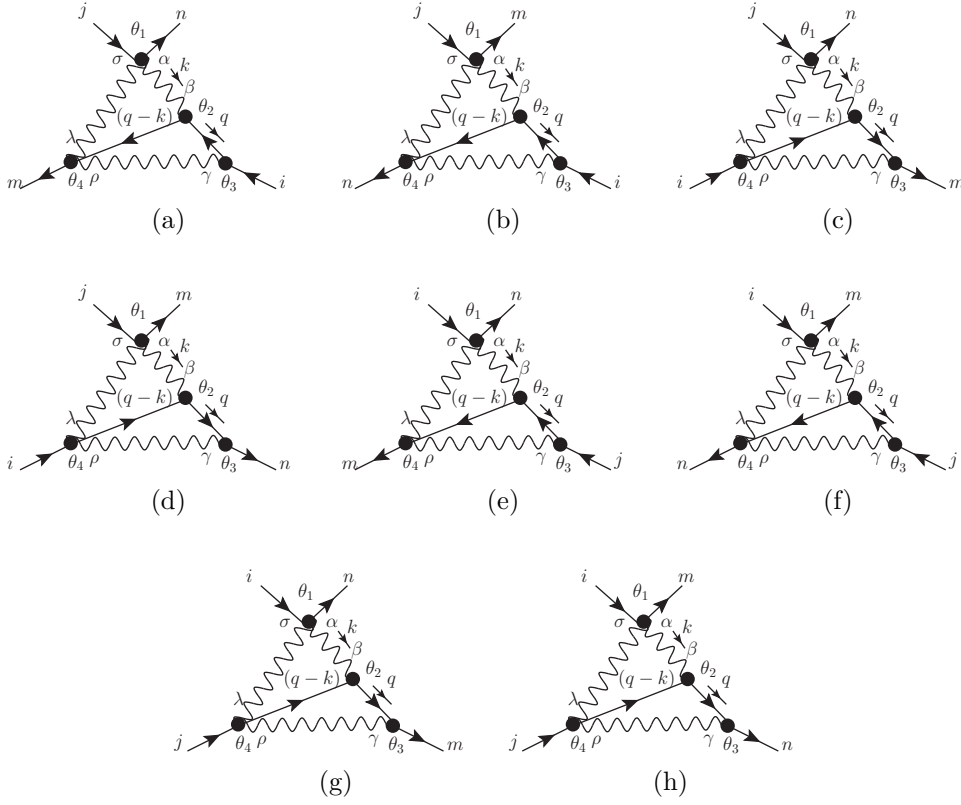
$$\mathcal{S}_{(\bar{\Phi}\Phi)^2}^{(D24)} = \frac{1}{8} \left( \frac{(a-b)^3}{32\pi^2\epsilon} \right) i g^6 (\delta_{in}\delta_{mj} + \delta_{jn}\delta_{mi}) \int_{\theta} \bar{\Phi}_i \Phi_m \Phi_n \bar{\Phi}_j . \quad (\text{B.88})$$


 Figure B.26:  $\mathcal{S}_{(\Phi\Phi)^2}^{(D24)}$ 

$D25 - a$	$\delta_{jn}\delta_{im}$	$D25 - b$	$\delta_{mj}\delta_{ni}$	$D25 - c$	$\delta_{jn}\delta_{im}$
$D25 - d$	$\delta_{mj}\delta_{ni}$	$D25 - e$	$\delta_{mj}\delta_{ni}$	$D25 - f$	$\delta_{jn}\delta_{im}$
$D25 - g$	$\delta_{mj}\delta_{ni}$	$D25 - h$	$\delta_{jn}\delta_{im}$		

Table B.17: Values of the diagrams in Figure B.27 with common factor

$$-\frac{1}{16} \left( \frac{(a-b)(a^2+b^2)}{32\pi^2\epsilon} \right) i g^6 \int_{\theta} \bar{\Phi}_i \Phi_m \Phi_n \bar{\Phi}_j .$$


 Figure B.27:  $\mathcal{S}_{(\overline{\Phi}\Phi)^2}^{(D25)}$ 

$\mathcal{S}_{(\overline{\Phi}\Phi)^2}^{(D25-a)}$  in the Figure B.27 is

$$\mathcal{S}_{(\overline{\Phi}\Phi)^2}^{(D25-a)} = \frac{1}{32} i g^6 \delta_{im} \delta_{jn} \int_{\theta} \overline{\Phi}_i \Phi_m \Phi_n \overline{\Phi}_j \int \frac{d^D k d^D q}{(2\pi)^{2D}} \times \left\{ \frac{8(a b^2 - a^2 b)(k \cdot q) q^2 + 2(a^3 + a^2 b - a b^2 - b^3) k^2 q^2}{(k^2)^2 (q-k)^2 (q^2)^2} \right\}, \quad (\text{B.89})$$

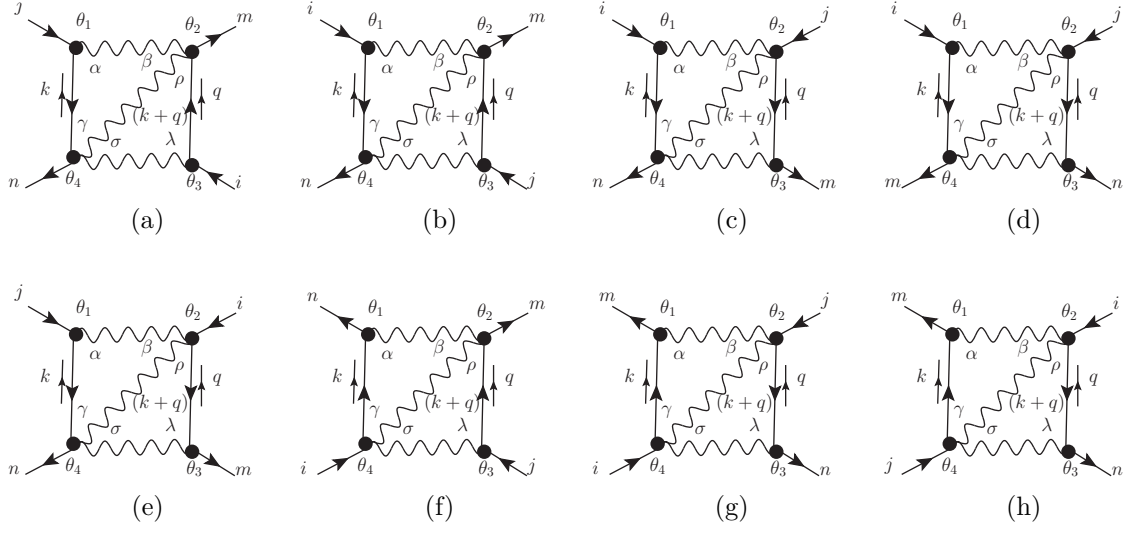
using Eqs. (C.14) and (C.16), then adding  $\mathcal{S}_{(\overline{\Phi}\Phi)^2}^{(D25-a)}$  to  $\mathcal{S}_{(\overline{\Phi}\Phi)^2}^{(D25-h)}$  with the values in Table B.17, we find

$$\mathcal{S}_{(\overline{\Phi}\Phi)^2}^{(D25)} = -\frac{1}{4} \frac{(a-b)(a^2+b^2)}{32\pi^2 \epsilon} i g^6 (\delta_{im} \delta_{jn} + \delta_{jm} \delta_{in}) \int_{\theta} \overline{\Phi}_i \Phi_m \Phi_n \overline{\Phi}_j. \quad (\text{B.90})$$

$\mathcal{S}_{(\overline{\Phi}\Phi)^2}^{(D26-a)}$  in the Figure B.28 is

$$\mathcal{S}_{(\overline{\Phi}\Phi)^2}^{(D26-a)} = \frac{1}{32} i \delta_{im} \delta_{nj} g^6 \int_{\theta} \overline{\Phi}_i \Phi_m \Phi_n \overline{\Phi}_j \int \frac{d^D k d^D q}{(2\pi)^{2D}} \left\{ \frac{-2a(a-b)^2 k^2 q^2}{(k^2)^2 (k+q)^2 (q^2)^2} \right\}, \quad (\text{B.91})$$

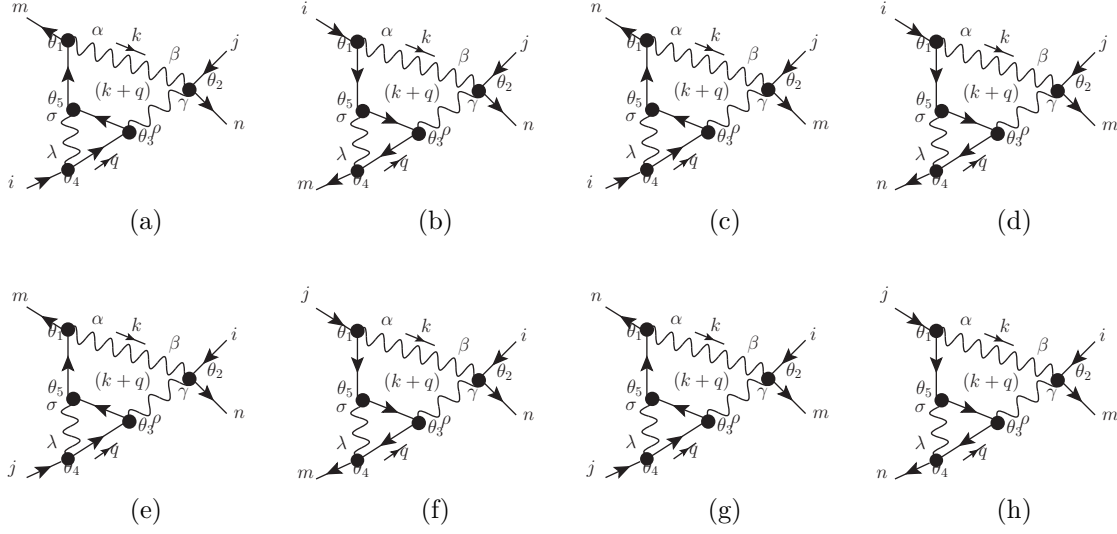



 Figure B.28:  $\mathcal{S}_{(\overline{\Phi}\Phi)^2}^{(D26)}$ 

$D26 - a$	$\delta_{im}\delta_{nj}$	$D26 - b$	$\delta_{jm}\delta_{ni}$	$D26 - c$	$-\delta_{jm}\delta_{ni}$
$D26 - d$	$-\delta_{im}\delta_{nj}$	$D26 - e$	$-\delta_{im}\delta_{nj}$	$D26 - f$	$-\delta_{jm}\delta_{ni}$
$D26 - g$	$\delta_{im}\delta_{nj}$	$D26 - h$	$\delta_{jm}\delta_{ni}$		

Table B.18: Values of the diagrams in Figure B.28 with common factor

$$\frac{1}{16} \left( \frac{a(a-b)^2}{32\pi^2\epsilon} \right) i g^6 \int_{\theta} \overline{\Phi}_i \Phi_m \Phi_n \overline{\Phi}_j .$$


 Figure B.29:  $\mathcal{S}_{(\overline{\Phi}\Phi)^2}^{(D27)}$ 

$D27 - a$	$\delta_{im}\delta_{jn}$	$D27 - b$	$\delta_{im}\delta_{jn}$	$D27 - c$	$\delta_{jm}\delta_{in}$
$D27 - d$	$\delta_{jm}\delta_{in}$	$D27 - e$	$\delta_{jm}\delta_{in}$	$D27 - f$	$\delta_{jm}\delta_{in}$
$D27 - g$	$\delta_{im}\delta_{jn}$	$D27 - h$	$\delta_{im}\delta_{jn}$		

 Table B.19: Values of the diagrams in Figure B.29 with common factor  $\frac{1}{32} \left( \frac{(a-b)^3}{32\pi^2\epsilon} \right) i g^6 \int_{\theta} \overline{\Phi}_i \Phi_m \Phi_n \overline{\Phi}_j$ .

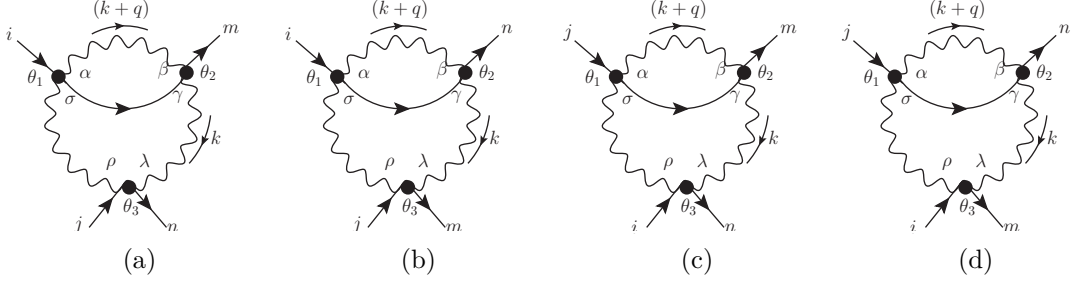
using Eq. (C.14), then adding  $\mathcal{S}_{(\overline{\Phi}\Phi)^2}^{(D26-a)}$  to  $\mathcal{S}_{(\overline{\Phi}\Phi)^2}^{(D26-h)}$  with the values in Table B.18, we find

$$\mathcal{S}_{(\overline{\Phi}\Phi)^2}^{(D26-a)} = \mathcal{S}_{(\overline{\Phi}\Phi)^2}^{(D26)} = 0. \quad (\text{B.92})$$

$\mathcal{S}_{(\overline{\Phi}\Phi)^2}^{(D27-a)}$  in the Figure B.29 is

$\mathcal{S}_{(\overline{\Phi}\Phi)^2}^{(D26-a)}$  in the Figure B.28 is

$$\mathcal{S}_{(\overline{\Phi}\Phi)^2}^{(D27-a)} = \frac{1}{128} i g^6 \delta_{im} \delta_{jn} \int_{\theta} \overline{\Phi}_i \Phi_m \Phi_n \overline{\Phi}_j \int \frac{d^D k d^D q}{(2\pi)^{2D}} \left\{ \frac{-4(a-b)^3 (k^2)^2 q^2}{(k^2)^3 (k+q)^2 (q^2)^2} \right\}, \quad (\text{B.93})$$


 Figure B.30:  $\mathcal{S}_{(\Phi\Phi)^2}^{(D28)}$ 

$D28 - a$	$\delta_{im}\delta_{jn}$	$D28 - b$	$\delta_{jm}\delta_{in}$	$D28 - c$	$\delta_{jm}\delta_{in}$
$D28 - d$	$\delta_{im}\delta_{jn}$				

 Table B.20: Values of the diagrams in Figure B.30 with common factor  $\frac{1}{4} \left( \frac{a^3 + 2ab^2}{32\pi^2\epsilon} \right) i g^6 \int_{\theta} \bar{\Phi}_i \Phi_m \Phi_n \bar{\Phi}_j$ .

using Eq. (C.14), then adding  $\mathcal{S}_{(\Phi\Phi)^2}^{(D27-a)}$  to  $\mathcal{S}_{(\Phi\Phi)^2}^{(D27-h)}$  with the values in Table B.19, we find

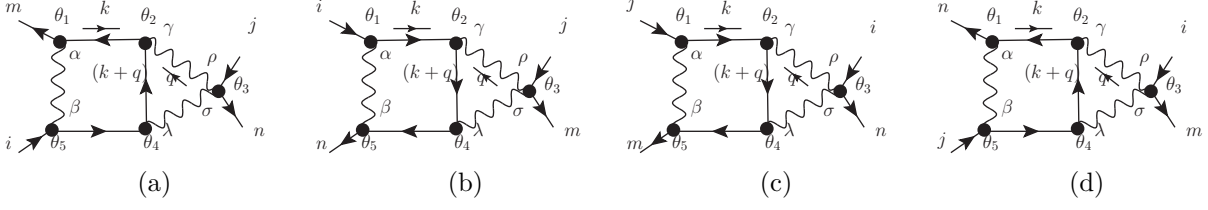
$$\mathcal{S}_{(\Phi\Phi)^2}^{(D27)} = \frac{1}{8} \left( \frac{(a-b)^3}{32\pi^2\epsilon} \right) i g^6 (\delta_{im}\delta_{jn} + \delta_{jm}\delta_{in}) \int_{\theta} \bar{\Phi}_i \Phi_m \Phi_n \bar{\Phi}_j. \quad (\text{B.94})$$

$\mathcal{S}_{(\Phi\Phi)^2}^{(D28-a)}$  in the Figure B.30 is

$$\mathcal{S}_{(\Phi\Phi)^2}^{(D28-a)} = -\frac{1}{8} i g^6 \delta_{im}\delta_{jn} \int_{\theta} \bar{\Phi}_i \Phi_m \Phi_n \bar{\Phi}_j \int \frac{d^D k d^D q}{(2\pi)^{2D}} \left\{ \frac{4ab^2(k \cdot q) + (2a^3 + 6ab^2)k^2}{(k^2)^2(k+q)^2q^2} \right\}, \quad (\text{B.95})$$

using Eqs. (C.14) and (C.16), then adding  $\mathcal{S}_{(\Phi\Phi)^2}^{(D28-a)}$  to  $\mathcal{S}_{(\Phi\Phi)^2}^{(D28-d)}$  with the values in Table B.20, we find

$$\mathcal{S}_{(\Phi\Phi)^2}^{(D28)} = \frac{1}{2} a \left( \frac{a^2 + 2b^2}{32\pi^2\epsilon} \right) i g^6 (\delta_{im}\delta_{jn} + \delta_{jm}\delta_{in}) \int_{\theta} \bar{\Phi}_i \Phi_m \Phi_n \bar{\Phi}_j. \quad (\text{B.96})$$


 Figure B.31:  $\mathcal{S}_{(\overline{\Phi}\Phi)^2}^{(D29)}$ 

$D29 - a$	$\delta_{mi}\delta_{jn}$	$D29 - b$	$\delta_{mj}\delta_{in}$	$D29 - c$	$\delta_{mj}\delta_{in}$
$D29 - d$	$\delta_{mi}\delta_{jn}$				

Table B.21: Values of the diagrams in Figure B.31 with common factor

$$\frac{1}{32} \left( \frac{(a-b)(a+b)^2}{32\pi^2\epsilon} \right) i g^6 \int_{\theta} \overline{\Phi}_i \Phi_m \Phi_n \overline{\Phi}_j .$$

$\mathcal{S}_{(\overline{\Phi}\Phi)^2}^{(D29-a)}$  in the Figure B.31 is

$$\mathcal{S}_{(\overline{\Phi}\Phi)^2}^{(D29-a)} = \frac{1}{128} i g^6 \delta_{mi}\delta_{jn} \int_{\theta} \overline{\Phi}_i \Phi_m \Phi_n \overline{\Phi}_j \int \frac{d^D k d^D q}{(2\pi)^{2D}} \times \left\{ \frac{-32(a^2b - ab^2)(k \cdot q)(k^2)^2 - 4(a^3 + 5a^2b - 5ab^2 - b^3)(k^2)^2 q^2}{(k^2)^3 (k+q)^2 (q^2)^2} \right\}, \quad (\text{B.97})$$

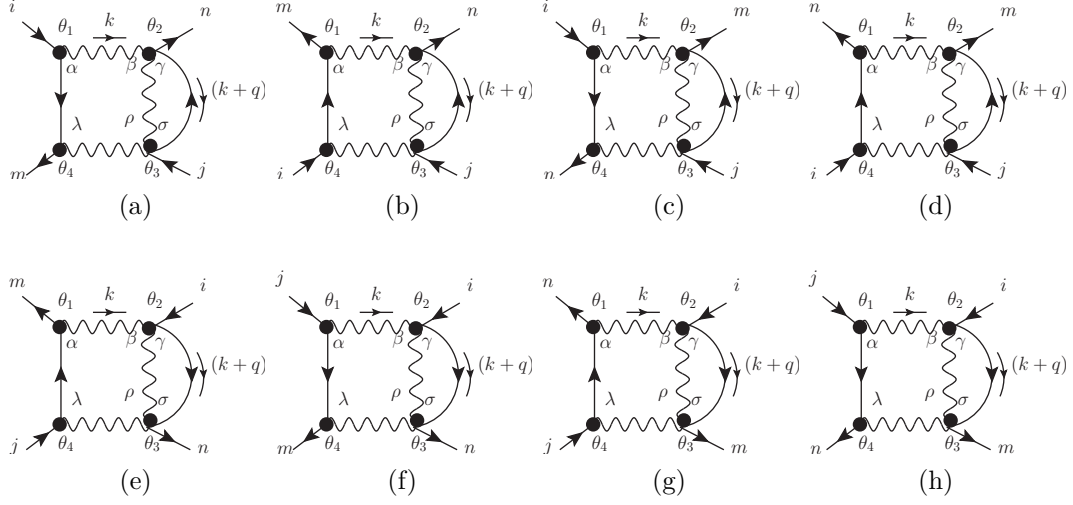
using Eqs. (C.14) and (C.16), then adding  $\mathcal{S}_{(\overline{\Phi}\Phi)^2}^{(D29-a)}$  to  $\mathcal{S}_{(\overline{\Phi}\Phi)^2}^{(D29-d)}$  with the values in Table B.21, we find

$$\mathcal{S}_{(\overline{\Phi}\Phi)^2}^{(D29)} = \frac{1}{16} \left( \frac{(a-b)(a+b)^2}{32\pi^2\epsilon} \right) i g^6 (\delta_{mi}\delta_{jn} + \delta_{mj}\delta_{in}) \int_{\theta} \overline{\Phi}_i \Phi_m \Phi_n \overline{\Phi}_j . \quad (\text{B.98})$$

$D30 - a$	$\delta_{nj}\delta_{mi}$	$D30 - b$	$\delta_{nj}\delta_{mi}$	$D30 - c$	$\delta_{ni}\delta_{mj}$
$D30 - d$	$\delta_{ni}\delta_{mj}$	$D30 - e$	$\delta_{ni}\delta_{mj}$	$D30 - f$	$\delta_{ni}\delta_{mj}$
$D30 - g$	$\delta_{nj}\delta_{mi}$	$D30 - h$	$\delta_{nj}\delta_{mi}$		

Table B.22: Values of the diagrams in Figure B.32 with common factor

$$\frac{1}{32} \left( \frac{b^3 + 5a^2b - 4ab^2 - 2a^3}{32\pi^2\epsilon} \right) i g^6 \int_{\theta} \overline{\Phi}_i \Phi_m \Phi_n \overline{\Phi}_j .$$


 Figure B.32:  $\mathcal{S}_{(\Phi\Phi)^2}^{(D30)}$ 

$D31 - a$	$\delta_{ni}\delta_{jm}$	$D31 - b$	$\delta_{nj}\delta_{im}$	$D31 - c$	$-\delta_{ni}\delta_{jm}$
$D31 - d$	$-\delta_{nj}\delta_{im}$	$D31 - e$	$-\delta_{nj}\delta_{im}$	$D31 - f$	$-\delta_{ni}\delta_{jm}$
$D31 - g$	$\delta_{ni}\delta_{jm}$	$D31 - h$	$\delta_{nj}\delta_{im}$		

 Table B.23: Values of the diagrams in Figure B.33 with common factor  $\frac{1}{16} \left( \frac{a^2 b - a^3}{32\pi^2 \epsilon} \right) i g^6 \int_{\theta} \bar{\Phi}_i \Phi_m \Phi_n \bar{\Phi}_j$ .

$\mathcal{S}_{(\Phi\Phi)^2}^{(D30-a)}$  in the Figure B.32 is

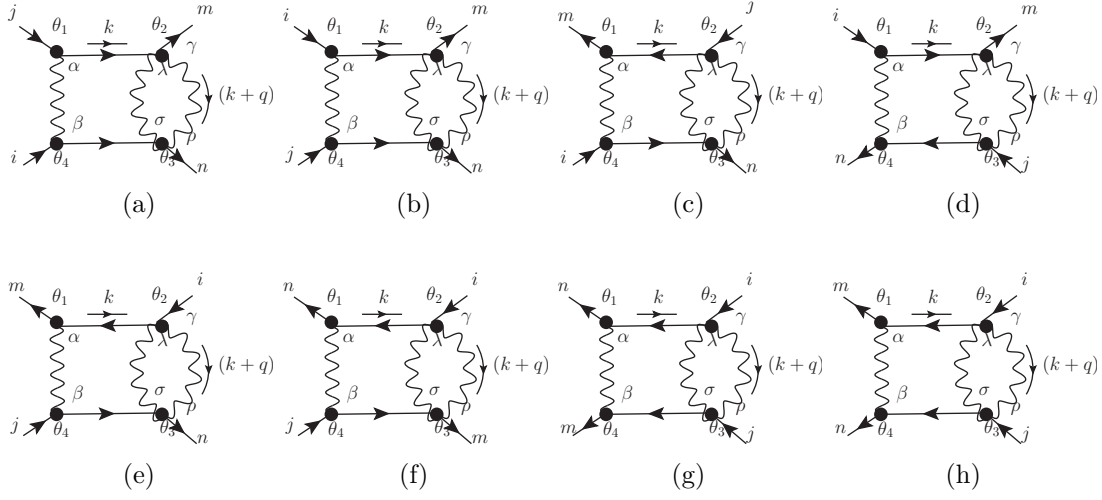
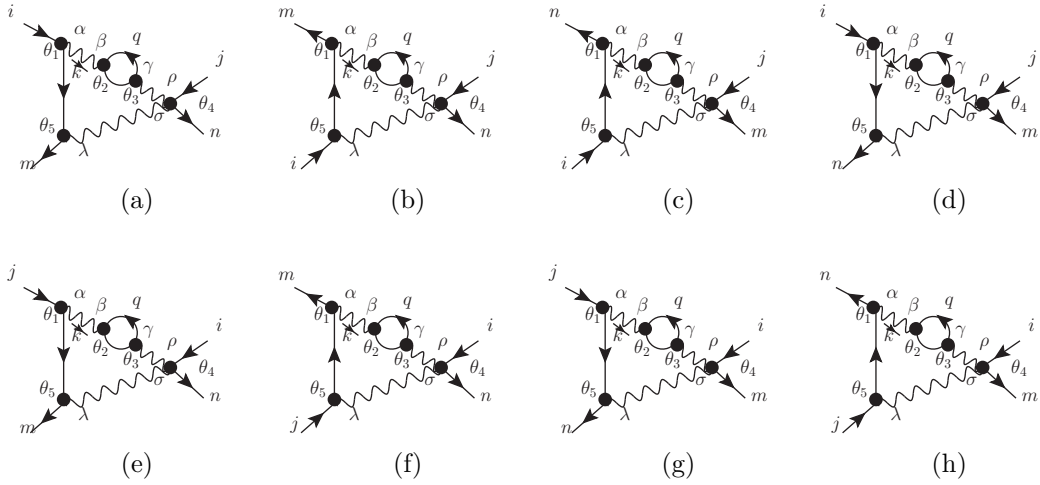
$$\mathcal{S}_{(\Phi\Phi)^2}^{(D30-a)} = -\frac{1}{32} i \delta_{nj} \delta_{mi} g^6 \int_{\theta} \bar{\Phi}_i \Phi_m \Phi_n \bar{\Phi}_j \int \frac{d^D k d^D q}{(2\pi)^{2D}} \left\{ \frac{-2b(a-b)^2 (k \cdot q) k^2 - 2a(a-b)^2 (k^2)^2}{(k^2)^3 (k+q)^2 q^2} \right\}, \quad (\text{B.99})$$

using Eqs. (C.14) and (C.16), then adding  $\mathcal{S}_{(\Phi\Phi)^2}^{(D30-a)}$  to  $\mathcal{S}_{(\Phi\Phi)^2}^{(D30-h)}$  with the values in Table B.22, we find

$$\mathcal{S}_{(\Phi\Phi)^2}^{(D30)} = -\frac{1}{8} \left( \frac{(a-b)^2 (2a-b)}{32\pi^2 \epsilon} \right) i g^6 (\delta_{nj} \delta_{mi} + \delta_{ni} \delta_{mj}) \int_{\theta} \bar{\Phi}_i \Phi_m \Phi_n \bar{\Phi}_j. \quad (\text{B.100})$$

$\mathcal{S}_{(\Phi\Phi)^2}^{(D31-a)}$  in the Figure B.33 is

$$\mathcal{S}_{(\Phi\Phi)^2}^{(D31-a)} = \frac{1}{64} i \delta_{ni} \delta_{jm} g^6 \int_{\theta} \bar{\Phi}_i \Phi_m \Phi_n \bar{\Phi}_j \int \frac{d^D k d^D q}{(2\pi)^{2D}} \left\{ \frac{-4(a^3 - a^2 b) (k^2)^2}{(k^2)^3 (k+q)^2 q^2} \right\}, \quad (\text{B.101})$$

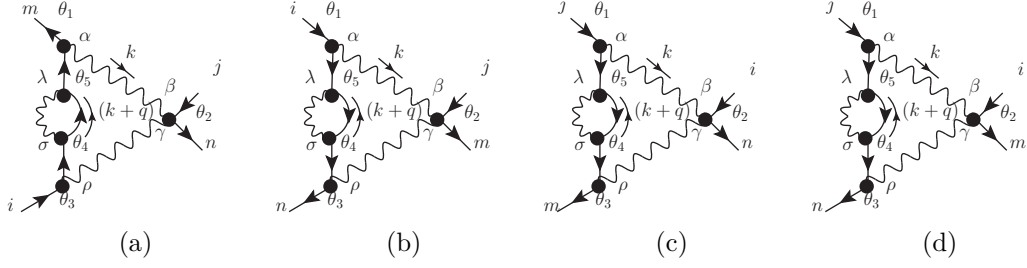

 Figure B.33:  $\mathcal{S}_{(\overline{\Phi}\Phi)^2}^{(D31)}$ 

 Figure B.34:  $\mathcal{S}_{(\overline{\Phi}\Phi)^2}^{(D32)}$ 

using Eq. (C.14), then adding  $\mathcal{S}_{(\overline{\Phi}\Phi)^2}^{(D31-a)}$  to  $\mathcal{S}_{(\overline{\Phi}\Phi)^2}^{(D31-h)}$  with the values in Table B.23, we find

$$\mathcal{S}_{(\overline{\Phi}\Phi)^2}^{(D31)} = 0. \quad (\text{B.102})$$

$\mathcal{S}_{(\overline{\Phi}\Phi)^2}^{(D32-a)}$  in the Figure B.34 is

$$\mathcal{S}_{(\overline{\Phi}\Phi)^2}^{(D32-a)} = -\frac{1}{128} i N g^6 \delta_{mi} \delta_{jn} \int_{\theta} \overline{\Phi}_i \Phi_m \Phi_n \overline{\Phi}_j \int \frac{d^D k d^D q}{(2\pi)^{2D}} \left\{ \frac{4(a-b)^3 (k^2)^2 (2(k \cdot q) + k^2 + 2q^2)}{(k^2)^4 (k+q)^2 q^2} \right\}, \quad (\text{B.103})$$


 Figure B.35:  $\mathcal{S}_{(\Phi\Phi)^2}^{(D33)}$ 

$D33 - a$	$\delta_{im}\delta_{jn}$	$D33 - b$	$\delta_{jm}\delta_{in}$	$D33 - c$	$\delta_{jm}\delta_{in}$
$D33 - d$	$\delta_{im}\delta_{jn}$				

 Table B.24: Values of the diagrams in Figure B.35 with common factor  $\frac{1}{16} \left( \frac{a(a-b)^2}{32\pi^2\epsilon} \right) i g^6 \int_{\theta} \bar{\Phi}_i \Phi_m \Phi_n \bar{\Phi}_j$ .

using Eqs. (C.14), (C.16), then adding  $\mathcal{S}_{(\Phi\Phi)^2}^{(D32-a)}$  to  $\mathcal{S}_{(\Phi\Phi)^2}^{(D32-h)}$ , we find

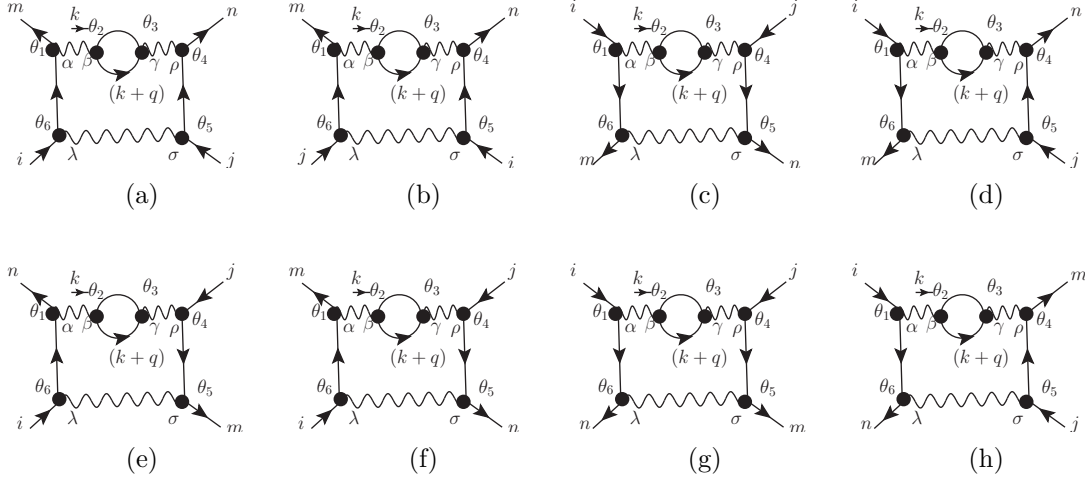
$$\mathcal{S}_{(\Phi\Phi)^2}^{(D32-a)} = \mathcal{S}_{(\Phi\Phi)^2}^{(D32)} = 0. \quad (\text{B.104})$$

$\mathcal{S}_{(\Phi\Phi)^2}^{(D33-a)}$  in the Figure B.35 is

$$\begin{aligned} \mathcal{S}_{(\Phi\Phi)^2}^{(D33-a)} &= \frac{1}{128} i g^6 \delta_{im} \delta_{jn} \int_{\theta} \bar{\Phi}_i \Phi_m \Phi_n \bar{\Phi}_j \\ &\times \int \frac{d^D k d^D q}{(2\pi)^{2D}} \left\{ \frac{-4(a-b)^3 (k^2)^2 q^2 - 16a(a-b)^2 (k^2)^2 (k^2 + (k \cdot q))}{(k^2)^4 (k+q)^2 q^2} \right\}, \end{aligned} \quad (\text{B.105})$$

using Eqs. (C.14), (C.16), then adding  $\mathcal{S}_{(\Phi\Phi)^2}^{(D33-a)}$  to  $\mathcal{S}_{(\Phi\Phi)^2}^{(D33-d)}$  with the values in the Table B.24, we find

$$\mathcal{S}_{(\Phi\Phi)^2}^{(D33)} = \frac{1}{8} \left( \frac{a(a-b)^2}{32\pi^2\epsilon} \right) i g^6 (\delta_{im}\delta_{jn} + \delta_{jm}\delta_{in}) \int_{\theta} \bar{\Phi}_i \Phi_m \Phi_n \bar{\Phi}_j. \quad (\text{B.106})$$


 Figure B.36:  $\mathcal{S}_{(\overline{\Phi}\Phi)^2}^{(D34)}$ 

$D35 - a$	$\delta_{im} \delta_{nj}$	$D35 - b$	$\delta_{jm} \delta_{ni}$	$D35 - c$	$\delta_{im} \delta_{nj}$
$D35 - d$	$\delta_{jm} \delta_{ni}$	$D35 - e$	$\delta_{jm} \delta_{ni}$	$D35 - f$	$\delta_{im} \delta_{nj}$
$D35 - g$	$\delta_{jm} \delta_{ni}$	$D35 - h$	$\delta_{im} \delta_{nj}$		

 Table B.25: Values of the diagrams in Figure B.37 with common factor  $-\frac{1}{32} \left( \frac{a(a-b)^2}{32\pi^2\epsilon} \right) i g^6 \int_{\theta} \overline{\Phi}_i \Phi_m \Phi_n \overline{\Phi}_j$ .

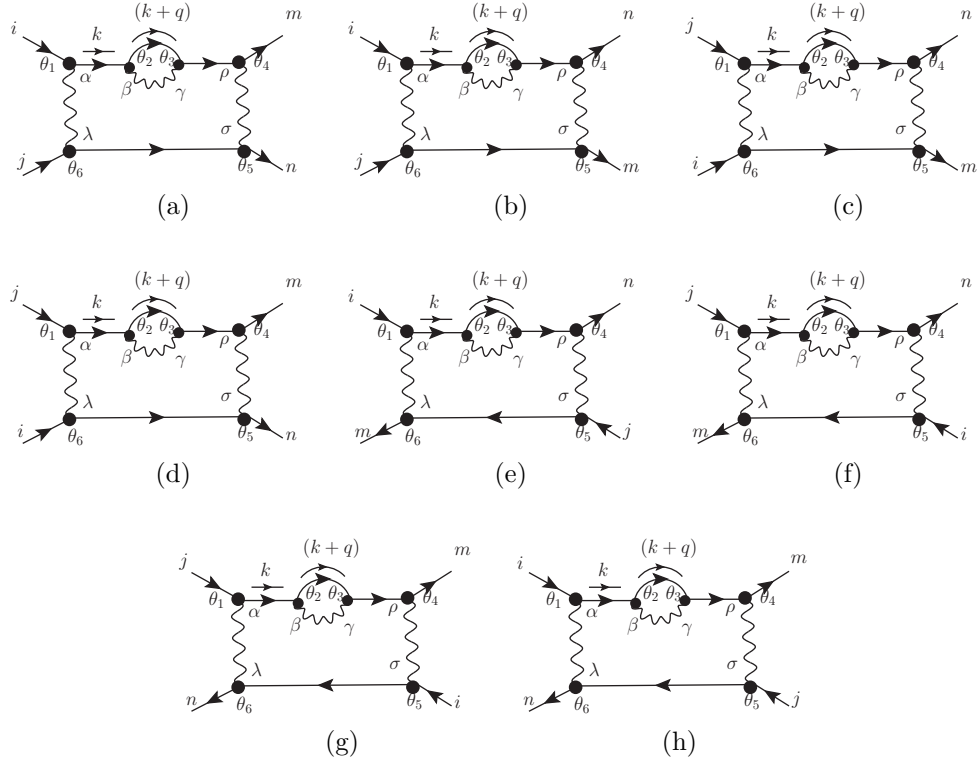
$\mathcal{S}_{(\overline{\Phi}\Phi)^2}^{(D34-a)}$  in the Figure B.36 is

$$\mathcal{S}_{(\overline{\Phi}\Phi)^2}^{(D34-a)} = \frac{1}{64(8)} i g^6 N \delta_{im} \delta_{nj} \int_{\theta} \overline{\Phi}_i \Phi_m \Phi_n \overline{\Phi}_j \int \frac{d^D k d^D q}{(2\pi)^{2D}} \left\{ \frac{8(a-b)^3 (k^2)^3 (2(k \cdot q) + k^2 + 2q^2)}{(k^2)^5 (k+q)^2 q^2} \right\}, \quad (\text{B.107})$$

using Eqs. (C.14), (C.16), then adding  $\mathcal{S}_{(\overline{\Phi}\Phi)^2}^{(D34-a)}$  to  $\mathcal{S}_{(\overline{\Phi}\Phi)^2}^{(D34-h)}$ , we find

$$\mathcal{S}_{(\overline{\Phi}\Phi)^2}^{(D34-a)} = \mathcal{S}_{(\overline{\Phi}\Phi)^2}^{(D34)} = 0. \quad (\text{B.108})$$



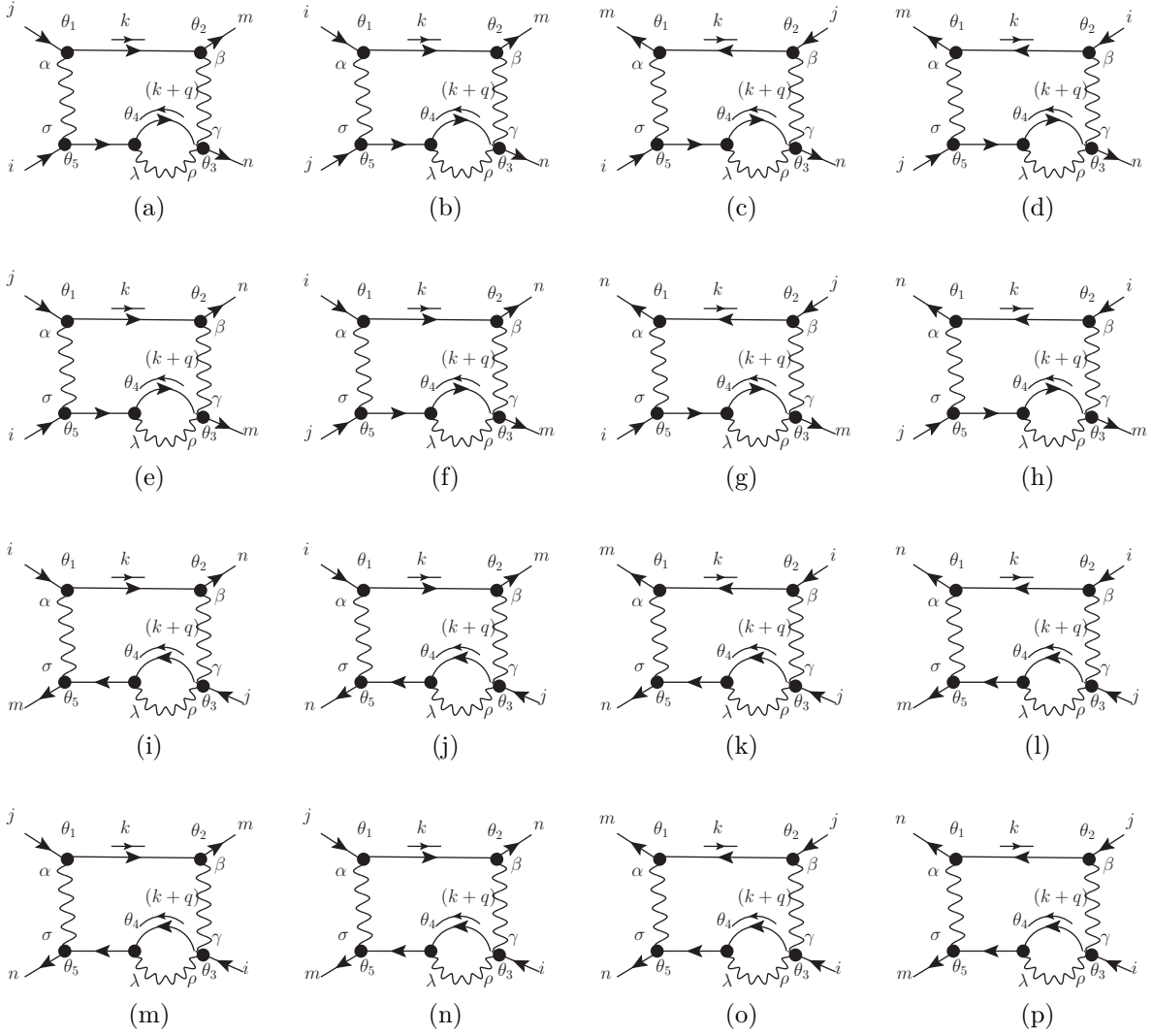

 Figure B.37:  $\mathcal{S}_{(\Phi\Phi)^2}^{(D35)}$ 

$\mathcal{S}_{(\Phi\Phi)^2}^{(D35-a)}$  in the Figure B.37 is

$$\begin{aligned} \mathcal{S}_{(\Phi\Phi)^2}^{(D35-a)} &= \frac{1}{64(8)} i \delta_{im} \delta_{nj} g^6 \int_{\theta} \bar{\Phi}_i \Phi_m \Phi_n \bar{\Phi}_j \\ &\times \int \frac{d^D k d^D q}{(2\pi)^{2D}} \left\{ \frac{32 a (a-b)^2 (k^2)^3 ((k \cdot q) + k^2) + 8 (a-b)^3 (k^2)^3 q^2}{(k^2)^5 (k+q)^2 q^2} \right\}, \quad (\text{B.109}) \end{aligned}$$

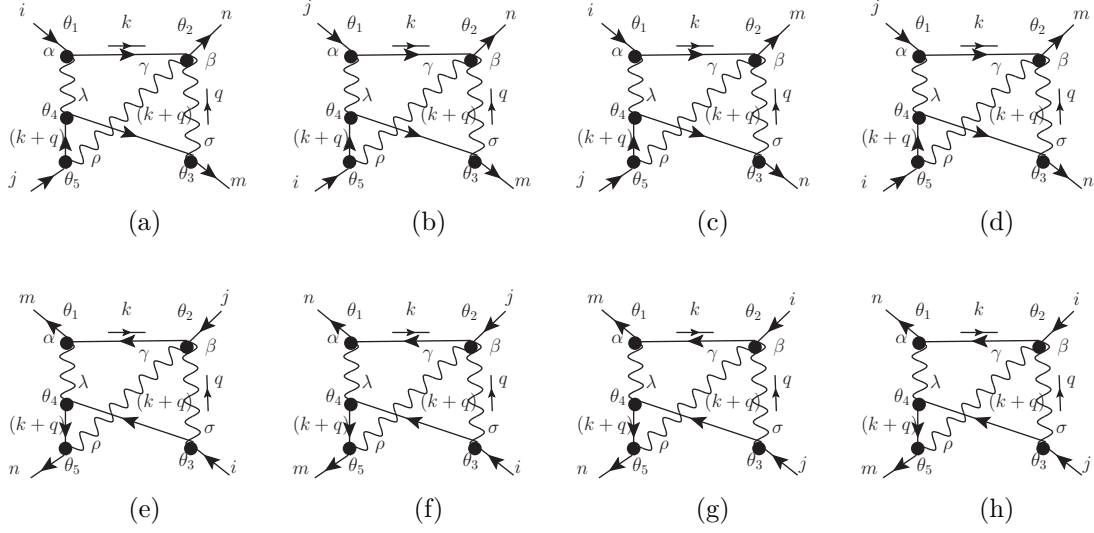
using Eqs. (C.14), (C.16), then adding  $\mathcal{S}_{(\Phi\Phi)^2}^{(D35-a)}$  to  $\mathcal{S}_{(\Phi\Phi)^2}^{(D35-h)}$  with the values in Table B.25, we find

$$\mathcal{S}_{(\Phi\Phi)^2}^{(D35)} = -\frac{1}{8} \left( \frac{a(a-b)^2}{32\pi^2 \epsilon} \right) i g^6 (\delta_{im} \delta_{nj} + \delta_{jm} \delta_{ni}) \int_{\theta} \bar{\Phi}_i \Phi_m \Phi_n \bar{\Phi}_j. \quad (\text{B.110})$$


 Figure B.38:  $\mathcal{S}_{(\Phi\Phi)^2}^{(D36)}$ 

$D36 - a$	$\delta_{mj}\delta_{ni}$	$D36 - b$	$\delta_{mi}\delta_{nj}$	$D36 - c$	$\delta_{mj}\delta_{ni}$
$D36 - d$	$\delta_{mi}\delta_{nj}$	$D36 - e$	$\delta_{mi}\delta_{nj}$	$D36 - f$	$\delta_{mj}\delta_{ni}$
$D36 - g$	$\delta_{mi}\delta_{nj}$	$D36 - h$	$\delta_{mj}\delta_{ni}$	$D36 - i$	$\delta_{mj}\delta_{ni}$
$D36 - j$	$\delta_{mi}\delta_{nj}$	$D36 - k$	$\delta_{mi}\delta_{nj}$	$D36 - l$	$\delta_{mj}\delta_{ni}$
$D36 - m$	$\delta_{mj}\delta_{ni}$	$D36 - n$	$\delta_{mi}\delta_{nj}$	$D36 - o$	$\delta_{mj}\delta_{ni}$
$D36 - p$	$\delta_{mi}\delta_{nj}$				

 Table B.26: Values of the diagrams in Figure B.38 with common factor  $\frac{1}{64} \left( \frac{3a^3 - 7a^2b + 5ab^2 - b^3}{32\pi^2\epsilon} \right) i g^6 \int_{\theta} \bar{\Phi}_i \Phi_m \Phi_n \bar{\Phi}_j$ .


 Figure B.39:  $\mathcal{S}_{(\Phi\Phi)^2}^{(D37)}$ 

$\mathcal{S}_{(\Phi\Phi)^2}^{(D36-a)}$  in the Figure B.38 is

$$\mathcal{S}_{(\Phi\Phi)^2}^{(D36-a)} = -\frac{1}{128} i g^6 \delta_{mj} \delta_{ni} \int_{\theta} \bar{\Phi}_i \Phi_m \Phi_n \bar{\Phi}_j \times \int \frac{d^D k d^D q}{(2\pi)^{2D}} \left\{ \frac{8a (a-b)^2 (k^2)^3 + 4(a^3 - a^2 b - a b^2 + b^3) (k \cdot q) (k^2)^2}{(k^2)^4 (q+k)^2 q^2} \right\}, \quad (\text{B.111})$$

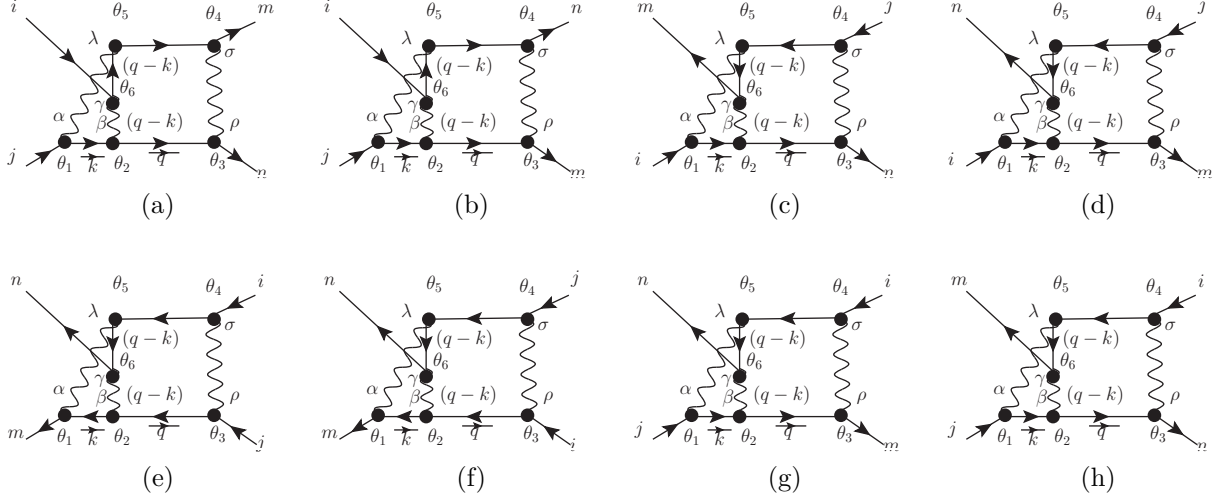
using Eqs. (C.14) and (C.16), then adding  $\mathcal{S}_{(\Phi\Phi)^2}^{(D36-a)}$  to  $\mathcal{S}_{(\Phi\Phi)^2}^{(D36-p)}$  with the values in Table B.26, we find

$$\mathcal{S}_{(\Phi\Phi)^2}^{(D36)} = \frac{1}{8} \left( \frac{(a-b)^2 (3a-b)}{32\pi^2 \epsilon} \right) i g^6 (\delta_{mi} \delta_{nj} + \delta_{mj} \delta_{ni}) \int_{\theta} \bar{\Phi}_i \Phi_m \Phi_n \bar{\Phi}_j. \quad (\text{B.112})$$

$\mathcal{S}_{(\Phi\Phi)^2}^{(D37-a)}$  in the Figure B.39 is

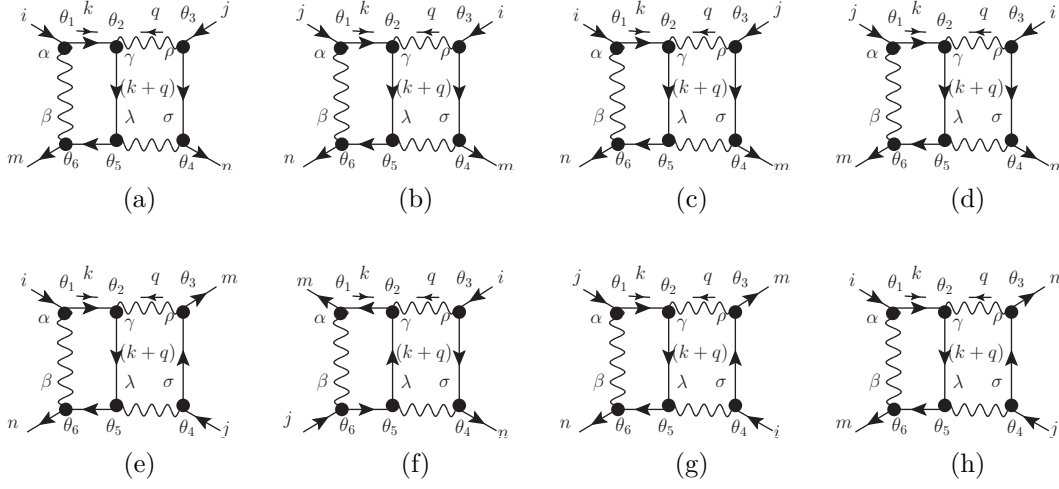
$$\mathcal{S}_{(\Phi\Phi)^2}^{(D37-a)} = \mathcal{S}_{(\Phi\Phi)^2}^{(D37)} = 0, \quad (\text{B.113})$$

because of  $D$ 's manipulations.


 Figure B.40:  $\mathcal{S}_{(\overline{\Phi}\Phi)^2}^{(D38)}$ 

$D38 - a$	$-\delta_{jn}\delta_{im}$	$D38 - b$	$-\delta_{jm}\delta_{in}$	$D38 - c$	$\delta_{jm}\delta_{in}$
$D38 - d$	$\delta_{im}\delta_{jn}$	$D38 - e$	$-\delta_{jm}\delta_{in}$	$D38 - f$	$-\delta_{im}\delta_{jn}$
$D38 - g$	$\delta_{jm}\delta_{in}$	$D38 - h$	$\delta_{im}\delta_{jn}$		

 Table B.27: Values of the diagrams in Figure B.40 with common factor  $\frac{1}{64} \left( \frac{(a-b)^3}{32\pi^2\epsilon} \right) i g^6 \int_{\theta} \overline{\Phi}_i \Phi_m \Phi_n \overline{\Phi}_j$ .


 Figure B.41:  $\mathcal{S}_{(\Phi\Phi)^2}^{(D39)}$ 

$\mathcal{S}_{(\Phi\Phi)^2}^{(D38-a)}$  in the Figure B.40 is

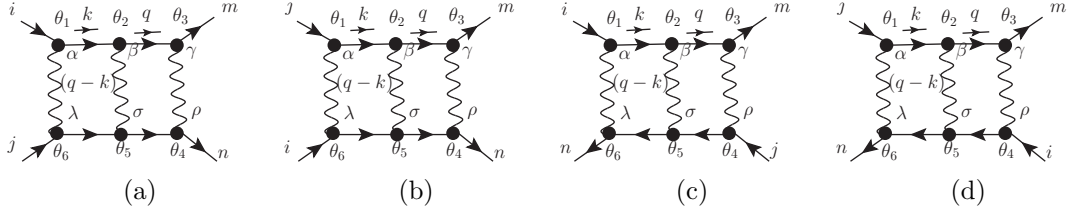
$$\begin{aligned} \mathcal{S}_{(\Phi\Phi)^2}^{(D38-a)} &= \frac{1}{64(8)} i \delta_{jn} \delta_{im} g^6 \int_{\theta} \bar{\Phi}_i \Phi_m \Phi_n \bar{\Phi}_j \int \frac{d^D k d^D q}{(2\pi)^{2D}} \left\{ -4 a^2 b (k \cdot q)^2 k^2 q^2 \right. \\ &\quad + 4 a^2 b (k \cdot q)^2 (q^2)^2 + a^2 b k_{\alpha\beta} k_{\gamma\delta} q^{\alpha\delta} q^{\beta\gamma} k^2 q^2 - a^2 b k_{\alpha\beta} k_{\gamma\delta} q^{\alpha\delta} q^{\beta\gamma} (q^2)^2 \\ &\quad + 8 (a-b)^3 k^2 (q^2)^2 (k-q)^2 + 2 a^2 b (k^2)^2 (q^2)^2 - 2 a^2 b k^2 (q^2)^3 \Big\} \\ &\quad \times \frac{1}{(k^2)^2 (q^2)^3 [(q-k)^2]^2}, \end{aligned} \quad (\text{B.114})$$

using Eqs. (C.14) and (C.24), then adding  $\mathcal{S}_{(\Phi\Phi)^2}^{(D38-a)}$  to  $\mathcal{S}_{(\Phi\Phi)^2}^{(D38-h)}$  with the values in Table B.27, we find

$$\mathcal{S}_{(\Phi\Phi)^2}^{(D38)} = 0. \quad (\text{B.115})$$

$\mathcal{S}_{(\Phi\Phi)^2}^{(D39-a)}$  in the Figure B.41 is

$$\begin{aligned} \mathcal{S}_{(\Phi\Phi)^2}^{(D39-a)} &= -\frac{1}{64(8)} i \delta_{im} \delta_{jn} g^6 \int_{\theta} \bar{\Phi}_i \Phi_m \Phi_n \bar{\Phi}_j \int \frac{d^D k d^D q}{(2\pi)^{2D}} \left\{ 16 (a-b)^3 (k \cdot q) (k^2)^2 q^2 \right. \\ &\quad + (8 a^3 - 22 a^2 b + 24 a b^2 - 8 b^3) (k^2)^2 (q^2)^2 - 4 a^2 b (k \cdot q)^2 k^2 q^2 \\ &\quad \left. + a^2 b q_{\alpha\beta} q_{\gamma\delta} k^{\alpha\gamma} k^{\beta\delta} k^2 q^2 \right\} \frac{1}{(k^2)^3 (k+q)^2 (q^2)^3}, \end{aligned} \quad (\text{B.116})$$


 Figure B.42:  $\mathcal{S}_{(\overline{\Phi}\Phi)^2}^{(D40)}$ 

$D40 - a$	$-\delta_{im}\delta_{jn}$	$D40 - b$	$-\delta_{jm}\delta_{in}$	$D40 - c$	$\delta_{im}\delta_{jn}$
$D40 - d$	$\delta_{jm}\delta_{in}$				

Table B.28: Values of the diagrams in Figure B.42 with common factor

$$\frac{1}{16} \left( \frac{a(a-b)^2}{32\pi^2\epsilon} \right) i g^6 \int_{\theta} \overline{\Phi}_i \Phi_m \Phi_n \overline{\Phi}_j .$$

using Eqs. (C.14), (C.16) and (C.20), then adding  $\mathcal{S}_{(\overline{\Phi}\Phi)^2}^{(D39-a)}$  to  $\mathcal{S}_{(\overline{\Phi}\Phi)^2}^{(D39-h)}$ , we find

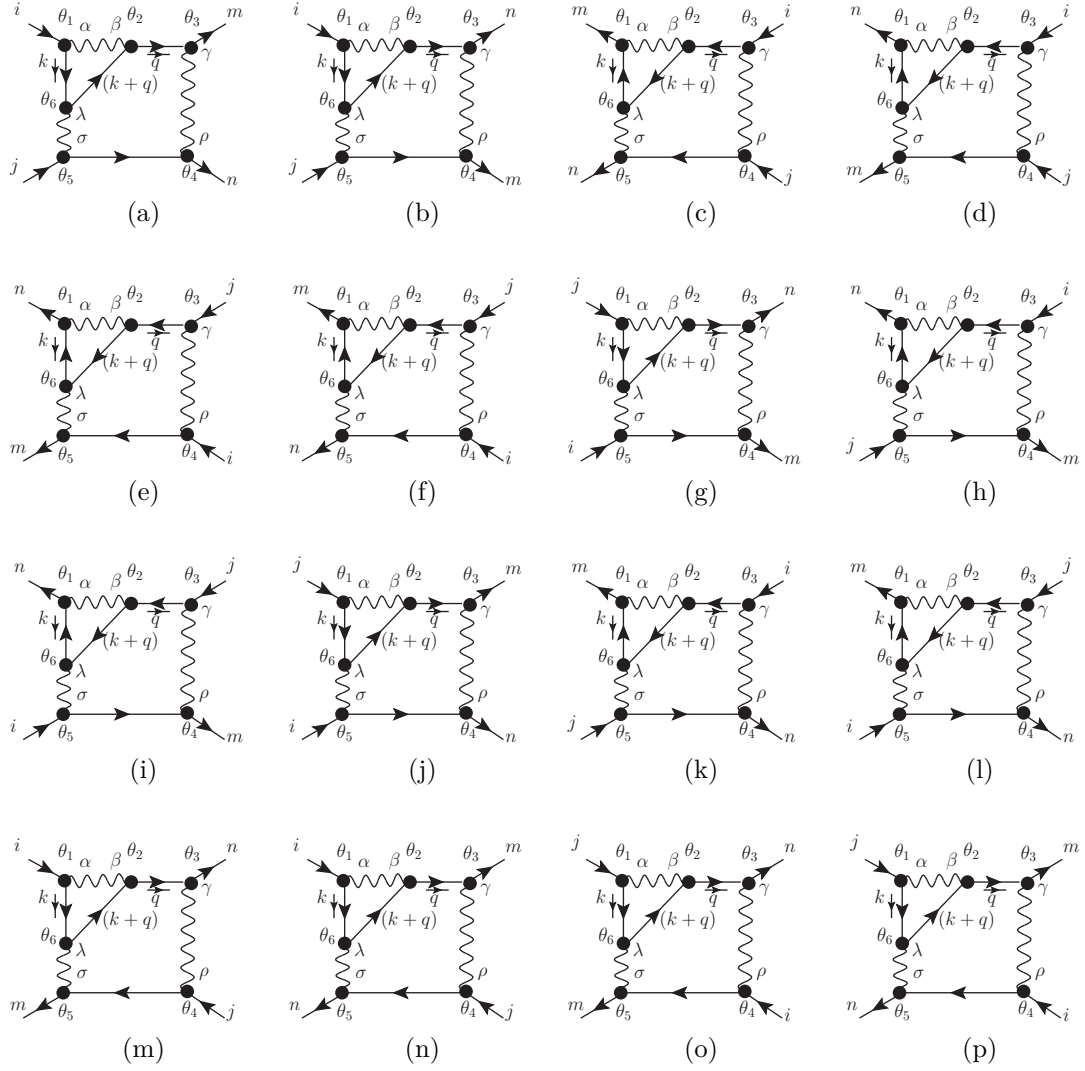
$$\mathcal{S}_{(\overline{\Phi}\Phi)^2}^{(D39-a)} = \mathcal{S}_{(\overline{\Phi}\Phi)^2}^{(D39)} = 0 . \quad (\text{B.117})$$

$\mathcal{S}_{(\overline{\Phi}\Phi)^2}^{(D40-a)}$  in the Figure B.42 is

$$\mathcal{S}_{(\overline{\Phi}\Phi)^2}^{(D40-a)} = -\frac{1}{64(8)} i \delta_{im}\delta_{jn} g^6 \int_{\theta} \overline{\Phi}_i \Phi_m \Phi_n \overline{\Phi}_j \int \frac{d^D k d^D q}{(2\pi)^{2D}} \left\{ \frac{-32 a (a-b)^2 (k^2)^2 (q^2)^2}{(k^2)^3 (q-k)^2 (q^2)^3} \right\} , \quad (\text{B.118})$$

using Eq. (C.14), then adding  $\mathcal{S}_{(\overline{\Phi}\Phi)^2}^{(D40-a)}$  to  $\mathcal{S}_{(\overline{\Phi}\Phi)^2}^{(D40-d)}$  with the values in Table B.28, we find

$$\mathcal{S}_{(\overline{\Phi}\Phi)^2}^{(D40)} = 0 . \quad (\text{B.119})$$


 Figure B.43:  $\mathcal{S}_{(\Phi\Phi)^2}^{(D41)}$ 

$D41 - a$	$\delta_{im} \delta_{nj}$	$D41 - b$	$\delta_{jm} \delta_{ni}$	$D41 - c$	$\delta_{im} \delta_{nj}$
$D41 - d$	$\delta_{jm} \delta_{ni}$	$D41 - e$	$\delta_{im} \delta_{nj}$	$D41 - f$	$\delta_{jm} \delta_{ni}$
$D41 - g$	$\delta_{im} \delta_{nj}$	$D41 - h$	$\delta_{jm} \delta_{ni}$	$D41 - i$	$\delta_{im} \delta_{nj}$
$D41 - j$	$\delta_{jm} \delta_{ni}$	$D41 - k$	$\delta_{im} \delta_{nj}$	$D41 - l$	$\delta_{jm} \delta_{ni}$
$D41 - m$	$\delta_{jm} \delta_{ni}$	$D41 - n$	$\delta_{im} \delta_{nj}$	$D41 - o$	$\delta_{im} \delta_{nj}$
$D41 - p$	$\delta_{jm} \delta_{ni}$				

Table B.29: Values of the diagrams in Figure B.43 with common factor

$$\frac{1}{64} \left( \frac{(b-a)^3}{32\pi^2\epsilon} \right) i g^6 \int_{\theta} \bar{\Phi}_i \Phi_m \Phi_n \bar{\Phi}_j .$$

$\mathcal{S}_{(\overline{\Phi}\Phi)^2}^{(D41-a)}$  in the Figure B.43 is

$$\begin{aligned} \mathcal{S}_{(\overline{\Phi}\Phi)^2}^{(D41-a)} = & -\frac{1}{64(8)} i \delta_{im} \delta_{nj} g^6 \int_{\theta} \overline{\Phi}_i \Phi_m \Phi_n \overline{\Phi}_j \int \frac{d^D k d^D q}{(2\pi)^{2D}} \left\{ 4 (2a^3 - a^2 b) (k \cdot q)^2 (q^2)^2 \right. \\ & + (8b^3 - 12a^3 + 26a^2 b - 24ab^2) k^2 (q^2)^3 - a^3 q_{\alpha\beta} q_{\gamma\delta} k^{\alpha\delta} k^{\beta\gamma} \\ & \left. + (a^2 b - a^3) k_{\alpha\beta} k_{\gamma\delta} q^{\alpha\delta} q^{\beta\gamma} \right\} \frac{1}{(k^2)^2 (k+q)^2 (q^2)^4}, \end{aligned} \quad (\text{B.120})$$

using Eqs. (C.14) and (C.20), then adding  $\mathcal{S}_{(\overline{\Phi}\Phi)^2}^{(D41-a)}$  to  $\mathcal{S}_{(\overline{\Phi}\Phi)^2}^{(D41-p)}$  with the values in Table B.29, we find

$$\mathcal{S}_{(\overline{\Phi}\Phi)^2}^{(D41)} = \frac{1}{8} \left( \frac{(b-a)^3}{32\pi^2 \epsilon} \right) i g^6 (\delta_{im} \delta_{nj} + \delta_{jm} \delta_{ni}) \int_{\theta} \overline{\Phi}_i \Phi_m \Phi_n \overline{\Phi}_j. \quad (\text{B.121})$$



# Appendix C

## Useful integrals

In this appendix we compute a set of general integrals that will be needed in the computation of the Feynman superdiagrams considered in this thesis.

### C.1 One loop integrals

We will start by considering some massive integrals, which will be the base for the derivation of the massless integrals that we will need, as shown in the next subsection.

First we quote the one loop integral in Minkowski space-time [79],

$$\begin{aligned}\mathcal{I}_1(A, p, m) &= \int \frac{d^D l}{(2\pi)^D} \frac{1}{[l^2 + m^2 + x(2p \cdot l + p^2)]^A} \\ &= i\mu^\epsilon \frac{\Gamma\left(A - \frac{D}{2}\right)}{(4\pi)^{D/2} \Gamma(A)} \left[x(1-x)p^2 + m^2\right]^{\frac{D}{2}-A},\end{aligned}\tag{C.1}$$

where  $d^D l \equiv \mu^\epsilon d^{3-\epsilon} l$  and  $D = 3 - \epsilon$ . Using this result we can obtain the set of integrals that will be needed in this thesis. For convenience, we will look for expressions where the momenta with uncontracted indices always appearing as bispinors. Let us start with the definitions,

$$p^2 \equiv \frac{1}{2} p^{\alpha\beta} p_{\alpha\beta}, \quad p \cdot l \equiv \frac{1}{2} p^{\alpha\beta} l_{\alpha\beta}.\tag{C.2}$$

Using the properties in Eqs. (2.10) and (2.11), we have

$$\frac{\partial}{\partial p^{\alpha\beta}} p^{\theta\sigma} = \partial_{\alpha\beta} p^{\theta\sigma} = \frac{1}{2} \left( \delta_\alpha^\theta \delta_\beta^\sigma + \delta_\beta^\theta \delta_\alpha^\sigma \right).\tag{C.3}$$

Then, by derivation with respect to  $p$  in Eq. (C.1), we obtain

$$\frac{\partial}{\partial p^{\alpha\beta}} \left( \int \frac{d^D l}{(2\pi)^D} \left\{ \frac{1}{[l^2 + m^2 + x(2p \cdot l + p^2)]^A} \right\} \right) = i \frac{\Gamma\left(A - \frac{D}{2}\right)}{(4\pi)^{D/2} \Gamma(A)} [x(1-x)p^2 + m^2]^{\frac{D}{2}-A} \quad (\text{C.4})$$

where

$$\frac{\partial}{\partial p^{\alpha\beta}} \left\{ \frac{1}{[l^2 + m^2 + x(2p \cdot l + p^2)]^A} \right\} = -A x [l^2 + m^2 + x(2p \cdot l + p^2)]^{-(A+1)} (l_{\theta\sigma} + p_{\theta\sigma}), \quad (\text{C.5})$$

and

$$\frac{\partial}{\partial p^{\alpha\beta}} \left\{ [x(1-x)p^2 + m^2]^{\frac{D}{2}-A} \right\} = x(1-x) p_{\alpha\beta} \left( \frac{D}{2} - A \right) [x(1-x)p^2 + m^2]^{\frac{D}{2}-A-1}. \quad (\text{C.6})$$

Substituting Eqs. (C.5) and (C.6) in Eq. (C.4) and using Eq. (C.1), we obtain,

$$\begin{aligned} \mathcal{I}_2(A, p, m) &= \int \frac{d^D l}{(2\pi)^D} \frac{l_{\alpha\beta}}{[l^2 + m^2 + x(2p \cdot l + p^2)]^A} \\ &= i \mu^\epsilon \frac{\Gamma\left(A - \frac{D}{2}\right)}{(4\pi)^{D/2} \Gamma(A)} \left\{ \frac{(-x) p_{\alpha\beta}}{[x(1-x)p^2 + m^2]^{A-D/2}} \right\} = -x p_{\alpha\beta} \mathcal{I}_1(A, p, m), \end{aligned} \quad (\text{C.7})$$

where it was used that

$$A \Gamma(A) = \Gamma(A+1). \quad (\text{C.8})$$

Using a similar procedure, it is possible to obtain the following set of integrals:

$$\begin{aligned} \mathcal{I}_3(A, p, m) &= \int \frac{d^D l}{(2\pi)^D} \frac{l_{\mu\nu} l_{\alpha\beta}}{(l^2 + m^2 + x(2l \cdot p + p^2))^A} = x^2 p_{\mu\nu} p_{\alpha\beta} \mathcal{I}_1(A, p, m) \\ &\quad + \frac{1}{2(A-1)} (C_{\mu\alpha} C_{\nu\beta} + C_{\nu\alpha} C_{\mu\beta}) \mathcal{I}_1(A-1, p, m) \end{aligned} \quad (\text{C.9})$$

$$\begin{aligned} \mathcal{I}_4(A, p, m) &= \int \frac{d^D l}{(2\pi)^D} \frac{l_{\mu\nu} l_{\rho\sigma} l_{\alpha\beta}}{(l^2 + m^2 + x(2l \cdot p + p^2))^A} = -x^3 p_{\mu\nu} p_{\rho\sigma} p_{\alpha\beta} \mathcal{I}_1(A, p, m) \\ &\quad - \frac{x}{2(A-1)} \left\{ (C_{\mu\alpha} C_{\nu\beta} + C_{\nu\alpha} C_{\mu\beta}) p_{\rho\sigma} + (C_{\rho\mu} C_{\sigma\nu} + C_{\sigma\mu} C_{\rho\nu}) p_{\alpha\beta} \right. \\ &\quad \left. + (C_{\rho\alpha} C_{\sigma\beta} + C_{\sigma\alpha} C_{\rho\beta}) p_{\mu\nu} \right\} \mathcal{I}_1(A-1, p, m), \end{aligned} \quad (\text{C.10})$$

$$\begin{aligned}
 \mathcal{I}_5(A, p, m) &= \int \frac{d^D l}{(2\pi)^D} \frac{l_{\mu\nu} l_{\rho\sigma} l_{\alpha\beta} l_{\theta\lambda}}{(l^2 + m^2 + x(2l \cdot p + p^2))^A} = x^4 p_{\mu\nu} p_{\rho\sigma} p_{\alpha\beta} p_{\theta\lambda} \mathcal{I}_1(A, p, m) \\
 &+ \frac{x^2}{2(A-1)} \left\{ (C_{\mu\alpha} C_{\nu\beta} + C_{\nu\alpha} C_{\mu\beta}) p_{\rho\sigma} p_{\theta\lambda} + (C_{\rho\mu} C_{\sigma\nu} + C_{\sigma\mu} C_{\rho\nu}) p_{\alpha\beta} p_{\theta\lambda} \right. \\
 &+ (C_{\rho\alpha} C_{\sigma\beta} + C_{\sigma\alpha} C_{\rho\beta}) p_{\mu\nu} p_{\theta\lambda} + (C_{\theta\mu} C_{\lambda\nu} + C_{\lambda\mu} C_{\theta\nu}) p_{\rho\sigma} p_{\alpha\beta} \\
 &+ (C_{\theta\alpha} C_{\lambda\beta} + C_{\lambda\alpha} C_{\theta\beta}) p_{\mu\nu} p_{\rho\alpha} + (C_{\theta\rho} C_{\lambda\sigma} + C_{\lambda\rho} C_{\theta\sigma}) p_{\mu\nu} p_{\alpha\beta} \left. \right\} \mathcal{I}_1(A-1, p, m) \\
 &+ \frac{1}{4(A-1)(A-2)} \left\{ (C_{\mu\alpha} C_{\nu\beta} + C_{\nu\alpha} C_{\mu\beta}) (C_{\theta\rho} C_{\lambda\sigma} + C_{\lambda\rho} C_{\theta\sigma}) \right. \\
 &+ (C_{\rho\mu} C_{\sigma\beta} + C_{\sigma\mu} C_{\rho\nu}) (C_{\theta\alpha} C_{\lambda\beta} + C_{\lambda\alpha} C_{\theta\beta}) \\
 &+ (C_{\rho\alpha} C_{\sigma\beta} + C_{\sigma\alpha} C_{\rho\beta}) (C_{\theta\mu} C_{\lambda\nu} + C_{\lambda\mu} C_{\theta\nu}) \left. \right\} \mathcal{I}_1(A-2, p, m), \tag{C.11}
 \end{aligned}$$

## C.2 Two loops massless integrals

In this section we obtain a set of integrals that will be needed in our calculations of the renormalization group functions. Therefore, we present only the divergent parts of the integrals, and also the mass parameter is chosen to be zero. Let us start with

$$\begin{aligned}
 \mathcal{I}_6 &= \int \frac{d^D k d^D q}{(2\pi)^{2D}} \frac{q_{\alpha\beta}}{(k+p)^2 (q+k)^2 q^2} = \int_0^1 dx \int \frac{d^D k d^D q}{(2\pi)^{2D}} \frac{q_{\alpha\beta}}{(k+p)^2 [q^2 x + (1-x)(q+k)^2]^2} \\
 &= \int_0^1 dx \int \frac{d^D k d^D q}{(2\pi)^{2D}} \frac{q_{\alpha\beta}}{(k+p)^2 [q^2 + (1-x)(2q \cdot k + k^2)]^2},
 \end{aligned}$$

using Eq. (C.7), we can calculate the integration in  $q$ ,

$$\mathcal{I}_6 = i \mu^\epsilon \frac{\Gamma(2-D/2)}{(4\pi)^{D/2}} \int_0^1 dx \frac{(x-1)}{[x(1-x)]^{2-D/2}} \int \frac{d^D k}{(2\pi)^D} \frac{k_{\alpha\beta}}{(k+p)^2 (k^2)^{2-D/2}},$$

then using the Feynman formula,

$$\frac{1}{A^\alpha B^\beta \dots} = \frac{\Gamma(\alpha + \beta + \dots)}{\Gamma(\alpha) \Gamma(\beta) \dots} \int_0^1 dy dx \dots \frac{\delta(1-x-y-\dots) x^{\alpha-1} y^{\beta-1} \dots}{(Ax + By + \dots)^{\alpha+\beta+\dots}}, \tag{C.12}$$

we can rewrite  $\mathcal{I}_6$  as,

$$\mathcal{I}_6 = i \mu^\epsilon \frac{\Gamma(3-D/2)}{(4\pi)^{D/2}} \int_0^1 dx dy \frac{(x-1) y^{1-D/2}}{[x(1-x)]^{2-D/2}} \int \frac{d^D k}{(2\pi)^D} \frac{k_{\alpha\beta}}{[k^2 + (1-y)(2k \cdot p + p^2)]^{3-D/2}}.$$

Using again Eq. (C.7) to evaluate the integration in  $k$ , we obtain

$$\mathcal{I}_6 = -\mu^{2\epsilon} \frac{\Gamma(\epsilon)}{(4\pi)^{3-\epsilon}} \int_0^1 dx dy \frac{(x-1)(y-1)\sqrt{y}^{\epsilon-1}}{\sqrt{x(1-x)}^{1+\epsilon}} \frac{p_{\alpha\beta}}{[y(1-y)p^2]^\epsilon}.$$

Finally, expanding in  $\epsilon$  and integrating in  $x$  and  $y$ , the integral  $I_6$  can be written as

$$\mathcal{I}_6 = -\frac{\Gamma(\epsilon)}{96\pi^2} p_{\alpha\beta} \left( 1 - \epsilon \left\{ \ln \left[ \frac{p^2}{4\pi\mu^2} \right] - 3 \right\} \right),$$

where  $\Gamma(\epsilon) = \frac{1}{\epsilon} - \gamma + \ln 4\pi + 1$ . Therefore,

$$\mathcal{I}_6 = \int \frac{d^D k d^D q}{(2\pi)^{2D}} \frac{q_{\alpha\beta}}{(k+p)^2 (q+k)^2 q^2} = -\frac{p_{\alpha\beta}}{96\pi^2\epsilon}, \quad (\text{C.13})$$

omitting all finite terms. Using a similar procedure it is possible to obtain the following integrals:

$$\mathcal{I}_7 = \int \frac{d^D k d^D q}{(2\pi)^{2D}} \frac{1}{(k+p)^2 (q+k)^2 q^2} = -\frac{1}{32\pi^2\epsilon}. \quad (\text{C.14})$$

$$\mathcal{I}_8 = \int \frac{d^D k d^D q}{(2\pi)^{2D}} \frac{k_{\alpha\beta}}{(k+p)^2 (q+k)^2 q^2} = \frac{p_{\alpha\beta}}{48\pi^2\epsilon}. \quad (\text{C.15})$$

$$\mathcal{I}_9 = \int \frac{d^D k d^D q}{(2\pi)^{2D}} \frac{k_{\alpha\beta} q_{\theta\lambda}}{(k+p)^2 k^2 (q+k)^2 q^2} = \frac{1}{192\pi^2\epsilon} (C_{\alpha\theta} C_{\beta\lambda} + C_{\beta\theta} C_{\alpha\lambda}). \quad (\text{C.16})$$

$$\mathcal{I}_{10} = \int \frac{d^D k d^D q}{(2\pi)^{2D}} \frac{k_{\mu\nu} k_{\theta\lambda}}{(k+p)^2 k^2 (k+q)^2 q^2} = -\frac{1}{96\pi^2\epsilon} (C_{\mu\theta} C_{\nu\lambda} + C_{\nu\theta} C_{\mu\lambda}). \quad (\text{C.17})$$

$$\begin{aligned} \mathcal{I}_{11} = \int \frac{d^D k d^D q}{(2\pi)^{2D}} \frac{q_{\mu\lambda} k_{\zeta\theta} k_{\kappa\rho}}{(k+p)^2 k^2 (k+q)^2 q^2} = & -\frac{1}{480\pi^2\epsilon} \{ (C_{\mu\zeta} C_{\lambda\theta} + C_{\lambda\zeta} C_{\mu\theta}) p_{\kappa\rho} \\ & + (C_{\zeta\kappa} C_{\theta\rho} + C_{\theta\kappa} C_{\zeta\rho}) p_{\mu\lambda} + (C_{\mu\kappa} C_{\lambda\rho} + C_{\lambda\kappa} C_{\mu\rho}) p_{\zeta\theta} \}. \end{aligned} \quad (\text{C.18})$$

$$\begin{aligned} \mathcal{I}_{12} = \int \frac{d^D k d^D q}{(2\pi)^{2D}} \frac{k_{\lambda\theta} k_{\mu\nu} k_{\kappa\rho} q_{\sigma\gamma}}{(k+p)^2 k^2 (k+q)^2 k^2 q^2} \\ = \frac{1}{960\pi^2\epsilon} \{ (C_{\lambda\mu} C_{\theta\nu} + C_{\theta\mu} C_{\lambda\nu}) (C_{\kappa\sigma} C_{\rho\gamma} + C_{\rho\sigma} C_{\kappa\gamma}) + (C_{\lambda\kappa} C_{\theta\rho} + C_{\theta\kappa} C_{\lambda\rho}) \times \\ (C_{\mu\sigma} C_{\nu\gamma} + C_{\nu\sigma} C_{\mu\gamma}) + (C_{\lambda\sigma} C_{\theta\gamma} + C_{\theta\sigma} C_{\lambda\gamma}) (C_{\mu\kappa} C_{\nu\rho} + C_{\nu\kappa} C_{\mu\rho}) \}. \end{aligned} \quad (\text{C.19})$$

We consider another integral, which will be more complicated, to wit

$$\begin{aligned}\mathcal{I}_{13} &= \int \frac{d^D k d^D q}{(2\pi)^{2D}} \frac{k_{\delta\theta} k_{\sigma\rho} q_{\beta\gamma} q_{\alpha\lambda}}{(k+p)^2 (p+q)^2 (k-q)^2 k^2 q^2} \\ &= \Gamma(3) \int_0^1 dx dy y \int \frac{d^D k d^D q}{(2\pi)^{2D}} \frac{k_{\delta\theta} k_{\sigma\rho} q_{\beta\gamma} q_{\alpha\lambda}}{(k+p)^2 k^2 [q^2 + 2q \cdot a + a^2 + c^2]^3},\end{aligned}$$

with  $c^2 = b^2 - a^2$ ,  $a = (1-x)yp - xyk$  and  $b^2 = y(1-x)p^2 + xyk^2$ . Using Eq. (C.9), we can write

$$\begin{aligned}\mathcal{I}_{13} &= \frac{i\mu^\epsilon}{(4\pi)^{D/2}} \int_0^1 dx dy \left\{ \underbrace{\int \frac{d^D k}{(2\pi)^D} \frac{k_{\delta\theta} k_{\sigma\rho} k_{\beta\gamma} k_{\alpha\lambda}}{(k+p)^2 k^2 [k^2 + l_1 p^2 + 2l_2 k \cdot p]^{3-D/2}}}_{\ast} \right. \\ &\quad \times \frac{x^2 y^3 \Gamma(3-D/2)}{[\sqrt{xy(1-xy)}]^{6-D}} + \underbrace{\int \frac{d^D k}{(2\pi)^D} \frac{k_{\delta\theta} k_{\sigma\rho}}{(k+p)^2 k^2 [k^2 + l_1 p^2 + 2l_2 k \cdot p]^{2-D/2}}}_{\boxtimes} \\ &\quad \left. \times \frac{1}{2} (C_{\beta\alpha} C_{\gamma\lambda} + C_{\gamma\alpha} C_{\beta\lambda}) \frac{y \Gamma(2-D/2)}{[\sqrt{xy(1-xy)}]^{4-D}} \right\} + \mathcal{O}(p^2),\end{aligned}$$

where

$$l_1 = \frac{(1-x)[1-y(1-x)]}{x(1-xy)}, \quad l_2 = \frac{y(1-x)}{1-xy}.$$

From the first integral,

$$\begin{aligned}\ast &= \frac{i\mu^\epsilon \Gamma(3-D)}{4(4\pi)^{D/2} \Gamma(3-D/2)} \{ (C_{\delta\sigma} C_{\theta\rho} + C_{\theta\sigma} C_{\delta\rho}) (C_{\beta\alpha} C_{\gamma\lambda} + C_{\gamma\alpha} C_{\beta\lambda}) \\ &\quad + (C_{\delta\beta} C_{\theta\gamma} + C_{\theta\beta} C_{\delta\gamma}) (C_{\sigma\alpha} C_{\rho\lambda} + C_{\rho\alpha} C_{\sigma\lambda}) + (C_{\delta\alpha} C_{\theta\lambda} + C_{\theta\alpha} C_{\delta\lambda}) \\ &\quad \times (C_{\sigma\beta} C_{\rho\gamma} + C_{\rho\beta} C_{\sigma\gamma}) \} \int_0^1 dz dw \frac{w [\sqrt{1-w}]^{4-D}}{[f^2]^{3-D}} + \mathcal{O}(p),\end{aligned}$$

where  $f^2 = d^2 - e^2$ ,  $d^2 = [w(1-z) + (1-w)l_1]p^2$  and  $e = [w(1-z) + (1-w)l_2]p$ .

From the second integral,

$$\begin{aligned}\boxtimes &= \frac{i\mu^\epsilon \Gamma(3-D)}{2(4\pi)^{D/2} \Gamma(2-D/2)} (C_{\delta\sigma} C_{\theta\rho} + C_{\theta\sigma} C_{\delta\rho}) (C_{\beta\alpha} C_{\gamma\lambda} + C_{\gamma\alpha} C_{\beta\lambda}) \\ &\quad \times \int_0^1 dz dw \frac{w [\sqrt{1-w}]^{2-D}}{[f^2]^{3-D}} + \mathcal{O}(p).\end{aligned}$$

Substituting  $\ast$  and  $\boxtimes$  in  $\mathcal{I}_{13}$ , we have

$$\begin{aligned} \mathcal{I}_{13} = & \int \frac{d^D k d^D q}{(2\pi)^{2D}} \frac{k_{\delta\theta} k_{\sigma\rho} q_{\beta\gamma} q_{\alpha\lambda}}{(k+p)^2 (p+q)^2 (k-q)^2 k^2 q^2} = -\frac{1}{5(384\pi^2\epsilon)} \{6(C_{\delta\sigma} C_{\theta\rho} + C_{\theta\sigma} C_{\delta\rho}) \\ & \times (C_{\beta\alpha} C_{\gamma\lambda} + C_{\gamma\alpha} C_{\beta\lambda}) + (C_{\delta\beta} C_{\theta\gamma} + C_{\theta\beta} C_{\delta\gamma}) (C_{\sigma\alpha} C_{\rho\lambda} + C_{\rho\alpha} C_{\sigma\lambda}) \\ & + (C_{\delta\alpha} C_{\theta\lambda} + C_{\theta\alpha} C_{\delta\lambda}) (C_{\sigma\beta} C_{\rho\gamma} + C_{\rho\beta} C_{\sigma\gamma})\}. \end{aligned} \quad (\text{C.20})$$

By similar means, we can find the following set of integrals:

$$\begin{aligned} \mathcal{I}_{14} = & \int \frac{d^D k d^D q}{(2\pi)^{2D}} \frac{q_{\lambda\theta} k_{\beta\rho}}{(k+p)^2 (p+q)^2 (k-q)^2 q^2} = \int \frac{d^D k d^D q}{(2\pi)^{2D}} \frac{q_{\lambda\theta} k_{\beta\rho}}{(k+p)^2 (p+q)^2 (k-q)^2 k^2} \\ & = -\frac{1}{192\pi^2\epsilon} (C_{\lambda\beta} C_{\theta\rho} + C_{\theta\beta} C_{\lambda\rho}), \end{aligned} \quad (\text{C.21})$$

$$\begin{aligned} \mathcal{I}_{15} = & \int \frac{d^D k d^D q}{(2\pi)^{2D}} \frac{q_{\mu\beta} q_{\theta\lambda}}{(k+p)^2 (p+q)^2 (k-q)^2 q^2} = \int \frac{d^D k d^D q}{(2\pi)^{2D}} \frac{k_{\mu\beta} k_{\theta\lambda}}{(k+p)^2 (p+q)^2 (k-q)^2 k^2} \\ & = -\frac{1}{96\pi^2\epsilon} (C_{\mu\theta} C_{\beta\lambda} + C_{\beta\theta} C_{\mu\lambda}), \end{aligned} \quad (\text{C.22})$$

$$\begin{aligned} \mathcal{I}_{16} = & \int \frac{d^D k d^D q}{(2\pi)^{2D}} \frac{q_{\mu\nu} q_{\lambda\theta} k_{\rho\sigma}}{(k+p)^2 (q+p)^2 (k-q)^2 q^2} = \int \frac{d^D k d^D q}{(2\pi)^{2D}} \frac{k_{\mu\nu} k_{\lambda\theta} q_{\rho\sigma}}{(k+p)^2 (q+p)^2 (k-q)^2 k^2} \\ & = \frac{1}{320\pi^2\epsilon} \{ (C_{\lambda\rho} C_{\theta\sigma} + C_{\theta\rho} C_{\lambda\sigma}) p_{\mu\nu} + (C_{\mu\rho} C_{\nu\sigma} + C_{\nu\rho} C_{\mu\sigma}) p_{\lambda\theta} \\ & + \frac{8}{3} (C_{\mu\lambda} C_{\nu\theta} + C_{\nu\lambda} C_{\mu\theta}) p_{\rho\sigma} \}, \end{aligned} \quad (\text{C.23})$$

$$\begin{aligned} \mathcal{I}_{17} = & \int \frac{d^D k d^D q}{(2\pi)^{2D}} \frac{k_{\delta\theta} k_{\sigma\rho} q_{\beta\gamma} q_{\alpha\lambda}}{(k+p)^2 (q^2)^2 [(k-q)^2]^2} = \int \frac{d^D k d^D q}{(2\pi)^{2D}} \frac{k_{\delta\theta} k_{\sigma\rho} q_{\beta\gamma} q_{\alpha\lambda}}{(k^2)^2 (q+p)^2 [(k-q)^2]^2} \\ & = \frac{1}{4(160\pi^2\epsilon)} \left\{ -\frac{2}{3} (C_{\delta\sigma} C_{\theta\rho} + C_{\theta\sigma} C_{\delta\rho}) (C_{\beta\alpha} C_{\gamma\lambda} + C_{\gamma\alpha} C_{\beta\lambda}) + (C_{\delta\beta} C_{\theta\gamma} + C_{\theta\beta} C_{\delta\gamma}) \times \right. \\ & \left. (C_{\sigma\alpha} C_{\rho\lambda} + C_{\rho\alpha} C_{\sigma\lambda}) + (C_{\delta\alpha} C_{\theta\lambda} + C_{\theta\alpha} C_{\delta\lambda}) (C_{\sigma\beta} C_{\rho\gamma} + C_{\rho\beta} C_{\sigma\gamma}) \right\}. \end{aligned} \quad (\text{C.24})$$

### C.3 Integrals used in the gauge superfield corrections

In this section we compile a set of Tables, with the divergent results for the specific integrals associated to each of the diagrams that contribute to the two-point vertex function of the gauge superfield, based on the results presented in the last subsection.

$\mathcal{I}^{(a)}$		$\mathcal{I}^{(a)}$	
$(k \cdot p) k_{\alpha\beta}$	$-2 p_{\alpha\beta} I_d$	$(k \cdot q) k_{\alpha\beta}$	$-2 p_{\alpha\beta} I_d$
$(k \cdot p) q_{\alpha\beta}$	$p_{\alpha\beta} I_d$	$p_{\beta\gamma} q_{\alpha\delta} k^{\gamma\delta}$	$3 p_{\alpha\beta} I_d$
$C_{\beta\gamma} C^{\delta\epsilon} k_{\alpha\epsilon} q_{\delta\zeta} k^{\gamma\zeta}$	$2 p_{\alpha\beta} I_d$	$k_{\alpha\gamma} k_{\beta\delta} p^{\gamma\delta}$	$2 p_{\alpha\beta} I_d$
$k_{\beta\gamma} q_{\alpha\delta} p^{\gamma\delta}$	$-p_{\alpha\beta} I_d$	$k_{\alpha\beta} k^2$	$4 p_{\alpha\beta} I_d$
$p_{\alpha\beta} k^2$	$-6 p_{\alpha\beta} I_d$	$q_{\alpha\beta} k^2$	$-2 p_{\alpha\beta} I_d$
$C_{\beta\gamma} q_{\alpha\delta} k^{\gamma\delta}$	$3 C_{\beta\alpha} I_d$	$C_{\beta\alpha} k^2$	$-6 C_{\beta\alpha} I_d$

Table C.1: Integrals of diagram  $\mathcal{S}_{\Gamma\Gamma}^{(a)}$  in the two-point vertex function of gauge superfield, with  $I_d = \frac{1}{192\pi^2\epsilon}$  and  $\mathcal{I}^{(a)} \equiv \int \frac{d^D k d^D q}{(2\pi)^{2D}} \frac{1}{(k+p)^2 (k+q)^2 q^2 k^2}$ .

$\mathcal{I}^{(a)}$		$\mathcal{I}^{(a)}$	
$(k \cdot p) k_{\alpha\beta}$	$-2 p_{\alpha\beta} I_d$	$p_{\alpha\gamma} q_{\beta\delta} k^{\gamma\delta}$	$3 p_{\alpha\beta} I_d$
$C_{\alpha\gamma} C^{\delta\epsilon} k_{\beta\delta} p_{\epsilon\zeta} k^{\gamma\zeta}$	$2 p_{\alpha\beta} I_d$	$k_{\alpha\gamma} k_{\beta\delta} p^{\gamma\delta}$	$2 p_{\alpha\beta} I_d$
$C_{\alpha\gamma} C^{\delta\epsilon} k_{\delta\zeta} q_{\beta\epsilon} p^{\gamma\zeta}$	$-3 p_{\alpha\beta} I_d$	$k_{\alpha\beta} k^2$	$4 p_{\alpha\beta} I_d$
$p_{\alpha\beta} k^2$	$-6 p_{\alpha\beta} I_d$	$q_{\alpha\beta} k^2$	$-2 p_{\alpha\beta} I_d$
$C_{\alpha\gamma} q_{\beta\delta} k^{\gamma\delta}$	$3 C_{\alpha\beta} I_d$	$C_{\beta\alpha} k^2$	$-6 C_{\beta\alpha} I_d$

Table C.2: Integrals of diagram  $\mathcal{S}_{\Gamma\Gamma}^{(b)}$  in the two-point vertex function of gauge superfield, with  $I_d = \frac{1}{192\pi^2\epsilon}$  and  $\mathcal{I}^{(a)} \equiv \int \frac{d^D k d^D q}{(2\pi)^{2D}} \frac{1}{(k+p)^2 (k+q)^2 q^2 k^2}$ .

$\mathcal{I}^{(b)}$		$\mathcal{I}^{(b)}$	
$(k \cdot p) (k \cdot q) k_{\alpha\beta}$	$p_{\alpha\beta} I_d$	$C_{\alpha\gamma} C_{\beta\delta} (k \cdot q) p_{\epsilon\zeta} k^{\gamma\zeta} k^{\delta\epsilon}$	$-p_{\alpha\beta} I_d$
$C_{\alpha\gamma} C_{\beta\delta} (k \cdot p) q_{\epsilon\zeta} k^{\gamma\epsilon} k^{\delta\zeta}$	$p_{\alpha\beta} I_d$	$C_{\alpha\gamma} C_{\beta\delta} p_{\epsilon\zeta} q_{\eta\theta} k^{\gamma\theta} k^{\delta\zeta} k^{\epsilon\eta}$	$-p_{\alpha\beta} I_d$
$(k \cdot q) k_{\alpha\gamma} k_{\beta\delta} p^{\gamma\delta}$	$-p_{\alpha\beta} I_d$	$C_{\alpha\gamma} C^{\delta\epsilon} k_{\beta\zeta} k_{\epsilon\eta} q_{\delta\theta} k^{\gamma\theta} p^{\eta\zeta}$	$p_{\alpha\beta} I_d$
$k_{\alpha\beta} k_{\gamma\delta} k_{\epsilon\zeta} p^{\delta\zeta} q^{\gamma\epsilon}$	$2 p_{\alpha\beta} I_d$	$(k \cdot p) k_{\alpha\gamma} k_{\beta\delta} q^{\delta\gamma}$	$p_{\alpha\beta} I_d$
$k_{\alpha\gamma} k_{\beta\delta} k_{\epsilon\zeta} p^{\delta\epsilon} q^{\zeta\gamma}$	$-p_{\alpha\beta} I_d$	$(k \cdot p) k_{\alpha\beta} k^2$	$-2 p_{\alpha\beta} I_d$
$(k \cdot q) k_{\alpha\beta} k^2$	$-2 p_{\alpha\beta} I_d$	$(k \cdot q) p_{\alpha\beta} k^2$	$3 p_{\alpha\beta} I_d$
$(k \cdot p) q_{\alpha\beta} k^2$	$p_{\alpha\beta} I_d$	$C_{\alpha\gamma} C_{\beta\delta} p_{\zeta\epsilon} k^{\gamma\zeta} k^{\delta\epsilon} k^2$	$2 p_{\alpha\beta} I_d$
$C_{\alpha\gamma} C_{\beta\delta} q_{\epsilon\zeta} k^{\gamma\zeta} k^{\delta\epsilon} k^2$	$-2 p_{\alpha\beta} I_d$	$C_{\alpha\gamma} C_{\beta\delta} q_{\epsilon\zeta} k^{\gamma\epsilon} k^{\delta\zeta} k^2$	$-2 p_{\alpha\beta} I_d$
$k_{\alpha\gamma} k_{\beta\delta} p^{\delta\gamma} k^2$	$2 p_{\alpha\beta} I_d$	$k_{\beta\gamma} q_{\alpha\delta} p^{\gamma\delta} k^2$	$-p_{\alpha\beta} I_d$
$C_{\alpha\gamma} C_{\beta\delta} q_{\epsilon\zeta} k^{\delta\epsilon} p^{\gamma\zeta} k^2$	$3 p_{\alpha\beta} I_d$	$k_{\beta\gamma} p_{\alpha\delta} q^{\gamma\delta} k^2$	$3 p_{\alpha\beta} I_d$
$C_{\alpha\gamma} C_{\beta\delta} k_{\epsilon\zeta} p^{\delta\zeta} q^{\gamma\epsilon} k^2$	$3 p_{\alpha\beta} I_d$	$C_{\alpha\gamma} C_{\beta\delta} p_{\epsilon\zeta} k^{\delta\epsilon} q^{\gamma\zeta} k^2$	$-p_{\alpha\beta} I_d$
$k_{\alpha\gamma} k_{\beta\delta} q^{\delta\gamma} k^2$	$-2 p_{\alpha\beta} I_d$	$C_{\alpha\gamma} C_{\beta\delta} k_{\epsilon\zeta} p^{\gamma\zeta} q^{\delta\epsilon} k^2$	$3 p_{\alpha\beta} I_d$
$k_{\alpha\beta} k^4$	$4 p_{\alpha\beta} I_d$	$p_{\alpha\beta} k^4$	$-6 p_{\alpha\beta} I_d$
$q_{\alpha\beta} k^4$	$-2 p_{\alpha\beta} I_d$	$C_{\beta\alpha} (k \cdot q) k^2$	$3 C_{\beta\alpha} I_d$
$C_{\beta\gamma} q_{\alpha\delta} k^{\gamma\delta} k^2$	$3 C_{\beta\alpha} I_d$	$C_{\alpha\gamma} q_{\beta\delta} k^{\gamma\delta} k^2$	$3 C_{\alpha\beta} I_d$
$C_{\beta\gamma} k_{\alpha\delta} q^{\gamma\delta} k^2$	$3 C_{\beta\alpha} I_d$	$C_{\alpha\gamma} k_{\beta\delta} q^{\gamma\delta} k^2$	$3 C_{\alpha\beta} I_d$
$C_{\beta\alpha} k^4$	$-6 C_{\beta\alpha} I_d$		

Table C.3: Integrals of diagram  $\mathcal{S}_{\Gamma\Gamma}^{(c)}$  in the two-point vertex function of gauge superfield, with  $I_d = \frac{1}{192\pi^2\epsilon}$  and  $\mathcal{I}^{(b)} \equiv \int \frac{d^D k d^D q}{(2\pi)^{2D}} \frac{1}{(k+p)^2 (k+q)^2 q^2 (k^2)^2}$ .

$\mathcal{I}^{(c)}$		$\mathcal{I}^{(c)}$	
$(k \cdot p) (k \cdot q) q_{\alpha\beta}$	$-p_{\alpha\beta} I_d$	$C_{\alpha\gamma} C_{\beta\delta} (p \cdot q) q_{\epsilon\zeta} k^{\gamma\zeta} k^{\delta\epsilon}$	0
$C_{\alpha\gamma} C^{\delta\epsilon} p_{\epsilon\zeta} q_{\beta\eta} q_{\delta\theta} k^{\gamma\theta} k^{\zeta\eta}$	$4 p_{\alpha\beta} I_d$	$C_{\alpha\gamma} C^{\delta\epsilon} k_{\epsilon\zeta} q_{\beta\eta} q_{\delta\theta} k^{\gamma\theta} p^{\zeta\eta}$	0
$C_{\beta\gamma} C^{\delta\epsilon} k_{\alpha\zeta} p_{\epsilon\eta} q_{\delta\theta} k^{\eta\theta} q^{\gamma\zeta}$	$2 p_{\alpha\beta} I_d$	$C_{\beta\gamma} C^{\delta\epsilon} k_{\alpha\zeta} k_{\epsilon\eta} q_{\delta\theta} p^{\eta\theta} q^{\gamma\zeta}$	$-2 p_{\alpha\beta} I_d$
$C_{\beta\gamma} C^{\delta\epsilon} k_{\alpha\zeta} k_{\delta\eta} q_{\epsilon\theta} p^{\eta\theta} q^{\gamma\zeta}$	$2 p_{\alpha\beta} I_d$	$C_{\beta\gamma} C^{\delta\epsilon} k_{\alpha\zeta} k_{\delta\eta} q_{\epsilon\theta} p^{\zeta\theta} q^{\gamma\eta}$	0
$k_{\alpha\gamma} k_{\delta\epsilon} q_{\beta\zeta} p^{\epsilon\zeta} q^{\delta\gamma}$	0	$C_{\alpha\gamma} C_{\beta\delta} (k \cdot q) p_{\epsilon\zeta} k^{\gamma\zeta} q^{\delta\epsilon}$	$p_{\alpha\beta} I_d$
$C_{\alpha\gamma} C_{\beta\delta} p_{\epsilon\zeta} q_{\eta\theta} k^{\gamma\eta} k^{\zeta\theta} q^{\delta\epsilon}$	0	$C_{\alpha\gamma} C_{\beta\delta} k_{\epsilon\zeta} q_{\eta\theta} k^{\gamma\theta} p^{\zeta\eta} q^{\delta\epsilon}$	$-4 p_{\alpha\beta} I_d$
$C_{\alpha\gamma} C_{\beta\delta} k_{\epsilon\zeta} q_{\eta\theta} k^{\gamma\eta} p^{\epsilon\theta} q^{\delta\zeta}$	$-4 p_{\alpha\beta} I_d$	$C_{\alpha\gamma} C_{\beta\delta} k_{\epsilon\zeta} p_{\eta\theta} k^{\gamma\theta} q^{\delta\zeta} q^{\epsilon\eta}$	0
$C_{\beta\gamma} C^{\delta\epsilon} k_{\alpha\zeta} k_{\delta\eta} p_{\epsilon\theta} q^{\gamma\theta} q^{\zeta\eta}$	0	$C_{\beta\gamma} C^{\delta\epsilon} k_{\alpha\zeta} k_{\delta\eta} p_{\epsilon\theta} q^{\gamma\eta} q^{\zeta\theta}$	$4 p_{\alpha\beta} I_d$
$(p \cdot q) k_{\alpha\beta} k^2$	$-p_{\alpha\beta} I_d$	$(k \cdot q) p_{\alpha\beta} k^2$	$-3 p_{\alpha\beta} I_d$
$(k \cdot p) q_{\alpha\beta} k^2$	$-p_{\alpha\beta} I_d$	$(k \cdot q) q_{\alpha\beta} k^2$	$4 p_{\alpha\beta} I_d$
$(p \cdot q) q_{\alpha\beta} k^2$	$-2 p_{\alpha\beta} I_d$	$p_{\alpha\gamma} q_{\beta\delta} k^{\gamma\delta} k^2$	$-3 p_{\alpha\beta} I_d$
$k_{\alpha\gamma} q_{\beta\delta} p^{\gamma\delta} k^2$	$p_{\alpha\beta} I_d$	$q_{\alpha\gamma} q_{\beta\delta} p^{\delta\gamma} k^2$	$2 p_{\alpha\beta} I_d$
$C_{\alpha\gamma} C_{\beta\delta} q_{\epsilon\zeta} k^{\gamma\epsilon} p^{\delta\zeta} k^2$	$-3 p_{\alpha\beta} I_d$	$C_{\alpha\gamma} C_{\beta\delta} p_{\epsilon\zeta} k^{\gamma\zeta} q^{\delta\epsilon} k^2$	$p_{\alpha\beta} I_d$
$C_{\alpha\gamma} C_{\beta\delta} k_{\epsilon\zeta} q^{\gamma\zeta} q^{\delta\epsilon} k^2$	$2 p_{\alpha\beta} I_d$	$C_{\alpha\gamma} C_{\beta\delta} p_{\epsilon\zeta} k^{\gamma\epsilon} q^{\delta\zeta} k^2$	$p_{\alpha\beta} I_d$
$C_{\alpha\gamma} C_{\beta\delta} k_{\epsilon\zeta} q^{\gamma\epsilon} q^{\delta\zeta} k^2$	$2 p_{\alpha\beta} I_d$	$C_{\alpha\gamma} C_{\beta\delta} k_{\epsilon\zeta} p^{\gamma\zeta} q^{\delta\epsilon} k^2$	$-3 p_{\alpha\beta} I_d$
$C_{\alpha\gamma} C_{\beta\delta} p_{\epsilon\zeta} q^{\gamma\epsilon} q^{\delta\zeta} k^2$	$2 p_{\alpha\beta} I_d$	$p_{\alpha\beta} k^4$	0
$q_{\alpha\beta} k^4$	0	$(k \cdot p) k_{\alpha\beta} q^2$	$-2 p_{\alpha\beta} I_d$
$(k \cdot p) q_{\alpha\beta} q^2$	$-p_{\alpha\beta} I_d$	$p_{\alpha\gamma} q_{\beta\delta} k^{\gamma\delta} q^2$	$-3 p_{\alpha\beta} I_d$
$C_{\alpha\gamma} C_{\beta\delta} p_{\epsilon\zeta} k^{\gamma\zeta} k^{\delta\epsilon} q^2$	$2 p_{\alpha\beta} I_d$	$C_{\alpha\gamma} C_{\beta\delta} q_{\epsilon\zeta} k^{\gamma\zeta} k^{\delta\epsilon} q^2$	$2 p_{\alpha\beta} I_d$
$k_{\alpha\gamma} k_{\beta\delta} p^{\delta\gamma} q^2$	$2 p_{\alpha\beta} I_d$	$k_{\alpha\gamma} q_{\beta\delta} p^{\gamma\delta} q^2$	$p_{\alpha\beta} I_d$
$C_{\alpha\gamma} C_{\beta\delta} q_{\epsilon\zeta} k^{\delta\epsilon} p^{\gamma\zeta} q^2$	$-3 p_{\alpha\beta} I_d$	$C_{\alpha\gamma} C_{\beta\delta} p_{\epsilon\zeta} k^{\gamma\zeta} q^{\delta\epsilon} q^2$	$p_{\alpha\beta} I_d$
$C_{\alpha\gamma} C_{\beta\delta} k_{\epsilon\zeta} p^{\gamma\zeta} q^{\delta\epsilon} q^2$	$-3 p_{\alpha\beta} I_d$	$C_{\alpha\gamma} C_{\beta\delta} p_{\epsilon\zeta} k^{\gamma\epsilon} q^{\delta\zeta} q^2$	$p_{\alpha\beta} I_d$
$C_{\alpha\gamma} C_{\beta\delta} k_{\epsilon\zeta} p^{\gamma\epsilon} q^{\delta\zeta} q^2$	$-3 p_{\alpha\beta} I_d$	$k_{\alpha\beta} k^2 q^2$	$6 p_{\alpha\beta} I_d$
$p_{\alpha\beta} k^2 q^2$	$-6 p_{\alpha\beta} I_d$	$C_{\alpha\gamma} q_{\beta\delta} q_{\epsilon\zeta} k^{\gamma\zeta} k^{\delta\epsilon}$	0
$C_{\alpha\gamma} q_{\beta\delta} q_{\epsilon\zeta} k^{\gamma\epsilon} k^{\zeta\delta}$	0	$C_{\beta\alpha} (k \cdot q) k_{\alpha\delta} q^{\gamma\delta}$	$-3 C_{\beta\alpha} I_d$
$C_{\beta\gamma} k_{\alpha\delta} k_{\epsilon\zeta} q^{\gamma\zeta} q^{\delta\epsilon}$	0	$C_{\alpha\gamma} C_{\beta\delta} C^{\epsilon\zeta} k_{\epsilon\eta} q_{\zeta\theta} k^{\gamma\theta} q^{\delta\eta}$	0
$C_{\beta\gamma} k_{\alpha\delta} k_{\epsilon\zeta} q^{\gamma\zeta} q^{\delta\epsilon}$	0	$C_{\alpha\gamma} q_{\beta\delta} k^{\gamma\delta} k^2$	$-3 C_{\alpha\beta} I_d$
$C_{\beta\gamma} k_{\alpha\delta} q^{\gamma\delta} k^2$	$-3 C_{\beta\alpha} I_d$	$C_{\alpha\gamma} q_{\beta\delta} k^{\gamma\delta} q^2$	$-3 C_{\alpha\beta} I_d$
$C_{\beta\gamma} k_{\alpha\delta} q^{\gamma\delta} q^2$	$-3 C_{\beta\alpha} I_d$	$C_{\beta\alpha} k^2 q^2$	$-6 C_{\beta\alpha} I_d$

Table C.4: Integrals of diagram  $\mathcal{S}_{\Gamma\Gamma}^{(d)}$  in the two-point vertex function of gauge superfield, with  $I_d = \frac{1}{192\pi^2\epsilon}$  and  $\mathcal{I}^{(c)} \equiv \int \frac{d^D k d^D q}{(2\pi)^{2D}} \frac{1}{(k+p)^2 (q+p)^2 (k-q)^2 q^2 k^2}$ .



# Bibliography

- [1] N. K. Nielsen. On the Gauge Dependence of Spontaneous Symmetry Breaking in Gauge Theories. *Nucl. Phys.*, B101:173–188, 1975.
- [2] P. Ramond. Dual theory for free fermions. *Phys. Rev. D*, 3:2415–2418, May 1971.
- [3] A. Neveu and J. H. Schwarz. Factorizable dual model of pions. *Nucl. Phys.*, B31:86–112, 1971.
- [4] A. Neveu and John H. Schwarz. Quark model of dual pions. *Phys. Rev. D*, 4:1109–1111, Aug 1971.
- [5] J.-L. Gervais and B. Sakita. Field theory interpretation of supergauges in dual models. *Nuclear Physics B*, 34(2):632 – 639, 1971.
- [6] Yu.A. Golfand and E.P. Likhtman. Extension of the Algebra of Poincare Group Generators and Violation of p Invariance. *JETP Lett.*, 13:323–326, 1971.
- [7] D.V. Volkov and V.P. Akulov. Possible universal neutrino interaction. *JETP Lett.*, 16:438–440, 1972.
- [8] J. Wess and B. Zumino. A lagrangian model invariant under supergauge transformations. *Phys. Lett.*, B49:52, 1974.
- [9] Sidney Coleman and Jeffrey Mandula. All possible symmetries of the  $s$  matrix. *Phys. Rev.*, 159(5):1251–1256, July 1967.
- [10] Rudolf Haag, Jan T. Łopuszański, and Martin Sohnius. All possible generators of supersymmetries of the  $s$ -matrix. *Nuclear Physics B*, 88(2):257 – 274, 1975.
- [11] Steven Weinberg. Precise relations between the spectra of vector and axial vector mesons. *Phys. Rev. Lett.*, 18:507–509, 1967.
- [12] Steven Weinberg. Current algebra and gauge theories. 2. NonAbelian gluons. *Phys. Rev.*, D8:4482–4498, 1973.
- [13] Jogesh C. Pati and Abdus Salam. Unified Lepton-Hadron Symmetry and a Gauge Theory of the Basic Interactions. *Phys. Rev.*, D8:1240–1251, 1973.

- [14] H. Georgi and S. L. Glashow. Unity of All Elementary Particle Forces. *Phys. Rev. Lett.*, 32:438–441, 1974.
- [15] Pran Nath and Richard L. Arnowitt. Generalized Supergauge Symmetry as a New Framework for Unified Gauge Theories. *Phys. Lett.*, B56:177–180, 1975.
- [16] Daniel Z. Freedman, P. van Nieuwenhuizen, and S. Ferrara. Progress Toward a Theory of Supergravity. *Phys. Rev.*, D13:3214–3218, 1976.
- [17] Stanley Deser and B. Zumino. Consistent Supergravity. *Phys. Lett.*, B62:335, 1976.
- [18] M. B. Green, J. H. Scharwz, and E. Witten. *Superstring Theory. Vol. 1: Introduction*. Cambridge Univ. Pr., 1988. 480 p.
- [19] M. B. Green, J. H. Scharwz, and E. Witten. *Superstring Theory. Vol. 2: Loop amplitudes, anomalies & phenomenology*. Cambridge Univ. Pr., 1988. 608 p.
- [20] Steven Weinberg. *The Quantum Theory of Fields. Vol. 3: Supersymmetry*. Cambridge Univ. Pr., 2000. 419 p.
- [21] R. Jackiw. Functional evaluation of the effective potential. *Phys. Rev.*, D9:1686, 1974.
- [22] L. Dolan and R. Jackiw. Gauge-invariant signal for gauge-symmetry breaking. *Phys. Rev. D*, 9:2904–2912, May 1974.
- [23] J. M. Frere and P. Nicoletopoulos. Gauge Invariant Content of the Effective Potential. *Phys. Rev.*, D11:2332, 1975.
- [24] Reijiro Fukuda and Taichiro Kugo. Gauge Invariance in the Effective Action and Potential. *Phys. Rev.*, D13:3469, 1976.
- [25] I. J. R. Aitchison and C. M. Fraser. Gauge Invariance and the Effective Potential. *Annals Phys.*, 156:1, 1984.
- [26] D. Johnston. Nielsen Identities in the 't Hooft Gauge. *Nucl. Phys.*, B253:687–700, 1985.
- [27] J. R. S. Do Nascimento and D. Bazeia. Gauge Invariance of the Effective Potential. *Phys. Rev.*, D35:2490–2494, 1987.
- [28] J. C. Breckenridge, M. J. Lavelle, and Thomas G. Steele. The Nielsen identities for the two point functions of QED and QCD. *Z. Phys.*, C65:155–164, 1995, hep-th/9407028.

- 
- [29] Paolo Gambino and Pietro Antonio Grassi. The Nielsen identities of the SM and the definition of mass. *Phys. Rev.*, D62:076002, 2000, hep-ph/9907254.
- [30] Sergio M. Iguri and Francisco D. Mazzitelli. Gauge fixing independence of test fields in Yang-Mills theories. 2001, hep-th/0107095.
- [31] A. Gerhold and A. Rebhan. Gauge dependence identities for color superconducting QCD. *Phys. Rev.*, D68:011502, 2003, hep-ph/0305108.
- [32] Adrian Lewandowski. Renormalization of Nielsen Identities. 2013, arXiv:1307.4055.
- [33] Sudhaker Upadhyay. Ward and Nielsen identities for ABJM theory in  $N = 1$  superspace. *Int. J. Mod. Phys.*, A31(19):1650112, 2016, arXiv:1607.00068.
- [34] Sidney R. Coleman and Erick J. Weinberg. Radiative Corrections as the Origin of Spontaneous Symmetry Breaking. *Phys.Rev.*, D7:1888–1910, 1973.
- [35] Marc Sher. Electroweak Higgs Potentials and Vacuum Stability. *Phys.Rept.*, 179:273–418, 1989.
- [36] V. Elias, Robert B. Mann, D.G.C. McKeon, and Thomas G. Steele. Optimal renormalization group improvement of two radiatively broken gauge theories. *Nucl.Phys.*, B678:147–196, 2004, hep-ph/0308301.
- [37] V. Elias, Robert B. Mann, D. G. C. McKeon, and Thomas G. Steele. Radiative electroweak symmetry-breaking revisited. *Phys. Rev. Lett.*, 91:251601, 2003, hep-ph/0304153.
- [38] F.A. Chishtie, V. Elias, Robert B. Mann, D.G.C. McKeon, and T.G. Steele. Stability of subsequent-to-leading-logarithm corrections to the effective potential for radiative electroweak symmetry breaking. *Nucl.Phys.*, B743:104–132, 2006, hep-ph/0509122.
- [39] V. Elias, R. B. Mann, D. G. C. McKeon, and T. G. Steele. Higher order stability of a radiatively induced 220 GeV Higgs mass. *Phys. Rev. D*, 72:037902, Aug 2005.
- [40] Krzysztof A. Meissner and Hermann Nicolai. Conformal Symmetry and the Standard Model. *Phys.Lett.*, B648:312–317, 2007, hep-th/0612165.
- [41] Krzysztof A. Meissner and Hermann Nicolai. Effective action, conformal anomaly and the issue of quadratic divergences. *Phys.Lett.*, B660:260–266, 2008, arXiv:0710.2840.
- [42] Krzysztof A. Meissner and Hermann Nicolai. Neutrinos, Axions and Conformal Symmetry. *Eur.Phys.J.*, C57:493–498, 2008, arXiv:0803.2814.

- [43] Krzysztof A. Meissner and Hermann Nicolai. Renormalization Group and Effective Potential in Classically Conformal Theories. *Acta Phys.Polon.*, B40:2737–2752, 2009, arXiv:0809.1338.
- [44] A.G. Dias, J.D. Gomez, A.A. Natale, A.G. Quinto, and A.F. Ferrari. Non-perturbative fixed points and renormalization group improved effective potential. *Physics Letters B*, 739(0):8 – 12, 2014.
- [45] F.A. Chishtie, T. Hanif, J. Jia, Robert B. Mann, D.G.C. McKeon, T. N Sherry, T. G. Steele. Can the Renormalization Group Improved Effective Potential be used to estimate the Higgs Mass in the Conformal Limit of the Standard Model? *Phys.Rev.*, D83:105009, 2011, arXiv:1006.5887.
- [46] T.G. Steele and Zhi-Wei Wang. Is Radiative Electroweak Symmetry Breaking Consistent with a 125 GeV Higgs Mass? 2012, arXiv:1209.5416.
- [47] Christoph Englert, Joerg Jaeckel, V.V. Khoze, and Michael Spannowsky. Emergence of the Electroweak Scale through the Higgs Portal. *JHEP*, 1304:060, 2013, arXiv:1301.4224.
- [48] Eung Jin Chun, Sunghoon Jung, and Hyun Min Lee. Radiative generation of the Higgs potential. 2013, arXiv:1304.5815.
- [49] Stanley Deser, R. Jackiw, and S. Templeton. Topologically massive gauge theories. *Ann. Phys.*, 140:372–411, 1982.
- [50] Jonathan F. Schonfeld. A mass term for three-dimensional gauge fields. *Nuclear Physics B*, 185(1):157 – 171, 1981.
- [51] R. E. Prange and S. M. Girvin, editors. *The Quantum Hall Effect, Graduate Text in Contemporary Physics*. Springer-Verlag, Berlin, 1990.
- [52] L.V. Avdeev, G.V. Grigorev, and D.I. Kazakov. Renormalizations in Abelian Chern-Simons field theories with matter. *Nucl.Phys.*, B382:561–580, 1992.
- [53] F. Ruiz Ruiz and P. van Nieuwenhuizen. Supersymmetric Yang-Mills-Chern-Simons theory. *Nucl. Phys. Proc. Suppl.*, 56B:269–274, 1997, hep-th/9701052.
- [54] A. C. Lehum, A. F. Ferrari, M. Gomes, and A. J. da Silva. Spontaneous gauge symmetry breaking in a SUSY Chern-Simons model. *Phys.Rev.*, 76:105021, 2007, arXiv:0709.3280 [hep-th].
- [55] A.F. Ferrari, E.A. Gallegos, M. Gomes, A.C. Lehum, J.R. Nascimento, A. J. da Silva. Coleman-Weinberg mechanism in a three-dimensional supersymmetric Chern-Simons-Matter model. *Phys.Rev.*, D82:025002, 2010, arXiv:1004.0982.

- [56] A.C. Lehum and A.J. da Silva. Spontaneous breaking of superconformal invariance in (2+1)D supersymmetric Chern-Simons-matter theories in the large N limit. *Phys.Lett.*, B693:393–398, 2010, arXiv:1008.1173.
- [57] Davide Gaiotto and Xi Yin. Notes on superconformal Chern-Simons-Matter theories. *JHEP*, 08:056, 2007, arXiv:0704.3740.
- [58] Andreas Gustavsson. Selfdual strings and loop space Nahm equations. *JHEP*, 04:083, 2008, arXiv:0802.3456.
- [59] Jonathan Bagger and Neil Lambert. Comments on multiple M2-branes. *JHEP*, 02:105, 2008, arXiv:0712.3738.
- [60] Jonathan Bagger and Neil Lambert. Gauge symmetry and supersymmetry of multiple M2-branes. *Phys.Rev.*, D77:065008, 2008, arXiv:0711.0955.
- [61] Miguel A. Bandres, Arthur E. Lipstein, and John H. Schwarz. Studies of the ABJM Theory in a Formulation with Manifest SU(4) R-Symmetry. *JHEP*, 09:027, 2008, arXiv:0807.0880.
- [62] E. Antonyan and Arkady A. Tseytlin. On 3d N=8 Lorentzian BLG theory as a scaling limit of 3d superconformal N=6 ABJM theory. *Phys. Rev.*, D79:046002, 2009, arXiv:0811.1540.
- [63] Ofer Aharony, Oren Bergman, Daniel Louis Jafferis, and Juan Maldacena. N=6 superconformal Chern-Simons-matter theories, M2-branes and their gravity duals. *JHEP*, 10:091, 2008, arXiv:0806.1218.
- [64] M. Naghdi. A Monopole Instanton-Like Effect in the ABJM Model. *Int. J. Mod. Phys.*, A26:3259–3273, 2011, arXiv:1106.0907.
- [65] Mir Faizal. M-Theory on Deformed Superspace. *Phys. Rev.*, D84:106011, 2011, arXiv:1111.0213.
- [66] Mir Faizal and Sudhaker Upadhyay. Spontaneous Breaking of the BRST Symmetry in the ABJM theory. *Phys. Lett.*, B736:288–292, 2014, arXiv:1407.6188.
- [67] Sudhaker Upadhyay and Diptarka Das. ABJM theory in Batalin-Vilkovisky formulation. *Phys. Lett.*, B733:63–68, 2014, arXiv:1404.2633.
- [68] Mir Faizal. M-Theory in the Gaugeon Formalism. *Commun. Theor. Phys.*, 57:637–640, 2012, arXiv:1201.1220.
- [69] J. M. Queiruga, A. C. Lehum, and Mir Faizal. Kahlerian effective potentials for Chern-Simons-matter theories. *Nucl. Phys.*, B902:58–68, 2016, arXiv:1511.03586.

- [70] Nikolas Akerblom, Christian Saemann, and Martin Wolf. Marginal Deformations and 3-Algebra Structures. *Nucl. Phys.*, B826:456–489, 2010, arXiv:0906.1705.
- [71] Marco S. Bianchi, Silvia Penati, and Massimo Siani. Infrared Stability of  $N = 2$  Chern-Simons Matter Theories. *JHEP*, 05:106, 2010, arXiv:0912.4282.
- [72] Marco S. Bianchi, Silvia Penati, and Massimo Siani. Infrared stability of ABJ-like theories. *JHEP*, 01:080, 2010, arXiv:0910.5200.
- [73] Marco S. Bianchi and Silvia Penati. The Conformal Manifold of Chern-Simons Matter Theories. *JHEP*, 01:047, 2011, arXiv:1009.6223.
- [74] I.L. Buchbinder, B.S. Merzlikin, and I.B. Samsonov. Two-loop effective potentials in general  $N=2$ ,  $d=3$  chiral superfield model. *Nucl.Phys.*, B860:87–114, 2012, arXiv:1201.5579.
- [75] I. L. Buchbinder and B. S. Merzlikin. On effective Kähler potential in  $N=2$ ,  $d=3$  SQED. *Nucl. Phys.*, B900:80–103, 2015, arXiv:1505.07679.
- [76] Wei Chen, G.W. Semenoff, and Yong-shi Wu. Scale and conformal invariance in Chern-Simons matter field theory. *Phys.Rev.*, D44:1625–1628, 1991.
- [77] Wei Chen, Gordon W. Semenoff, and Yong-Shi Wu. Two loop analysis of nonAbelian Chern-Simons theory. *Phys.Rev.*, D46:5521–5539, 1992, hep-th/9209005.
- [78] F. Ruiz Ruiz and P. van Nieuwenhuizen. BRS symmetry versus supersymmetry in Yang-Mills-Chern- Simons theory. *Nucl. Phys.*, B486:443–465, 1997, hep-th/9609074.
- [79] Pang-Ning Tan, Bayram Tekin, and Yutaka Hosotani. Maxwell Chern-Simons scalar electrodynamics at two loop. *Nucl.Phys.*, B502:483–515, 1997, hep-th/9703121.
- [80] V.S. Alves, M. Gomes, S.L.V. Pinheiro, and A.J. da Silva. A Renormalization group study of the  $(\phi^* \phi)^{**3}$  model coupled to a Chern-Simons field. *Phys.Rev.*, D61:065003, 2000, hep-th/0001221.
- [81] Alex G. Dias, M. Gomes, and A. J. da Silva. Dynamical breakdown of symmetry in  $(2+1)$  dimensional model containing the Chern-Simons field. *Phys. Rev.*, D69:065011, 2004, hep-th/0305043.
- [82] Warren Siegel. Supersymmetric Dimensional Regularization via Dimensional Reduction. *Phys.Lett.*, B84:193, 1979.
- [83] A.G. Dias and A.F. Ferrari. Renormalization Group and Conformal Symmetry Breaking in the Chern-Simons Theory Coupled to Matter. *Phys.Rev.*, D82:085006, 2010, arXiv:1006.5672.

- [84] L.V. Avdeev, D.I. Kazakov, and I.N. Kondrashuk. Renormalizations in supersymmetric and nonsupersymmetric nonAbelian Chern-Simons field theories with matter. *Nucl. Phys.*, B391:333–357, 1993.
- [85] John Collins. *Renormalization*. Cambridge Monographs on Mathematical Physics. Cambridge Univ. Pr., 1984.
- [86] A.R. Fazio, V.E.R. Lemes, M.S. Sarandy, and S.P. Sorella. The Diagonal ghost equation Ward identity for Yang-Mills theories in the maximal Abelian gauge. *Phys. Rev.*, D64:085003, 2001, hep-th/0105060.
- [87] J.M. Bell and J.A. Gracey. Momentum subtraction scheme renormalization group functions in the maximal Abelian gauge. *Phys. Rev.*, D88(8):085027, 2013, arXiv:1310.0243.
- [88] Luca Di Luzio and Luminita Mihaila. On the gauge dependence of the Standard Model vacuum instability scale. *JHEP*, 06:079, 2014, arXiv:1404.7450.
- [89] J.M. Bell and J.A. Gracey. Maximal abelian and Curci-Ferrari gauges in momentum subtraction at three loops. *Phys. Rev.*, D92:125001, 2015, arXiv:1511.00854.
- [90] A.G. Quinto and A.F. Ferrari. Nielsen identity and the renormalization group in an Abelian supersymmetric Chern-Simons model. *Phys. Rev.*, D94(8):085006, 2016, arXiv:1607.07505.
- [91] A.F. Ferrari, M. Gomes, A.C. Lehum, J.R. Nascimento, A.Yu. Petrov, A.J. da Silva. On the superfield effective potential in three dimensions. *Phys.Lett.*, B678:500–503, 2009, arXiv:0901.0679.
- [92] A.G. Quinto, A.F. Ferrari, and A.C. Lehum. Renormalization group improvement and dynamical breaking of symmetry in a supersymmetric Chern-Simons-matter model. *Nucl. Phys.*, B907:664–677, 2016, arXiv:1405.6118.
- [93] S.J. Gates, Marcus T. Grisaru, M. Rocek, and W. Siegel. Superspace, or one thousand and one lessons in supersymmetry. *Front. Phys.*, 58:1–548, 1983, hep-th/0108200.
- [94] I.L. Buchbinder and S.M. Kuzenko. *Ideas and methods of supersymmetry and supergravity: Or a walk through superspace*. Bristol, UK, 1998. 656 p.
- [95] J.S. Kang. Gauge Invariance of the Scalar-Vector Mass Ratio in the Coleman-Weinberg Model. *Phys. Rev.*, D10:3455, 1974.
- [96] C. Becchi, A. Rouet, and R. Stora. The Abelian Higgs-Kibble Model. Unitarity of the S Operator. *Phys. Lett.*, B52:344–346, 1974.

- [97] Lewis H. Ryder. *Quantum Field Theory*. Cambridge Univ. Pr., second edition edition, 1996.
- [98] Mark Srednicki. *Quantum Field Theory*. Cambridge University Press, 2007. 660 p.
- [99] E.A. Gallegos and A.J. da Silva. Dynamical (super)symmetry vacuum properties of the supersymmetric Chern-Simons-matter model. *Phys.Rev.*, D85:125012, 2012, arXiv:1111.2886.
- [100] A. C. Lehum and A. J. da Silva. Supersymmetry breaking in the three-dimensional nonlinear sigma model. *Phys. Rev.*, D88(6):067702, 2013, arXiv:1308.4713.
- [101] E.A. Gallegos and A.J. da Silva. Supergraph techniques for D=3,N=1 broken supersymmetric theories. *Phys.Rev.*, D84:065009, 2011, arXiv:1102.1989.
- [102] Christopher Ford. Multiscale renormalization group improvement of the effective potential. *Phys. Rev.*, D50:7531–7537, 1994, hep-th/9404085.
- [103] C. Ford and C. Wiesendanger. A Multiscale subtraction scheme and partial renormalization group equations in the O(N) symmetric  $\phi^4$  theory. *Phys. Rev.*, D55:2202–2217, 1997, hep-ph/9604392.
- [104] Thomas Hahn. Generating Feynman diagrams and amplitudes with FeynArts 3. *Comput. Phys. Commun.*, 140:418–431, 2001, hep-ph/0012260.
- [105] D. Binosi, J. Collins, C. Kaufhold, and L. Theussl. JaxoDraw: A Graphical user interface for drawing Feynman diagrams. Version 2.0 release notes. *Comput. Phys. Commun.*, 180:1709–1715, 2009, arXiv:0811.4113.
- [106] A.F. Ferrari. SusyMath: A Mathematica package for quantum superfield calculations. *Comput. Phys. Commun.*, 176:334–346, 2007, <http://fma.if.usp.br/~alysson/SusyMath>.
- [107] Sidney R. Coleman and Brian Russell Hill. No More Corrections to the Topological Mass Term in QED in Three-Dimensions. *Phys. Lett.*, B159:184–188, 1985.
- [108] C.Ford and D.R.T. Jones. The Effective potential and the differential equations method for Feynman integrals. *Phys. Lett.*, B274:409–414, 1992. [Erratum: *Phys. Lett.* B285,399(1992)].
- [109] V.Elias, D.G.C. McKeon, and T.N. Sherry. Summation of higher order effects using the renormalization group equation. *Int.J.Mod.Phys.*, A20:1065–1088, 2005, hep-th/0408152.